Towards the next generation of drug administration:

Evaluation of drug delivery systems

in vitro, in vivo, and in clinical settings

Inauguraldissertation

zur

Erlangung der Würde eines Doktors der Philosophie
vorgelegt der
Philosophisch-Naturwissenschaftlichen Fakultät
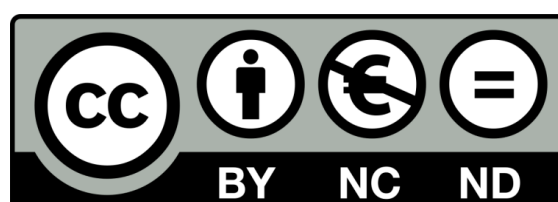der Universität Basel

von

Klara Kiene

aus Deutschland

Basel, 2019

Genehmigt von der Philosophisch-Naturwissenschaftlichen Fakultät auf Antrag von

Prof. Dr. Jörg Huwyler

Dr. med. Julia Bielicki

Basel, den 18. September 2018

Prof. Dr. Martin Spiess (Dekan)

"The pessimist sees difficulty in every opportunity.
The optimist sees the opportunity in every difficulty."

unknown

TABLE OF CONTENT AND LIST OF FIGURES

ZUSAMMENFASSUNG FÜR LAIEN

Eine zentrale Herausforderung aktueller Arzneimittelforschung besteht darin, dass neue und vielversprechende Wirkstoffe oft schlecht vom Körper aufgenommen oder schnell wieder abgebaut werden. Beides führt dazu, dass hohe Dosen an Wirkstoffen verabreicht werden müssen, um therapeutisch wirksam zu sein. Die hohen Dosen resultieren dann in immer stärkeren Nebenwirkungen. Um diese Herausforderung zu meistern, verpackt man Wirkstoffe häufig in Transportsysteme, welche den Wirkstoff an den Zielort bringen, und ihn vor vorzeitigem Abbau im Körper schützen. Solche Transportsysteme bestehen oft aus Polymeren und können ganz verschiedene Formen annehmen. Polymere sind Stoffe, die aus vielen sich wiederholenden Untereinheiten bestehen. Diese Untereinheiten können sowohl immer die gleichen sein, oder sich auch voneinander unterscheiden. Die Anzahl der Untereinheiten ist ebenfalls variabel. Es gibt natürliche Polymere, die in Lebewesen synthetisiert werden und daher auch Biopolymere genannt werden. Synthetische Polymere hingegen werden künstlich hergestellt oder entstehen bei der chemischen Weiterverarbeitung von Biopolymeren.

Ein erster Ansatz, Wirkstoffe an ihren Zielort zu transportieren, besteht darin, sie in winzig kleine Transportsysteme, so genannte **Nanopartikel**, zu packen. Nanopartikel sind so klein, dass man davon 1'000 bis 1'000'000 aneinanderreihen müsste, um einen Millimeter an Strecke zurückzulegen. Wir haben solche Nanopartikel aus synthetischen Polymerketten hergestellt und ihre Oberfläche so bearbeitet, dass sie ganz bestimmte Leberzellen (Hepatozyten) erkennen. Vereinfacht funktioniert das wie ein Schlüssel, der in ein dazugehöriges Schloss passt. Ein bestimmtes Protein an der Oberfläche eines Nanopartikels (quasi der Schlüssel) kann diesen an eine dazu passende Zelle andocken lassen, die sozusagen das Schloss, also den entsprechenden Rezeptor, vorweist. In Zellexperimenten konnten wir demonstrieren, dass solche modifizierten Nanopartikel besser von den passenden Zellen aufgenommen wurden als Nanopartikel, die keine modifizierte Oberfläche – also keinen passenden Schlüssel – hatten. Wir konnten ausserdem zeigen, dass solche Nanopartikel für unsere Zellen nicht giftig waren und bestätigten dies in ersten Versuchen mit Zebrafisch Embryos. Zebrafische sind ein sehr interessantes Tiermodell für die Arzneimittelentwicklung, da ihr Erbgut dem des Menschen relativ ähnlich ist. Zudem entwickeln sich die Embryos innerhalb weniger Tage – und das auch noch ausserhalb des Mutterleibs, im Gegensatz zu klassischen Labortieren wie Mäusen und Ratten. Man kann also die Embryonalentwicklung dieser Tiere sehr gut beobachten, was sie besonders für das Testen potenziell giftiger Substanzen interessant macht. Doch selbst wenn man herausfindet, dass eine Formulierung in Zebrafischen gut vertragen wird, ist es bisher nicht möglich, komplett auf weitere Tierversuche zu verzichten. Die potenziellen neuen Medikamente müssen noch einen langen Weg an

Tierversuchen und weiteren Charakterisierungen durchlaufen, bevor man sie für sicher genug erachtet, um sie das erste Mal an Menschen zu testen. Zebrafische bilden also quasi eine Zwischenstufe, um die nachfolgenden Tierversuche auf ein Minimum reduzieren zu können.

Als weiteres Transportsystem für Wirkstoffe haben wir aus Polymeren **Hydrogele** hergestellt. Diese bestehen aus miteinander verknüpften Polymerketten und wenn man sie stark vergrössert betrachtet, kann man eine netzartige Struktur erkennen. Je nach Ausgangsstoffen und Herstellungsmethode sind solche Hydrogele unterschiedlich stabil und haben unterschiedlich grosse Poren. Generell sind sie dadurch charakterisiert, dass sie grosse Mengen an Flüssigkeit aufnehmen und auch wieder abgeben können, weshalb sie gerne als Wundauflagen verwendet werden. Diese dürfen die Wunde nicht noch zusätzlich reizen, sondern sollen gut verträglich und ungiftig sein. Des Weiteren sollte das Material des Wundverbandes nicht mit der Wunde verkleben und ein feuchtes Wundmilieu schaffen, das heilungsfördernd ist.

Ein Polymer, das für solche Wundauflagen geeignet ist, heisst Chitosan. Chitosan ist ein natürliches Material, das unter anderem in der Schale von Krebstieren und den Zellwänden von Pilzen vorkommt. Wir haben Chitosan auf zwei verschiede Arten chemisch verändert. Beim Mischen dieser beiden unterschiedlich modifizierten Polymere bildete sich ein Gel. Wir konnten ein Protein in dieses Gel laden und zeigen, dass es verzögert auch wieder freigesetzt wurde. Dahinter steht die Idee, eine Wundauflage zu schaffen, die alle Substanzen in sich vereint, welche der Körper für die Wundheilung benötigt. Das sind zum Beispiel Stoffe, die die Neubildung von Blutgefässen oder frischen Hautzellen fördern. Insbesondere Patienten mit chronischen Wunden könnten von solchen Verbandsmaterialien profitieren, da ihre körpereigene Wundheilung aus verschiedensten Gründen gestört ist. Ein weiterer Vorteil des Gels, das wir hergestellt haben, ist die Möglichkeit, es gefrierzutrocknen. Gefriertrocknung ist ein Prozess zur schonenden Trocknung von Stoffen, ohne diese erhitzen zu müssen. Typische Beispiele aus dem Alltag sind Instant-Kaffee oder Früchte in Müslimischungen. Gefriergetrocknete Produkte sind wesentlich länger haltbar und einfacher zu transportieren als in ihrer unverarbeiteten Form. Unser gefriergetrocknetes Chitosan-Gel hatte eine watteähnliche Konsistenz und konnte durch den Kontakt mit Flüssigkeit erfolgreich wieder rehydriert (also gelförmig gemacht) werden. Das ist sehr vielversprechend für eine Wundauflage: Das getrocknete Gel könnte zum Beispiel auf eine nässende Wunde aufgelegt und luftdicht befestigt werden. Das Wundsekret würde zu einer Rehydrierung des Gels führen, die im Gel eingeschlossenen Wirkstoffe aus dem Gel könnten an die Wunde abgegeben werden, und die Wunde würde konstant feucht bleiben und könnte dementsprechend gut heilen.

Eine weitere Anwendungsmöglichkeit für Polymere als Wirkstoffträger sind **dünne Filme/Membranen**, die in den Mund genommen werden und sich dort innerhalb kurzer Zeit auflösen. Solche Filme sind maximal briefmarkengross und werden entweder auf die Zunge, unter die Zunge, in die Backentasche oder an den Gaumen geklebt. Dort lösen sie sich schnell auf und geben ihren Wirkstoff frei. Für Patienten sind solche Filme sehr angenehm, da sie nicht geschluckt werden müssen und deshalb einfach einzunehmen sind. Das ist vor allem für Menschen mit Schluckschwierigkeiten, wie Kinder oder ältere Patienten, relevant.

Wir haben einen solchen speziellen Film in einer klinischen Studie getestet. Dieser Film enthält winzige Mengen an Midazolam. Das ist eigentlich ein Schlaf- und Beruhigungsmittel. Es kann aber auch verwendet werden, um zu bestimmen, wie gut ein bestimmter Medikamenten-Abbaumechanismus bei einzelnen Patienten funktioniert. Der hier untersuchte Abbauweg wird durch das sogenannte Enzym CYP3A gesteuert und ist für mehr als 50% der handelsüblichen Medikamente relevant. Deshalb ist er auch anfällig für Wechselwirkungen: Einzelne Medikamente oder auch andere Substanzen (z.B. Grapefruitsaft) können ihn nämlich hemmen oder verstärken, so dass parallel verabreichte Medikamente viel langsamer oder schneller abgebaut werden als man das erwarten würde. Vernachlässigt man das bei der Verabreichung von Arzneimitteln, kann es für den Patienten zu gefährlichen Unter- oder Überdosierungen kommen. Eine Überprüfung dieser Enzymaktivität nennt man Phänotypisierung. Allerdings möchte man natürlich die Patienten bei einer Phänotypisierung mit Midazolam nicht jedes Mal sedieren (aufgrund der beruhigenden Eigenschaften von Midazolam), sondern nur ganz geringe Mengen davon verwenden. Je geringer jedoch eine verabreichte Menge, desto schwieriger ist es, diese genau herzustellen und zu verabreichen. Bisher geht das nur, wenn man die Midazolam-Lösung stark verdünnt. Einfacher und reproduzierbarer wäre eine fertige Formulierung, die eine solche winzige Dosis Midazolam bereits enthält und direkt verwendet werden kann. Wir konnten klinisch zeigen, dass ein Film aus Polymeren geeignet ist, winzige Mengen an Midazolam zu transportieren und Aussagen über die Enzymaktivität von CYP3A zu treffen. Insbesondere für die Phänotypisierung von Kindern und älteren Patienten wäre das sehr interessant, da die Probe weder geschluckt werden muss noch ausgespuckt werden kann. Die daraus resultierende Vereinfachung der Phänotypisierung stellt einen wichtigen Meilenstein auf dem Weg zu einem modernen, individualisierten und patientenzentrierten Behandlungsansatz dar. Allerdings sind natürlich noch viele weitere Untersuchungen nötig.

Eine Alternative für kinderfreundliche Arzneimittelformulierungen sind **Tabletten**, die bei Speichelkontakt schnell im Mund zerfallen. Wie bei den oben beschriebenen Filmen kann man auch

mit solchen Tabletten gut dosieren und trotzdem vermeiden, dass grosse Tabletten oder Kapseln geschluckt werden müssen. Leider gibt es bis heute nur sehr wenige solcher Formulierungen auf dem Markt – und noch weniger davon sind für Kinder zugelassen. Hier besteht also dringend Nachholbedarf. Allerdings muss man bei der Entwicklung von kinderfreundlichen Medikamenten darauf achten, wie Kinder deren Geschmack empfinden. Oft verweigern sie nämlich die Einnahme schlecht-schmeckender Arzneimittel. Das wiederum führt dann zu Therapieabbrüchen und unwirksamen Therapien.

Wir haben daher eine neu entwickelte, schnell-zerfallende Placebo-Tablette (also eine Tablette ohne aktiven Wirkstoff) an Kindern getestet. Von Erwachsenen war diese bereits als sehr positiv beurteilt worden. Man kann jedoch nicht direkt von Erwachsenen auf Kinder schliessen, da deren Mundgefühl und Geschmackssensoren sehr unterschiedlich sind. Darum wurden Kinder zwischen 2 und 10 Jahren gebeten, die Tabletten zu probieren. Wir haben dann einerseits beobachtet, wie die Kinder auf die Tabletten reagiert haben (z.B. ob sie weinen mussten oder sie direkt wieder ausspuckten) und wie die Eltern die Verabreichung bewerten (v.a. im Vergleich zu anderen Medikamenten, die sie bereits kennen). Bei den älteren Kindern haben wir ausserdem untersucht, wie schnell die Tablette im Mund zerfällt und wo danach Rückstände zu finden sind. Diese Kinder sollten auch bewerten, wie gut ihnen die Tablette geschmeckt hat, und ob sie noch eine zweite Tablette nehmen würden. Zusammenfassend kann gesagt werden, dass sowohl Kinder wie auch Eltern diese Tablette sehr gut akzeptierten und sehr positiv darauf reagierten. Auch Kinder, die sonst keine Tabletten, Kapseln oder flüssigen Arzneimittel schlucken wollen/können, fanden unsere Testtablette sehr lecker. Diese Art der Formulierung eröffnet also vielversprechende Möglichkeiten: Solche schnell zerfallenden Tabletten könnten als Transportsysteme für viele verschiedene Wirkstoffe dienen, die bisher nicht in kindgerechter oder nur in schlecht schmeckender flüssiger Form verfügbar sind.

Zusammenfassend haben wir also verschiedenste innovative, grösstenteils polymerbasierte Applikationsformen für arzneiliche Wirkstoffe präklinisch und klinisch evaluiert und wichtige Erkenntnisse dazu gewonnen, wie die Wirkstoffverfügbarkeit weiter optimiert werden kann.

SUMMARY

Currently, many promising therapeutic compounds suffer from substantial drawbacks such as rapid clearance from circulation, poor bioavailability, or severe toxicity in patients. One option to face these challenges might be the usage of nanoparticles as drug delivery systems. There are different classes of formulations, so called nanomedicines, including drug-protein conjugates, drug-polymer conjugates, liposomes, micelles, and polymersomes. In general, main therapeutic fields for engineered nanomaterials are oncology, cardiovascular medicine, neurology, anti-inflammatory drugs, and anti-infectious treatment.

Herein (chapter 2.1), **polymersomes prepared of the diblock copolymer PDMS-*b*-PMOXA** are described. These were synthesised and modified to achieve targeting to the asialoglycoprotein receptor of hepatocytes. Conjugation of asialofetuin to the polymersomes' surface increased uptake of these polymersomes into hepatocytes, when compared to unmodified polymersomes. Moreover, a model compound was successfully encapsulated into the polymersomes and sustained release was achieved. Biocompatibility of the various polymersomes was assessed *in vitro*, and zebrafish embryos were utilised as a first vertebrate model to evaluate *in vivo* toxicity. In conclusion, the targeted drug delivery system was safe and well tolerated *in vitro* as well as *in vivo*. Successful drug encapsulation and release make it a promising tool for clinical applications in the field of hepatology. Further comprehensive investigations, especially regarding scalability of production process and *in vivo* characterisation would be needed before stepping forward to the clinics.

In addition to nanoparticles, polymers can also be used to synthesise hydrogels. Hydrogels are crosslinked networks formed by a hydrophilic macromolecular polymer. Their mesh like structure and physicochemical properties allow hydrogels to imbibe large amounts of water and to be used as drug delivery systems. Therefore, hydrogels are of special interest in the fields of drug delivery, biosensing, and tissue engineering.

In this work (chapter 2.2), a **self-assembling chitosan hydrogel** based on chemically modified chitosan (a natural polymer) was prepared. Chitosan is known to be biocompatible, biodegradable, bio-renewable, and non-toxic. In addition, it is tissue-regenerating, haemostatic, and immune-stimulating, making it a very promising hydrogel scaffold for wound dressing. The obtained self-assembling chitosan hydrogel had a porous structure enabling loading it with proteins and releasing them in a sustained manner. Moreover, the hydrogel was biodegradable and could be lyophilised. These characteristics make it a promising scaffold for application of therapeutic proteins in the treatment of

chronic wounds. It remains to be elucidated how this chitosan hydrogel loaded with therapeutic proteins would behave *in vitro* as well as *in vivo* before clinical applications could be considered.

Another application for polymers are buccal films (BFs). BFs can be loaded with drugs and enable oral absorption of these drugs upon placing the BFs into the oral cavity, either sublingual, buccal, or palatal. Besides fast onset of action and reduced first pass metabolism, BFs are easy to be administered, even to vulnerable patient populations such as geriatric or paediatric patients who have difficulties with swallowing liquid or solid oral dosage formulations. This makes BFs – amongst other potential applications – highly valuable for phenotyping purposes, especially for these patient groups. Phenotyping is particularly important for drugs with a narrow therapeutic window that need to be carefully dosed, based on the patient's individual metabolic capacity. One main metabolising enzyme is cytochrome P450 3A (CYP3A). It is assumed that CYP3A is involved in the metabolism of more than 50% of the marketed drugs. Consequently, such an essential metabolism pathway will be frequently affected by various drug-drug interactions including either inhibition of CYP3A enzymes or increase of CYP3A expression. Enzyme activity can vary up to 400-fold and thus, plasma concentrations of co-administered drugs can change tremendously resulting in either reduced drug activity or toxic side effects. To phenotype CYP3A, the benzodiazepine midazolam is a well-accepted probe drug, but suffering from the drawback that patients are sedated during phenotyping with pharmacologically active midazolam doses. Therefore, a microdosing approach for phenotyping was recently developed. One elegant option to formulate and administer microdoses are BFs.

Herein (chapter 2.3), a clinical study investigating the usability of a **microdosed midazolam BF** for phenotyping is described. According to the outcomes, such a film can be considered an interesting novel diagnostic tool in the field of personalised medicine. Before making its step into clinical daily practice, it remains to be evaluated how the microdosed midazolam BF reflects increased or inhibited CP3A activity. Moreover, it would be necessary to test the film again in a greater variety of volunteers (e.g. different age or weight) to be able to generalise the results obtained from the former study.

As mentioned above, paediatric patients are a vulnerable population with the need for oral formulations that are easy and safe to administer. A medication's taste and the ability of children to swallow their medicine may greatly influence the selection of a drug, therefore therapy and prescribing practice. The medication palatability is essential for patient acceptance, therapeutic compliance and

successful outcome of a therapy. Not only BFs but also oral disintegrating tablets (ODTs) offer great options for this purpose.

To test the palatability of a **placebo ODT based on Functionalised Calcium Carbonate**, a clinical study with 40 children from 2 to 10 years was conducted, in a setup that considered the specific communication challenges with this target group – obviously children cannot be expected to give quantified feedback on likeability, taste, etc. (chapter 2.4). The tablet was highly accepted by children as well as by their parents. Such palatable, inert carrier ODTs could be formulated to contain a wide range of active pharmaceutical ingredients for oral delivery that are currently unavailable as child friendly formulations or exist only as bad tasting liquids. This includes frequently used and highly relevant drugs, such as antibiotics and steroids. Therefore, the tested ODT or similar child-appropriate solid oral dosage forms could improve world-wide access to high quality medicines and adherence for children in future.

In summary, a broad variety of innovative, mostly polymer-based application forms for drug ingredients have been preclinically and clinically evaluated and led to relevant insights on how drug availability could be further optimised.

ACKNOWLEDGEMENT

AIM OF THE THESIS

At first, the **synthetic diblock copolymer PDMS-*b*-PMOXA** was used to synthesise **polymersomes**. This included:

- Characterisation of their physicochemical properties: size, surface charge, stability in serum, loading capacity and release characteristics, and *in vitro* and early *in vivo* biocompatibility.
- Chemical surface modification with asialofetuin to target the asialoglycoprotein receptor of hepatocytes: assessment of targeting ability and clarification of uptake mechanism.
- Testing the circulation behaviour in zebrafish embryos: Does PMOXA add stealth properties?

At second, the **natural polymer chitosan** was used to formulate a **self-assembling hydrogel**. This involved:

- Chemical modification of chitosan to achieve maleimide and sulfhydryl coupling, respectively: prove successful modification.
- Showing gelation via Michael addition upon mixing aqueous solutions of the modified polymers: Microscopical evaluation of the gel's structure, assessment of swelling and degradation behaviour, loading and release of protein from the gel, lyophilisation of the gel to improve storage capability, comparison of chitosan gel to marketed hydrogel products.

At third, a polymer based **buccal film (BF) loaded with microdoses of midazolam** was tested in a **phenotyping study**. Necessary steps were:

- Preparation of buccal midazolam control solution and buccal application of both formulations to volunteers.
- Data analysis and evaluation if BF could be used for CYP3A phenotyping: AUC, C_{max}, t_{max}, $t_{1/2}$, CL/F of midazolam and 1'-OH-midazolam, respectively, and metabolic ratios of these.

At fourth, a **paediatric palatability study** with an **oral disintegrating tablet (ODT) based on Functionalised Calcium Carbonate** was conducted. This included:

- Study information and informed consent procedure with parents and their children.
- Palatability assessment and evaluation of ODT acceptance by children as well as their parents: child-appropriate questionnaire, ODT-acceptability questionnaire for parents, facial hedonic scale for taste assessment, disintegration time of ODT.

ABBREVIATIONS

ADME	absorption, distribution, metabolism, and excretion
ASGPR	asialoglycoprotein receptor
BF	buccal film
CNS	central nervous system
CYP450	cytochrome P450
CYP3A	cytochrome P450 3A
EGF	epidermal growth factor
EPR effect	enhanced permeability and retention effect
FCC	Functionalised Calcium Carbonate
FHS	facial hedonic scale
GIT	gastrointestinal tract
HPC	hydroxypropylcellulose
HPMC	hydroxypropylmethylcellulose
EMA	European Medicines Agency
MCC	microcrystalline cellulose
MPS	mononuclear phagocytic system
NCL	Nanotechnology Characterization Lab
ODT	oral disintegrating tablet
PDMS	poly(dimethylsiloxan)
PEG	polyethylene glycol
PIP	Paediatric Investigation Plan
PLGA	poly(lactide-co-glycolide)
PMOXA	poly(2-methyloxazoline)
rhEGF	recombinant human epidermal growth factor
rhVEGF	recombinant human vascular endothelial growth factor
STEP	Safety and Toxicity of Excipients for Paediatrics
TPP	sodium triphosphate
VEGF	vascular endothelial growth factor
1'-OH-midazolam	1'-hydroxymidazolam

1 INTRODUCTION

In this thesis, the focus is on development of different drug delivery systems – mainly based on polymers. At first, polymersomes, which were targeted towards hepatocytes, are described (chapters 1.1, 2.1, and 3.1). A self-assembling chitosan hydrogel for wound healing forms the second pillar of this thesis (chapters 1.2, 2.2, and 3.2). The third sub-chapter is about a polymeric buccal film for phenotyping that was tested in a pharmacokinetic clinical study (chapters 1.3, 2.3,and 3.3). The chapters 1.4, 2.4, and 3.4 refer to a study in children, assessing the palatability of an oral disintegrating tablet.

1.1 TARGETED NANOPARTICLES FOR HEPATIC DRUG DELIVERY

1.1.1 NANOMEDICINES FOR DRUG DELIVERY

Many promising therapeutic compounds suffer from disadvantages such as low bioavailability, rapid clearance, and high systemic toxicity. To tackle these hurdles, nanoparticles as drug delivery systems gained increasing interest within the last decades. So called nanomedicines – including different classes of formulations such as drug-protein conjugates, drug-polymer conjugates, liposomes, micelles, and polymersomes – definitely have a great potential [1, 2]. The European Commission defines engineered nanomaterials as "any intentionally manufactured material, containing particles, in an unbound state or as an aggregate or as an agglomerate and where, for 50% or more of the particles in the number size distribution, one or more external dimensions is in the size range 1 nm to 100 nm" [3]. Moreover, engineered nanomaterials are "designed for a specific purpose or function" [3]. Common characteristics are their small size, high surface to volume ratio, and adjustable physicochemical properties. In the next sections, some nanomaterials, which can be used for drug delivery purposes, are highlighted (Figure 1).
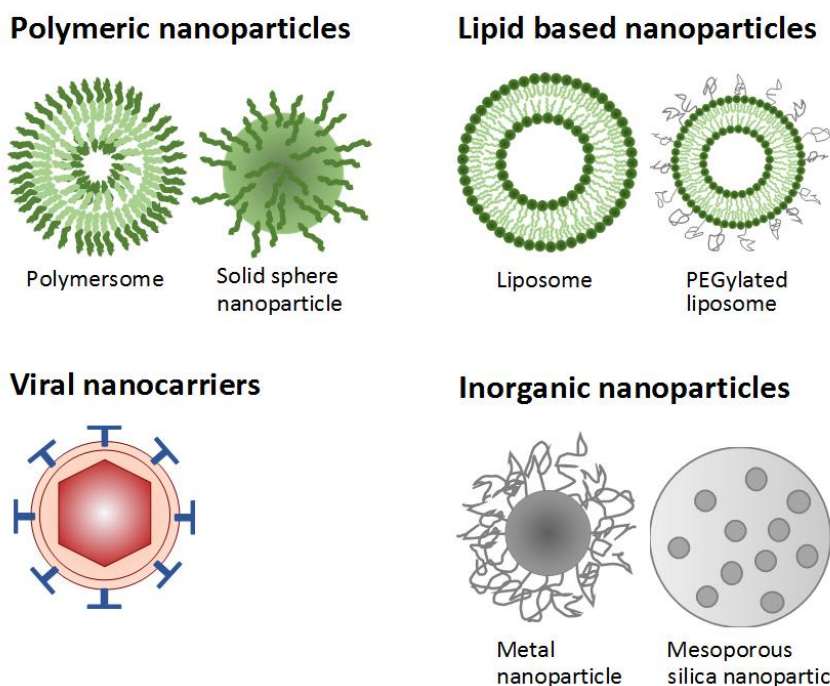
Figure 1. Schematic illustration of a selection of established nanocarriers platforms.

(I) Inorganic nanoparticles include gold particles, silica and magnetic nanocarriers, quantum dots, or graphene nanoparticles [4]. Usually, these are easy to synthesise and modify, in addition to good biocompatibility and favourable physicochemical properties. Such characteristics make inorganic nanomaterials well suited for targeted drug delivery, cancer therapies, bio-imaging, or theragnostic applications – a combination of diagnosis and treatment of a disease [4, 5].

(II) For gene delivery, **viral nanoparticles** were developed. Using genetically modified, recombinant viral vectors, therapeutic nucleic acids such as RNA or DNA could be delivered into target cells. These viral nanoparticles could avoid recognition by the host immune system [6]. Common vectors are retroviruses, adenoviruses, adeno-associated viruses, and herpes viruses [7].

(III) The most popular type of nanoparticles might be **lipid based nanoparticles.** These were the first class of nanomedicines, which was developed [8]. Lipid based nanoparticles are sub-divided depending on their morphology: e.g. liposomes, micelles, nanostructured lipid carriers, solid lipid nanoparticles, or lipid polymer hybrid nanoparticles [9, 10]. On one hand, natural occurring lipids such as phosphatidylcholine or phosphatidylinositol can be used as building blocks for lipid based nanocarriers. On the other hand, artificial synthetic lipids, often synthesised from glycerophosphocholine using acylation and enzyme catalysed reactions, build the ground for lipid nanoformulations. Common fields of application are gene delivery or drug delivery with triggered drug release [11, 12].

(IV) It is also possible to use polymers to prepare nanoparticles. **Natural polymers** such as polysaccharides (e.g. chitosan and cyclodextrins) or proteins (e.g. gelatine) are a well-accepted starting material for drug delivery systems [13–16]. High biocompatibility and biodegradability, low production costs, and structural flexibility are main advantages of biopolymers [16].

(V) In contrast to their natural counterparts, **synthetic polymers** are characterised by low batch-to-batch variability. As natural polymers, synthetic ones are biocompatible and biodegradable. Moreover, they show a highly versatile chemistry. This makes them popular for pharmaceutical applications, for example as solid-sphere nanoparticles, polymeric micelles, polymersomes, polymer-drug conjugates, dendrimers, or polyplexes [17]. Common synthetic polymers are poly(lactic acid), poly(lactide-co-glycolide) (PLGA), poly(ε-caprolactone), poly(dimethylsiloxan) (PDMS), poly(2-methyloxazoline) (PMOXA), or their copolymers [18–20]. Polymeric vesicles, called polymersomes, are formed by self-assembly of amphiphilic block-copolymers. Comparable to liposomes, polymersomes have an aqueous core in which hydrophilic compounds can be encapsulated. Hydrophobic or amphiphilic molecules can be integrated into the hydrophobic surrounding membrane. In comparison to lipid based vesicles, usually polymersomes have a thicker membrane [21], resulting in improved membrane stability concurrent with lower permeability. Depending on the chemical composition and modification, biological and physicochemical characteristics of polymersomes are highly tuneable [22–24]. By selecting the appropriate chemical composition of each polymer-block, the desired properties of polymersomes (e.g. improved drug encapsulation, biocompatibility, long circulation in blood stream, or stimuli-responsiveness) can be achieved. This results in a broad range of block-copolymers and therefore a huge variety of polymersomes. In addition, it is possible to chemically modify the surface of polymersomes and to link targeting moieties onto it. This provides additional chemical versatility. Several polymeric formulations consisting of the block copolymer PDMS-*b*-PMOXA have been reported recently. Biocompatibility of the individual polymer blocks as well as low cytotoxicity in various *in vitro* models are important advantages of PDMS and PMOXA copolymers [25–28]. Moreover, PMOXA-decorated liposomes displayed increased circulation times in blood [29] reminding of polyethylene glycol (PEG)-shielded nanocarriers [30]. It was suggested that PMOXA could serve as a potential PEG-substitute to shield nanoparticles from protein adsorption by adding stealth properties to their surface. In accordance with these findings, polymeric nanoreactors made of tri-block PMOXA-*b*-PDMS-*b*-PMOXA did neither induce a macrophage-mediated inflammatory response *in vitro* nor *in vivo* [31]. In chapter 2.1 of this thesis, polymersomes prepared of PDMS-*b*-PMOXA diblock copolymers are described.

Overall, main therapeutic areas for engineered nanomaterials are oncology [32], cardiovascular medicine [33, 34], neurology [35], anti-inflammatory drugs [34, 36], and anti-infectious treatment [37, 38].

1.1.2 Liver and liver diseases

In the field of anti-infectious treatments, one big topic are liver diseases such as hepatocellular carcinoma, viral hepatitis, or genetic and metabolic disorders. Liver diseases are already one of the leading causes of death. Unfortunately, incidence rates are still increasing [39]. The liver is the largest internal human organ (weighing approximately 1.5 kg in an adult). It is responsible for about 500 different functions in the human body. Its key-functions are metabolism and clearance of endo- and exogenous substances. Moreover, the liver stores proteins, fats, vitamins, or iron, and produces proteins such as clotting factors. Other important liver functions are cholesterol homeostasis and immune responses (the liver is one major player of the mononuclear phagocyte system, MPS) [40–44]. The liver (Figure 2) is built of hexagonal formed liver lobules, being the functional units [45]. Each liver lobule is supplied with oxygen and nutrients by peripheral blood flow from the hepatic artery and the portal vein through liver capillaries (i.e. sinusoids) to the central vein [46, 47]. Non-parenchymal liver cells such as sinusoidal endothelial cells, hepatic macrophages (Kupffer cells), stellate cells (Ito cells), and parenchymal cells (i.e. hepatocytes) form the liver lobules [48, 49]. Latter account for about 80% of the cytoplasmic liver mass. Hepatocytes are involved in many essential liver functions, for example metabolism of xenobiotics, protein synthesis and storage, transformation of carbohydrates, and bile and urea formation and secretion [50, 51]. Moreover, hepatocytes are considered as main pro-pathogenic cell type for many disorders including liver cancer [52], viral or parasitic liver infections [53], and genetic diseases with and without parenchymal damage (examples given in [54–58]). Therefore, hepatocytes represent a very relevant target for various therapy approaches.

The physiological function of the liver often hampers pharmacotherapies. On one hand, the liver is well known for its high drug uptake. On the other hand, rapid drug elimination – based on P-glycoprotein mediated efflux and non-specific drug uptake by Kupffer cells – hinder the treatment of liver diseases [59]. According to this, conventional therapeutic approaches with small molecules as well as novel therapeutic compounds (e.g. nucleic acids, proteins, or peptides) often show only low bioavailability and rapid clearance from the circulation. Therefore, increased drug doses are required resulting in dose-limiting side effects. Altogether, the development of alternative strategies to achieve efficient and specific drug delivery to hepatocytes is highly desirable [59, 60].
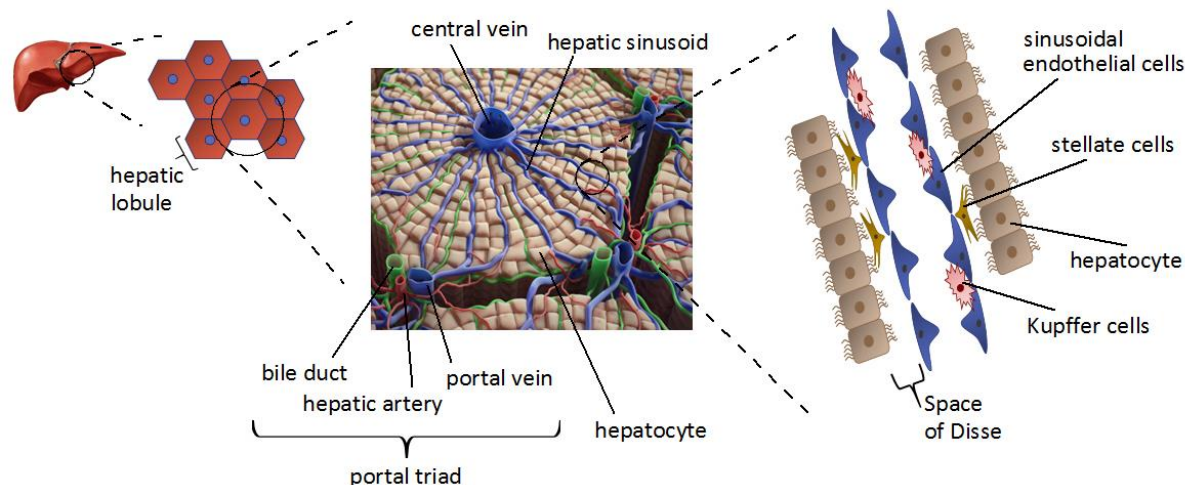
Figure 2. Schematic structure of the liver. The hepatic lobules are the functional units of the liver. Via portal vein and hepatic artery each lobule receives blood from the periphery. Bile is transported from the liver to the gastrointestinal tract through the bile duct. The hepatic arteries terminate in the hepatic sinusoids lined by sinusoidal endothelial cells. Kupffer cells are spread in the sinusoids' lumen. In the perisinusoidal Space of Disse stellate cells are located. The parenchyma is formed by hepatocytes. Figures were adapted from [61, 62].

1.1.3 ACTIVE TARGETING OF HEPATOCYTES

The common method to achieve nanoparticle accumulation in tumour tissue makes use of the enhanced permeability and retention (EPR) effect. Passage of nanoparticles through leakier vessels in tumour tissue and accumulation there over time is called passive targeting [63]. Additional targeting moieties on the surface of nanocarriers are promising, since they could further increase penetration of nanoparticles into solid tumours [64]. Such an approach would also help to decrease off-target exposure and reduce toxic side effects. Therefore, especially targeted nanomedicines allow to reduce the administered dose and to increase the efficiency of a therapy [65]. In the following section, four key characteristics, which nanomedicines should present to achieve successful hepatocyte drug delivery, are described [66].

(I) Pharmacokinetic properties of nanoparticles mainly depend on their building material, size, surface charge, and surface modification [67]. Nanoparticles should be smaller than 150 nm to pass the fenestration of liver sinusoids and to arrive at the hepatocytes. Moreover, with this size they are thought to be small enough not to be recognised by hepatic macrophages (i.e. Kupffer cells) [68]. The larger the nanoparticles the more rapidly they are cleared from circulation [69]. Also surface charge of nanoparticles determines their pharmacokinetic profile: Strongly positively charged nanoparticles easily interact with negatively charged cell surfaces, resulting in quick sequestration of these nanoformulations in the lung [70]. On the other hand, highly negative charge of nanoparticles triggers phagocytic clearance [71]. Ideally, nanoparticles that are meant to reach hepatocytes should have a

slightly negative surface potential (i.e. 0 to -10 mV) [72]. This could for example be achieved by PEGylation of nanoparticles. Formation of a bio-corona from serum proteins around such nanoparticles could be prevented – or at least reduced – and their unspecific uptake through phagocytosis is decreased [69, 73]. With such an approach the circulation half-life is increased, enhancing the chance of successful drug delivery to the target cell.

(II) In order to efficiently deliver a nanoparticulate formulation to hepatocytes, **active targeting** plays a crucial role. To be considered as ideal, a target receptor should (i) be abundantly expressed on the cell surface to enhance the binding probability and accessibility. (ii) Moreover, a target receptor should be exclusively or at least predominantly expressed on the target cell type to achieve selectivity. (iii) In addition, target receptors should be efficiently internalised to enable uptake of the nanoparticles into the cell [74, 75]. Ideally, the target receptor is internalised upon receptor binding. Receptor mediated endocytosis results in endosome-fusion with the lysosome membrane and a pH drop down to pH ≤ 6.0 [76]. Upon this pH-shift, the receptors are recycled, and the internalised nanoparticles can escape the endosome. Liver cells are very interesting in terms of targeting as they express many different receptors [77]. Main receptors on hepatocytes are glycoprotein receptors (e.g. asialoglycoprotein receptor, ASGPR) and mannose receptors [78]. Carbohydrate receptors such as the ASGPR are responsible for the uptake of glycoproteins, proteins, and cellular particles – for example heparin and apoptotic cells [79, 80]. The ASGPR is abundantly expressed on the surface of hepatocytes but only minimally on extra-hepatic cells [66]. Therefore, ASGPRs are the most important targets to reach the hepatocytes [81].

Liver diseases may result in pathological tissue alterations. These might have a big influence on the targeting strategy by changing the accessibility or expression of the target receptor [66]. Therefore, the success rate of targeted nanomedicines might be improved by combining diagnostic strategies (e.g. to assess targeting ability) with therapeutic approaches.

(III) The third important factor for effective development of targeted nanoparticles to hepatocytes is the **targeting ligand**. It is crucial to keep two things in mind: (i) Efficient and specific binding of the ligand to its receptor and (ii) optimisation of the ligand density on the nanoparticles' surface to balance too low targeting ability (not enough ligand molecules) and increased opsonisation due to too high ligand density [82]. Possible ligands for the aforementioned ASGPR are glycoproteins (e.g. asialofetuin, galactose, lactose, *N*-acetylglucosamine, or pullulan) or some viruses (e.g. hepatitis B or C virus) [83, 84].

(IV) As a fourth factor, the availability of suitable *in vitro* **and** *in vivo* **models** must be taken into consideration. During development of a targeted drug delivery system to hepatocytes it is necessary to preclinically test the resulting formulation with suitable *in vitro* and *in vivo* models.

1.1.4 ASGPR-SPECIFIC TARGETING OF PDMS-*B*-PMOXA POLYMERSOMES

As outlined in section 1.1.3, the ASGPR is well suited for hepatocyte-specific drug delivery. It is a calcium-dependent lectin receptor that specifically binds carbohydrates with terminal galactose or *N*-acetylglucosamine residues [85]. Its physiological function is the clearance of desialylated glycoproteins from circulation. Binding of a ligand triggers ASGP receptor internalisation via the clathrin-dependent pathway [86]. It is highly advantageous that the ASGPR is species independent. The human as well as the rodent ASGPR recognise the same carbohydrate patterns [87]. This makes the ASGPR a very interesting receptor for drug development, since *in vitro* experiments can be directly compared to first preclinical *in vivo* experiments.

To target the ASGPR, different asialofetuin-modified nanomaterials have already been used, such as polymer-lipid hybrid nanoparticles [88] and liposomes [89]. As described in section 1.1.1, polymeric nanocarriers are an interesting alternative to lipid based formulations [90]. Successful cellular targeting was recently achieved by modifying the surface of PDMS-*b*-PMOXA polymersomes with antibodies or peptides. The ligand-functionalised polymersomes were bound specifically to their target cells, followed by rapid cellular uptake [26, 28, 91]. This suggests that polymersomes made of PDMS-*b*-PMOXA are a promising biocompatible and versatile platform to design novel specific drug targeting systems. In chapter 2.1 a variety of polymersomes based on PDMS-*b*-PMOXA and modified with the targeting ligand asialofetuin are presented in detail. The focus was on formulation and surface modification of PDMS-*b*-PMOXA polymersomes for targeted drug delivery to hepatocytes. Potential toxicity of the resulting polymersomes was assessed *in vitro* using the human hepatocarcinoma derived HepG2 cell line. In addition, zebrafish embryos were utilised as a first vertebrate model to assess *in vivo* toxicity [92, 93].

Introduction – Targeted nanoparticles for hepatic drug delivery

1.2 CHITOSAN HYDROGEL TO TREAT CHRONIC WOUNDS

1.2.1 HYDROGELS FOR DRUG DELIVERY

Polymeric materials are not only used to formulate nanoparticles for systemic drug delivery as described in section 1.1. It is also possible to formulate mesh-like delivery systems for local drug delivery. Such delivery devices are made to release their cargo upon swelling and erosion as soon as they come in contact with water or body fluids, respectively, resulting in local drug release. It is obvious that such a drug delivery system has to consist of a non-toxic, biodegradable, and biocompatible matrix [94]. Talking about swellable systems, hydrogels are one option. Already in the 1960s, hydrogel research was founded by Wichterle and Lím. They synthesised hydrogels based on the copolymerisation of hydroxyl methacrylate and ethylene glycol dimethacrylate [95]. Hydrogels are crosslinked networks formed by a hydrophilic macromolecular polymer. Their polymeric backbone contains many hydrophilic moieties (e.g. hydroxyl, carboxylic, sulphate, or amine groups) and allows hydrogels to imbibe large amounts of water [96]. Their physical properties such as swelling, permeation, mechanical strength, and surface characteristics can be changed by structural modification [97]. Especially the fields of drug delivery, biosensing, and tissue engineering profit from hydrogel based drug delivery systems [98, 99]. Hydrogels are classified as physical or chemical hydrogels depending on the type of bonds that are formed during their fabrication process.

Physical hydrogels, also called reversible hydrogels, are formed by noncovalent binding strategies such as electrostatic interactions, hydrogen bonding, or hydrophobic forces. The main advantage of physical hydrogels is based on their non-covalent formation: no potentially toxic covalent linker molecules are required. But this is again also a drawback, since reversible hydrogels may lack mechanical strength and dissolve in an uncontrolled manner [98, 100].

In contrast, **chemical hydrogels** are stabilised and held together by covalent bonds wherefore they are termed permanent hydrogels. They are formed by irradiation chemistry, secondary polymerisation, or by using small crosslinker molecules resulting in irreversibly crosslinked polymer chains. Therefore, they show a stable network structure allowing absorption of water and diffusion-mediated drug release. However, the methods applied to form such permanent hydrogels might be less biocompatible than the ones leading to physically crosslinked hydrogels [100].

By using **pre-functionalised polymer chains** with reactive functional groups, a covalently crosslinked hydrogel can be prepared without need for any additional crosslinker molecule [101, 102]. For example, disulfide-bond formation between the single polymer chains [103], Schiff bases

reactions [104], or Michael addition [105, 106] result in such stable hydrogels. These combine the advantages of physically and chemically crosslinked gels.

Up to now, polymeric hydrogels were used for a broad variety of applications. In this section a few are shortly described: To fight the increasing antibiotic resistance in pathogenic microbes, locally applied antibiotics may offer an opportunity. For such **local antibiotic drug delivery**, hydrogels are a very interesting solution due to their high hydrophilicity, unique three-dimensional network structures, biocompatibility, cell adhesive properties, and even inherent antimicrobial activity [107]. The combination of antibacterial agents with nanomaterials such as hydrogels could help to lower the doses compared to systemically administered antibiotics. This is expected to alleviate the problems of resistance and undesired side effects to some extent. It is also possible to use polymeric hydrogels for **ocular drug delivery**. Such formulations are characterised by a prolonged drug release [108]. Additionally to ocular drug delivery, also **nasal drug delivery** is a field of hydrogel research [109]. The mucoadhesive properties of hydrogels result in prolonged residence time on the nasal mucosa increasing the contact time and therefore mucosal drug absorption. But not only topical application of hydrogels is an option. Also **injectable hydrogels** can be designed to deliver bio-therapeutic molecules [96, 110, 111]. These could serve as drug or gene delivery system or form a cell-growing depot in the body upon a single injection of an *in situ* forming hydrogel. For example, local intratumoural delivery of chemotherapeutics by injection of hydrogel drug depots is a very promising idea [112]. Other fascinating fields for hydrogel application are **tissue engineering** and **regenerative medicine** [113]. Mimicking key characteristics of natural tissue, i.e. retention of large amounts of water, effective mass transfer, and ability to form different shapes, makes hydrogels very interesting for these applications. Amongst others, one special focus is on hydrogels as bioactive materials to encapsulate stem cells [114]. Hydrogels could successfully mimic the three-dimensional shape of extracellular matrix, providing a friendly growth environment for stem cells.

1.2.2 CHITOSAN: ONE POSSIBLE NATURAL POLYMER TO FORMULATE HYDROGELS

Several different polymers can be chosen to create hydrogels. Comparable to the preparation of polymeric nanoparticles (chapter 1.1.1), synthetic and natural polymers are used, offering different advantages and disadvantages. **Natural polymers** originate from plants, algae, animals, or different microbial populations, which makes them comparatively inexpensive [96]. Advantages of natural polymers are biocompatibility, lack of toxicity, and good interaction with the surrounding tissue [96]. **Synthetic polymers** offer even broader opportunities to modify their mechanical and degradation properties. Therefore, **hybrid systems** out of natural and synthetic polymers have already been

designed [96]. Well known examples for synthetic polymers are poly(acrylamide), acrylic acid, PEG, pyrrolidone, or derivatives of them [107]. Polymers from natural sources include polysaccharides (e.g. hyaluronic acid, cyclodextrin, alginate, carboxymethyl cellulose, and chitosan) and protein based polymers (e.g. gelatine, fibrin, and collagen) [96]. In the following section, the natural polymer chitosan (Figure 3 B) is described in more detail. It is the most important derivative of chitin (Figure 3 A), which itself can be found in the exoskeleton of insects and marine invertebrates, in some microorganisms, and in the cell walls of fungi [115].
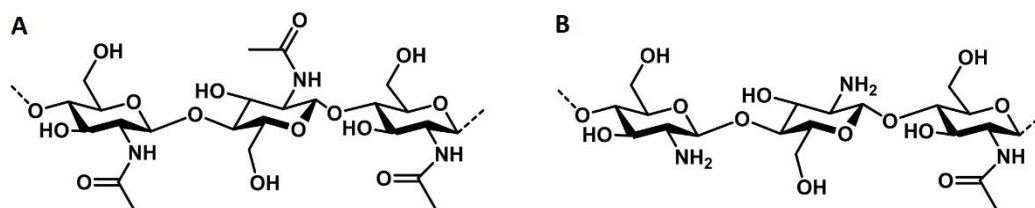
Figure 3. Chemical structure of A) chitin and B) chitosan.

Chitosan is partially de-*N*-acetylated chitin and consists of glucosamine and *N*-acetylglucosamine copolymers. Removing acetyl moieties from chitin (either by amide hydrolysis under alkaline conditions or by enzymatic hydrolysis) leads to chitosan [116]. It is preferred over its parent substance for biomedical applications due to its better solubility in water and organic solvents [117]. Chitosan combines biocompatible, biodegradable, bio-renewable, and non-toxic properties. Moreover, it is highly mucoadhesive and able to transiently open tight junctions [118]. Chitosan shows tissue regenerative effects [119], is fungi-static [120], haemostatic [121], hypocholesterolemic [122], tumour-suppressive [123], as well as immune-stimulating [124]. In addition to these many great properties, chitosan offers a huge potential for chemical and mechanical modifications to create new properties and functions. These make it a very promising scaffold for hydrogels.

De-*N*-acetylation of chitin results in free amino moieties in the chitosan backbone. Therefore, chitosan becomes soluble under acidic conditions due to protonation of the amino residues. Additionally, the viscosity and molecular weight of chitosan can be controlled by pH changes [115]. The relative proportion of glucosamine to *N*-acetylglucosamine determines many properties of the hetero-polymer such as solubility and acid-base behaviour [125]. In addition to the amino group, chitosan possesses two hydroxyl moieties on each glucoside residue. These can be easily modified in order to adjust biological, chemical, and physical properties [115]. As mentioned above, one main advantage of chitosan is its biodegradability. In a physiological environment harmless degradation products are formed by chitinase, chitosanase, or lysozyme [126]. These break the glycosidic bonds of the polysaccharide backbone, resulting in oligosaccharides of different length [127].

Chitosan is not only used in biomedicine [102, 127] but also in food industry [128–130], cosmetics [131, 132], or for water treatment [133, 134].

1.2.3 MODIFICATIONS OF CHITOSAN

In order to even broaden the spectrum of potential applications – especially for pharmaceutical purposes – the modification of polymers has gained huge attention [115]. The basis for many chitosan modifications is laid by the amino and hydroxyl moieties [135]. These can be used for several interactions with other polymers or biological molecules. The most common techniques to modify polymers, are blending and chemical functionalisation, including graft co-polymerisation [115].

Physical modification is achieved by **blending**. It results in physical mixtures (homogenous or more-phase structures) of at least two polymers. Compared to the former single polymers, blended polymers offer new physical properties [136] such as improved mechanical, chemical, structural, biological, or morphological characteristics. Advantages of blending are the short time required [137] and the huge variety of properties that can be tailored to certain applications [115]. Chitosan was for example blended with other hydrophilic polymers, i.e. poly(vinyl alcohol), poly(ethyl oxide), or poly(vinyl pyrrolidone) [138]. Among others, these blends were investigated as oral drug delivery systems [138], as well as to improve mechanical properties of medical products, and to achieve controlled drug delivery [115].

Functionalisation means chemical modification of the polymeric surface to improve certain properties such as adhesion or biocompatibility and to modify physico-chemical properties (e.g. electrostatic charging or permeation of polymeric surfaces). For example, carboxylic acid and hydroxyl moieties increase on one hand hydrogen bonding and on the other hand they enable further chemical covalent modifications [139]. Chitosan was modified by several methods, for example thiolation (as described in chapter 2.2), co-polymerisation, or alkylation [140, 141].

The method of **graft co-polymerisation** describes a process of covalently binding one polymer to the other. This might happen within seconds or even last for several hours [142, 143].

1.2.4 WOUND HEALING AND WOUND DRESSINGS

Wound dressings are used to facilitate wound healing. Among other characteristics, they should protect the wound from contamination, keep a moist wound environment in order to support wound closure, and ensure sustained and effective delivery of applied bioactive substances [144, 145]. Of

course, the perfect wound dressing would be skin. Therefore, researchers try to mimic this gold standard as close as possible. At the beginning of wound dressing research, wound dressings were mainly protective and had a passive role in the healing process. This approach has changed during the last decades towards specialised biocompatible materials supporting the natural process of wound healing [146]. By providing a moist wound environment, proliferation and migration of fibroblasts and keratinocytes is induced. Moreover, scar formation is reduced by enhanced collagen synthesis. These new materials are also recognised as very acceptable and beneficial by patients as they can be easily removed without causing pain and trauma during dressing change. In addition, they reduce wound exudates, or odour from a wound [147].

Such specialised wound dressings are particularly important for patients with chronic wounds. In diabetic ulcers, venous stasis ulcers, or decubitus ulcers, cutaneous wound healing is a major problem. The process of cutaneous wound healing is a very complex interaction between several factors, which – in most cases – results in timely restoration of an intact skin barrier. But this multistep process of wound healing is easily prone to interruption. Several pathologic factors might favour the formation of chronic wounds. Examples are peripheral vascular disease, which influences the wound's blood supply, immunosuppression or acquired immunodeficiency, metabolic diseases such as diabetes, certain medications (e.g. anticoagulants or corticoids), radiation therapy resulting in previous local tissue injury, or external factors like temperature, sustained pressure, and moisture. Chronic wounds are the result – difficult and expensive to treat. In the United States alone, the number of patients with chronic wounds is estimated to exceed 6.5 million; treating these patients requires more than US$ 25 billion per year [145].

Physiological wound healing (Figure 4) is characterised by three main phases: inflammation, fibroblast proliferation, and epithelialisation [148]. Uncomplicated wound healing results in a fine scar with little fibrosis, sometimes some wound contraction, and almost normal tissue architecture and organ function [148]. A **chronic wound** describes a healing process that does not happen in orderly or timely sequence, or where the result lacks structural integrity [149]. Abundant granulation tissue forms and often disproportionate fibrosis results in distinct scar contraction and loss of tissue function [148].

(I) Within the first 5 to 10 minutes after an injury, **haemostasis** begins and is supported by an intense vasoconstriction. To achieve successful tissue healing and regeneration, the wound is cleared from foreign material and dead tissue. Within 20 minutes after the trauma, the **inflammatory phase** starts. It is characterised by local vasodilation and increased capillary permeability. Haemostasis is supported by platelet adhesion and clot formation at the site of injury [148]. These platelets are the depot for many vasoactive substances and growth factors (i.e. epidermal growth factor, β-thromboglobulin,

platelet-derived growth factor, platelet factor 4, transforming growth factor β, angiogenesis factor, fibroblast growth factor, bradykinin, serotonin, prostacyclins, prostaglandins, histamine, and thromboxane) [150]. In addition, the complement cascade is initiated, and leukocytes are guided by chemotaxis to infiltrate the wound bed. Their interplay with lysosomal enzymes, free oxygen radicals, collagenases, elastases, and neutral proteases protects the wound from infections and keeps it clear from tissue debris. The increased capillary permeability allows neutrophils and monocytes to enter the interstitial space. Macrophages and lymphocytes start to replace the leukocytes. They guide fibroblasts to the wound, where these can adhere on a scaffold of mainly fibronectin and hyaluronate, produced 24-48 hours after injury [148, 151]. In addition to phagocytosis and cell migration, macrophages are also key drivers for tissue proliferation and subsequent collagen synthesis and degradation [148, 152].

(II) Within 2 to 3 days, the **fibroblast proliferation phase** starts and lasts for about one week. Fibroblasts produce essential substances for wound repair, i.e. collagen and glycosaminoglycans such as hyaluronic acid, chondroitin-4-sulfate, heparin sulfate, and dermatan sulfate. These are mainly involved in deposition and aggregation of collagen fibres, which are constantly produced during this time until about three weeks after injury. Rapid growth of endothelial cells and angiogenesis within the granulation tissue create a very active healing environment within the wound. The increasing content of collagen results in increasing wound tensile strength. Wound maturation is characterised by a homeostasis between collagen synthesis and degradation. Remodelling begins with collagen fibres reorganising into a more structured lattice. The extracellular matrix starts to be reorganised. The tensile strength of the wound further increases, but in best cases only 80% of the maximum tensile strength of healthy skin can be reached [145, 148].

(III) The **epithelialisation phase** represents another milestone of wound healing. Epithelial cells migrate and grow from the bottom of the wound to their edges, covering the complete wound. Epithelialisation involves mobilisation, migration, mitosis, and cellular differentiation of these cells. Already during the earlier phases, wound contraction is induced by specialised fibroblasts to minimise the wound size and close potential defects. However, if this process is not controlled properly, it can lead to disorganised structural integrity, loss of function, and hypertrophic scar formation [148].

During the different phases of physiological wound healing, granulation tissue – rich in capillaries, fibroblasts, inflammatory cells, and endothelial cells – is converting to a collagen matrix. Apoptosis is the key driver to create this relatively avascular and acellular structure. If this process of controlled apoptosis fails to occur in a timely manner, chronic wounds with high cellular activity and eventually abundant scar tissue will be the result [148].
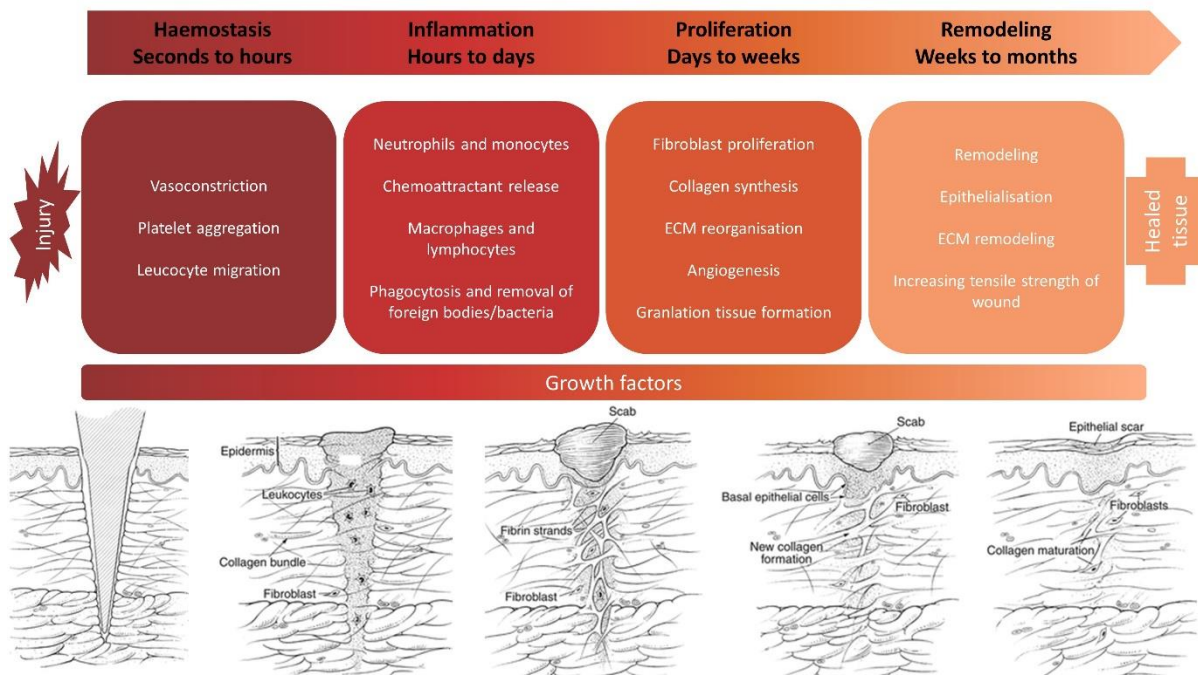
Figure 4. Phases of physiological wound healing. ECM – extracellular matrix. Figures were adapted from [153, 154].

The morbidity associated with chronic wounds has resulted in an increasing importance of good wound care. **Moist occlusive dressings** are used to support the inflammatory phase and re-epithelialisation [155]. Moreover, autolytic wound debridement – necessary for successful wound healing – is enabled in such a moist environment. In contrast, traditional **dry gauze dressings** inhibit this process and bear the risk for further injury when being removed from the wound. Therefore, classical wound dressings nowadays are **low adherent dressings**, which maintain a moist wound environment while allowing exudate to pass through a secondary dressing. Low adherent dressings are manufactured in such a way that they reduce adherence at the wound bed to make dressing changes as less painful as possible [155]. Another typical class of wound dressings are **semipermeable films**. These allow air and water vapour exchange whilst being impermeable to fluids and bacteria [155]. **Hydrocolloids** consist of a semipermeable film or foam as backing material crosslinked to a hydrophilic layer of for example gelatine, collagen, cellulose, or pectin. They form an occlusive, adhesive wound dressing that jellifies on the wound surface to promote a moist wound environment [144, 155]. In contrast, **hydrogels** are permeable to moisture vapour and oxygen. Depending on the secondary dressing, bacteria and fluids can permeate. As mentioned in section 1.2.1, hydrogels consist of a polymeric matrix containing large amounts of water and are able to donate this water to the wound bed resulting in a moist wound environment. The process of swelling and shrinkage is reversible, which allows hydrogels to adapt perfectly to the actual situation in the wound [146, 155]. For moderately

exudative wounds **foams** can be chosen. They are made from silicone or polyurethane foam and are permeable to oxygen and moisture vapour [145]. Another option are **alginate dressings**, which are used for highly exudative wounds. Upon contact with wound exudate they partly dissolve and form a hydrophilic gel [155]. It is also possible to use **collagen products** that help to attract cell populations necessary for wound healing and to reduce negative factors such as proteases and free radicals [145]. In addition, dressings can be **antimicrobial**, e.g. silver- or iodine-impregnated dressings, to treat burns and infected wounds [155]. It is also possible to produce **bioactive wound dressings**. These dressings contain agents beneficial for wound healing such as steroids, antibiotics, or growth factors [146]. The latter promote wound healing by supporting cell migration, proliferation and differentiation in the wound bed [156].

In chapter 2.2, a chitosan based hydrogel is described, which was prepared out of two chemically modified chitosan polymers. The gel formed as soon as the two polymers were mixed – without need for additional crosslinking agents. The hydrogel could be lyophilised and rehydrated successfully. In addition, loading and afterwards release of a model protein from this hydrogel was achieved. These properties make it a promising scaffold for biological wound dressings in the field of chronic wound treatment.

1.3 BUCCAL FILMS FOR PHENOTYPING: A PHARMACOKINETIC STUDY

1.3.1 CYP3A METABOLISM

Cytochrome P450 (CYP450) enzymes are a superfamily of 57 human enzymes. Their main functions are oxidative, reductive, and peroxidative metabolism of various exogenous and endogenous compounds (phase I metabolism). About 80% of the drugs on the market nowadays are metabolised via CYP450 [157]. Moreover, CYP450 enzymes are involved in cholesterol metabolism, bile-acid biosynthesis, steroid synthesis and metabolism, vitamin D_3 synthesis and metabolism, and retinoic acid hydroxylation. CYP450 enzymes are located in epithelial cells of the small intestine and in the smooth endoplasmic reticulum of hepatocytes [158].

Not all 57 human CYP450 variants are involved in drug metabolism. The five major drug metabolising CYP450 are CYP3A4, CYP2D6, CYP1A2, CYP2C9, and CYP2C19. These are responsible for about 60% of drug metabolism [159]. Not only in terms of activity but also when it comes to expression levels, the CYP3A family is the most abundant in human liver and intestine, accounting for about 50% of the CYP450 enzymes [160, 161]. CYP3A4 and CYP3A5 are the two most active enzymes of the CYP3A family. Both show very similar substrate specificity, which cannot be distinguished easily. Other members of this family show either only very low activity, such as CYP3A43, or are for example only expressed in foetuses, such as CYP3A7 [161]. CYP3A enzymes metabolise a very broad range of chemically unrelated drugs from almost every drug class. It is assumed that CYP3A is involved in the metabolism of more than 50% of the therapeutic agents undergoing oxidative alterations [161, 162]. Therefore, it is not surprising that such essential metabolism pathway can be easily affected by various drug-drug interactions. These include either inhibition of CYP3A enzymes or increase of CYP3A expression and therefore higher metabolic activity. As a result, enzyme activity may vary up to 400-fold [163]. Thus, plasma concentrations of co-administered drugs can change tremendously resulting in either reduced activity or toxic side effects. Some serious and well-known examples for such drug-drug interactions are presented below.

Co-administration of **CYP3A inhibitors** (e.g. diltiazem, verapamil, or nitroimidazole antifungal agents) with erythromycin (extensively metabolised by CYP3A) results in over-dosing with erythromycin and therefore prolonged cardiac repolarisation. Torsades de pointes may occur leading to sudden death [164]. Erythromycin itself is, due to its extensive metabolism by CYP3A, competitively inhibiting this enzyme subfamily. In combination with simvastatin this may result in myopathy or rhabdomyolysis, signs of intoxication with this lipid-lowering drug [165]. Another very important CYP3A inhibitor is grapefruit juice that is known to interact with more than 85 drugs. In combination with for example immunosuppressants like sirolimus or cyclosporine this may result in nephrotoxicity

and myelotoxicity [166]. Usually, CYP3A inhibition is reversible within two to three days once the inhibiting drug is stopped. However, some CYP3A inhibitors destroy the enzyme and new CYP3A must be synthesised. This is the case for example with diltiazem and macrolide antibiotics [161].

CYP3A inducers (e.g. rifampicin, phenobarbital, phenytoin, many glucocorticoids) up-regulate CYP3A expression. Therefore, previously active doses of CYP3A substrates may become ineffective, or toxic metabolites of these substrates can lead to intoxication. For example, oral contraceptives containing the CYP3A substrate etinylestradiol combined with CYP3A inducing agents may result in breakthrough vaginal bleeding or even pregnancy [161]. Moreover, patients taking the immunosuppressant cyclosporine or HIV-protease inhibitors co-administered with the potent CYP3A inducer St. John's wort may suffer from therapy failure [167, 168]. In contrast to CYP3A inhibition, the effects of CYP3A induction are not immediate as they are based on new CYP3A synthesis. Usually, it takes two to three weeks until steady-state levels are reached and several weeks until the induction effect is "washed-out", once the inducer is discontinued.

1.3.2 MIDAZOLAM FOR CYP3A PHENOTYPING

From the examples given above it becomes clear that especially drugs with a narrow therapeutic window need to be dosed very carefully based on the patient's individual metabolising activity. For clinical practice, this means that an easy and reliable phenotyping tool is needed to tailor dose recommendations in patient treatment. By administration of a test drug followed by measurement of the metabolic ratio (in blood plasma, urine, saliva, or tissue) the metabolic activity of a patient regarding the tested enzyme can be determined. Phenotyping provides information about the activity of a certain drug metabolising enzyme at a given time point. It reflects genetic factors as well as non-genetic and environmental factors (Figure 5). The main prerequisite for phenotyping is that the metabolism of the test drug is exclusively dependent on the tested enzyme [169, 170].
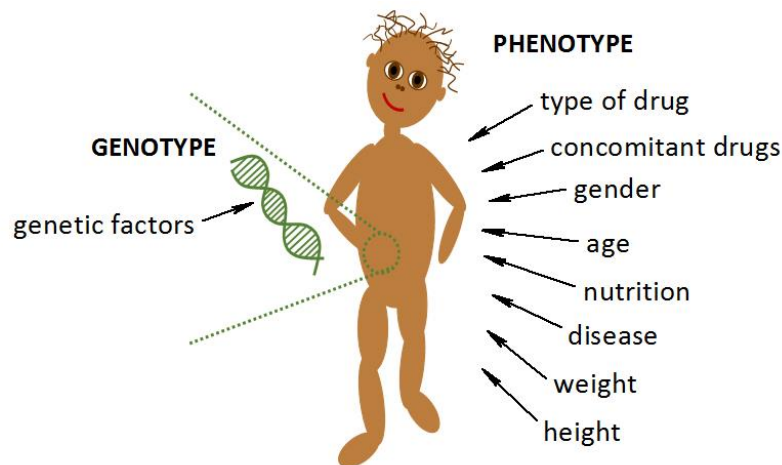
Figure 5. Difference between geno- and phenotype. The genotype of a person is exclusively determined by genetic factors whereas the phenotype also reflects several environmental influences on a person.

To phenotype CYP3A, midazolam is a well-accepted probe drug [163, 171–175]. This short-acting benzodiazepine is sedative, anxiolytic, anticonvulsive, and muscle-relaxant. For insomnia treatment typical doses are between 7.5-15 mg *per os*. Within 20 minutes, the sedative effect starts and after 7-8 hours of sleep the effect is usually resolved. After oral administration, midazolam has an absolute bioavailability of 30-50%, and the peak concentration is reached within one hour. The elimination half-life time is between 1.5-2.5 hours. Almost 100% of the midazolam dose are eliminated after biotransformation. The hepatic oxidative metabolism involves CYP3A4 and CYP3A5. These hydroxylate midazolam to 1'-hydroxymidazolam (1'-OH-midazolam) and 4'-hydroxymidazolam. This step is followed by either further hydroxylation to 1',4'-dihydroxymidazolam and/or glucuronidation and elimination via urine (Figure 6). The main metabolite in plasma and urine is 1'-OH-midazolam and 60-80% of the initial dose can be found in the urine as glucuronidated 1'-OH-midazolam. 1'-OH-midazolam is pharmacologically active (about 34% of the effect of orally administered midazolam) and plasma concentrations of this metabolite reach about 30-50% of the parent substance [176, 177].

Intravenously administered midazolam is used as sedative, as pre-medication before anaesthetic induction, or directly for anaesthesia. The total doses range between 1-7.5 mg. Already after 2 minutes, first effects appear and within 5-10 minutes the peak concentration is reached. Intravenously administered midazolam is metabolised extensively by CYP3A as well. The main metabolite is – comparable to oral administration – 1'-OH-midazolam. Its plasma concentration reaches about 12% of midazolam. The pharmacological effect of 1'-OH-midazolam after intravenous administration is not as significant as after oral administration (about 10%). The metabolism and

elimination pathway is of course the same as for oral midazolam, with a half-life time of 1.5-2 hours, and comparable hydroxylation and glucuronidation patterns [176].
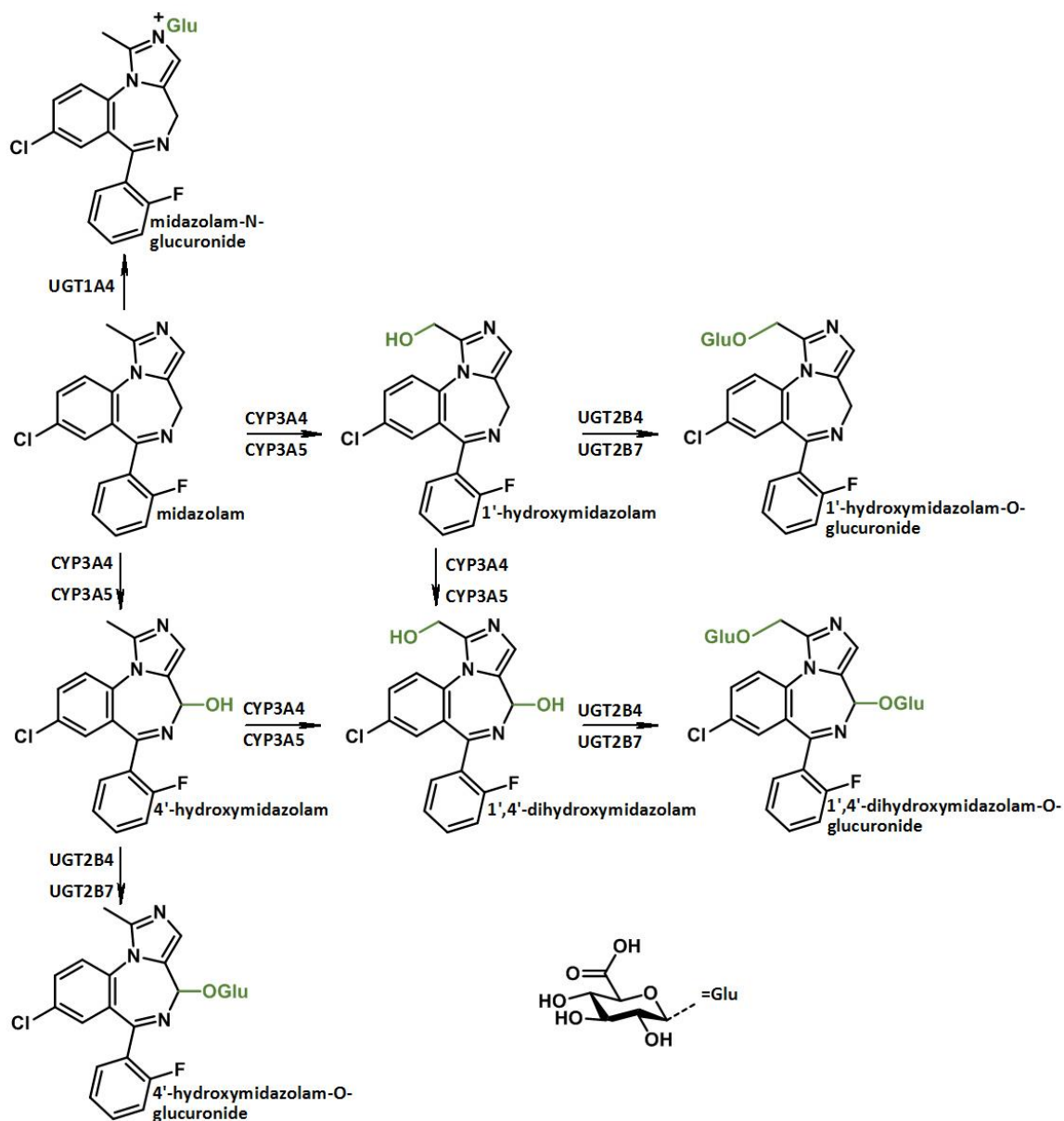
Figure 6. Metabolism of midazolam. CYP3A4 and CYP3A5 transform midazolam to 1'-hydroxymidazolam, 4'-hydroxymidazolam, and 1',4'-dihydroxymidazolam. All metabolites and the parent substance undergo rapid glucuronidation via uridine diphosphate-glucuronosyl-transferases (UGTs) followed by elimination via urine. UGTs are divided into two subfamilies, UGT1 and UGT2 [178–181].

From the information above, it becomes clear that midazolam is very well suited to serve as phenotyping test drug to determine the activity of CYP3A. For this purpose, plasma concentrations of midazolam as well as its main metabolite 1'-OH-midazolam are measured. By using metabolic ratios of parent to metabolite plasma concentrations, the CYP3A activity of every single patient can be determined and dose recommendations for CYP3A drugs could be made. In order to avoid sedation of

every tested patient due to pharmacologically active midazolam doses, a microdosing approach for phenotyping was recently developed [174]. Halama and co-workers found that oral midazolam kinetics are linear over a 30'000-fold range and already doses as small as 300 ng can be used to predict drug interactions with strong CYP3A inhibitors [174]. However, the development of drug formulations containing microdoses as well as their administration remain a challenge. One opportunity to tackle this is to use microdosed oral films.

1.3.3 ORAL FILMS

In general, oral films are divided into oral disintegrating films and buccal films (BFs). **Oral disintegrating films** can be either mucoadhesive or non-mucoadhesive and they disintegrate rapidly in the oral cavity. After swallowing them they are absorbed in the gastrointestinal tract (GIT). Depending on the amount and type of drug that they are containing an oral absorption is also possible. **BFs** are always mucoadhesive and the oral absorption of drug results in a fast onset of action. BFs can be placed either sublingual, buccal, or palatal. Regarding oral absorption, the residence time of the drug within the oral cavity plays an important role. Additionally, one should consider the oral mucosa saturation. Beside the fast onset of action, main advantages of oral absorption are that the drugs are not destroyed by harsh conditions in the GIT nor are they exposed to first pass metabolism. Therefore, it is possible to lower the required dose strength what again improves the safety and efficacy profile of a drug [182].

Oral films possess several advantages. Due to their appellative form and their inherent ease of administration they are very well accepted by patients. This is particularly important for special patient populations such as paediatric or geriatric patients who might have difficulties with swallowing [183]. Moreover, oral films can hardly be spit out. That makes them also well suited for bedridden or non-cooperative patients. In addition to high compliance, oral films are beneficial for drugs with a narrow therapeutic window and for those requiring a precise dose adaption in phases of initial drug monitoring. Not only with regards to patients, but also in direct comparison to other oral formulations, oral films offer many advantages. In contrast to several oral disintegrating tablets, oral films are more stable, resistant, flexible, and better portable. Moreover, the dosing accuracy and ease of administration of oral films is preferable compared to liquid oral formulations requiring a careful volume measurement and often cautious shaking before administration. In terms of transportation, it is also better to work with oral films, since they require much less space and weight. Moreover, liquid oral solutions tend to have stability issues. Major drawbacks of oral films are their instability in very humid regions and their limited ability to load higher amounts of active pharmaceutical ingredients. The latter challenge was already tackled by some companies and Gas-X Strips® are an example that a

drug load of more than 50% is possible. Due to the fact that oral films are in direct and comparably long contact to the oral mucosa, taste masking is an important question to be discussed [182]. Additionally, oral films are not suited for active pharmaceutical ingredients that are unstable at mucosal pH or that are irritating the oral mucosa [183].

Comparable to the formulations described in sections 1.1 and 1.2, polymers are also the key component of oral films. One or more polymers control the properties of the resulting films: their mucoadhesiveness, disintegration time, mechanical strength, elasticity, handling properties, and drug loading capacity [182]. In the following paragraph, the polymers that were used to formulate the midazolam BF (chapter 2.3) are highlighted.

Cellulose derivatives are often used for oral films. To formulate the midazolam-containing BF, hypromellose, hydroxypropyl cellulose and microcrystalline cellulose were processed. Hypromellose, short for **hydroxypropylmethylcellulose (HPMC)**, is one of the most used excipients. HPMC is partly O-methylated (-OCH$_3$) and O-(2-hydroxypropylated) (-OCH$_2$-CH(OH)-CH$_3$) cellulose (Figure 7 A). As chitosan (section 1.2.2), HPMC exists in several grades with different molecular weights (i.e. 10-150 kDa) and varying degree of substitution resulting in tuneable oral film properties [184]. It was shown that the HPMC grade influences the dissolution profile and drug substance release. The higher the hydroxypropyl/methoxyl ratio the slower was the release [185]. Moreover, polymers with a higher viscosity due to increased branching and/or longer polymer chains tend to produce more resistant, stiff, and extensible polymeric matrices [182]. It is well known that a combination of HPMC with microcrystalline cellulose and plasticisers such as PEG 400 (as it is presented in chapter 2.3) results in good film forming properties [186]. Another cellulose derivative is **hydroxypropylcellulose (HPC)**. Herein, the hydroxyl residues of cellulose are hydroxypropylated (-OCH$_2$-CH(OH)-CH$_3$) (Figure 7 B). As HPMC, HPC exists in several substitution grades with different molecular weights between 60-1200 kDa [184]. Using HPC for film formation results in mechanically stable films with good carrying capacity and moderate bioadhesive properties [182, 187]. HPC is soluble in many different solvents [184]. This enables researchers to flexibly select the solvent according to the solubility of the drug that should be loaded into the oral film. **Microcrystalline cellulose (MCC)** (Figure 7 C) is partly depolymerised α-cellulose with a resulting polymerisation degree around 120-300. In comparison to unmodified cellulose powder, MCC is easier to be compressed, shows improved flowability, and is mechanically more stable. Moreover, MCC is very useful as disintegrant due to wicking effects as soon as it comes in contact with liquid [184].

Another common polymer used for film formation is **starch**. It is a promising biopolymer because of its wide availability, biodegradability, and low costs [188]. Starch is a combination of amylopectin

(Figure 7 D) and amylose (Figure 7 E), typically in a ratio of 75-85% amylopectin and 15-25% amylose [184]. To prepare strength, water resistant, thermally stable, and easily processable films, starch is usually blended with other polymers [188]. For the midazolam BF, described in this work, hydrolysed starch in the form of maltose (Figure 7 F) was used [182]. Films containing such Maltodextrins are characterised by fast disintegration and dissolution times [189].

The synthetic macromolecule **PEG 400** is a polycondensation product of ethylenoxide (Figure 7 G). PEGs exist in various polymerisation grades with molecular weights ranging mainly from 200 to 7000 g/mol. PEG 200 to PEG 600 are liquid at room temperature, whereas PEGs with a higher molecular weight are semisolid or solid at this temperature. PEGs can be used for many different purposes, such as solvent, solubility enhancer, lubricant, embedding material, basis for ointments or suppositories, or as plasticiser [184]. In the midazolam BF PEG 400 is used as plasticiser.
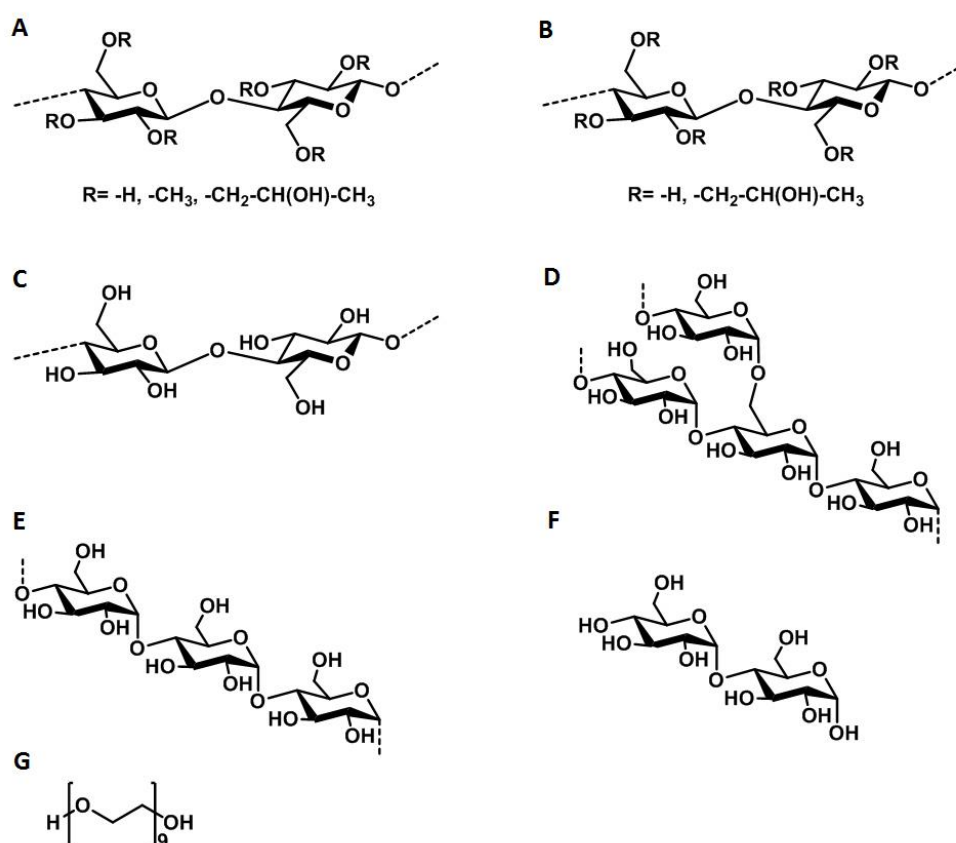
Figure 7. Chemical structures of common polymers used in oral films. A) hydroxypropylmethylcellulose (HPMC), B) hydroxypropylcellulose (HPC), C) microcrystalline cellulose (MCC), D) amylopectin, E) amylose, F) maltose, and G) polyethylenglycol (PEG) 400.

In chapter 2.3, the use of a BF containing microdoses of midazolam is described. It was applied onto the palatal mucosa of healthy volunteers and the plasma concentrations of midazolam and 1'-OH-midazolam were determined for 12 hours. It was shown that the BF described in this study

facilitated oral absorption of midazolam, resulting in plasma concentrations that would be comparable to intravenously administered midazolam. Moreover, the plasma concentration-time profiles of this microdosed BF and a buccal solution containing the same amount of midazolam were comparable if the solution was administered into the buccal cavity, resulting in oral absorption as well. With respect to the presented results it would be also possible to perform a limited sampling strategy using the BF, as it was already proposed for other CYP3A phenotyping methods [190]. To use microdosed midazolam BFs for phenotyping would be very attractive especially for vulnerable patient populations where adverse drug reactions and drug-drug interactions are highly expected and where drug administration may create some difficulties. Amongst others, this is the case for paediatric patients [191, 192] as well as geriatric patients with multimorbidity [193].

1.4 ORAL DISINTEGRATING TABLETS: A PALATABILITY STUDY IN CHILDREN

1.4.1 PAEDIATRIC PATIENTS

The paediatric population is very heterogeneous. Physical, cognitive, and psychosocial abilities develop gradually but also individually with flowing transitions between the different age categories. Therefore, it is necessary to consider each paediatric patient as individual depending on the development. In the following sections, the paediatric age groups are described [194, 195].

(I) Preterm newborn infants (born before 37 weeks of pregnancy [196]) include 25-week gestation newborns, weighing 500 g, as well as 30-week gestation babies with 1500 g, or low-birth-weight newborns. It is obvious that this group presents special challenges regarding studies of medicinal products due to the unique pathophysiology and responses to therapies of preterm newborn infants. It should be always evaluated whether these children are immature or growth-retarded. For this purpose, several factors might be considered: (i) Their gestational age at birth and age after birth has to be kept in mind [194]. The corrected age refers to the age calculated from the expected date of delivery [195]. (ii) The activity of hepatic and renal clearance mechanisms is not fully developed [195, 197]. (iii) Fast and highly variable development of physiological and pharmacological processes results in rapidly changing dose recommendations. (iv) Protein binding differs from older children. Moreover, displacement issues, e.g. bilirubin, need to be kept in mind. (v) Preterm newborns possess only an immature blood-brain barrier, which is not able to protect the central nervous system (CNS) from potentially toxic substances. (vi) The skin barrier is not as efficient as in older paediatric patients. Due to increased transdermal absorption potential intoxication with medicinal products or other chemicals might occur. (vii) Distinct cardiac (e.g. patent ductus arteriosus) and pulmonary (e.g. respiratory distress syndrome) conditions are specific for neonates and must be monitored carefully. Moreover, preterm newborn infants show unique susceptibilities such as intraventricular haemorrhage [194, 195].

(II) Term newborn infants (aged 0 to 27 days) are comparable to preterm newborn infants regarding the physiological and pharmacological principles discussed above, with the difference that term newborns are developmentally more mature. Compared to older children, term newborn babies differ significantly: (i) The blood-brain barrier is still not fully developed allowing the entrance of potentially toxic substances into the CNS. (ii) Their body water and fat content vary from older children and their body-surface-area-to-weight ratio is much higher resulting in different volumes of distribution of medicinal products compared to older paediatric patients. (iii) It is more difficult to predict the oral bioavailability in newborns than in older children. The gastrointestinal absorption is influenced by several factors such as surface area, gastric and intestinal pH, intestinal mobility and transit time, tissue

perfusion, and maturation of transporters and receptors. All of them develop and mature over time. (iv) Highly variable and rapidly changing metabolism pathways require dose adjustments on at least weekly (if not daily) basis. For this purpose, not only pharmacokinetic changes but also pharmacodynamic changes should be considered [194, 195].

(III) Infants and toddlers (aged 28 days to 23 months) are characterised by (i) rapid CNS development and (ii) maturation of their immune system. (iii) They grow quickly and changes in body composition such as age-related changes in fat, muscle, and total body water composition might have significant impact on volume of distribution, peak plasma concentrations, and half-lives. (iv) The oral absorption becomes more predictable and (v) metabolic pathways such as hepatic and renal clearance continue to mature rapidly [194, 195]. Aged 1 to 2 years, the children's clearance of many compounds (based on mg/kg) can exceed the adults' one [197]. It has to be kept in mind that the maturation of clearance pathways is strongly influenced by inter-individual fluctuations [194].

(IV) Children (aged 2 to 11 years) possess (i) mostly mature clearance pathways with often more active clearance capacities than adults. (ii) During this long period of time, psychomotor development is very important and might be easily affected by CNS-active drugs. (iii) The effects and acceptance of medicinal products can be determined more easily than in younger children due to increased cognitive and motor skills. Moreover, skeletal growth, weight gain, school attendance, and school performance can be measured to gather information about ongoing therapies. (iv) Towards the end of this age period, puberty starts to begin [194]. Typically, onset of puberty in girls is from 8 to 9 years of age, which is a little bit earlier than in boys (around 10 years or older) [198]. With this period, clearance capacity may change significantly, what makes dose adjustments necessary [194]. Due to the very broad range of developmental differences within this population of 2 to 11 year-old children, the European Committee for Medicinal Products for Human Use divided it into two subgroups: **preschool children** (aged 2 to 5 years) and **school-going children** (6 to 11 years old) [199, 200].

(V) Adolescents (aged 12 to 16-18 years, depending on the region) are the oldest group of paediatric patients. (i) The main difference to younger children is the sexual maturation. Sex hormones might interfere with drugs and medicinal products may delay the adolescent's development. For certain drugs, pregnancy testing, review of sexual activity, as well as information about correct use of contraceptives becomes necessary. (ii) During adolescence, neurocognitive abilities develop further and body growth continues. Medicinal products that impede these developments should be used carefully, since they might have an impact on pubertal growth spurt affecting the final height of a person [194]. (iii) Hormonal changes during the development of adolescents can also influence many diseases such as increasing insulin resistance in diabetes mellitus patients [201] or recurrence of

seizures around menarche [202]. (iv) The use of recreational drugs such as alcohol [203] or tobacco [204] by adolescent patients might have a huge impact on concomitant medicinal products resulting in over- or under-dosing.

When comparing paediatric patients with adults, the differences are not limited to drug metabolism and absorption but also include organs of perception, meaning their ability to smell and taste. Already between 2 and 6 days of age, the neonates' olfactory ability starts to develop. This enables them to locate a food source and to discriminate their mother from other unknown mothers [205]. Children were reported to be more sensitive to taste than adults, mainly due to much higher density of taste pores and fungiform papillae on the tongue. Moreover, it was stated that the sense of taste is developing during childhood, being not yet completely mature in 8 to 9 year old children [206]. Therefore, palatability testing in adults cannot replace palatability testing in children. How palatability can be tested in children is described in more detail in section 1.4.3.

1.4.2 PAEDIATRIC FORMULATIONS

From the information about paediatric age groups, which was outlined above, it becomes clear that children are not small adults. At the moment there is a lack of medicinal products available as paediatric friendly formulations and tested for use in children [194]. So far, paediatricians need to prepare and administer unlicensed formulations by manipulating adult dosage forms ("off-label use"). This includes splitting or crushing tablets, opening capsules, dispersing tablets or capsules in liquids and taking proportions of them, cutting suppositories, or applying injectable solutions by other routes. It is obvious that such manipulations might have huge impact on bioavailability and safety of a medicinal product [199]. To improve the quality, efficacy, and safety of paediatric medicines, age-appropriate formulations of medicinal products for use in children are necessary. Already in 2001, the European Medicines Agency (EMA) recommended to test paediatric formulations in children [199, 207]. In addition to deeper and more exact information on the consequences of off-label use, the manufacturers were asked to perform paediatric investigations with the products intended for paediatric use. This so called Paediatric Investigation Plan (PIP) has been required by EU paediatric regulations since 2006, including an overview of planned measures or performed studies before authorising a drug for use in children [199]. One main aim was that children will gain access to medicinal products with a positive risk-benefit balance [191].

The development of age-appropriate formulations for children is challenging due to different aspects. Child friendly medicines have to allow for accurate dosing and need to show good palatability to support patient's compliance with the therapy [207]. Therefore, liquid or small particulate dosage

forms are preferred for children [208]. So far, there is not much known about the acceptability of different dosage forms, administration volumes, dosage form size, taste, and acceptability as well as safety of excipients with regard to age and developmental status of the child [199]. Interregional differences make it necessary to produce different types of formulations, flavours, and colours. According to different age classes, several galenical formulations may be needed, such as liquids, suspensions, or for example chewable tablets. Moreover, all these formulations need to exist in several drug concentrations keeping the aforementioned paediatric age groups in mind [207]. To be considered child-appropriate, a medicinal product needs to address following criteria [208]:

(I) To achieve **sufficient bioavailability** the site and route of absorption and the properties of the drug formulation need to be kept in mind. For children, the main route of administration is *per os* [192, 200]. Important points to consider when administering a peroral drug are varying gastrointestinal transit times, incomplete intestinal drug absorption, changing pH conditions along with the passage through the GIT, drug-food interactions, instability of the drug under gastric conditions, and the first-pass effect. As already mentioned in section 1.4.1, the gastric fluid of newborns and infants is in an almost neutral pH range. It takes one year until infants have a pH of 1-2 at fastened state, which is the normal value for grown-ups. This makes enteric coatings inappropriate for infants under 1 year. Moreover, the transit time through the GIT might deviate a lot from adults. Alternatives to the peroral administration are rectal, buccal, transdermal, nasal, inhalative, or parenteral administration routes. However, bioavailability remains a challenge in all these formulations and their advantages must be balanced against their drawbacks to find the optimal formulation for every single patient [192, 208].

(II) To be considered as **safe**, **excipients** need to be non-toxic, inert, non-allergenic, and form non-toxic metabolites in the body of a child [208]. It has to be kept in mind that not every excipient, which is safe in adults, can be chosen for paediatric formulations [195, 209]. To gain more information on substances, which are suited for paediatric formulations and which ones have to be omitted, European and US Paediatric Formulation Initiatives teamed up. They created a database to collect and easily access relevant information about Safety and Toxicity of Excipients for Paediatrics (STEP) [209–211]. With regards to toxicity, solid oral dosage forms are preferable against liquid formulations, which require more often potentially toxic excipients. On the other hand, dose administration and adaption are easier with liquid formulations. It becomes more and more obvious that it is necessary to balance many different factors when formulating medicines for children [208].

(III) Palatability and acceptability of a medicinal formulation are important parameters to be considered when treating children. In a Danish study, almost half of the children receiving liquid or solid oral dosage forms had difficulties in taking their medication. Main problems, parents and

caregivers were facing when administering oral formulations, were taste of the medicine and difficulties of children in swallowing solid medications. The younger the children, the more pronounced the difficulties were [212]. Bad palatability may result in poor adherence ending up in treatment failure, complications, and eventually the development of drug resistance [213]. To improve acceptance, possible options include dispersing small-sized pellets in food or juices and offering training in swallowing tablets to children [208, 214].

(IV) Another key factor to be considered when formulating medicines for children is an **adequate dose uniformity**. Liquid formulations have the advantage to be easily adjustable by volume adaption. However, a certain level of accuracy and training is necessary to ensure exact dosing [215]. Unfortunately, many dosing devices for liquid formulations are not very exact [216]. When it comes to solid dosage forms the difficulties further increase. Splitting is less accurate and special coatings around the tablets might be destroyed by crushing or cutting [217]. To overcome these problems, multiparticulate systems such as pellets, micropellets [218], or minitablets [219] have been developed. These cover broad dosing ranges and can be safely and easily tailored to individual patients' needs.

(V) To make a medicinal product efficient, **easy and safe administration** are very important points to be reflected. Medication errors can happen at any time of the application process. Typical mistakes are incorrect dosage or frequency of drug administration, prescription mistakes, wrong route of administration, interactions with food or other drugs, or inadequate communication between medicinal personal, parents, and other caregivers [220]. To reduce these pitfalls, buccal drug formulations present an attractive alternative to classic oral dosage forms by combining easy administration with the advantages of solid formulations such as drug stability and non-toxic excipients [208]. Moreover, e-prescribing, medication reconciliation, barcode systems, clinical pharmacists in medical settings, improved training of medicinal staff, standardisation of equipment used by laypersons, precise and clear product information and clear package design are needed to overcome sound-alike and look-alike confusions [208, 220].

(VI) The **socio-cultural acceptability** of medicinal products must be considered to avoid stigmatisation of patients. Therefore, drug administration should be – where possible – adjusted to the daily life making use of controlled release formulations or delivery systems facilitating drug administration also in school environments [199]. Moreover, preferences regarding galenical formulations should be respected to enhance patient adherence [208].

1.4.3 Paediatric palatability testing

As mentioned above, palatability and acceptability of a medicine are important parameters to be considered when treating children. So far, there has not been much systematic methodological research on how to evaluate taste and mouthfeel of age-appropriate formulations in paediatric patient populations. To assess the acceptability of a medication, taste and smell can be evaluated quantitatively by using indirect analytical methods and taste/smell sensors. Moreover, a qualitative analysis is possible by taste panels, also called consumer testing. It is known that adults and children have different sensory feelings [205, 206]. Therefore, the EMA considers children the most suitable target population for taste assessment of paediatric formulations [199]. However, children are a very vulnerable patient population and should only be considered for clinical trials if research cannot be performed with adults. If research with children is unavoidable, the least vulnerable patient population, i.e. older children, should be included. In all cases, the decision should be based on target population, possibility of extrapolation, and the scientific validity of the planned approach [221]. The EMA clearly states that "in principle, healthy children should not be enrolled as healthy volunteers, because they cannot consent and are vulnerable like children with a disease or condition. […] Exceptions could be where healthy children participate in palatability testing such as swill and spit taste testing for a new flavoured medicine" [221].

When planning a clinical trial with children, it is necessary to adapt the methods to the child's developmental stage and to focus on practical and ethical considerations and limitations [222]. According to the EMA, key elements to consider before designing a palatability study are that (i) children have a shorter attention span, and therefore the test should be as short as possible. (ii) Children are easily diverted with other things than the trial. This makes it necessary to design and perform the trial as motivating as possible and to give the children the impression of having fun during the trial. (iii) It is very important that every child participating in the trial can understand the procedure. The researcher is asked to describe the procedures to the children as child friendly as possible, e.g. by using cartoons. (iv) Children are easily confused and become taste-fatigue if there are too many variables during a trial. Therefore, variables should be limited to a maximum of four. Generally, the EMA considers children older than 4 years as capable of participating in taste trials. The key characteristics of children, which were mentioned above, are the more prominent the younger the child is. This results in failure rate variations up to 50% for younger children, depending on the design and duration of the test. Moreover, younger children have difficulties in communicating their feelings and preferences [199].

Amongst others, there are two common principles to evaluate palatability of a formulation in children: verbal judgement and facial hedonic scales (FHS, Figure 8 A). Children younger than 5 years seem to be less capable to express taste preferences and differences between test formulations compared to older children. To obtain reliable estimation of taste acceptance in younger children, the verbal method is preferred over the FHS [223]. This means, when asked for sensory experience, children will be able to state whether they had liked the probe substance or not, referring to their acceptance of a taste. But when it comes to preferences between several formulations they might be overstrained in discriminating between taste, after-taste, texture, smell, or appearance of the formulation. Moreover, Davies and Tuleu concluded that children from 3 years on are capable of using an FHS, whereas visual analogue scales (Figure 8 B) are more widely applied for children older than 6 years [222]. In addition, the facial expression of the volunteer himself may help to gather more information on the acceptance of the tested formulation. Reliability of the outcome might be further increased by involving parents, guardians, or health providers. The EMA suggests asking them about any discomfort or other observations in relation to the acceptance of the study medication by their children [221].
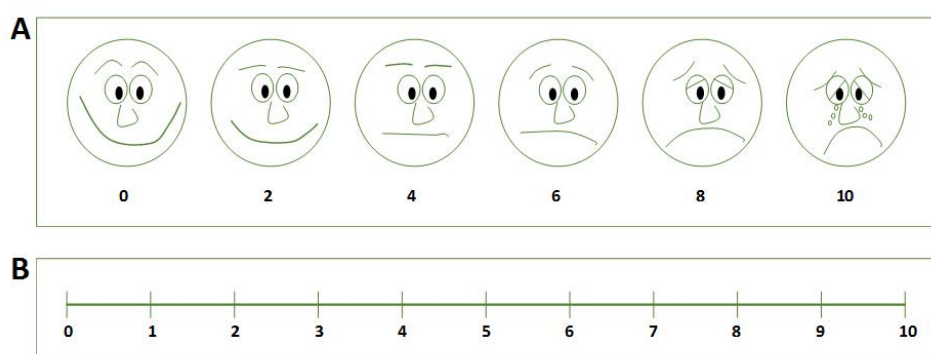
Figure 8. Tools commonly used to rate perception of children. These are well-established for paediatric pain assessment. A) Facial hedonic scale, FHS. The child should point at the face that describes its feelings the best. On the backside each face is linked to a number (often between 0 to 10), which can be used for evaluation by clinicians. B) Visual analogue scale. Older children are able to rate their perception directly in numbers. They are asked to point out which number describes best what they feel at the moment (e.g. from "no pain" corresponding to 0 to "unbearable pain" corresponding to 10). Figures were adapted from [224].

In the herein presented work, the palatability of an oral disintegrating tablet (ODT) in 40 children (aged 2 to 10 years) attending the outpatient department at University Children's Hospital of Basel (UKBB) for minor surgical ailments was tested. The ODT has been evaluated before in adult volunteers, showing very good acceptability and palatability [225]. But as already outlined above, it is necessary to perform palatability testing of paediatric formulations in paediatric patients. Therefore, a palatability assessment of these placebo ODTs was conducted in children who were divided according to the age classes defined in section 1.4.1: pre-school children were aged 2 to 5 years and the older

population was 6 to 10 years old. Keeping in mind the difficulties of younger children to communicate preferences between several formulations, the focus was on acceptance of the palatability of the test formulation. The younger children were asked child appropriate questions and their spontaneous verbal judgement was recorded. For the older subpopulation these questions were combined with an FHS. In addition, the parents of every child were asked to compare drug formulations – which they are already familiar with – with the ODT. It was of additional interest to elaborate and critically evaluate the suitability of the questionnaire to generate data about palatability in healthy children.

2   RESULTS

2.1 PDMS-*B*-PMOXA POLYMERSOMES FOR HEPATOCYTE TARGETING AND ASSESSMENT OF TOXICITY

Klara Kiene, Susanne H. Schenk, Fabiola Porta, Alexandra Ernst, Dominik Witzigmann, Philip Grossen, Jörg Huwyler

Department of Pharmaceutical Sciences, Division of Pharmaceutical Technology, University of Basel, Klingelbergstrasse 50, 4056 Basel, Switzerland

Research paper

PDMS-*b*-PMOXA polymersomes for hepatocyte targeting and assessment of toxicity

Klara Kiene, Susanne H. Schenk, Fabiola Porta, Alexandra Ernst, Dominik Witzigmann, Philip Grossen, Jörg Huwyler *

Department of Pharmaceutical Sciences, Division of Pharmaceutical Technology, University of Basel, Klingelbergstrasse 50, 4056 Basel, Switzerland

ARTICLE INFO

ABSTRACT

Nanoparticles, such as polymersomes, can be directed to the hepatic asialoglycoprotein receptor to achieve targeted drug delivery. In this study, we prepared asialofetuin conjugated polymersomes based on the amphiphilic di-block copolymer poly(dimethylsiloxane)-*b*-poly(2-methyloxazoline) (PDMS-*b*-PMOXA). They had an average diameter of 150 nm and formed monodisperse vesicles. Drug encapsulation and sustained release was monitored using the hydrophilic model compound carboxyfluorescein. Asialoglycoprotein receptor specific uptake by HepG2 cells *in vitro* was energy dependent and could be competitively inhibited by the free targeting ligand. Mechanistic uptake studies revealed intracellular trafficking of asialofetuin conjugated polymersomes from early endosomes and to the lysosomal compartment. Polymersomes showed no toxicity in the MTT assay up to co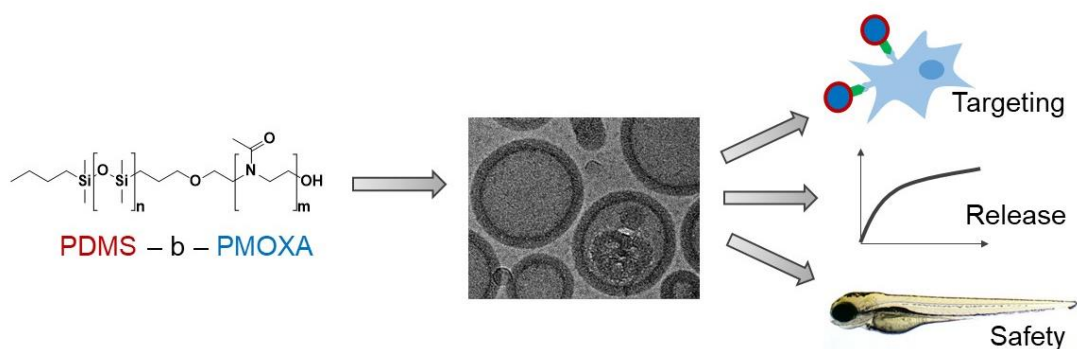ncentrations of 500 µg/mL. In addition, acute toxicity and tolerability of our PDMS-*b*-PMOXA polymersome formulations was assessed *in vivo* using zebrafish embryos as a vertebrate screening model. In conclusion, a hepatocyte specific drug delivery system was designed, which is safe and biocompatible and which can be used to implement liver-specific targeting strategies.

1. Introduction

Liver diseases such as hepatocellular carcinoma, viral hepatitis, or genetic and metabolic disorders belong to the leading causes of death, and the incidence rates are still increasing [1]. Though the liver is well known for its high drug uptake, available pharmacotherapies are often not adequate. Rapid drug elimination including P-glycoprotein mediated efflux and non-specific drug uptake by Kupffer cells makes the treatment of liver diseases difficult [2]. Therapeutic approaches using conventional small molecular weight drugs or novel therapeutic compounds such as nucleic acids, proteins, or peptides suffer from drawbacks including

dose-limiting side effects, low bioavailability and rapid clearance from the blood stream. To overcome these challenges, there is an urgent need to develop alternative strategies for efficient drug delivery to the liver. Hepatocytes represent more than 80% of the resident hepatic cells and for several diseases they act as the most relevant target. Therefore, a specific delivery of pharmaceutical compounds to this cell type would be highly desirable [2,3].

In the search for alternative drug delivery systems, nanomedicines (including different classes of formulations such as drug-protein conjugates, drug-polymer conjugates, liposomes, micelles and polymersomes) have a great potential [4,5]. Among the particulate drug nanocarriers, liposomes are the most extensively studied, and there is now a range of clinically approved liposomes-based products that improve therapeutic outcome in patients. In 2016, only a few polymer-based nanocarriers were on the market, for example paclitaxel-loaded micelles. (For an extensive review on nanoparticle-based medicines see Refs. [4,6,7]).

Targeted nanomedicines [8] offer the possibility to increase the efficiency of drug treatment and to minimize toxic side effects since local drug accumulation and specific uptake reduce off-target exposure and allow for reduction of the administered dose. In terms of liver diseases, the asialoglycoprotein receptor (ASGPR) provides an opportunity to target hepatocytes [9]. The ASGPR is abundantly expressed on the surface of parenchymal liver cells

but minimally on extra-hepatic cells [10]. Up to now, different nanomaterials have been modified with asialofetuin such as PLGA/DOPE hybrid nanoparticles [11] and liposomes [12] in order to target the ASGPR.

Recently, polymersomes have been studied as nanocarriers for drug delivery [13]. Polymersomes are vesicles formed by self-assembly of amphiphilic block copolymers. Similar to liposomes, polymersomes offer the ability to encapsulate hydrophilic compounds in the aqueous core and to integrate hydrophobic or amphiphilic molecules into the hydrophobic part of their surrounding membrane. Compared to phospholipid based liposomes, polymersomes are characterized by a thicker membrane (8–21 nm) [14], which leads to enhanced membrane stability concurrent with lower permeability and improved storage properties. The precise biological and physicochemical characteristics of polymersomes are highly tunable (for review see [15–17]). By appropriate selection of the chemical composition of each polymer block, a broad range of block copolymers can be synthesized that confer polymersomes with a variety of specific properties such as improved drug encapsulation, biocompatibility, long circulation in blood stream, or stimuli-responsiveness. Chemical groups on the surface of polymersomes that allow conjugation of targeting moieties provide additional chemical versatility. No polymersome formulations have achieved FDA approval to date, and there are only few clinical trials in progress [4,6,7].

Recently, several reports on polymersomes formed by block copolymers consisting of poly(dimethylsiloxan) (PDMS) and poly (2-methyloxazoline) (PMOXA) have been published. The individual polymer blocks have been reported to be biocompatible [18] and polymersomes based on PDMS and PMOXA copolymers exhibited low cytotoxicity in various *in vitro* models [18–21]. PMOXA-decorated liposomes displayed increased circulation times in blood [22]. Konradi et al. [23] suggested that PMOXA could serve as a potential PEG substitute for rendering surfaces resistant to protein adsorption, i.e., adding stealth properties to the surfaces. In accordance to these findings, polymeric nanoreactors made of tri-block PMOXA-*b*-PDMS-*b*-PMOXA did not induce a macrophage-mediated inflammatory response *in vitro* and *in vivo* [24]. Antibody or peptide functionalized PDMS-*b*-PMOXA polymersomes have recently been used for cellular targeting. The ligand-targeted PDMS-*b*-PMOXA polymersomes were shown to bind specifically to their target cells, followed by rapid cellular uptake [19,21,25]. This suggests that polymersomes made of PDMS-*b*-PMOXA present a promising biocompatible and versatile platform to design novel specific drug targeting systems.

In this study, we present various formulations of polymersomes based on PDMS-*b*-PMOXA. We incorporated carboxyfluorescein as a model compound and demonstrated a slow drug release from these vesicles *in vitro*. In addition, we focused on the formulation of PDMS-*b*-PMOXA polymersomes for targeted drug delivery to hepatocytes and assessed potential toxicity of the resulting polymersomes. As a hepatocyte specific target, we chose the ASGPR. Its naturally occurring ligand asialofetuin, was selected as targeting moiety [9,12] and was covalently attached to PDMS-*b*-PMOXA polymersomes. We investigated the specific cellular uptake of AF modified polymersomes and we confirmed their biocompatibility *in vitro* using the human hepatocarcinoma derived HepG2 cell line. In addition, we used zebrafish embryos as a vertebrate model to assess *in vivo* toxicity [26,27].

2. Materials and methods

2.1. Materials

Poly(dimethylsiloxane)$_{67}$-block-poly(2-methyloxazoline)$_{15}$ and amino end functionalized poly(dimethylsiloxane)$_{67}$-block-poly

(2-methyloxazoline)$_{15}$-NH$_2$ diblock copolymers (PDMS-*b*-PMOXA and PDMS-*b*-PMOXZ-NH$_2$, respectively) were obtained from Polymer Source Inc. (Montreal, Canada). Asialofetuin type II, fetuin, N -ethyl-N'-(3-dimethylaminopropyl)carbodiimide hydrochloride (EDAC), 2-iminothiolane, 5(6)-carboxyfluorescein, Hoechst 33342, and other reagents were of analytical grade and were obtained by Sigma-Aldrich (Buchs, Switzerland). 3-(4,5-dimethylthiazol-2-yl)-2,5-diphenyltetrazolium bromide (MTT) and dimethylsulfoxide (DMSO) were of analytical grade and purchased from Carl Roth GmbH (Karlsruhe, Germany). HiLyte Fluor 488 NHS ester was obtained from Anaspec Inc. (Fremont, CA, USA). p-maleimidophenyl isocyanate was obtained from Thermo Fisher (Zug, Switzerland).

Amicon Ultra-4 centrifugal filters (MWCO of 30 kDa and100 kDa) were from Sigma Aldrich (Buchs, Switzerland). Whatman Nucleopore Polycarbonate filters were from VWR International GmbH (Dietikon, Switzerland). Spectra/Pore dialysis membranes (MWCO 3.5 kDa and 14 kDa) were from Carl Roth GmbH (Karlsruhe, Germany). Superose 6 prep grade was from GE Healthcare (Otelfingen, Switzerland).

Rabbit anti-EEA1 (Ab2900) and rabbit anti-LAMP1 (Ab24170) polyclonal antibodies were obtained from abcam (Cambridge, UK), goat anti-rabbit Dylight 633 conjugate and CellMask deep red plasma membrane stain were from ThermoFisher Scientific (Waltham, MA, USA).

Dulbecco's modified Eagle medium (DMEM, high glucose), Dulbecco's phosphate buffered saline (DPBS without calcium and magnesium, pH 7.2), 0.25% Trypsin/EDTA, 100× Penicillin/ Streptomycin solution, and poly-ᴅ-lysine hydrobromide (MW 70,000–150,000) were obtained from Sigma Aldrich (Buchs, Switzerland). Fetal calf serum was purchased from Amimed (Bioconcept, Allschwil, Switzerland).

2.2. Formulation of polymersomes

Polymer vesicles were prepared using the thin film rehydration method as described by Egli et al. [19]. For rehydration of the polymer film DPBS was used and the resulting opalescent suspension was consecutively extruded through a series of polycarbonate filters with an average pore diameter of 0.4, 0.2 and 0.1 μm (each 5 extrusions; LipEx 10 mL extruder, Transferra Nanosciences Inc., BC, Canada).

2.3. Coupling of asialofetuin or fetuin to polymersomes

1.5 mg asialofetuin (AF) or fetuin (F) were dissolved in 500 μL DPBS/1 mM EDTA, pH 8.0. To thiolate the proteins, a 430-fold molar excess of 2-iminothiolane (Traut's reagent) was added and the reaction was carried out under stirring (350 rpm) at RT for 1 h. The resulting thiolated proteins were purified using Amicon Ultra-4 centrifugal filter units (MWCO 30 kDa) and concentrated to approximately 120 μL in DPBS/1 mM EDTA.

In parallel, PDMS-*b*-PMOXA polymersomes (1 mL, 5 mg/mL) were activated by adding 10 μL of p-maleimidophenyl isocyanate solution (7.84 mM). The reaction was carried out overnight at RT with stirring (350 rpm). Unreacted p-maleimidophenyl isocyanate was removed using Amicon Ultra-4 centrifugal filter units (MWCO 100 kDa) and the final maleimide activated polymersomes were re-suspended in 1 mL DPBS/1 mM EDTA.

Proteins were then covalently linked to the polymersomes via Michael addition. 1 mL of activated polymersome suspension was mixed with the thiolated proteins (120 μL) and stirred (350 rpm) at RT overnight. The resulting protein modified polymersomes were purified by gel filtration chromatography (Superose 6 Prep grade, elution buffer DPBS). Polymersome containing fractions were pooled and re-concentrated to a final volume of 1 mL in DPBS

using Amicon Ultra-4 centrifugal filters (MWCO 100 kDa). The final polymersomes (5 mg/mL) were stored at 4 °C.

2.4. Fluorescent labeling of unmodified polymersomes

To label unmodified polymersomes with HiLyte Fluor 488, 17.5 mg PDMS-*b*-PMOXA was mixed with 7.5 mg PDMS-*b*-PMOXZ-NH$_2$ and dissolved in 5 mL ethanol. Subsequent polymersome formation and extrusion was performed as described above. 1 mL of the resulting NH$_2$-functionalized polymersomes (5 mg/mL) was combined with 72 µL EDAC stock solution (1 mg/mL in H$_2$O) and 4.1 µL of HiLyte Fluor 488 NHS ester solution (20 mg/mL in DMSO). The labeling reaction was carried out with stirring (500 rpm) at RT overnight. Unbound dye was removed by dialysis (MWCO 14 kDa) against DPBS.

2.5. Fluorescent labeling of asialofetuin and fetuin, coupling to polymersomes

For the labeling reaction, 1.5 mg of AF or F were dissolved in 0.5 mL of 0.05 M borate buffer, pH 8.5. Next, 50 µL EDAC stock solution (1 mg/mL in H$_2$O) and 10 µL of HiLyte Fluor 488 NHS ester solution (20 mg/mL in DMSO, 10-fold molar excess) were added to the protein solutions. The labeling reactions were carried out with stirring (350 rpm) at RT for 1 h. Unbound dye was removed using Amicon Ultra-4 centrifugal filters (MWCO 30 kDa) and labeled proteins were re-suspended in 0.5 mL DPBS/1 mM EDTA, pH 8.0. HiLyte Fluor 488 labeled proteins were then thiolated and covalently linked to p-maleimidophenyl isocyanate activated PDMS-*b*-PMOXA polymersomes as described in the previous section. All steps were carried out with light protection.

2.6. Encapsulation of carboxyfluorescein and release assay

PDMS-*b*-PMOXA polymersome formulation was performed as described in Section 2.2. However, to incorporate carboxyfluorescein (CF) into the polymersomes we used 15 mM 5(6)-carboxyfluorescein in DPBS for rehydration of the polymer film. Unincorporated CF was removed by extensive dialysis (MWCO 14 kDa) against DPBS at 4 °C. All steps were performed under light protection. The loading capacity was determined after particle disruption with 50% DMSO by fluorescence measurement (λex = 490 nm and λem = 520 nm; SpectraMax M2e, Molecular Devices, Sunnyvale, CA, USA).

To determine the *in vitro* CF release, we used a micro dialysis device (MWCO 3.5 kDa). Briefly, 200 µL samples were dialyzed against 5 mL release buffer at 4 °C, RT (23 °C), or at 37 °C. At indicated intervals 200 µL samples were withdrawn from the buffer compartment and the relative fluorescent intensity of the released CF was measured. After each measurement the samples were returned to the acceptor compartment to keep the volume constant.

2.7. Characterization of polymersomes

Dynamic light scattering (DLS) and Zeta potential measurement were carried out using the Delsa™ Nano C particle sizer (Beckman Coulter Inc., Nyon, Switzerland). Size distribution was analyzed using the CONTIN algorithm (DelsaNano UI software version 3.73/2.30, Beckman Coulter Inc.) and zeta potential was assessed using the Smoluchowski equation [28].

For cryogenic transmission electron microscopy (Cryo-TEM) analysis, a suspension of polymersomes (5 mg/mL) in DPBS was deposited on glow-discharged holey carbon grids (Quantifoil 3.5/1, Cu 200 mesh, Grosslöbichau Germany) and blotted 1 s before plunge freezing in liquid ethane using a Vitrobot mark4 device

(FEI Co., Hillsboro, OR, USA). The frozen grids were stored in liquid nitrogen before transferring them into a cryo-holder (Gatan, Pleasanton, CA, USA). A Philips CM200 FEG TEM at 200 kV accelerating voltage in low-dose mode was used for analysis (Philips, Amsterdam, Netherlands).

2.8. Cell culture

The liver hepatocarcinoma cell line HepG2 was cultured in DMEM high glucose (4500 mg/L) supplemented with 10% fetal calf serum, and Penicillin-Streptomycin. Cells were incubated routinely in a humidified CO$_2$-incubator (5% CO$_2$) at 37 °C.

2.9. In vitro uptake and flow cytometry

HepG2 cells were seeded into 12 well plates (5×10^5 cells/well) and allowed to adhere overnight. The next day the medium was replaced and the cells were incubated with different HiLyte Fluor 488 labeled PDMS-*b*-PMOXA polymersome formulations (1 mg/mL diluted in medium). For competitive inhibition, the cells were pre-incubated for 1 h with an excess of free AF (final concentration 1 mg/mL), before adding the polymersomes. After indicated incubation periods the cells were detached with 2.5% trypsin/EDTA and cellular uptake was analyzed by flow cytometry using a FACS Canto II (BD Bioscience, San Jose, CA, USA). Data were analyzed using FlowJo V9/X software (TreeStart, Ashland, OR, USA).

2.10. In vitro uptake and confocal laser scanning microscopy

HepG2 cells (5×10^5 cells/well) were seeded on poly-D-lysine-coated ibidi 4 well µ-slides (Vitaris AG, Baar, Switzerland) and exposed to different HiLyte Fluor 488 labeled polymersome formulations as described in the previous section. After 4 h of incubation, nuclei were counterstained with Hoechst 33342 (1 µg/mL) and cells were incubated with CellMask Deep Red plasma membrane stain (0.5 µg/mL). Cells were analyzed immediately by confocal laser scanning microscopy using an Olympus FV-1000 inverted microscope (Olympus LtD., Tokyo, Japan) equipped with a 60× UPlanFL N oil-immersion objective (NA 1.40). Images were processed using Olympus FluoView software (v3.1).

2.11. Intracellular localization

HepG2 cells were seeded into 12 well plates (2×10^5 cells/well) on poly-D-lysine-coated glass cover slips (# 1.5, Menzel, Braunschweig, Germany) and allowed to adhere over night. Next day the medium was replaced and cells were incubated for the indicated periods of time with HiLyte Fluor 488-labeled AF modified polymersomes (1 mg/mL diluted in cell culture medium).

Cells were fixed with 2% PFA (RT, 15 min) and blocked with 5% BSA in DPBS. Immunostaining was performed over night at 4 °C with rabbit anti-EEA1 (early endosomes, 1:500 in 5% BSA) or rabbit anti-LAMP1 (lysosomes, 1:500 in 5% BSA), followed by the detection antibody goat anti-rabbit Dylight 633 (1:1000 in 5% BSA). The nuclei were counterstained with Hoechst 33342 (1 µg/mL). Images were acquired on an Applied Precision widefield DeltaVision Core Microscope (GE Healthcare, Otelfingen, Switzerland) with a CoolSNAP HQ2 camera, a 60× Plan Apo oil objective (NA 1.4), and softWoRx image acquisition software. Pearson's correlation coefficient (PCC) was calculated using ImageJ software with the JACoP ImageJ plugin.

2.12. MTT cell viability assay

Cell viability of HepG2 cells incubated with different concentrations of unmodified PDMS-PMOXA polymersomes was measured

using the MTT-assay as described elsewhere [20]. Absorbance measurements were performed in a 96 well micro-titre plate reader at 540 nm (SpectraMax M2e).

2.13. Zebrafish housing and breeding

All procedures on live zebrafish (*Danio rerio*) were carried out following the Swiss legislation on animal welfare. The zebrafish wildtype line AB/Tübingen was kindly provided by Prof. M. Affolter (Biozentrum, Universty of Basel, Switzerland) and were maintained at standard conditions as described elsewhere [29]. Eggs were obtained by random mating of three adult males and four females in small breeding tanks. Fertilized zebrafish eggs were collected the next day, transferred to $0.5\times$ E2 medium [29], and maintained at 28 °C. Healthy embryos were selected under a Leica S8APO stereomicroscope (Leica Microsystems AG, Heerbrugg, Switzerland) within 4 h post fertilization (hpf). All embryos used in one experiment were derived from the same spawn of eggs to allow for direct statistical comparison between treated and control groups.

2.14. Assessment of toxicity using zebrafish embryos

To assess embryonic toxicity, healthy zebrafish embryos (4 hpf) were incubated in 24 well plates containing 500 µg polymersomes/mL of the different polymersome formulations diluted in $0.5\times$ E2 medium or $0.5\times$ E2 medium as untreated control. Each sample and replicate consisted of 30 embryos in a 24 well plate (6×5 embryos). The embryos were transferred daily to new wells containing fresh test solutions. Every 24 h, all embryos were examined under the stereomicroscope for mortality, morphological abnormalities, and hatching rate. The experiments were terminated 96 hpf when most embryos have hatched. To study the consequences of dechorionation on toxicity, the chorion of 24 hpf embryos was removed before exposure to the different polymersome formulations.

2.15. Statistical analysis

Results are expressed as means ± standard deviation (SD), $n \geq 3$. Wherever indicated, significance was determined by one-way analysis of variance (ANOVA) followed by Bonferroni's *post hoc* test using OriginPro (Version 9.1.0, OriginLab Corporation, Northampton, MA, USA). Statistically significant values ($p < 0.01$) were marked with an asterisk.

3. Results

3.1. Characterization of PDMS-b-PMOXA polymersomes

In the present study, we developed asialofetuin (AF) modified polymersomes as nanocarriers for active targeting of hepatocytes. The polymersomes were composed of the amphiphilic diblock copolymer PDMS-*b*-PMOXA and were formulated using the film rehydration method as described earlier [19]. In order to obtain targeted polymersomes, unmodified PDMS-*b*-PMOXA polymersomes were activated and covalently functionalized with thiolated AF via Michael addition as shown in Fig. 1. For visualization in targeting studies, AF was first labeled with HiLyte Fluor 488 prior to thiolation and coupling to the polymersomes. As a negative control, fetuin (F) modified polymersomes were synthesized using the same chemical strategy.

All PDMS-*b*-PMOXA polymersome variants were routinely analyzed by DLS for average size and size distribution. The results and the abbreviation used for the different formulations are

summarized in Table 1. The average of the mean hydrodynamic diameters of individual polymersome formulations were between 148.4 nm and 161.3 nm and the polydispersity indexes (PDI) varied between 0.082 and 0.175. The different modifications did not significantly alter polymersome size ($p < 0.01$). The PDI values were less than 0.2 in all formulations, suggesting monodispersity of the preparations. Zeta-potentials were slightly negative and stayed in the range of -1.3 mV to -5.9 mV (measured in DPBS).

The different polymersome formulations were also analyzed by Cryo-TEM to confirm size and vesicle morphology (Fig. 2A). Cryo-TEM clearly shows hollow spheres with an average membrane thickness 19.6 ± 2.5 nm (n = 104). The average diameters of the polymersomes were 122.1 ± 33.1 nm (n = 58, unmodified PPs), 131.3 ± 25.5 nm (n = 35, PP-F), and 117 ± 21.9 nm (n = 33, PP-AF). The corresponding PDIs varied between 0.03 and 0.086, and were calculated as PDI = $(SD/mean)^2$ [30]. The variability observed in the average diameter as compared to DLS measurement is due to intrinsic differences in the used techniques. Cryo-TEM analysis is performed with the polymersomes in a frozen state that conserves the native structure of the polymersomes. DLS measures the hydrodynamic diameter, which takes the hydration layer surrounding the polymersomes into account, resulting in apparent larger diameters.

The integrity of the particles was tested under forced stress conditions. Unmodified PDMS-*b*-PMOXA polymersomes were diluted in DPBS, 3% BSA/DPBS, or 50% FCS/DPBS and incubated for 7 d at 37 °C. Average size and size distribution were analyzed by DLS. As outlined in Fig. 2B no statistically significant changes in particle diameters occurred over time. A slight increase in apparent size (approximately 15%) was recognized in samples that were exposed to 3% BSA or 50% FCS, which possibly can be explained by changes in the hydration layer due to protein binding. The calculated PDIs stayed below 0.2 over the 7 d of exposure indicating stability of the polymersomes at the tested conditions. In addition, the polymersomes could be stored in DPBS at 4 °C for at least 4 months without significant change in particle size and PDI, and without loss of functionality as confirmed by cellular uptake experiments (data not shown).

3.2. Encapsulation of carboxyfluorescein and release profile

We used CF as a hydrophilic model compound to test for drug loading and release from polymersomes. CF was encapsulated into PDMS-*b*-PMOXA polymersomes by the thin film hydration method. The resulting PP-CFs were analyzed by DLS for size and size distribution (Table 1). The zeta-potential remained close to neutrality (-5.9 mV). The calculated loading capacity of CF was 1.5 ± 0.2 nmol CF per mg of polymersomes.

The release of CF from the polymersomes into DPBS at different temperatures was monitored using a micro dialysis setup. The cumulative release profiles of CF are shown in Fig. 2C. In DPBS CF release was temperature dependent and occurred in a slow and sustained manner over a long period of time. No initial burst release was observed at any of the tested temperatures and no plateau was reached within the duration of the experiment (96 h). CF release at 37 °C reached $7.7 \pm 1.3\%$ after 8 h, the curve flatted then slightly and continued to reached $17.8 \pm 1.8\%$ after 24 h and $45.1 \pm 2.0\%$ at 96 h. At RT (23 °C) a similar curve was found, however, the maximal release at 96 h was $23.5 \pm 1.8\%$. At 4 °C, $7.8 \pm 2.6\%$ of the encapsulated CF was recovered from the acceptor compartment after 96 h.

At this point, the release profiles were evaluated in buffers containing naturally occurring serum proteins. CF release was tested in 3% BSA/DPBS and in 50% FCS/DPBS for 48 h at 37 °C. During the first 24 h, the release profiles of CF in protein containing buffers were similar to DPBS alone (statistically no significant difference),
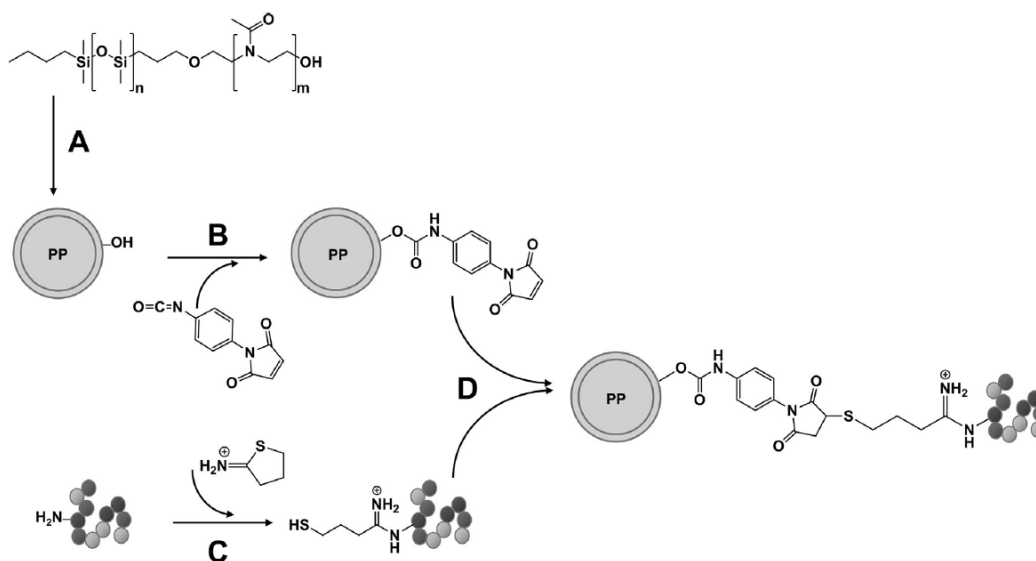
Fig. 1. Preparation of asialofetuin targeted PDMS-*b*-PMOXA polymersomes. (A) Formulation of PDMS-*b*-PMOXA polymersomes (PP) using the thin film rehydration method. (B) Modification of the polymersomes' surface using p-maleimidophenyl isocyanate in order to obtain maleimide-functionalized polymersomes and (C) in parallel thiolation of proteins (asialofetuin or fetuin) using 2-iminothiolane (Traut's activation). (D) Finally, maleimide-functionalized polymersomes and Traut's modified proteins are covalently linked via Michael addition to achieve protein-decorated polymersomes.

Table 1
Size and polydispersity index of PDMS-*b*-PMOXA based polymersomes.

Abbreviation	Full name of polymersome	Diameter (nm)	PDI
PP	PDMS-PMOXA polymersome	156.9 ± 8.8	0.082 ± 0.041
PP-F	PP modified with F	155.4 ± 15.0	0.097 ± 0.015
PP-AF	PP modified with AF	149.8 ± 7.9	0.103 ± 0.019
PP-488	PP modified with HiLyte Fluor 488	161.3 ± 10.2	0.175 ± 0.057
PP-F-488	PP modified with HiLyte Fluor 488 labeled F	148.4 ± 6.3	0.098 ± 0.039
PP-AF-488	PP modified with HiLyte Fluor 488 labeled AF	149.3 ± 1.5	0.098 ± 0.027
PP-CF	PP loaded with CF	155.9 ± 17.5	0.133 ± 0.034

Hydrodynamic diameters (DLS-intensity peaks) and polydispersity index (PDI) of different polymersome formulations were measured by dynamic light scattering (DLS). Measurements were performed in DPBS. Data represent mean values ± SD (n = 5). Abbreviations used for the different formulations are indicated.

however, after 48 h, the release of CF in 3% BSA/DPBS or 50% FCS/DPBS was significantly lower than in DPBS alone (see supplementary information S1).

3.3. Targeted delivery of asialofetuin modified polymersomes to HepG2 cells

We used AF modified polymersomes to specifically target the ASGPR on hepatic cells. AF is a naturally occurring ligand of the ASGPR in which the terminal sialic acids are removed, leaving several bi- and tri-antennary glycans that bind with high affinity to the ASGPR [31]. As a negative control we used F, which still contains sialic acid modifications that prevent binding to the ASGPR.

In order to visualize polymersomes *in vitro*, we labeled the conjugated targeting-proteins (AF or F). The resulting PP-AF-488 and PP-F-488 vesicles were analyzed by DLS to ensure similar size and monodispersity (Table 1). Fluorescence correlation spectroscopy (FCS) has been performed as described earlier [32] and was used to determine the protein labeling efficiency and to assess the number of labeled protein molecules conjugated per molecule of unmodified polymersome (see supplementary information S2). Our results indicate a labeling efficiency of two fluorophores per molecule AF or F, and a coupling efficiency of 17 molecules of AF-488 per PP-AF-488 and eleven molecules of F-488 per PP-F-488.

To study targeted uptake, HepG2 cells were incubated with PP-488, PP-F-488, and PP-AF-488. After 1, 2, or 4 h incubation at 37 °C, the cells were detached by trypsinization, and cellular uptake was analyzed by flow cytometry. For quantification and better visualization, mean fluorescence intensities (MFI) were normalized to untreated control cells (Fig. 3). Cells incubated for 4 h with unmodified PP-488 showed only a minor increase in MFI of 2.5 ± 0.06 as compared to control cells. In contrast, if the cells were incubated with PP-AF-488 for 4 h, a significant gradual increase in MFI was observed from 1 h (MFI = 2.8 ± 0.03), 2 h (MFI = 6.1 ± 0.06) to 4 h (MFI = 13.5 ± 0.17), indicating an ASGPR mediated uptake mechanism.

To further demonstrate ASGPR specific uptake of PP-AF-488, we pre-incubated HepG2 cells with an excess of unlabeled AF (1 mg/mL). Competitive inhibition of uptake was visualized by confocal laser scanning microscopy (Fig. 4A). After 4 h of incubation at 37 °C, a distinct intracellular pattern of fluorescent particles was observed in HepG2 cells that were incubated with PP-AF-488. No such signal was detectable in cells that were incubated with untargeted PP-488 or which were pre-incubated with free unlabeled AF. In addition, no uptake of fluorescent particles occurred at 4 °C. To quantify cellular uptake of the fluorescent particles under the different conditions, the cells were analyzed by flow cytometry. The measured mean fluorescence intensities (MFI) were normalized to untreated control cells (Fig. 4B). Again, free AF inhibited uptake of PP-AF-488 and the MFI decreased from 13.5 ± 0.17 (PP-AF-488) to 2.7 ± 0.05 (PP-AF-488 pre-incubated with free AF), which is the
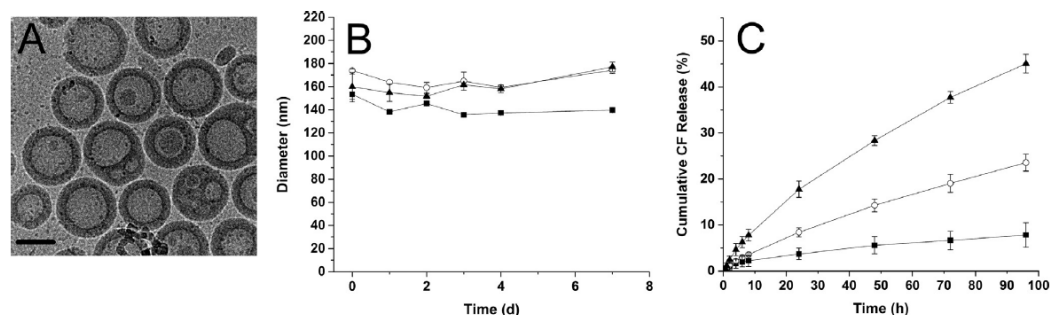
Fig. 2. Characterization of PDMS-b-PMOXA polymersomes by cryogenic transmission electron microscopy (Cryo-TEM) and drug release profiles. (A) Cryo-TEM image of unmodified PDMS-b-PMOXA polymersomes shows the formation of hollow spheres. Scale bar = 100 nm. (B) Stability of PDMS-b-PMOXA polymersomes in different buffers at 37 °C. Changes in hydrodynamic diameters (DLS-intensity peaks) were measured by dynamic light scattering (DLS). Black squares: DPBS, open circles: 3% BSA/DPBS, and black triangles: 50% FCS/DPBS. Values are means ± SD (n = 3). (C) Cumulative release profile of carboxyfluorescein from polymersomes in DPBS. Carboxyfluorescein release was measured at different temperatures. Black triangles: 37 °C, open circles: RT (23 °C), and black squares: 4 °C. SD is shown with error bars (n = 3).
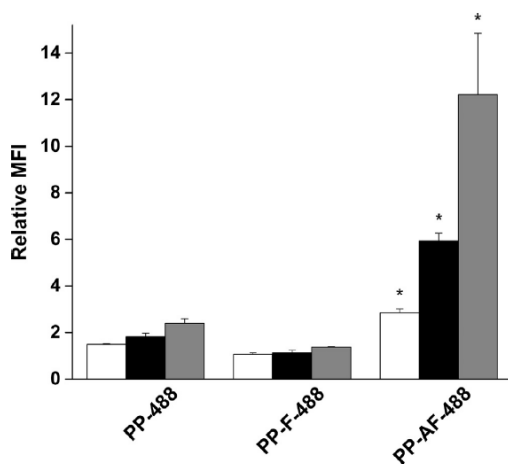
Fig. 3. Time dependent cellular uptake of targeted and non-targeted polymersomes. HepG2 cells were incubated with PP-488, PP-F-488, and PP-AF-488 for 1 h (white), 2 h (black), and 4 h (grey). Cells were analyzed by flow cytometry to quantify uptake of the differently modified polymersomes. Mean fluorescence intensity (MFI) was normalized to untreated control cells. SD is shown with error bars (n = 3), *p < 0.01.

level of non-targeted PP-488 (MFI = 2.5 ± 0.06). Moreover, low temperature (4 °C) completely inhibited PP-AF-488 internalization (MFI = 1.1 ± 0.02).

3.4. Intracellular localization

To determine the subcellular localization of AF targeted polymersomes, HepG2 cells were incubated with PP-AF-488 for 1, 2, and 4 h, followed by staining with anti-human EEA1 antibodies or anti-human LAMP1 to detect early endosomes or lysosomes, respectively. Within the first 2 h, PP-AF-488 mainly co-localized with EEA1 (Fig. 5A). After 4 h, colocalization with EEA1 decreased markedly, whereas colocalization with LAMP1 has increased over time and peaked at 4 h (Fig. 5B).

To quantify the colocalization of PP-AF-488 with early endosomes and lysosomes the Pearson's correlation coefficients (PCC) [33] were calculated. This coefficient describes the degree

of correlation of the fluorophore signals, in our case HiLyte Fluor 488 for PP-AF-488 and Dylight 633 for the detection of EEA1 and LAMP1. The PCCs for colocalization of PP-AF-488 with EEA1 and LAMP1 are shown in Fig. 5C. After 1 and 2 h of exposure of PP-AF-488 to HepG2 cells, the calculated PPCs for EEA1 (early endosomes) were 0.511 ± 0.158 (1 h), and 0.606 ± 0146 (2 h), while after 4 h it decreased to 0.281 ± 0.035. On the other hand, the calculated PCCs for LAMP1 (lysosomes) gradually increased from 0.178 ± 0.110 (1 h), to 0.389 ± 0.159 (2 h), to 0.545 ± 0.087 (4 h).

3.5. Assessment of cell viability in vitro – MTT assay

Unmodified PDMS-b-PMOXA polymersomes have been shown to be non-toxic in HepG2 cells up to 300 μg/mL [20]. In this study, we functionalized polymersomes with AF and F. To ensure that these surface modifications did not alter cell viability, we performed MTT cell viability assays using HepG2 cells. Cell viability was normalized to untreated cells (100% viability, negative control). As a positive control, HepG2 cells were exposed to 40 μM Terfenadine (5.01 ± 0.52% cell viability, data not shown). There was no major loss in cell viability in HepG2 cells after incubation for 24 h with the different PP-formulations (25–500 μg/mL, Fig. 6). Calculated cell viability was between 79.96 ± 4.57% and 99.41 ± 7.19% (normalized to untreated control cells) for all tested formulations up to 500 μg/mL.

3.6. Cytotoxicity in vivo in zebrafish

To investigate whether our polymersomes exhibit adverse effects in vivo, zebrafish embryos were exposed for 4 d (starting 4 hpf) to the different PP-formulations. Nanoparticles were diluted in 0.5× E2 embryo medium to a final concentration of 500 μg/mL, which was the highest polymersome concentration tested in vitro and was shown to be non-toxic in HepG2 cells. The integrity of the nanoparticles in 0.5× E2 medium was confirmed by measuring hydrodynamic diameter and PDI using DLS. To avoid bacterial contaminations and to investigate cumulative effects of the PP-formulations on zebrafish development, the medium containing the respective nanoparticles was changed daily. Zebrafish embryos were examined every 24 h up to 96 hpf for malformations such as yolk sac edema, pericardial edema, tail and head malformations. In addition, hatching and survival rates were monitored. Fig. 7A shows percentage of cumulative mortality, malformations, and hatching rate at 96 hpf. Mean mortality rate was less than 2.5% and less than 5% of all larvae showed malformations (mostly
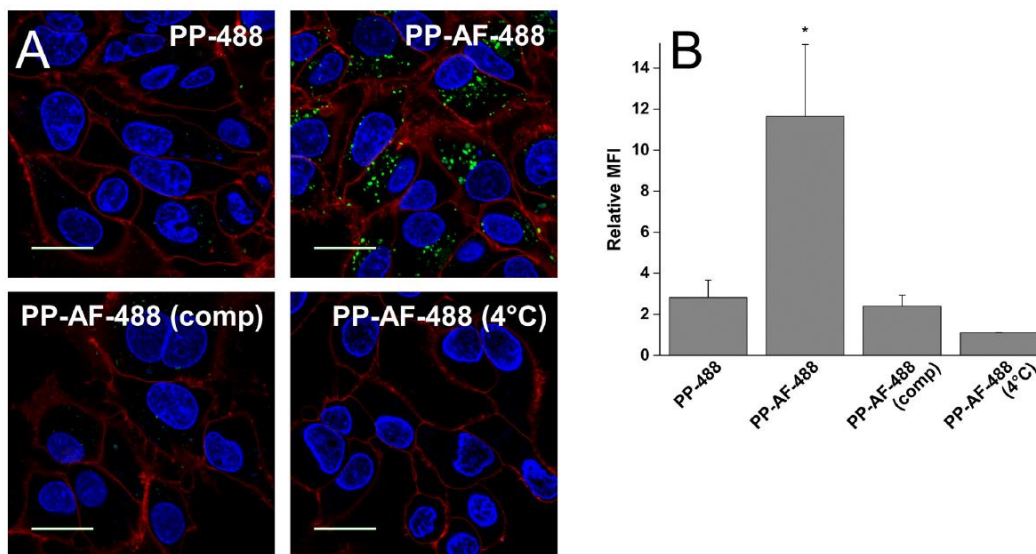
Fig. 4. Asialoglycoprotein receptor specific uptake of PP-AF-488 by HepG2 cells. PP-488 (negative control) and PP-AF-488: cells were incubated with the indicated polymersomes for 4 h at 37 °C. PP-AF-488 (comp): for competitive inhibition studies HepG2 cells were pre-incubated for 1 h with an excess of free asialofetuin prior to adding PP-AF-488. PP-AF-488 (4 °C): HepG2 cells were incubated at 4 °C in the presence of PP-AF-488. (A) Confocal laser scanning microscopy. Nuclei are stained with Hoechst 33342 (blue) and cell membranes are stained with CellMask Deep Red plasma membrane stain (red). HiLyte Fluor 488 labeled polymersomes (PP-488, PP-AF-488) are visualized in green. Scale bar = 20 μm. (B) Uptake determined by flow cytometry is shown as mean fluorescence intensity (MFI) normalized to untreated control cells. SD is shown with error bars (n = 3), *p < 0.01.
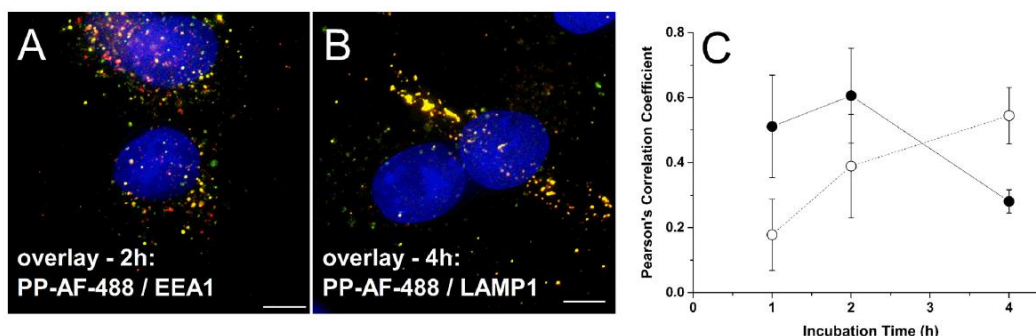
Fig. 5. Intracellular trafficking of PP-AF-488 in HepG2 cells. Cells were exposed to PP-AF-488 and intracellular localization of the particles was visualized by specific immunostaining of subcellular organelles. anti-EEA1 antibodies were used to visualize early endosomes and anti-LAMP1 antibodies were used to stain lysosomes. (A) Colocalization of PP-AF-488 with EEA1 in HepG2 cells after 2 h of incubation and (B) colocalization of PP-AF-488 with LAMP1 in HepG2 cells after 4 h of incubation. Nuclei are stained blue (Hoechst 33342), PP-AF-488 particles are in green (HiLyte 488), and respective subcellular organelles endosomes are red (Dylight 633). Yellow dots: Colocalization of PP-AF-488 and the respective organelle. Scale bar = 5 μm. (C) Pearson's correlation coefficients for PP-AF-488 and EEA1 (black circles), and PP-AF-488 and LAMP1 (open circles, dotted line). Cellular trafficking of asialofetuin modified polymersomes from early to late endosomes within 4 h is shown. SD is shown with error bars (n = 5).

pericardial edema, sometimes combined with a bent tail, Fig. 7B + C). There was no statistical significant difference between all tested conditions. A slight delay in pigmentation was observed 48 – 52 hpf in the embryo group that was exposed to the unmodified PPs. However, these embryos "catched up" and normal development was restored at 72 hpf. At 96 hpf more than 95% of the larvae had hatched. As outlined in Fig. 7A, no major differences in the hatching rates were observed.

To exclude perturbing effects by the chorion that surrounds the developing zebrafish, embryos were dechorionized (24 hpf) prior

to exposing them to the different PP-formulations. The medium was replaced daily and the developing embryos were observed for survival and malformations. In accordance with the previous experiment, no difference regarding malformations and overall survival were observed (data not shown).

4. Discussion

For effective hepatocyte specific drug delivery, polymersomes must present several specific characteristics [13,34,35]. The
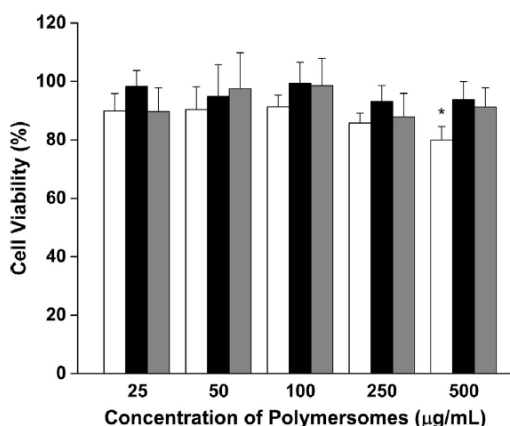
Fig. 6. MTT-assay. Cell viability of HepG2 cells after incubation for 24 h with increasing concentrations of differently modified PPs: PP (white), PP-F (black), PP-AF (grey). Cell viability is expressed as % viable cells relative to untreated control cells (100%). SD is shown with error bars (n = 8), *p < 0.01.

particles should be small in size to pass hepatic fenestration and reach their targets. They must be capable for drug loading and release, and should be stable enough to prevent premature loss of cargo. To target specific organs or cells, the core material should be versatile and allow surface modification with ligands for a targeted uptake. Finally, the polymersomes must be non-toxic, and upon injection into the bloodstream they should avoid opsonization in order to increase circulation half-life.

4.1. Characterization of polymersomes

In this paper, we present the development of stable polymersomes based on the block-copolymer PDMS-*b*-PMOXA. We

covalently modified them with AF for hepatocyte specific cell targeting. The resulting polymersomes were of similar size and all formulations had a hydrodynamic diameter around 150 nm. This size makes our polymersomes suitable for liver targeting as it is still sufficient to pass the numerous open fenestrations in the endothelial lining of the sinusoids (average diameter approximately 150 nm) and to have access to hepatocytes located beneath [36]. The zeta potential of our polymersomes was slightly negative (-1.3 mV to -5.9 mV). This is ideal, since highly positively charged nanoparticles tend to exhibit a higher cytotoxicity than negatively charged particles [37]. In addition, cationic nanoparticles are less suitable for *in vivo* use since they rapidly accumulate in the lung after intravenous injection [38].

Our polymersome formulations were stable for at least 4 months if stored in DPBS at 4 °C, confirming previous observations using vesicles formed by a similar block copolymer (PMOXA-*b*-PDMS-*b*-PMOXA) [39].

4.2. Encapsulation of carboxyfluorescein and release

Most nanomedicines have to be injected into systemic blood circulation. Therefore, membrane stability is a desirable characteristic for drug containing vesicles and it helps to control drug release in order to prevent premature, i.e., unwanted loss of cargo. Polymersomes are known to be less permeable for a variety of molecules compared to liposomes. For example, they are an order of magnitude less permeable to water than liposomes [40]. To demonstrate that PDMS-*b*-PMOXA forms tight vesicles, we encapsulated CF into polymersomes and subsequently measured CF release into DPBS at different temperatures over a period of 96 h. As a result, we showed a sustained CF release at 37 °C, but only minor leakage at 4 °C. Recently, Figueiredo et al. [21] encapsulated doxorubicin into PDMS-*b*-PMOXA polymersomes. In contrast to our findings they observed a burst effect within the first 4 h (29% release) and reached a maximal release of 40% within 48 h. This observation might be due to differences in the physico-chemical
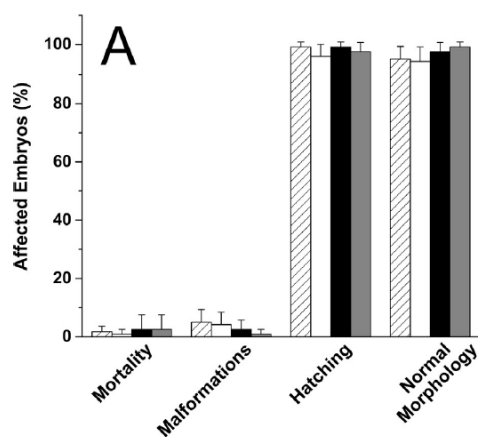
Fig. 7. Toxicity of differently modified polymersomes in zebrafish (96 hpf). (A) Percentages of mortality in the early zebrafish larvae, larvae affected by morphological malformations, hatching rate, and larvae with normal morphology are shown. The following polymersome formulations were tested and compared to control (no polymersomes, shaded): PP (white), PP-F (black), and PP-AF (grey). Values are means ± SD (n = 30). (B, C) Representative images of zebrafish embryos 96 hpf. Panel B: embryo with normal morphology, Panel C: embryo with malformations (PE pericardial edema, TM tail malformation). Scale bar = 1 mm.
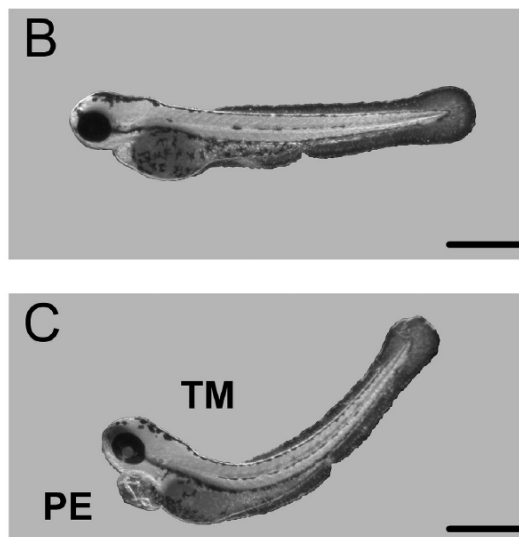
properties of the encapsulated compounds (CF versus doxorubicin) that could result in different release profiles. On the other hand, differences in block co-polymer composition used for drug encapsulation and in purification protocols may lead to altered membrane permeability for the encapsulated compounds [21].

Using the standard thin film rehydration method the achieved loading capacity of CF in PDMS-b-PMOXA polymersomes was low. However, to achieve therapeutic effects, alteration of pharmacokinetics is the most important factor, since already a low percentage of nanoparticles delivered to the diseased tissue may offer a benefit to the patients [41]. Nanoparticles can shift the balance in off- and on-target accumulation thereby reducing severe side effects of encapsulated drugs [41]. Nevertheless, to improve encapsulation efficiency, alternative encapsulation methods can be used [15]. For example, the encapsulation efficiency of Doxorubicin was 3-fold higher using the co-solvent method (13%) compared to the film rehydration method (4%) [21]. A more recent technology, namely microfluidics, represents a sophisticated way for solvent-switch that combines vesicle formation and drug loading at the same time. Microfluidics has been used to encapsulate doxorubicin or the poorly water-soluble propofol into liposomes with high efficiency exceeding standard encapsulation technologies [42,43].

4.3. Asialoglycoprotein receptor specific uptake by HepG2 cells and endosomal trafficking

An essential step during drug delivery is the cell specific uptake of nanocarriers and their intracellular localization. To decrease side effects, avoidance of unspecific uptake of the nanoparticles is a prerequisite for *in vivo* implementation of targeting strategies. As described elsewhere, a prolonged incubation time (24 h) was needed to allow uptake of unmodified PDMS-b-PMOXA polymersomes in HepG2 cells [20]. Therefore, we developed a hepatocyte specific targeting strategy based on the ASGPR, a lectin-type receptor that is highly and predominately expressed on parenchymal liver cells [10]. We showed in this paper that enhanced uptake within 4 h can be achieved by using AF to specifically target polymersomes to the ASGPR. Uptake experiments at 4 °C and competitive inhibition with the free ligand confirmed that cellular uptake of the targeted nanoparticles is an energy-dependent process and specifically mediated by the ASGPR. The ASGPR is a well-characterized receptor that is responsible for clearance of desialylated glycoproteins from circulation by endocytosis. The mechanism of cellular uptake by this receptor was extensively studied [44,45] and comprises receptor binding, internalization via clathrin coated vesicles, fusion with the endosomal compartment and delivery to lysosomes. In the present study, mechanistic studies were carried out to clarify whether binding of AF conjugated nanoparticles to the ASGPR would interfere with the processes of subcellular trafficking. In accordance to the pathway described for free AF [45], internalized AF-targeted particles co-localized with the early endosome and eventually accumulated within the lysosome.

Importantly, the mechanism of cellular entry of nanoparticles and their final sub-cellular distribution can have great influence on the performance of the drug. Lysosomal accumulation will not be a problem for drugs that are stable at the low pH found in lysosomes. Other therapeutics such as nucleic acids, proteins or peptides would be rapidly degraded and inactivated if delivered to the lysosome. With respect to drug delivery, additional technologies might be necessary to promote endosomal escape and to avoid lysosomal degradation of such therapeutics: e.g., co-application of endosomal escape enhancers [46], or modification of the polymer backbone [47,48,16]. An exception could be enzyme replacement therapy, as used for the treatment of lysosomal storage diseases, e.g., Gaucher's disease [49,50]. Encapsulated in PP-AF nanocarriers

the respective enzyme would be protected from degradation and clearance in the blood stream. After AF-targeted uptake and endocytosis, the enzyme would be delivered to the lysosomes and exert its therapeutic effect where it is needed to degrade accumulated disease causing substrates in the liver.

4.4. Cytotoxicity in vitro and in vivo

Clinically successful nanomaterials should be non-toxic and easily eliminated from the body to avoid toxic accumulation and side effects. In the past, various cells lines were exposed to different formulations of PDMS-b-PMOXA based polymersomes and all of them were shown to be non-toxic within the tested concentration range [19–21]. Since toxic effects of nanoparticles not only depend on the nanomaterial itself but also on particle size, shape, surface charge, and surface modifications, every new formulation needs to be tested *de novo* [51,52]. We used the MTT cell viability assay to assess toxic effects of different polymersome formulations on HepG2 cells. For all concentrations and formulations tested cell viability was at least 80%. These data confirm that functionalization did not alter cell viability and thus our polymersome formulations can be considered biocompatible *in vitro*.

However, *in vitro* cytotoxicity assays can only be used to obtain an initial estimate on nanoparticle toxicity. The *in vivo* situation is much more complex and the *in vitro* – *in vivo* correlation is often only moderate [53,54]. Most biological active compounds cause complex responses in animals that cannot be predicted by cell culture models alone. Studies in rodents are expensive, time consuming and require a large number of animals. To overcome these limitations, zebrafish embryos are increasingly used to assess toxic effects *in vivo* [55,56,53]. The zebrafish model offers several advantages such as, small size, high reproducibility, rapid and *ex utero* embryonic development, and almost total transparency up to 120 hpf. The cardiovascular, nervous and digestive systems are similar to mammals. In addition, zebrafish and humans share highly conserved signaling pathways with high level of genomic homology [57,27]. Therefore, zebrafish are becoming increasingly recognized as a vertebrate model for "intermediate" toxicity screening not only for small molecules, but also for nanoparticles before turning to experiments in rodents [55,56,53,54].

Following well-established protocols to assess developmental *in vivo* toxicity, we exposed healthy zebrafish embryos for 96 hpf to the highest concentration of different PP formulations that have been shown to be non-toxic *in vitro* (500 μg/mL). To exclude that the chorion surrounding the developing embryo is protecting the embryos from harmful effects by our nanoparticles, the experiment has been performed with intact embryos and dechorionized embryos. Neither intact nor dechorionized zebrafish embryos showed any signs of toxicity (equal hatching rate, no malformations), suggesting good biocompatibility of our polymersomes. In addition, preliminary experiments indicate that even upon direct injection of our polymersomes into the blood circulation of 72 hpf zebrafish embryos (using a microinjection device) did not result in acute toxicity such as seizures, denaturation of body fluids, or heart failures and the fish survived up to 144 hpf when they were sacrificed (data not shown). We conclude from these experiments that our polymersomes are well tolerated within a typical dose range suggested for use of nanomedicines [58,52].

An important prerequisite for nanoparticle targeting is that they do not activate an inflammatory response, leading to recognition by the mononuclear phagocyte system (MPS) and rapid clearance from blood circulation. It is known that PMOXA can add stealth properties to the surface of nanoparticles allowing prolonged circulation times in the blood stream [23,24,59]. However, there are some conflicting reports concerning induction of inflammation by PMOXA containing nanoparticles. Using the tri-block copolymer

PMOXA-*b*-PDMS-*b*-PMOXA, De Vocht et al. found no immune-stimulatory effect on murine macrophages *in vitro* nor *in vivo* upon intra-peritoneal injection [24]. On the other hand, Kiestead et al. injected rats with PMOXA-modified liposomes and reported induction of an IgM response and enhanced blood clearance upon second injection similar to polyethylene glycol (PEG)-modified liposomes [59]. This effect, called "accelerated blood clearance (ABC) phenomenon", is of clinical concern because it decreases the efficiency of encapsulated drugs. Several approaches to attenuate the induction of the ABC phenomenon have been proposed such as changing the administration scheme or co-encapsulation of drugs with immunosuppressive activity [60]. In terms of our PDMS-*b*-PMOXA polymersomes, further investigations are needed to evaluate the *in vivo* fate of the polymersomes after (repeated) intravenous injection and to study the *in vivo* efficacy of the AF targeting.

5. Conclusions

In this paper we successfully functionalized PDMS-*b*-PMOXA based polymersomes with AF for hepatocyte specific targeting and receptor-mediated endocytosis. *In vitro* experiments confirmed ASGPR specific uptake of AF-functionalized polymersomes by the HepG2 cell line. AF conjugation increased polymersome uptake in HepG2 cells, compared to unmodified polymersomes, without inducing any significant cytotoxicity. Biocompatibility of our polymersome formulations was further confirmed *in vivo* using the zebrafish model. In addition, we encapsulated CF into PDMS-*b*-PMOXA polymersomes and demonstrated a slow and sustained drug release at 37 °C.

In conclusion, we achieved a targeted drug delivery system that is safe and well tolerated *in vitro* and *in vivo*. The possibility for drug encapsulation and release makes it a promising tool for potential clinical applications in the field of hepatology. Further studies are required to investigate its pharmacokinetics and biodistribution in higher vertebrates such as rodents.

Acknowledgements

Appendix A. Supplementary material

Supplementary data associated with this article can be found, in the online version, at http://dx.doi.org/10.1016/j.ejpb.2017.07.002.

References

[1] R. Williams, Global challenges in liver disease, Hepatology 44 (2006) 521–526, http://dx.doi.org/10.1002/hep.21347.
[2] K. Poelstra, J. Prakash, L. Beljaars, Drug targeting to the diseased liver, J. Control. Release. 161 (2012) 188–197, http://dx.doi.org/10.1016/j.jconrel.2012.02.011.
[3] L.H. Reddy, P. Couvreur, Nanotechnology for therapy and imaging of liver diseases, J. Hepatol. 55 (2011) 1461–1466, http://dx.doi.org/10.1016/j.jhep.2011.05.039.
[4] A. Wicki, D. Witzigmann, V. Balasubramanian, J. Huwyler, Nanomedicine in cancer therapy: Challenges, opportunities, and clinical applications, J. Control. Release. 200 (2015) 138–157, http://dx.doi.org/10.1016/j.jconrel.2014.12.030.
[5] S. Tinkle, S.E. Mcneil, M. Stefan, R. Bawa, G. Borchard, Nanomedicines : addressing the scientific and regulatory gap, Ann. N. Y. Acad. Sci. 131 (2014) 35–56, http://dx.doi.org/10.1111/nyas.12403.
[6] E. Pérez-Herrero, A. Fernández-Medarde, Advanced targeted therapies in cancer: drug nanocarriers, the future of chemotherapy, Eur. J. Pharm. Biopharm. 93 (2015) 52–79, http://dx.doi.org/10.1016/j.ejpb.2015.03.018.
[7] P. Grossen, D. Witzigmann, S. Sieber, J. Huwyler, PEG-PCL-based nanomedicines: a biodegradable drug delivery system and its application, J. Control. Release. 260 (2017) 46–60, http://dx.doi.org/10.1016/j.jconrel.2017.05.028.
[8] D.M. Webster, P. Sundaram, M.E. Byrne, Injectable nanomaterials for drug delivery: carriers, targeting moieties, and therapeutics, Eur. J. Pharm. Biopharm. 84 (2013) 1–20, http://dx.doi.org/10.1016/j.ejpb.2012.12.009.
[9] A.A. D'Souza, P.V. Devarajan, Asialoglycoprotein receptor mediated hepatocyte targeting—strategies and applications, J. Control. Release. 203 (2015) 126–139, http://dx.doi.org/10.1016/j.jconrel.2015.02.022.
[10] D. Witzigmann, L. Quagliata, S.H. Schenk, C. Quintavalle, L.M. Terracciano, J. Huwyler, Variable asialoglycoprotein receptor 1 expression in liver disease: Implications for therapeutic intervention, Hepatol. Res. 46 (2016) 686–696, http://dx.doi.org/10.1111/hepr.12599.
[11] S. Díez, I. Miguéliz, C. Tros de Ilarduya, Targeted cationic poly(D,L-lactic-co-glycolic acid) nanoparticles for gene delivery to cultured cells, Cell. Mol. Biol. Lett. 14 (2009) 347–362, http://dx.doi.org/10.2478/s11658-009-0003-7.
[12] P. Detampel, D. Witzigmann, S. Krähenbühl, J. Huwyler, Hepatocyte targeting using pegylated asialofetuin-conjugated liposomes, J. Drug Target. 22 (2014) 232–241, http://dx.doi.org/10.3109/1061186X.2013.860982.
[13] D.E. Discher, F. Ahmed, Polymersomes, Annu. Rev. Biomed. Eng. 8 (2006) 323–341, http://dx.doi.org/10.1146/annurev.bioeng.8.061505.095838.
[14] D.E. Discher, A. Eisenberg, Polymer vesicles, Science 297 (2002) 967–973, http://dx.doi.org/10.1126/science.1074972.
[15] L. Messager, J. Gaitzsch, L. Chierico, G. Battaglia, Novel aspects of encapsulation and delivery using polymersomes, Curr. Opin. Pharmacol. 18 (2014) 104–111, http://dx.doi.org/10.1016/j.coph.2014.09.017.
[16] T. Thambi, J.H. Park, D.S. Lee, Stimuli-responsive polymersomes for cancer therapy, Biomater. Sci. 4 (2016) 55–69, http://dx.doi.org/10.1039/c5bm00268k.
[17] H. De Oliveira, J. Thevenot, S. Lecommandoux, Smart polymersomes for therapy and diagnosis: fast progress toward multifunctional biomimetic nanomedicines, Wiley Interdiscip. Rev. Nanomed. Nanobiotechnol. 4 (2012) 525–546, http://dx.doi.org/10.1002/wnan.1183.
[18] P. Broz, S.M. Benito, C. Saw, P. Burger, H. Heider, M. Pfisterer, S. Marsch, W. Meier, P. Hunziker, Cell targeting by a generic receptor-targeted polymer nanocontainer platform, J. Control. Release. 102 (2005) 475–488, http://dx.doi.org/10.1016/j.jconrel.2004.10.014.
[19] S. Egli, M.G. Nussbaumer, V. Balasubramanian, M. Chami, N. Bruns, C. Palivan, W. Meier, Biocompatible functionalization of polymersome surfaces: a new approach to surface immobilization and cell targeting using polymersomes, J. Am. Chem. Soc. 133 (2011) 4476–4483, http://dx.doi.org/10.1021/ja110275f.
[20] M. Camblin, P. Detampel, H. Kettiger, D. Wu, V. Balasubramanian, J. Huwyler, Polymersomes containing quantum dots for cellular imaging, Int. J. Nanomedicine. 9 (2014) 2287–2298, http://dx.doi.org/10.2147/IJN.S59189.
[21] P. Figueiredo, V. Balasubramanian, M.-A. Shahbazi, A. Correia, D. Wu, C.G. Palivan, J.T. Hirvonen, H.A. Santos, Angiopep2-functionalized polymersomes for targeted doxorubicin delivery to glioblastoma cells, Int. J. Pharm. 511 (2016) 794–803, http://dx.doi.org/10.1016/j.ijpharm.2016.07.066.
[22] S. Zalipsky, C. Hansen, J. Oaks, T. Allen, Evaluation of blood clearance rates and biodistribution of poly(2-oxazoline)-grafted liposomes, J. Pharm. Sci. 85 (1996) 133–137, http://dx.doi.org/10.1021/js9504043.
[23] R. Konradi, B. Pidhatika, A. Mühlebach, M. Textor, Poly-2-methyl-2-oxazoline: a peptide-like polymer for protein-repellent surfaces, Langmuir 24 (2008) 613–616, http://dx.doi.org/10.1021/la702917z.
[24] C. De Vocht, A. Ranquin, R. Willaert, J.A. Van Ginderachter, T. Vanhaecke, V. Rogiers, W. Versées, P. Van Gelder, J. Steyaert, Assessment of stability, toxicity and immunogenicity of new polymeric nanoreactors for use in enzyme replacement therapy of MNGIE, J. Control. Release 137 (2009) 246–254, http://dx.doi.org/10.1016/j.jconrel.2009.03.020.
[25] L.-H. Dieu, D. Wu, C.G. Palivan, V. Balasubramanian, J. Huwyler, Polymersomes conjugated to 83–14 monoclonal antibodies: in vitro targeting of brain capillary endothelial cells, Eur. J. Pharm. Biopharm. 88 (2014) 316–324, http://dx.doi.org/10.1016/j.ejpb.2014.05.021.
[26] L.I. Zon, R.T. Peterson, In vivo drug discovery in the Zebraf, Nat. Rev. Drug Discov. 4 (2005) 35–44, http://dx.doi.org/10.1038/nrd1606.
[27] C. Chakraborty, A.R. Sharma, G. Sharma, S.-S. Lee, Zebrafish: a complete animal model to enumerate the nanoparticle toxicity, J. Nanobiotechnol. 14 (2016), http://dx.doi.org/10.1186/s12951-016-0217-6.
[28] A. Sze, D. Erickson, L. Ren, D. Li, Zeta-potential measurement using the Smoluchowski equation and the slope of the current-time relationship in electroosmotic flow, J. Colloid Interface Sci. 261 (2003) 402–410, http://dx.doi.org/10.1016/S0021-9797(03)00142-5.

[29] M. Westerfield, The Zebrafish Book, A guide for the Laboratory Use of Zebrafish (Danio rerio), 5th ed., University of Oregon Press, Eugene, 2007.
[30] U. Nobbmann, PDI from an individual peak in DLS, 2015. <http://www.materials-talks.com/blog/2015/03/31/pdi-from-an-individual-peak-in-dls/> (accessed June 9, 2017).
[31] D. Witzigmann, P. Detampel, F. Porta, J. Huwyler, Isolation of multiantennary N-glycans from glycoproteins for hepatocyte specific targeting via the asialoglycoprotein receptor, RSC Adv. 6 (2016) 97636–97640, http://dx.doi.org/10.1039/C6RA18297F.
[32] P. Grossen, G. Québatte, D. Witzigmann, C. Prescianotto-Baschong, L.-H. Dieu, J. Huwyler, Functionalized solid-sphere PEG-b-PCL nanoparticles to target brain capillary endothelial cells in vitro, J. Nanomater. 2016 (2016) 1–13, http://dx.doi.org/10.1155/2016/7818501.
[33] S. Bolte, F.P. Cordelieres, A guided tour into subcellular colocalisation analysis in light microscopy, J. Microsc. 224 (2006) 213–232, http://dx.doi.org/10.1111/j.1365-2818.2006.01706.x.
[34] J. Nicolas, S. Mura, D. Brambilla, N. Mackiewicz, P. Couvreur, Design, functionalization strategies and biomedical applications of targeted biodegradable/biocompatible polymer-based nanocarriers for drug delivery, Chem. Soc. Rev. 42 (2013) 1147–1235, http://dx.doi.org/10.1039/c2cs35265f.
[35] H. Nakamura, F. Jun, H. Maeda, Development of next-generation macromolecular drugs based on the EPR effect: challenges and pitfalls, Expert Opin. Drug Deliv. 12 (2015) 53–64, http://dx.doi.org/10.1517/17425247.2014.955011.
[36] A. Pathak, S.P. Vyas, K.C. Gupta, Nano-vectors for efficient liver specific gene transfer, Int. J. Nanomed. 3 (2008) 31–49.
[37] E. Fröhlich, The role of surface charge in cellular uptake and cytotoxicity of medical nanoparticles, Int. J. Nanomed. 7 (2012) 5577–5591, http://dx.doi.org/10.2147/IJN.S36111.
[38] H. Ishiwata, N. Suzuki, S. Ando, H. Kikuchi, T. Kitagawa, Characteristics and biodistribution of cationic liposomes and their DNA complexes, J. Control. Release 69 (2000) 139–148, http://dx.doi.org/10.1016/S0168-3659(00)00293-5.
[39] S. Litvinchuk, Z. Lu, P. Rigler, T.D. Hirt, W. Meier, Calcein release from polymeric vesicles in blood plasma and PVA hydrogel, Pharm. Res. 26 (2009) 1711–1717, http://dx.doi.org/10.1007/s11095-009-9881-7.
[40] B.M. Discher, Y.-Y. Won, D.S. Ege, J.C.-M. Lee, F.S. Bates, D.E. Discher, D.A. Hammer, Polymersomes: tough vesicles made from diblock copolymers, Science 284 (80-) (1999) 1143–1146, http://dx.doi.org/10.1126/science.284.5417.1143.
[41] T. Lammers, F. Kiessling, M. Ashford, W. Hennink, G. Storm, Cancer nanomedicine: Is targeting our target?, Nat Rev. Mater. 1 (2016) 1–4, http://dx.doi.org/10.1038/natrevmats.2016.76.
[42] F. Kong, X. Zhang, M. Hai, Micro fluidics fabrication of monodisperse biocompatible phospholipid vesicles for encapsulation and delivery of hydrophilic drug or active compound, Langmuir 30 (2014) 3905–3912, http://dx.doi.org/10.1021/la404201m.
[43] E. Kastner, V. Verma, D. Lowry, Y. Perrie, Micro fluidic-controlled manufacture of liposomes for the solubilisation of a poorly water soluble drug, Int. J. Pharm. 485 (2015) 122–130, http://dx.doi.org/10.1016/j.ijpharm.2015.02.063.
[44] G. Ashwell, J. Harford, Carbohydrate-Specific Receptors of the Liver, Annu. Rev. Biochem. 51 (1982) 531–554, http://dx.doi.org/10.1146/annurev.bi.51.070182.002531.
[45] L.M. Bareford, P.W. Swaan, Endocytic mechanisms for targeted drug delivery, Adv. Drug Deliv. Rev. 59 (2007) 748–758, http://dx.doi.org/10.1017/CBO9781107415324.004.
[46] H. Fuchs, A. Weng, R. Gilabert-Oriol, Augmenting the efficacy of immunotoxins and other targeted protein toxins by endosomal escape enhancers, Toxins (Basel) 8 (2016), http://dx.doi.org/10.3390/toxins8070200.
[47] G. Sahay, J. Oh, A.V. Kabanov, T.K. Bronich, Biomaterials The exploitation of differential endocytic pathways in normal and tumor cells in the selective targeting of nanoparticulate chemotherapeutic agents, Biomaterials 31 (2010) 923–933, http://dx.doi.org/10.1016/j.biomaterials.2009.09.101.
[48] D. Ma, Enhancing endosomal escape for nanoparticle mediated siRNA delivery, Nanoscale 6 (2014) 6415–6425, http://dx.doi.org/10.1039/c4nr00018h.
[49] P.K. Mistry, G. Lopez, R. Schiffmann, N.W. Barton, N.J. Weinreb, E. Sidransky, Gaucher disease circa 2016: progress and ongoing challenges, Mol. Genet. Metab. 120 (2016) 8–21, http://dx.doi.org/10.1016/j.ymgme.2016.11.006.
[50] F.M. Platt, B. Boland, A.C. van der Spoel, Lysosomal storage disorders: the cellular impact of lysosomal dysfunction, J. Cell Biol. 199 (2012) 723–734, http://dx.doi.org/10.1083/jcb.201208152.
[51] L. Shang, K. Nienhaus, G.U. Nienhaus, Engineered nanoparticles interacting with cells: size matters, J. Nanobiotechnol. 12 (2014), http://dx.doi.org/10.1186/1477-3155-12-5.
[52] H. Kettiger, D. Sen, L. Schiesser, J.M. Rosenholm, J. Huwyler, Comparative safety evaluation of silica-based particles, Toxicol. Vitr. 30 (2015) 355–363, http://dx.doi.org/10.1016/j.tiv.2015.09.030.
[53] L. Bodewein, F. Schmelter, S. Di, H. Hollert, R. Fischer, M. Fenske, Differences in toxicity of anionic and cationic PAMAM and PPI dendrimers in zebra fi sh embryos and cancer cell lines, Toxicol. Appl. Pharmacol. 305 (2016) 83–92, http://dx.doi.org/10.1016/j.taap.2016.06.008.
[54] L.Y. Rizzo, S.K. Golombek, M.E. Mertens, Y. Pan, D. Laaf, J. Broda, J. Jayapaul, D. Möckel, V. Subr, W.E. Hennik, G. Storm, U. Simon, W. Jahnen-Dechent, F. Kiessling, T. Lammers, In vivo nanotoxicity testing using the zebrafish embryo assay, J. Mater. Chem. B, Mater Biol. Med. (2013), http://dx.doi.org/10.1039/C3TB20528B.ln.
[55] J. Duan, Y. Yu, H. Shi, L. Tian, C. Guo, P. Huang, X. Zhou, S. Peng, Z. Sun, Toxic effects of silica nanoparticles on zebrafish embryos and larvae, PLOSone 8 (2013) 4–12, http://dx.doi.org/10.1371/journal.pone.0074606.
[56] D.A. Mosselhy, W. He, D. Li, Silver nanoparticles: in vivo toxicity in zebrafish embryos and a comparison to silver nitrate, J. Nanoparticle Res. 18 (2016) 1–15, http://dx.doi.org/10.1007/s11051-016-3514-y.
[57] G.J. Lieschke, P.D. Currie, Animal models of human disease: zebrafish swim into view, Nat. Rev. Genet. 8 (2010) 353–367, http://dx.doi.org/10.1038/nrg2091.
[58] C. Blaise, F. Gagne, J.F. Férard, P. Eullaffroy, Ecotoxicity of selected nano-materials to aquatic organisms, Environ. Toxicol. 23 (2008) 591–598, http://dx.doi.org/10.1002/tox.20402.
[59] P.H. Kierstead, H. Okochi, V.J. Venditto, T.C. Chuong, S. Kivimae, J.M.J. Fréchet, F.C. Szoka, The effect of polymer backbone chemistry on the induction of the accelerated blood clearance in polymer modified liposomes, J. Control. Release 213 (2015) 1–9, http://dx.doi.org/10.1016/j.jconrel.2015.06.023.
[60] A.S. Abu Lila, H. Kiwada, T. Ishida, The accelerated blood clearance (ABC) phenomenon : Clinical challenge and approaches to manage, J. Control. Release 172 (2013) 38–47, http://dx.doi.org/10.1016/j.jconrel.2013.07.026.

Supporting information

PDMS-*b*-PMOXA polymersomes for hepatocyte targeting and assessment of toxicity

Encapsulation of Carboxyfluorescein and Release Profile

The polymersomes were loaded with Carboxyfluorescein (CF) as described in section 2.6 of the article. The release profile of CF in buffers containing naturally occurring serum protein was evaluated: CF release was tested in 3% BSA in DPBS and in 50% FCS in DPBS for 48 h at 37°C.
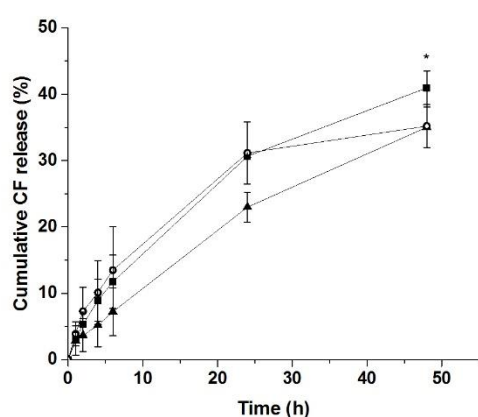
Figure S1. Release profiles of PP-CF in buffers containing naturally occurring serum protein. The release profiles of CF in 3% BSA are represented by black triangles, the release of CF in 50% FCS is shown with open circles, and the black squares depict the release of CF in DPBS. SD is shown with error bars (n = 3), *p < 0.01.

Fluorescence Correlation Spectroscopy

Fluorescence correlation spectroscopy (FCS) measurements were performed as described elsewhere [1] with an inverted Zeiss 510-Meta/Confocor2 laser-scanning microscope (Carl Zeiss AG, Feldbach, Switzerland) equipped with an argon laser (488 nm) and a water immersion objective (Zeiss C-Apochromat 40x, NA 1.2). 15 µL of the samples of HiLyte Fluor 488, HiLyte Fluor 488 labelled proteins, and polymersomes conjugated to HiLyte Fluor 488 labelled proteins were measured at RT on a cover glass (Huber & Co., Reinach, Switzerland). Fluctuation in fluorescence intensity was analysed in terms of an autocorrelation function (average of 30 measurements over 10 s). Diffusion times of the samples were independently measured and fixed in the fitting procedure to reduce the amount of free fitting parameters. Molecular brightness measurements were used to evaluate the number of HiLyte Fluor 488 per molecule of protein and the number of HiLyte Fluor 488 labelled protein per polymersome.
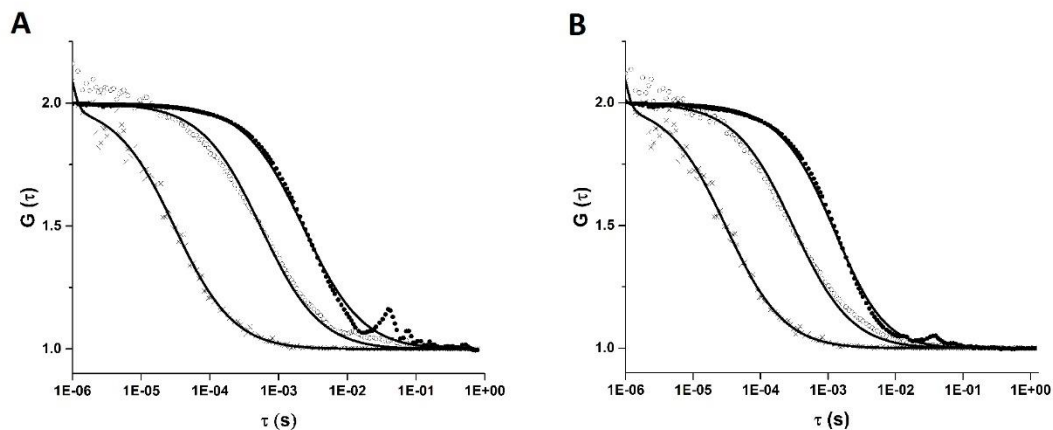
Figure S2. Fluorescence correlation spectroscopy analysis of polymersomes conjugated to HiLyte 488 fluorescently labelled protein. A) Normalised autocorrelation curves of free HiLyte 488 (crosses), HiLyte 488 labelled asialofetuin (AF-488, open circles), and polymersomes conjugated to AF-488 (PP-AF-488, black circles). Different diffusion times of free HiLyte 488 (31 µs), AF-488 (557 µs), and PP-AF-488 (2307 µs) indicated the successful conjugation of the polymersomes. B) Normalised autocorrelation curves of free HiLyte 488 (crosses), HiLyte 488 labelled fetuin (F-488, open circles), and polymersomes conjugated to F-488 (PP-F-488, black circles). Different diffusion times of free HiLyte 488 (31 µs), F-488 (308 µs), and PP-FF-488 (2315 µs) indicated the successful conjugation of the polymersomes. Autocorrelation curves represent the averages of 30 measurements over 10 seconds.

References

1. Grossen P, Québatte G, Witzigmann D, et al (2016) Functionalized solid-sphere PEG-b-PCL nanoparticles to target brain capillary endothelial cells in vitro. Journal of Nanomaterials 2016: doi: 10.1155/2016/7818501

2.2 SELF-ASSEMBLING CHITOSAN HYDROGEL: A DRUG-DELIVERY DEVICE ENABLING THE SUSTAINED RELEASE OF PROTEINS

Klara Kiene, Fabiola Porta, Buket Topacogullari, Pascal Detampel, Jörg Huwyler

Department of Pharmaceutical Sciences, Division of Pharmaceutical Technology, University of Basel, Klingelbergstrasse 50, 4056 Basel, Switzerland

Applied Polymer
JOURNAL OF
SCIENCE

Self-assembling chitosan hydrogel: A drug-delivery device enabling the sustained release of proteins

Klara Kiene, Fabiola Porta, Buket Topacogullari, Pascal Detampel ⓘ, Jörg Huwyler

Division of Pharmaceutical Technology University of Basel, Basel 4056, Switzerland
Correspondence to: J. Huwlyer (E-mail: joerg.huwyler@unibas.ch)

ABSTRACT: The development of a self-assembling hydrogel, prepared from maleimide-modified and thiolated chitosan (CS), is described. Under mild reaction conditions, the natural CS polymer was coupled with either maleimide or sulfhydryl moieties in a one-step synthesis. Subsequently, these CS polymers spontaneously formed a covalently crosslinked CS hydrogel when mixed. The three-dimensional network structure was visualized with scanning electron microscopy. The swelling and degradation behavior was evaluated, and viscosity measurements were conducted. The gel was loaded with the model protein albumin, and prolonged release was achieved. These properties were preserved after lyophilization and rehydration. This makes the hydrogel a promising scaffold for biological wound dressings for the treatment of chronic wounds. © 2017 Wiley Periodicals, Inc. J. Appl. Polym. Sci. **2017**, *134*, 45638.

INTRODUCTION

In the 1960s, the foundation for hydrogel research was created by Wichterle and Lím. They synthesized hydrogels based on the copolymerization of hydroxyl methacrylate with the crosslinker ethylene glycol dimethacrylate.[1] Since then, hydrogels have attracted great attention in the fields of drug delivery, biosensing, and tissue engineering.[2,3] Hydrogel-based drug-delivery systems can be used for targeted delivery, the extension of circulation time, the reduction of toxicity and side effects, and the transport of fragile bioactive molecules, such as proteins. Hydrogels retain the proteins in their three-dimensional (3D) network structure to protect the proteins' active form and to prevent them from denaturation during administration.[2,4,5]

Hydrogels can be prepared through different strategies. On the one hand, polymer chains can be physically associated by noncovalent binding strategies, namely, electrostatic, hydrophobic, or hydrogen-bonding forces. These approaches of reversible linkage do not require any potentially toxic covalent linker molecule. This makes them safe for clinical application. The main disadvantages of physically crosslinked hydrogels are their weak mechanical strength and uncontrolled dissolution. On the other hand, it is possible to form hydrogels by covalent interactions between the polymer chains. With irradiation chemistry, small crosslinker molecules, or secondary polymerization, the irreversible crosslinking of polymer chains can be achieved. Because permanent covalent crosslinked hydrogels show a stable network structure, they allow for the absorption of water and permit drug release by diffusion. To overcome the drawbacks of additional crosslinker molecules, it is possible to use prefunctionalized polymer chains with reactive functional groups.[6,7] One method for covalent crosslinking without the need for crosslinking reagents or catalysts is *in situ* gelation through the formation of disulfide bonds between the single polymer chains.[8] Moreover, hydrogels can be formed by Schiff bases.[9] Another example for covalent crosslinking under mild reaction conditions is Michael addition, which requires the simple mixing of two components. The approach of self-assembling hydrogels combines the advantages of physically and chemically crosslinked hydrogels.[10,11]

To form hydrogels, natural or synthetic polymers can be chosen. An important natural biopolymer is chitosan (CS), which is used extensively for drug delivery to various organs of the human body.[12,13] CS is partially deacetylated chitin and is composed of copolymers of glucosamine and *N*-acetyl glucosamine.[14,15] CS is soluble in acidic solutions because of the protonation of amino moieties but hardly soluble at physiological pH. In physiological environments, various enzymes, such as bacterial chitosanase or lysozyme, degrade CS and form harmless degradation products.[16] CS and its derivatives have been
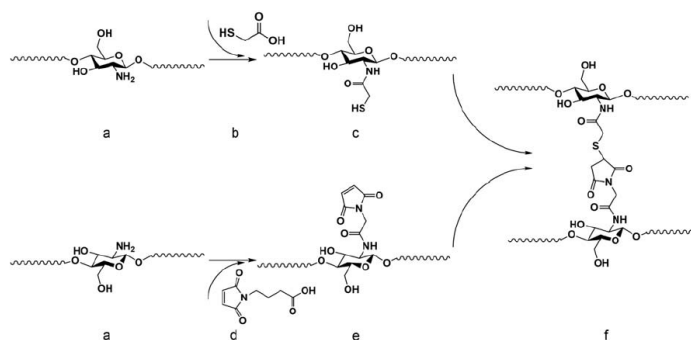
Figure 1. (a) Modification of CS (b) with either thioglycolic acid (c) resulting in SH–CS or (d) by the addition of 4-maleimidobutyric acid (e) leading to Mal–CS. The mixture of aqueous solutions of the two polymers led to covalent crosslinking via (f) Michael addition and gelation.

shown to be bioadhesive and to promote cell proliferation and, consequently, tissue regeneration.[6,14,17] CS has a low toxicity[18] and is biocompatible and biodegradable.[19] Furthermore, CS has a strong antimicrobial activity.[20]

Although cutaneous wound healing is a major problem in diabetic ulcers, venous stasis ulcers, and decubitus ulcers, hydrogels carrying bioactive proteins are promising improvements compared to conventional wound dressings.[21] The number of patients with chronic wounds is estimated to exceed 6.5 million in the United States alone; this has led to an annual spending of US$25 billion on the treatment of chronic wounds.[22] Among several characteristics, an optimal hydrogel has to keep the wound moist while removing wound exudate,[23] present an ideal release profile of therapeutic proteins on the wound, and be lyophilized for easy storage and application.

To address this health problem, in this study, we coupled CS in a one-step synthesis under mild reaction conditions with either maleimide or sulfhydryl groups. The results were two types of modified polymer. Subsequently, these CS polymers were combined to form a self-assembling covalently crosslinked CS hydrogel. The gel was loaded with the model protein albumin and used either immediately or after lyophilization and rehydration. Under both conditions, prolonged protein release was achieved.

RESULTS AND DISCUSSION

Analysis and Chemical Modification of CS

The CS polymer was either thiolated with thioglycolic acid or modified with a maleimide moiety according to a procedure from the literature.[24] Subsequently, a self-assembling CS hydrogel was prepared (Figure 1).

The unmodified CS was analyzed before the experiments to determine its molecular weight and degree of deacetylation. A molecular weight of 250 ± 20 kDa was determined according to Morris et al.[25] (this weight corresponds to 1300–1500 monomers). With ^{1}H-NMR, we determined the degree of deacetylation to be 70% (data not shown).[26]

With Fourier transform infrared spectroscopy, the successful modification of CS to maleimide–chitosan (Mal–CS) and thiolated chitosan (SH–CS) was confirmed. The comparison of the unmodified CS to Mal–CS revealed maleimide-specific peaks at 1706 cm^{-1} (alkene bonds) and 1521 cm^{-1} (carbonyl bonds). Characteristic peaks of SH–CS were seen at 2570 cm^{-1} (sulfhydryl groups), 1518 cm^{-1} (carbonyl bonds), and 1247 cm^{-1} (carbon–sulfur bonds; Figure S1, Supporting Information).[27,28]

Formation and Analysis of the Hydrogel

Most current CS derivatives, which are used as intermediates or precursors for further conjugation, are prepared from multistep reactions and/or under harsh conditions.[29–32] In contrast, the modification of CS to either Mal–CS or SH–CS performed in this study was a one-step reaction under mild and aqueous conditions and did not require harsh organic solvents. Gelation was recognizable directly after the two polymer solutions were mixed. This was indicative of strong covalent interactions of the polymer chains due to successful modification with either maleimide or sulfhydryl moieties.

Morphology. The morphological appearance of the hydrogel was examined by scanning electron microscopy (SEM; Figure 2). The 3D network structure showed pore diameters between 5 and 100 μm, which were comparable to those of other CS hydrogels.[33]

Rheology, Swelling, and Degradation. The rheology of the CS hydrogel showed a clear pseudo-plasticity, that is, shear-thinning or thixotropic flow behavior [Figure 3(a,b)]. When the shear rate was increased, the viscosity decreased, and at shear rates above 150 s^{-1}, an equilibrium was established between structural breakdown and rebuilding; this resulted in a steady-state plateau in the viscosity. Upon decreasing the shear rate, the viscosity and, thus, the structure of the gel recovered completely; this behavior followed a hysteresis loop. This indicated that the hydrogel was capable of resisting shear stress up to at least 200 s^{-1} without being destroyed. The decrease in the viscosity from approximately 14 to 2 Pa s of our gel with increasing shear rate up to 100 s^{-1} was comparable to the results found by Mikešová et al. (2% CS solution),[34] whereas the CS-containing gels of Wu et al.[35] showed either higher
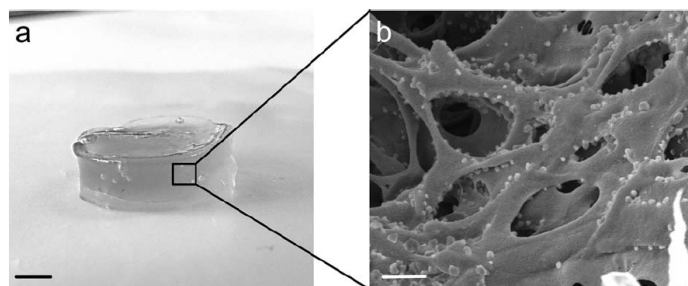
Figure 2. Macroscopic and microscopic structures of the CS hydrogel. (a) The CS hydrogel after crosslinking via Michael addition. Scale bar = 0.2 cm. (b) SEM analysis of the CS hydrogel showing a porous structure. Scale bar = 3 μm.

viscosities or significantly lower ones than our CS hydrogel, depending on the formulation. Argüelles-Monal et al.[36] investigated CS crosslinked with glutaraldehyde and showed changing rheology behavior as well according to different stoichiometric ratios between the polymer and crosslinker. Ratios of less than 1 were reflected by viscosities much lower than the ones of our gel, and the viscosity values of gels with a stoichiometric ratio of 5 were in the range 8000–9000 Pa s. A comparison between three different formulations of our CS hydrogel revealed no significant differences in the viscosity and shear stress ($p < 0.01$). The original gel was formed by mixing 1:1 Mal–CS and SH–CS, and the compared gels had ratios of 1:2 and 1:3, respectively (data not shown). As we did not measure significant differences in the viscosity and shear stress of the 1:1, 1:2, and 1:3 mixed hydrogels (Mal–CS:SH–CS), we decided to test the release of the model protein, bovine serum albumin (BSA), in the main formulation, namely, the 1:1 mixture.

We assumed that our hydrogel would be applied directly on the wound and subsequently fixed by a secondary occlusive dressing. Under these conditions, wound exudate is absorbed by the lyophilisate, the gel is evenly spread, and moisture is preserved. The spreadability of the CS hydrogel was compared to those of two marketed hydrogels, Prontosan Wound Gel and Prontosan Wound Gel X. Both gels are used clinically for the cleansing and moisturizing of skin wounds and burns, and to prevent the formation of biofilms. Prontosan Wound Gel is a thin gel,

whereas Prontosan Wound Gel X shows a viscous consistency.[37] The spreadability curve of the CS hydrogel was similar to that of Prontosan Wound Gel X, whereas the curves of Prontosan Wound Gel and our CS hydrogel differed significantly [$p < 0.01$, Figure 3(c)]. This indicated that the CS hydrogel would behave in a manner comparable to that of the licensed reference product (Prontosan Wound Gel X) once it is applied to a wound.

In another control experiment, lysozyme (1 mg/mL) was added to the hydrogel to destroy the gel structure through hydrolysis of the β(1-4)-glycosidic bonds between N-acetyl glucosamine and glucosamine of the CS backbone. This led to a significantly reduced viscosity compared to the intact hydrogel (data not shown). The destruction of the hydrogel's viscosity by the addition of lysozyme showed that the backbone was still biodegradable, even though the single polymers were chemically modified.

This latter finding confirmed results from the swelling and degradation studies. In these experiments, the hydrogel was exposed to either acetic buffer (pH 5.0), phosphate-buffered saline (PBS pH 7.4), or a lysozyme solution (1 mg/mL). In an acidic environment, the gel almost doubled in mass (1.8-fold swelling) because of protonation of the amine moieties of CS (pK_a = 6.5); this led to excellent wettability of the gel at acidic pH. In contrast, at physiological pH, the hydrogel showed a swelling of 1.3-fold on the basis of the lower degree of protonation of the amine moieties and, therefore, showed a reduced wettability
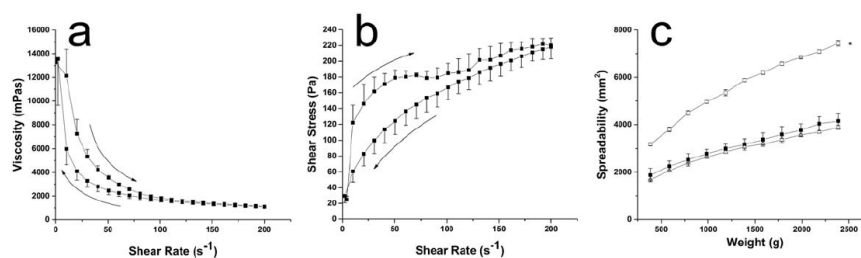
Figure 3. Rheology data of the CS hydrogel. (a) The viscosity decreased with increasing shear rate and reached a steady state at about 150 s^{-1}. Thixotropic behavior was observed when the shear rate was ceased. (b) Flow curve of the CS hydrogel in which the shear rate is plotted against the shear stress. Arrows indicate the temporal direction of the hysteresis loops. (c) The spreadability of the CS hydrogel (black squares), Prontosan Wound Gel (open circles), and Prontosan Wound Gel X (open triangles). The values are expressed as means plus the standard deviations (SDs; $n = 3$), *$p < 0.01$.
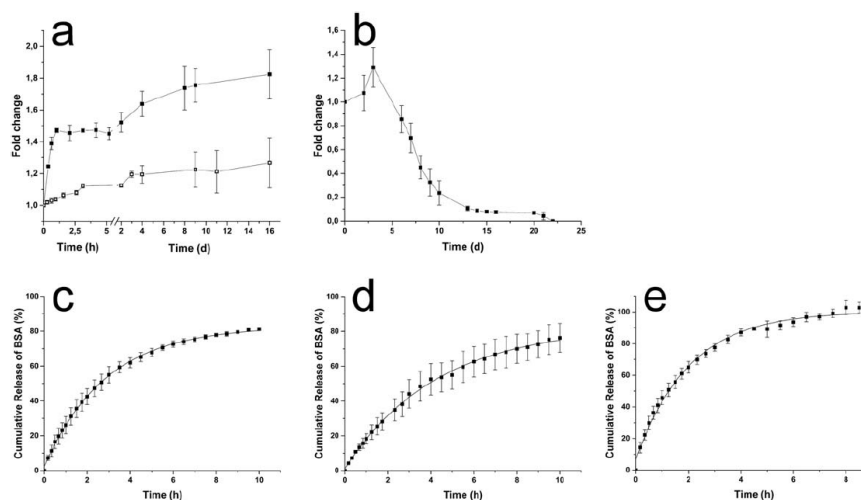
Figure 4. Swelling behavior and cumulative protein release profiles. (a) Nondestructive swelling of the hydrogel either in an acidic environment (black squares) or under physiological conditions (open squares). Incubation in an acetic buffer (pH 5.0) led to a 1.8-fold increase in the weight, whereas swelling in physiological buffer (PBS, pH 7.4) resulted in an almost 1.3-fold mass rise. (b) Incubation of the hydrogel with lysozyme led to the complete destruction of the gel due to the enzymatic breakdown of the CS backbone structure. (c) Sustained release profile of BSA from the preloaded CS hydrogel directly after gelation. Fifty percent of BSA was released after 2.5 h. (d) Sustained release of BSA from the lyophilized, preloaded CS hydrogel, which was rehydrated before release testing. After 3.9 h, 50% of BSA was released. (e) Release profile of the postloaded CS hydrogel, in which 50% of BSA was released within 1.2 h. The values are expressed as means ± SDs ($n = 3$).

compared to the gel at pH 5.0 [Figure 4(a)]. When the hydrogel was incubated in a lysozyme solution, a destructive swelling process was observed. This process was divided into two phases. During the first 3 days, the gel showed a nondestructive swelling behavior comparable to swelling under physiological conditions (1.3-fold). Thereafter, the degradation process became predominant; this resulted in complete degradation of the hydrogel within 3 weeks [Figure 4(b)].

BSA Release. To investigate the drug-release properties of the CS hydrogel, BSA was used as a model protein, as it has a medium size, is easily available, and is known to be stable during lyophilization.[38] Three different hydrogel preparations were tested for their release properties: two preloaded gels and one postloaded formulation. To make the preloaded gels, SH–CS was dissolved in a BSA solution and Mal–CS was dissolved in PBS; then, the two aqueous solutions were mixed. Thereafter, the spontaneously formed gels were either taken directly for release testing [gel 1, Figure 4(c)] or lyophilized so the release properties could be determined after rehydration [gel 2, Figure 4(d)]. The third formulation, the postloaded hydrogel, was prepared without BSA before gelation. Afterward, this hydrogel was lyophilized and soaked with a BSA solution before release testing [gel 3, Figure 4(e)]. The release profiles were fitted according to eq. (1), where C_{max} is the maximal cumulative release, k represents the rate constant, and t is the soaking time. The time needed to reach 50% release is defined as $t_{1/2}$ [eq. (2)]. The results are summarized in Table I.

$$\text{Cumulative release of BSA } (\%) = C_{max}[1-\exp(-kt)] \quad (1)$$

$$t_{1/2} = -\frac{\ln\left(1 - \frac{0.5}{C_{max}}\right)}{k} \quad (2)$$

Postloaded hydrogels released 50% of the protein within less than 1.5 h. The release of BSA was two times slower in the preloaded hydrogels. With postloaded gels, the complete liberation of BSA was observed. The preloaded gels released approximately 80% of BSA; this was indicative of the retention of residual BSA within the gel. There was no difference ($p < 0.01$) with respect to BSA release between the lyophilized and freshly prepared hydrogels. There was also no significant difference ($p < 0.01$) between release at pH 7.4 and release at pH 8.0 in any of the gels (data not shown).

Moreover, equivalence between the lyophilized and freshly prepared preloaded hydrogels was determined with the similarity factor f_2 according to U.S. Food and Drug Administration guidelines.[39] The two release profiles of the preloaded gels were

Table I. Curve Fitting of the Release Profiles of BSA from Three Different CS Hydrogels According to Eq. (1)

Parameter	Gel 1 [Figure 4(c)]	Gel 2 [Figure 4(d)]	Gel 3 [Figure 4(e)]
C_{max} (%)	81.7	81.6	98.3
$t_{1/2}$ (h)	2.5	3.9	1.2
r^2	0.998	0.998	0.988

equivalent, and there was no influence of lyophilization ($f_2 = 52$). In contrast, the postloaded CS hydrogel was not equivalent to its preloaded counterpart ($f_2 = 34$).

In addition, with the application of Higuchi's model,[40,41] the release profiles of all three gel variations scaled almost linearly with the square root of time (r^2 for all of the gels ≥ 0.96, Figure S2, Supporting Information); this indicated that the releases were diffusion mediated.[42]

We concluded that variations in the loading procedure or lyophilization resulted in only a modest change in the total protein release (i.e., 82–100% protein release within 10 h). The release over 10 h was in a similar range as that of the CS gel formulation of Alemdaroğlu et al.;[43] their gel was loaded with epidermal growth factor (EGF) and aimed at treating second-degree burn wounds in rats. In their in vitro study, the release rate of EGF was 97.3% after 24 h, and in vivo, the EGF loaded gels were repeatedly applied for 14 days (one application per day). This resulted in a better and faster epithelization than in the control groups without EGF. Daily reapplication of the device would make our hydrogel a very good candidate for the 23% of chronic wounds that require daily dressing changes.[22,44] The 1 day of release is in sharp contrast to other published CS hydrogels, which show a very slow release of their loaded cargos over 10–20 days. This could be explained by the ionic or covalent interactions between the cargo proteins and scaffold.[45–47] Thus, different types of gels have to be chosen, depending on their intended use.

Wound Healing. The cutaneous wound-healing process is based on a perfectly organized interplay of highly regulated factors, and numerous diseases may affect this cascade of events involved in wound healing.[21] A biological dressing based on carboxymethyl-cellulose is already on the market under the trade name Regranex. It releases becaplermin, a platelet-derived growth factor, and has been shown to be effective.[48] In addition, several clinical studies with a variety of other growth factors are currently ongoing. The biopolymer CS presented in this study is a possible alternative to this type of wound dressing. In fact, CS-derived products are already used clinically.[49,50] To preserve a moist wound environment, our lyophilized hydrogel should be fixed with an occlusive secondary dressing. Thanks to its porous structure, swelling, and release properties, the gel will take up excess of liquid and prevent the wound from drying out by releasing water when necessary. Such a protein-loaded hydrogel might be beneficial for the treatment of chronic wounds, especially diabetic ulcers, venous stasis ulcers, and decubitus ulcers.[22] Particularly infected ulcers need, in addition to appropriate antibiotic therapy and regular wound debridement, daily dressing changes.[44] For these patients, our hydrogel wound dressing, which combines the antimicrobial properties of CS and the complete release of entrapped protein within less than 1 day, offers an additional advantage.[20] A moist wound dressing, such as our CS hydrogel, is easily removed from wounds, reduces pain during dressing changes, and therefore, increases patient compliance. Moreover, biodegradation of the CS backbone by lysozyme, which is present in almost all body liquids,[51] increases the removability of the hydrogel as well. Additionally, the hydrogel herein described was

easily lyophilized; this revealed a mechanically stable, cottonlike structure afterward. This makes it an easily storable and manageable wound-dressing device.

Although intact skin shows a pH around 5.5, wounds have the tendency to show a slightly alkaline pH.[52] This is also the range in which many proteolytic enzymes, which can be used for the therapy of chronic wounds, are active (e.g., fribrinolysin or collagenase).[52] When the release of BSA from the our hydrogel was examined, no change in the release profiles between physiologic and slightly basic pH was observed. This makes the hydrogel suitable for the transport of proteolytic enzymes, which could be used for the therapy of chronic wounds. However, there is a broad variety of therapeutic biologics, and each one may display a different release profile from the hydrogel because of various intermolecular interactions. Therefore, the release profile of any new biologic drug from a CS hydrogel needs to be investigated, and the hydrogel's efficiency in treating chronic wounds should be confirmed in future clinical trials. A reaction between the our model protein albumin with the maleimide moieties of CS during gelation is unlikely because free cysteines are not present in BSA.[53] However, possible interactions of Mal–CS with free cysteines in other peptides or proteins has to be considered. Such interactions could potentially be beneficial and used to prolong the release profile of the cargo from the CS scaffold.

CONCLUSIONS

In this study, a self-assembling CS hydrogel was formed under physiological conditions by chemical modification of the biopolymer CS. After gel formation, a porous structure was obtained, and thixotropic flow behavior was observed. The hydrogel could be lyophilized and was shown to be degradable by hydrolysis of the CS backbone structure. In addition, the model protein albumin was successfully loaded into the hydrogel, and a sustained release profile was observed. Therefore, the application of this new gel as a scaffold for therapeutic proteins in the treatment of chronic wounds is envisioned.

REFERENCES

1. Wichterle, O.; Lím, D. Nature **1960**, 185, 117.

2. Hoffman, A. S. Adv. Drug Delivery Rev. **2002**, 54, 3.

3. Peppas, N. A.; Hilt, J. Z.; Khademhosseini, A.; Langer, R. Adv. Mater. **2006**, 18, 1345.

4. Kiyonaka, S.; Sada, K.; Yoshimura, I.; Shinkai, S.; Kato, N.; Hamachi, I. Nat. Mater. **2004**, 3, 58.

5. Lee, K. Y.; Yuk, S. H. Prog. Polym. Sci. **2007**, 32, 669.

6. Berger, J.; Reist, M.; Mayer, J. M.; Felt, O.; Peppas, N. A.; Gurny, R. *Eur. J. Pharm. Biopharm.* **2004**, *57*, 19.

7. Bhattarai, N.; Gunn, J.; Zhang, M. *Adv. Drug Delivery Rev.* **2010**, *62*, 83.

8. Wu, Z. M.; Zhang, X. G.; Zheng, C.; Li, C. X.; Zhang, S. M.; Dong, R. N.; Yu, D. M. *Eur. J. Pharm. Sci.* **2009**, *37*, 198.

9. Tan, H.; Chu, C. R.; Payne, K. A.; Marra, K. G. *Biomaterials* **2009**, *30*, 2499.

10. Nie, W.; Yuan, X.; Zhao, J.; Zhou, Y.; Bao, H. *Carbohydr. Polym.* **2013**, *96*, 342.

11. Pritchard, C. D.; O'Shea, T. M.; Siegwart, D. J.; Calo, E.; Anderson, D. G.; Reynolds, F. M.; Thomas, J. A.; Slotkin, J. R.; Woodard, E. J.; Langer, R. *Biomaterials* **2011**, *32*, 587.

12. Bernkop-Schnürch, A.; Dünnhaupt, S. *Eur. J. Pharm. Biopharm.* **2012**, *81*, 463.

13. Giri, T. K.; Thakur, A.; Alexander, A.; Ajazuddin, Badwaik, H.; Tripathi, D. K. *Acta Pharm. Sin. B* **2012**, *2*, 439.

14. Rani, M.; Agarwal, A.; Negi, Y. S. *BioResources* **2010**, *5*, 2765.

15. Shukla, S. K.; Mishra, A. K.; Arotiba, O. A.; Mamba, B. B. *Int. J. Biol. Macromol.* **2013**, *59*, 46.

16. Chhabra, P.; Tyagi, P.; Bhatnagar, A.; Mittal, G.; Kumar, A. *J. Pharm. Bioallied Sci.* **2016**, *8*, 300.

17. Berger, J.; Reist, M.; Mayer, J. M.; Felt, O.; Gurny, R. *Eur. J. Pharm. Biopharm.* **2004**, *57*, 35.

18. Kato, Y.; Onishi, H.; Machida, Y. *Biomaterials* **2004**, *25*, 907.

19. Vongchan, P.; Sajomsang, W.; Subyen, D.; Kongtawelert, P. *Carbohydr. Res.* **2002**, *337*, 1239.

20. Delezuk, J. A. M.; Ramírez-Herrera, D. E.; de Ávila, B. E.-F.; Wang, J. *Nanoscale* **2017**, *9*, 2195.

21. Han, G.; Ceilley, R. *Adv. Ther.* **2017**, *34*, DOI: 10.1007/s12325-017-0478-y.

22. Lindholm, C.; Searle, R. *Int. Wound J.* **2016**, *13*, 5.

23. Moura, L. I. F.; Dias, A. M. A.; Carvalho, E.; de Sousa, H. C. *Acta Biomater.* **2013**, *9*, 7093.

24. Kast, C. E.; Bernkop-Schnürch, A. *Biomaterials* **2001**, *22*, 2345.

25. Morris, G. A.; Castile, J.; Smith, A.; Adams, G. G.; Harding, S. E. *Carbohydr. Polym.* **2009**, *76*, 616.

26. Lavertu, M.; Xia, Z.; Serreqi, A. N.; Berrada, M.; Rodrigues, A.; Wang, D.; Buschmann, M. D.; Gupta, A. *J. Pharm. Biomed. Anal.* **2003**, *32*, 1149.

27. Brugnerotto, J.; Lizardi, J.; Goycoolea, F. M.; Argüelles-Monal, W.; Desbrières, J.; Rinaudo, M. *Polymer* **2001**, *42*, 3569.

28. Kumirska, J.; Czerwicka, M.; Kaczyński, Z.; Bychowska, A.; Brzozowski, K.; Thöming, J.; Stepnowski, P. *Mar. Drugs* **2010**, *8*, 1567.

29. Matsumoto, M.; Udomsinprasert, W.; Laengee, P.; Honsawek, S.; Patarakul, K.; Chirachanchai, S. *Macromol. Rapid Commun.* **2016**, *37*, 1618.

30. Ahmadi, F.; Oveisi, Z.; Samani, S. M.; Amoozgar, Z. *Res. Pharm. Sci.* **2015**, *10*, 1.

31. Chen, X.-G.; Park, H.-J. *Carbohydr. Polym.* **2003**, *53*, 355.

32. Jia, Z.; Shen, D.; Xu, W. *Carbohydr. Res.* **2001**, *333*, 1.

33. Liu, X.; Chen, Y.; Huang, Q.; He, W.; Feng, Q.; Yu, B. *Carbohydr. Polym.* **2014**, *110*, 62.

34. Mikešová, J.; Hašek, J.; Tishchenko, G.; Morganti, P. *Carbohydr. Polym.* **2014**, *112*, 753.

35. Wu, J.; Liu, J.; Shi, Y.; Wan, Y. *J. Mech. Behav. Biomed. Mater.* **2016**, *64*, 161.

36. Argüelles-Monal, W.; Goycoolea, F. M.; Peniche, C.; Higuera-Ciapara, I. *Polym. Gels Networks* **1998**, *6*, 429.

37. B. Braun Medical AG. Product Information. https://www.bbraun.com/content/dam/catalog/bbraun/bbraunProductCatalog/S/AEM2015/en-01/b6/flyer-prontosan-woundgelandwoundgelx.pdf.bb-.49161896/flyer-prontosan-woundgelandwoundgelx.pdf (accessed June 16, 2017).

38. Lewis, L. M.; Johnson, R. E.; Oldroyd, M. E.; Ahmed, S. S.; Joseph, L.; Saracovan, I.; Sinha, S. *AAPS PharmSciTech* **2010**, *11*, 1580.

39. U.S. Department of Health and Human Services, Food and Drug Administration (FDA), Center for Drug Evaluation and Research (CDER), Guidance for Industry - Dissolution Testing of Immediate Release Solid Oral Dosage Forms, U. S. Food and Drug Administration, Center for Drug Evaluation and Research (Silver Spring, MD) **1997**.

40. Higuchi, T. *J. Pharm. Sci.* **1961**, *50*, 874.

41. Siepmann, J.; Peppas, N. A. *Int. J. Pharm.* **2011**, *418*, 6.

42. Hiemstra, C.; Zhong, Z.; van Steenbergen, M. J.; Hennink, W. E.; Feijen, J. *J. Controlled Release* **2007**, *122*, 71.

43. Alemdaroğlu, C.; Değim, Z.; Çelebi, N.; Zor, F.; Öztürk, S.; Erdoğan, D. *Burns* **2006**, *32*, 319.

44. Hilton, J. R.; Williams, D. T.; Beuker, B.; Miller, D. R.; Harding, K. G. *Clin. Infect. Dis.* **2004**, *39*, S100.

45. Chang, Y.; Xiao, L. *J. Macromol. Sci. Part A* **2010**, *47*, 608.

46. Hu, H.; Yu, L.; Tan, S.; Tu, K.; Wang, L.-Q. *Carbohydr. Res.* **2010**, *345*, 462.

47. Liu, X.; Yu, B.; Huang, Q.; Liu, R.; Feng, Q.; Cai, Q.; Mi, S. *Int. J. Biol. Macromol. A* **2016**, *93*, 314.

48. Smiell, J. M.; Wieman, T. J.; Steed, D. L.; Perry, B. H.; Sampson, A. R.; Schwab, B. H. *Wound Repair Regen.* **1999**, *7*, 335.

49. Akncbay, H.; Senel, S.; Ay, Z. Y. *J. Biomed. Mater. Res. B* **2007**, *80*, 290.

50. Mo, X.; Cen, J.; Gibson, E.; Wang, R.; Percival, S. L. *Wound Repair Regen.* **2015**, *23*, 518.

51. Hankiewicz, J.; Swierczek, E. *Clin. Chim. Acta* **1974**, *57*, 205.

52. Dissemond, J.; Witthoff, M.; Brauns, T. C.; Haberer, D.; Goos, M. *Hautarzt* **2003**, *54*, 959.

53. Bujacz, A. *Acta Crystallogr. D* **2012**, *68*, 1278.

55

Results – Self-assembling chitosan hydrogel: a drug delivery device enabling sustained release of proteins

Supporting information

Self-assembling chitosan hydrogel: a drug delivery device enabling sustained release of proteins

Experimental section

Materials and equipment

N-(3-dimethylaminopropyl)-N'-ethylcarbodiimide hydrochloride (EDAC) was supplied by Carl Roth GmbH (Karlsruhe, Germany). Bovine serum albumin (BSA), chitosan from shrimp shells (C3646) and thioglycolic acid (TGA) were purchased from Sigma-Aldrich (Buchs, Switzerland). 4-maleimidobutyric acid and N-hydroxysuccinimide (NHS) were obtained from TCI Europe N.V. (Zwijndrecht, Belgium). All other chemicals were of analytical grade as well and used as obtained. Milli-Q water with a resistivity of 18.2 MΩ/cm was obtained with a Milli-Q Advantage A10 System, purchased from Millipore (Billerica, MA). Prontosan® Wound Gel and Prontosan® Wound Gel X (B. Braun Medical AG, Sempach, Switzerland) were purchased from a public pharmacy in Switzerland.

Analysis and chemical modification of chitosan

The molecular weight of chitosan was determined by viscosity measurement [1] and the degree of deacetylation was analysed by ^{1}H NMR spectroscopy [2]. ^{1}H NMR spectra were recorded on a Bruker Avance III spectrometer operating at 500.13 for ^{1}H, equipped with a 5 mm BBI probe with a z-gradient. The spectra were measured in a mixture of D_2O/DCl (Armar Chemicals, Döttingen, Switzerland) at 70°C using standard Bruker pulse sequences. Spectra were processed by a Bruker TopSpin 3.0 software.

Modification of chitosan was performed according to the literature procedure [3]. Maleimide coupling was achieved as follows: To 50 mL of a 0.5% (wt/vol) solution of chitosan in Milli-Q water (pH adjusted to 5.5 with 1 M hydrochloric acid (HCl)), 4-maleimidobutyric acid, dissolved in dimethylsulfoxide (80% wt/vol), was added resulting in a concentration of 0.8% (wt/vol). EDAC and NHS were added in the same molarity as 4-maleimidobutyric acid. To obtain maleimide-chitosan, the reaction was stirred overnight at room temperature (RT). To thiolate chitosan, 1.1 vol% of TGA was added to 50 mL of a 0.5% (wt/vol) chitosan solution (pH 5.5) and EDAC and NHS were added in the same molarity. The reaction was stirred overnight at RT. Purification of both modified polymers was performed by extensive dialysis (molecular weight cut off (MWCO) 14 kDa) against 5 mM HCl at 4°C. Subsequently, maleimide-chitosan and thiolated chitosan were recovered by freeze drying (Christ Epsilon 2-6D, Adolf Kühner AG, Birsfelden, Switzerland).

Qualitative Infrared analysis (FTIR, ALPHA equipped with a single reflection ATR module, Bruker Optik GmbH, Ettlingen, Germany) was carried out with lyophilised samples of the modified chitosan compared to unmodified chitosan. Spectra were recorded in the middle infrared (4500 cm^{-1} to 400 cm^{-1}) with a spectral resolution of 4 cm^{-1} in the absorbance mode for 64 scans at RT. Spectra were processed by a Bruker OPUS/Mentor software.

Formation of chitosan hydrogel

40 mg/mL of lyophilised thiolated chitosan and 18 mg/mL of lyophilised maleimide-chitosan, respectively, were dissolved in Dulbecco's phosphate-buffered saline (PBS), pH 7.4. The solutions were formed under stirring overnight at RT. Afterwards they were mixed in a 1:1 ratio, referred to the weight of lyophilised chitosan, and allowed to crosslink overnight at RT.

Analysis of the chitosan hydrogel

For the analysis of the surface morphology by scanning electron microscopy (SEM), the hydrogels were lyophilised, glued on an aluminium sample holder and sputtered with 20 nm gold (Leica EM ACE 600 – Double Sputter Coater, Leica Microsystems, Wetzlar, Germany). Pictures were conducted using a Nova NanoSEM 230 (FEI, Hillsboro, OR) with an acceleration voltage of 5 kV, a magnification of 4691x, 6.9 mm working distance, a spotsize of 2.5, mode SE and scanmode ETD.

Rheology measurements were conducted with a cone-plate Haake Mars 40 Rheometer (Thermo Fisher Scientific Inc., Cambridge, UK). The cone had a diameter of 20 mm and an angle of 1° (gap 0.048 mm). Rotational viscosity was measured at 20°C by linearly increasing the shear rate from zero to 200.0 s^{-1} during 60.0 s followed by 30.0 s of rotation at a shear rate of 200.0 s^{-1} and again 60.0 s of linearly decreasing shear rate down to zero.

The spreadability of the hydrogel was measured according to Münzel *et al.* [4] using Equation S1, where *d* is the average of the diameter of the gel's surface under a certain weight. The spreadability of commercially purchased Prontosan® Wound Gel and Prontosan® Wound Gel X was compared to the spreadability of our chitosan hydrogel.

$$spreadability = d^2 * \pi/4$$ (Equation S1)

Swelling and degradation properties of the hydrogel were examined in PBS pH 7.4, acetic buffer pH 5 and a 1 mg/mL lysozyme solution. The weight was measured at certain time points by taking the gels

out of the medium, gently removing excess of water and weighing afterwards. Subsequently, the gels were placed back into the medium again.

To test the protein release, the chitosan hydrogel was loaded with 1.8% (wt/vol) BSA. The release was monitored using a micro dialysis approach (MWCO 300 kDa). The dialysis was carried out against PBS, pH 7.4 and pH 8.0, for 32 hours at RT. To measure the BSA concentration, 1 mL of medium was taken out at certain time points and placed back into the medium after measurement to keep constant volume. By using UV-Vis spectroscopy (Bucher Biotec AG, Basel, Switzerland) the concentration of released BSA was determined. FDA "Guidance for Industry" was used to calculate the similarity factor f_2 (Equation S2) where n is the number of time points, R_t is the release value of the reference gel at time t, and T_t is the release value of the compared gel at time t. For curves to be considered similar, f_2 values greater than 50 (50-100) ensure sameness or equivalence of the two curves and, thus, of the performance of the two products [5].

$$f_2 = 50 * \log\left\{\left(1 + \left(\frac{1}{n}\right)\Sigma_{t=1}^{n}(R_t - T_t)^2\right)^{-0.5} * 100)\right\} \qquad \text{(Equation S2)}$$

To determine statistical significance, one-way analysis of variance (ANOVA) followed by Bonferroni's *post hoc* test using statistical software of OriginPro 2016 (OriginLab Corporation, Northampton, MA) was performed, $p < 0.01$. The same software was used for curve fittings, based on Equation 1.
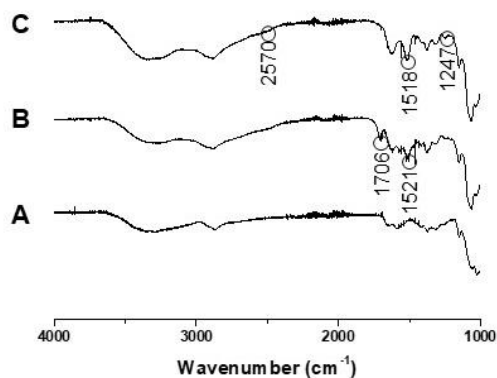
Figure S1. FTIR spectra of A) of unmodified chitosan, B) maleimide chitosan, and C) thiolated chitosan.
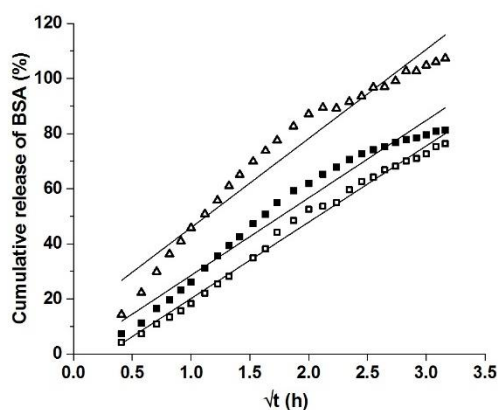
Figure S2. Linear regression of cumulative release profiles of BSA versus square root of time. Black squares represent the pre-loaded gel, which was used directly for release testing (gel 1). The pre-loaded and lyophilised gel (gel 2) is shown with open squares. The open triangles depict the values of release from the post-loaded chitosan hydrogel (gel 3). For detailed description of the formulations please see Figure 4c-e and Table 1.

References

1. G. A. Morris, J. Castile, A. Smith, et al (2009) Macromolecular conformation of chitosan in dilute solution: A new global hydrodynamic approach. Carbohydr Polym 76(4):616-621. doi:10.1016/j.carbpol.2008.11.025

2. M. Lavertu, Z. Xia, A. N. Serreqi, et al (2003) A validated 1H NMR method for the determination of the degree of deacetylation of chitosan. J Pharm Biomed Anal 32(6):1149-1158. doi:10.1016/S0731-7085(03)00155-9.

3. C. E. Kast, A. Bernkop-Schnürch (2001) Thiolated polymers – thiomers: development and in vitro evaluation of chitosan-thioglycolic acid conjugates. Biomaterials 22(17):2345-2352. doi:10.1016/S0142-9612(00)00421-X.

4. K. Münzel, J. Büchi, O.-E. Schultz (1959) Galenisches Praktikum. Wissenschaftliche Verlagsgesellschaft m.b.H. Stuttgart

5. U.S. Department of Health and Human Services, Food and Drug Administration (FDA), Center for Drug Evaluation and Research (CDER) (1997) Guidance for industry – dissolution testing of immediate release solid oral dosage forms.

2.3 MICRODOSED MIDAZOLAM FOR THE DETERMINATION OF CYTOCHROME P450 3A ACTIVITY: DEVELOPMENT AND CLINICAL EVALUATION OF A BUCCAL FILM

Klara Kiene[1], Noriyuki Hayasi[2], Jürgen Burhenne[3], Ryo Uchitomi[2], Claudia Sünderhauf[4], Yasmin Schmid[4], Manuel Haschke[4,5], Walter Emil Haefeli[3], Stephan Krähenbühl[4], Gerd Mikus[3], Hirohiko Inada[2], Jörg Huwyler[1]

[1] Department of Pharmaceutical Sciences, Division of Pharmaceutical Technology, University of Basel, Klingelbergstrasse 50, 4056 Basel, Switzerland

[2] Kyukyu Pharmaceutical Co., Ltd., 32-7 Hibari, Imizu City, Toyama 939-0351 Japan

[3] Department of Clinical Pharmacology and Pharmacoepidemiology, Heidelberg University Hospital, Im Neuenheimer Feld 410, 69120 Heidelberg, Germany

[4] Clinical Pharmacology & Toxicology, University Hospital Basel, Schanzenstrasse 55, 4031 Basel, Switzerland
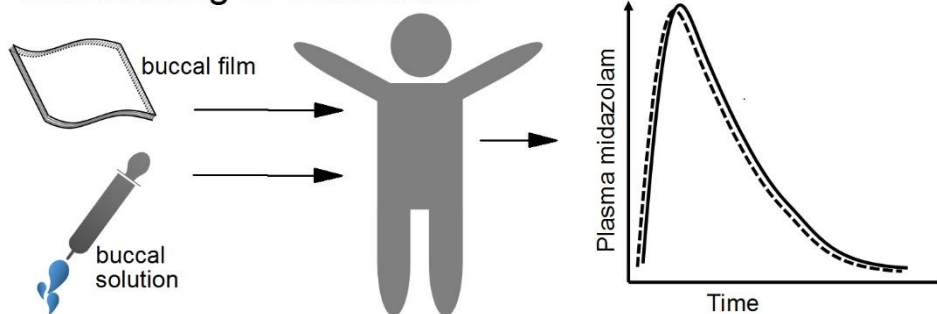
Microdosed midazolam for the determination of cytochrome P450 3A activity: Development and clinical evaluation of a buccal film

Klara Kiene[a], Noriyuki Hayasi[b], Jürgen Burhenne[c], Ryo Uchitomi[b], Claudia Sünderhauf[d], Yasmin Schmid[d], Manuel Haschke[d,1], Walter Emil Haefeli[c], Stephan Krähenbühl[d], Gerd Mikus[c], Hirohiko Inada[b], Jörg Huwyler[a,*]

[a] Department of Pharmaceutical Sciences, Division of Pharmaceutical Technology, University of Basel, Klingelbergstrasse 50, 4056 Basel, Switzerland
[b] Kyukyu Pharmaceutical Co., Ltd., 32-7 Hibari, Imizu City, Toyama 939-0351, Japan
[c] Department of Clinical Pharmacology and Pharmacoepidemiology, Heidelberg University Hospital, Im Neuenheimer Feld 410, 69120 Heidelberg, Germany
[d] Clinical Pharmacology & Toxicology, University Hospital Basel, Schanzenstrasse 55, 4031 Basel, Switzerland

ABSTRACT

Cytochrome P450 3A (CYP3A) isozymes metabolize about 50% of all marketed drugs. Their activity can be modulated up to 400-fold, which has great impact on individual dose requirements for CYP3A substrates. The activity of CYP3A can be monitored using the CYP3A substrate midazolam. To avoid pharmacological midazolam effects during phenotyping, a microdosing approach is preferred. However, the preparation of microdosed dosage forms remains a challenge. Fast dissolving buccal films are therefore proposed to facilitate this task.

It was the aim of the present study to clinically evaluate a novel buccal film containing microdoses of midazolam for assessment of CYP3A activity.

In a randomized, open-label crossover design, the pharmacokinetics of midazolam and its active hydroxy-metabolite, 1′-OH-midazolam, was assessed in 12 healthy volunteers after administration of single microdoses of midazolam (30 μg) as buccal film or buccal solution.

The buccal film did rapidly disintegrate, was well tolerated, and no adverse events occurred. The film and the solution showed very similar midazolam plasma concentration-time profiles but were not bioequivalent according to EMA and FDA guidelines. For C_{max}, AUC_{0-12h}, and $AUC_{0-\infty}$ the geometric mean ratios of film to solution, with their 90% confidence intervals in parentheses, were 1.15 (1.00–1.32), 1.16 (1.04–1.28), and 1.19 (1.08–1.31), respectively. As a proxy for CYP3A activity, molar metabolic ratios of midazolam and 1′-OH-midazolam were analyzed over time, which revealed good correlations already 1 h or 2 h after application of the film or the solution, respectively.

The tested midazolam buccal film is a convenient dosage form that facilitates administration of a phenotyping probe considerably and may potentially be used in special patient populations such as pediatric patients.

Clinical Trials.gov Identifier: NCT03204578

1. Introduction

To adjust pharmacotherapy according to individual patient's needs and to define appropriate dosing regimens, information is needed on the activity of drug metabolizing enzymes. To this end, phenotyping of important metabolic pathways can be performed (Stoll et al., 2013).

a

b

Fig. 1. In vitro characterization of the midazolam buccal film (BF). a) The area of the BF is 14 mm × 20 mm. It has a height of approximately 50 μm and contains 30 μg of midazolam. The cross-section shows the three-layered structure. b) In vitro cumulative release of midazolam from BFs according to the monograph *Dissolution test* in the *General Tests, Processes* and *Apparatus* monograph of the Japanese Pharmacopoeia. All test samples disintegrated completely within 1 min and the release profile reached almost 100% within 5 min. Values are given as mean ± SD, $n = 6$.

About 50% of all marketed drugs are metabolized in the liver by CYP3A isozymes (Zhou, 2008; Burk and Wojnowski, 2004). This group of enzymes is part of the superfamily of mixed function oxidases, is expressed in the liver and, to a lower extend, in the small intestine and other tissues (Thummel et al., 1996; Paine et al., 1996). Enzyme polymorphisms and co-medication can modulate CYP3A activity up to 400-fold (Backman et al., 1998). Therefore, dose requirements of CYP3A substrates may vary consider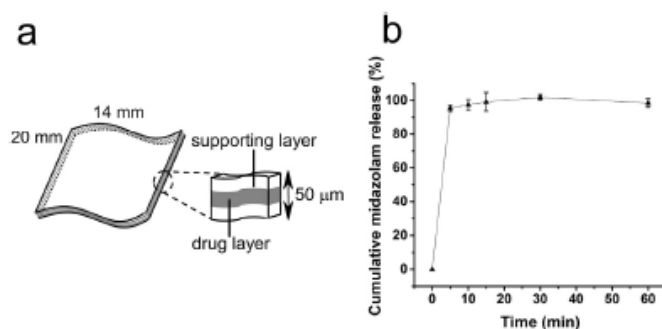ably intra- and inter-individually. CYP3A activity can be used as a biomarker to predict optimal dosing of CYP3A metabolized drugs (Stoll et al., 2013). This strategy may improve therapeutic efficacy and minimize the risk for adverse drug effects.

Determination of CYP3A activity is increasingly performed with microdoses of the CYP3A substrate midazolam, thus avoiding pharmacological adverse effects (i.e., sedation) during phenotyping (Halama et al., 2013; Hohmann et al., 2015). However, so far, no midazolam drug product with microdose strength is on the market. Therefore, microdoses have to be prepared for each patient in a laborious and error-prone dilution process from a regular strength drug solution.

Midazolam is anxiolytic and sedative. Therapeutic doses vary with intent of treatment and patient's constitution. Oral doses for pre-medication are between 7.5 and 15 mg (Roche Pharma (Schweiz) AG, 2015), which is similar to doses used for phenotyping (typically 2–7.5 mg). Because such doses show pharmacological effects, especially in patients with low CYP3A activity, a microdosing approach for CYP phenotyping was developed (Halama et al., 2013). Accordingly, we used in the present study a single midazolam microdose of 30 μg. Oral midazolam pharmacokinetics is linear over a 30,000-fold range, and already doses as small as 300 ng can be used to monitor drug interactions with strong CYP3A inhibitors (Halama et al., 2013).

Implementation of microdosing protocols involves two important challenges. First, there should be a good correlation of the pharmacokinetic parameters between conventional and microdoses of probe drugs. Previous studies have successfully shown comparability of conventional and microdoses (Halama et al., 2013). Second, administration of microdoses is a technological challenge because appropriate drug formulations are not readily available. To address the technical and handling challenges of microdosing, a novel buccal film (BF) formulation was developed. The BF is a three-layered solid dosage form (Borges et al., 2015) containing 30 μg of midazolam. In contrast to a buccal solution (prepared from the intravenous formulation of Dormicum®,

used as a reference in the present study), a BF would allow for precise dosing and administration to special patient groups such as small children (Orlu et al., 2017). In addition, solid dosage forms have a higher stability, a longer shelf life, and are less susceptible to microbial contamination. It was therefore the aim of the present study to clinically evaluate a novel BF formulation and to test whether this BF can be used for CYP3A phenotyping.

2. Methods

2.1. Trial design and study settings

This was a single-center, open-label, randomized 2-period crossover trial in 12 healthy volunteers of both sexes (6 men and 6 women) comparing midazolam pharmacokinetics after administration as buccal solution or BF. Healthy volunteers were recruited considering inclusion and exclusion criteria after pre-study clinical, medical, and laboratory examinations. The recruitment criteria can be found in the supporting information. Participants arrived on study days fasting for at least 10 h. Consumption of alcoholic and caffeinated beverages, grapefruit juice, smoking, as well as intake of other medication including herbal drugs (e.g., St. John's Wort), vitamins, trace elements, and other dietary supplements were not allowed during the study period to exclude possible drug-drug interactions.

2.2. Interventions

On the first study day, participants were assigned by block randomization to one of two treatment sequences (AB or BA). Treatment in period A was a BF (Fig. 1a) containing 30 μg of midazolam, provided by Kyukyu Pharmaceutical Co., Ltd. (Toyama, Japan). Treatment in period B consisted of a single 30 μg midazolam dose administered as buccal solution (Dormicum® V 5 mg/5 mL diluted with 5% glucose solution to obtain a midazolam concentration of 30 μg/500 μL) (Table 1). Treatment periods were divided by a 7-day washout period between administrations.

On each visit, participants received the dosing according to treatment sequence by buccal application. They were asked to keep the formulation in the oral cavity for 2 min after application, followed by drinking of 200 mL intake of water. Pharmacokinetic blood sampling was performed pre-dose and at defined time points during 12 h. After 4 h, the participants were free to consume food and permitted beverages.

Table 1
Study treatments.

Treatment A	Buccal film (BF) containing 30 μg of midazolam as a single buccal application of the BF without swallowing for 2 min, followed by drinking of 200 mL water.
Treatment B (reference)	Dilution of Dormicum® V (5 mg/5 mL) solution with 5% glucose solution in order to obtain a midazolam solution in a dose strength of 30 μg/500 μL. Single buccal application of the solution without swallowing for 2 min, followed by drinking of 200 mL water.

2.3. Analytical methods and outcomes

Plasma concentrations of midazolam and 1'-OH-midazolam were determined by a validated ultra-performance liquid chromatography coupled to tandem mass spectrometry (Burhenne et al., 2012). Limits of quantification were 0.093 pg/mL for midazolam and 0.255 pg/mL for 1'-OH-midazolam. Standard pharmacokinetic parameters were calculated with the Microsoft Excel add-in PKSolver using non-compartmental analysis (Zhang et al., 2010). To estimate the terminal elimination rate constant and the area under the concentration-time curve from time zero to infinity ($AUC_{0-\infty}$), four time points were included during the terminal log-linear phase (EMA, 2010). All pharmacokinetic parameters, except time to peak concentration (t_{max}), which was directly derived from the data, were determined using non-compartmental analysis. Statistical analysis was done with Microsoft Excel 2016 (Microsoft Corporation, Redmond, USA) and graphical analysis was performed using OriginPro (Version 9.1.0, OriginLab Corporation, Northampton, USA).

2.4. Sample size/statistical considerations

The sample size used in this project is consistent with phase 1 studies (FDA, 2001; FDA, 2003) and no formal sample size calculation had been performed. Data was analyzed descriptively. AUC from time zero to 12 h (AUC_{0-12h}), $AUC_{0-\infty}$, peak concentration (C_{max}), half-life time ($t_{1/2}$), and molar metabolic ratios were described with their geometric mean and two-sided 90% confidence intervals. t_{max} was expressed as median and total range (Halama et al., 2013). According to Katzenmaier and co-workers, estimated metabolic clearance (eCl_{met}) was calculated (Katzenmaier et al., 2011). Bioequivalence was evaluated according to the pertinent guidelines of the European Medicines Agency (EMA) and the US Food and Drug Administration (FDA): 90% confidence intervals of the geometric mean ratios of BF to solution with respect to C_{max}, AUC_{0-12h} and $AUC_{0-\infty}$ must be within the 80–125% interval (EMA, 2010; FDA, 2001; FDA, 2003). Bioequivalence measures (i.e., AUC and C_{max}) were log-transformed using natural logarithms.

Differences of the means of $AUC_{0-\infty}$, AUC_{0-12h}, and C_{max} were analyzed with a post hoc power analysis using G*Power Version 3.1.9.2, ($\alpha = 0.05$) (Faul et al., 2007; Faul et al., 2009; University of Düsseldorf - Group, n.d.).

2.5. Midazolam-containing buccal film

The midazolam-containing BF is a thin film consisting of a midazolam-containing drug layer located between two supporting layers (Fig. 1a). The quantitative composition of the midazolam BF is given in Table 2. Starting materials were tested according to European Pharmacopoeia, Japanese Pharmacopoeia, Japanese Pharmaceutical Excipients, and Japanese Standards of Food Association. Excipients and solvents were mixed until a homogenous paste was formed. The supporting layer was prepared in a continuous process by deposition of the

Table 2
Quantitative composition of midazolam BF (BF: buccal film, DL: drug layer, SL: supporting layer).

Components	Amount in a 30 μg midazolam BF (mg)
Midazolam (DL, marker substance)	0.030
Hypromellose (SL, coating agent)	4.00
Titanium oxide (SL, coating agent)	0.50
Hydroxypropylcellulose (DL, base)	7.50
Microcrystalline cellulose (DL, disintegrant)	2.50
Hydrogenated maltose starch syrup, powder (DL, disintegrant)	2.50
Macrogol 400 (DL and SL, plasticizer)	0.70
Saccharin sodium hydrate (DL, sweetening agent)	0.20

paste onto a polyester support (transparent polyethylene terephthalate, thickness of approximately 75 μm) and drying it at 70 °C for 1.7 min. Afterwards, it was overcoated with the midazolam-containing drug layer and dried at 70 °C for 2.5 min. Thus, a two-layer sheet was produced. Two two-layer sheets were combined face-to-face forming a three-layered film with a thickness of 50 μm where the midazolam-containing layer is covered by two supporting layers. From this film, samples with a size of 14 mm × 20 mm were cut, packed in polymer-aluminum laminate, and sealed. Each produced batch was analyzed with respect to outer appearance, drug content, content uniformity, and water content. Water content was measured using Karl Fischer Titration according to the Japanese Pharmacopoeia XVII. Dissolution tests were performed according to the monograph *Dissolution test* in the *General Tests, Processes and Apparatus* monograph of the Japanese Pharmacopoeia. Due to assay sensitivity, dissolution tests were performed with 100 μg midazolam BFs in 900 mL of water at 50 rpm and 37.5 °C. After 5, 10, 15, and 30 min, respectively, 5 mL of the dissolution medium were withdrawn and filtered through a 0.45 μm filter prior to analysis with ultra-performance liquid chromatography (ACQUITY UPLC, Waters, Tokyo, Japan). The column was made from stainless steel, 3.0 mm inner diameter, 100 mm in length, packed with octadecylsilanized silica gel (2.2 μm particle diameter), and worked at a constant temperature of 40 °C. The mobile phase was an 18:8:5 mixture of 0.026 mol/L disodium hydrogen phosphate dehydrate aqueous solution, pH 5.0, methanol, and acetonitrile. Flow rate was 1.0 mL/min and samples were detected using an ultraviolet absorption photometer at 220 nm.

3. Results

In the present study, an innovative BF formulation of midazolam was used for microdosing. Content of midazolam in each BF was 30.36 μg ± 1.13 μg. BFs disintegrated within 1 min and dissolution studies at 37.5 °C revealed a complete drug release within 5 min (Fig. 1b). Additional data can be found in the supporting information.

During the study, 12 volunteers were successfully exposed, and no adverse events occurred. All datasets could be used for analysis and statistical evaluation. Plasma concentration-time profiles of midazolam and 1'-OH-midazolam were overlapping for BF and the reference solution (Fig. 2). The corresponding pharmacokinetic parameters are given in Table 3. The ratio of midazolam to its metabolite 1'-OH-midazolam was stable from 1 h on (Fig. 3a, b) and similar for BF and solution, as indicated by a quotient of around 1 of the BFs molar ratios to the solution's molar ratios (Fig. 3c). During 1 h to 4 h after administration, there was no significant difference ($p > 0.05$). The comparison of single time point measurements of the parent-to-metabolite concentration ratios with corresponding ratios of the AUC_{0-12h} resulted in good correlations with $R^2 = 0.94$ for the solution after 2 h, whereas for the BF, the best correlation was already achieved after 1 h ($R^2 = 0.86$) (Fig. 3d, e).

The geometric mean ratios of BF to solution, with their 90% confidence intervals in parentheses, were 1.15 (1.00–1.32) for C_{max}, 1.16 (1.04–1.28) for AUC_{0-12h}, and 1.19 (1.08–1.31) for $AUC_{0-\infty}$, respectively (Table 4).

The G*Power post hoc power analysis ($\alpha = 0.05$) revealed a power of 0.7 for $AUC_{0-\infty}$, 0.45 for AUC_{0-12h}, and 0.27 for C_{max}, respectively.

4. Discussion

Midazolam content of BFs varied by ± 3.7%. This is well below the ± 15% threshold defined by regulatory authorities. Thus, content uniformity is assured. Stability tests were performed with samples stored in their primary packaging at 60 °C and at ambient humidity (see supporting information). Storage for 3 weeks under these stress conditions reveled < 4% loss of midazolam and no increase in water content. We conclude that BFs can be stored for prolonged periods of time (i.e., covering at least the duration of the clinical trial) at ambient

79

Results – Microdosed midazolam for the determination of CYP 3A activity: development and clinical evaluation of a BF
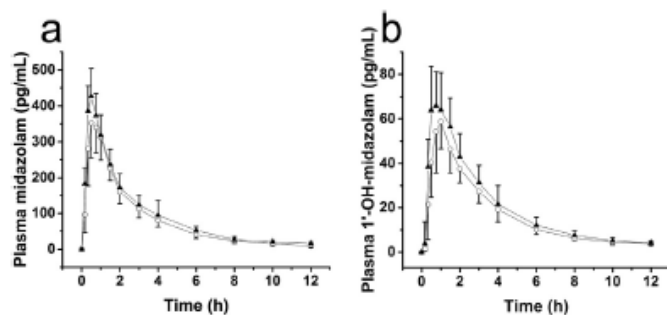
Fig. 2. Plasma concentration-time profiles of a) midazolam and b) 1'-OH-midazolam after application of one midazolam buccal film (black triangles) compared to an equal dose (30 µg) of a buccal midazolam solution (open circles). Values are represented as geometric means and their 90% confidence interval, $n = 12$ healthy volunteers.

Table 3

Pharmacokinetic parameters after administration of 30 µg of midazolam as buccal solution or buccal film (BF). t_{max} is given as median ($n = 12$) with its range in parenthesis, all other parameters as geometric means ($n = 12$) with corresponding 90% CI in parenthesis (AUC$_{0-12h}$, AUC$_{0-\infty}$: area under the plasma concentration-time profile from time zero to 12 h or infinity, respectively, BF: buccal film, CI: confidence interval, CL: clearance, C$_{max}$: peak concentration, eCL$_{met}$: estimated metabolic clearance, F: bioavailability, t$_{1/2}$: elimination half-life, t$_{max}$: time to peak concentration).

Parameter	Solution[a]	BF[a]
Midazolam		
AUC$_{0-12h}$ midazolam (pg/mL·h)	988 (842–1134)	1147 (998–1296)
AUC$_{0-\infty}$ midazolam (pg/mL·h)	1059 (898–1220)	1265 (1104–1426)
C$_{max}$ midazolam (pg/mL)	385 (309–462)	446 (386–506)
t$_{max}$ midazolam (h)	0.63 (0.33–1.00)	0.50 (0.33–0.75)
t$_{1/2}$ midazolam (h)	3.25 (2.71–3.79)	3.96 (2.88–5.03)
CL/F midazolam (mL/h)	28.3 (21.2–35.5)	23.7 (17.7–29.8)
eCL$_{met}$ (mL/min)	240 (192–299)	230 (188–280)
1'-OH-midazolam		
AUC$_{0-12h}$ 1'-OH-midazolam (pg/mL·h)	202 (173–231)	249 (207–290)
AUC$_{0-\infty}$ 1'-OH-midazolam (pg/mL·h)	229 (198–260)	277 (234–320)
t$_{max}$ 1'-OH-midazolam (h)	0.75 (0.33–1.00)	0.75 (0.33–1.50)
t$_{1/2}$ 1'-OH-midazolam (h)	4.02 (3.07–4.97)	4.12 (3.52–4.72)
Metabolic ratios		
Molar metabolic ratio: AUC$_{0-12h}$ (midazolam)/AUC$_{0-12h}$ (1'-OH-midazolam)	5.12 (4.12–6.12)	4.84 (4.20–5.48)
Molar metabolic ratio: AUC$_{0-\infty}$ (midazolam)/AUC$_{0-\infty}$ (1'-OH-midazolam)	4.86 (3.86–5.86)	4.79 (4.18–5.40)
Molar metabolic ratio: concentration ratio at 2 h (solution) and at 1 h (BF)	4.49 (3.49–5.50)	5.22 (4.16–6.29)

[a] t_{max} is given as median ($n = 12$) with its range in parenthesis, all other parameters as geometric means ($n = 12$) with corresponding 90% CI in parenthesis.

temperature without exceeding the 10% threshold for drug degradation as recommended by regulatory authorities. Microdoses of midazolam were completely released from the BFs within 5 min as demonstrated by dissolution studies performed in accordance with the Japanese Pharmacopoeia. The BFs can therefore be considered as a rapidly disintegrating drug formulation allowing for precise microdosing of midazolam.

The main prerequisite for implementation of microdosing protocols is a good correlation of the pharmacokinetic parameters between conventional and microdoses of probe drugs. Halama and co-workers, as well as Hohmann and co-workers dealt with this question. They showed that midazolam pharmacokinetics are linear over a 30,000-fold dose range (Halama et al., 2013). Even independently of the route of midazolam administration (orally vs. intravenously), their study showed

that essentially no pharmacokinetic parameter varied between microgram and milligram doses. Moreover, they concluded that inter- as well as intra-individual variability of microdoses and milligram doses of midazolam does not differ (Hohmann et al., 2015). Based on these considerations, a clinical trial was initiated using a 2×2 (i.e., 2-sequence, 2-period, 2-treatment) crossover design involving 12 volunteers. To assess the BF as drug delivery device for microdoses of midazolam, we compared a BF to a buccal solution. Obtained plasma concentration versus time profiles were very similar for both formulations and both the parent drug and the 1'-OH metabolite. Despite this similarity, bioequivalence was not reached according to criteria defined by regulatory authorities such as the EMA and FDA (EMA, 2010; FDA, 2001; FDA, 2003). These assume bioequivalence if 90% confidence intervals of the geometric mean ratios of two dosage forms fall within a range of 0.8–1.25. This applies for both C$_{max}$ and AUC. Indeed, a post hoc power analysis revealed that the sample size in our study was not large enough to draw final conclusions with respect to bioequivalence. It should be noted that in the present study the volunteers were asked to keep the BF and the reference solution for 2 min in the oral cavity before they were allowed to drink a glass of water. Interestingly, this led to higher than expected exposure levels. C$_{max}$ and AUC$_{0-\infty}$ of midazolam were about 3-fold higher compared to Halama et al. (Halama et al., 2013) and Burhenne et al. (Burhenne et al., 2012) after application of 30 µg oral midazolam. We therefore assume that in our trial midazolam was mainly absorbed buccally within the 2 min in the oral cavity (Zhang et al., 2002). This resulted in plasma concentrations, which are in the same concentration range as intravenously applied midazolam. A ratio of 1:3 dosing difference of intravenous to oral was also used by Hohmann and co-workers (Hohmann et al., 2015) to compensate for first-pass metabolism following oral drug administration.

It is important to note that phenotyping relies on metabolic ratios and not on absolute drug concentrations. Since the BF's molar ratios and the solution's molar ratios were similar, we assume that both formulations are suited for phenotyping CYP3A activity, even if they are not bioequivalent. Metabolic ratios can be determined based on AUC or plasma concentrations at a defined point in time. There was a good correlation between AUC based ratios and single point concentration ratios 2 h post dosing (solution) and 1 h post dosing (BF). This is in agreement with Donzelli et al. (Donzelli et al., 2014), where metabolic ratios were determined 2 h after oral application of the phenotyping probe as a solution. In the latter study, a correlation with an $R^2 > 0.8$ was considered to reliably predict enzyme activity. In contrast to our approach, some authors proposed to use limited sampling strategies for CYP3A phenotyping (Kim et al., 2002; Lee et al., 2006). Here, changes in plasma concentrations of the parent (and not parent to metabolite ratios) are used to determine enzymatic activity. However, there are conflicting reports regarding the reliability of limited sampling strategies since partial AUCs were found to be not suitable to assess hepatic CYP3A activity after intravenous midazolam administration (Masters

80
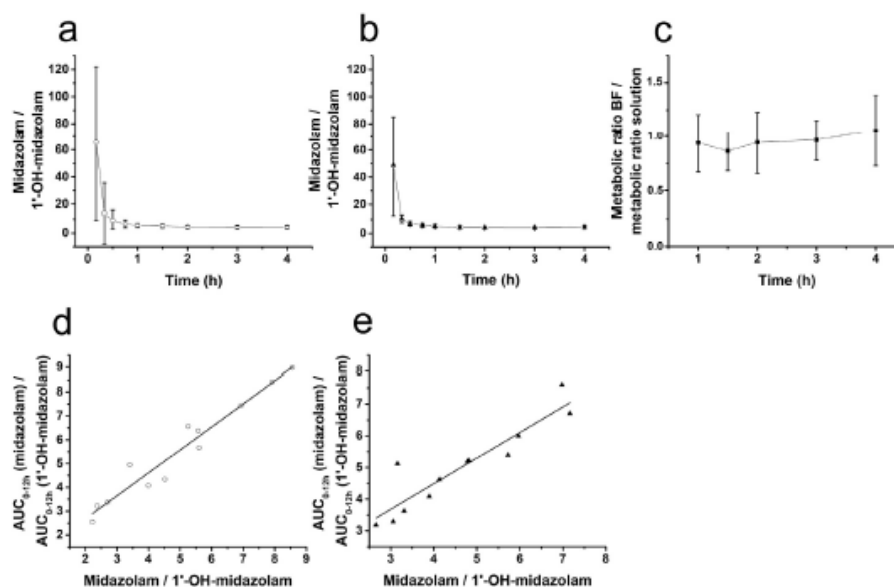
Fig. 3. Plasma concentration ratios of midazolam to 1′-OH-midazolam shown for a) the buccal solution, and b) the buccal film (BF). c) To compare both dosage forms, for each individual volunteer the quotient of the metabolic ratios (BFs ratio to solution's ratio) was calculated. According to this analysis, there was no significant difference between 1 h to 4 h after administration ($p > 0.05$). Values are given as geometric means and their 90% confidence interval, $n = 12$. d) and e) show the comparison of single time point measurements of the parent-to-metabolite plasma concentration ratios with corresponding ratios of the AUC_{0-12h} 2 h after administration of the solution the correlation was $R^2 = 0.94$ (d), whereas for the BF, the best correlation was already achieved after 1 h ($R^2 = 0.86$) (e).

Table 4

Bioequivalence analysis for C_{max}, AUC_{0-12h}, and $AUC_{0-\infty}$. Geometric mean ratios of BF to solution are represented with their 90% CI (AUC_{0-12h}, $AUC_{0-\infty}$: area under the plasma concentration-time profile from time zero to 12 h or infinity, respectively, BE: bioequivalence, BF: buccal film, CI: confidence interval, C_{max}: peak concentration).

BE parameter	Geometric mean ratio (90% CI)
C_{max}	1.15 (1.00-1.32)
AUC_{0-12h}	1.16 (1.04-1.28)
$AUC_{0-\infty}$	1.19 (1.08-1.31)

et al., 2015), in particular if less than four sampling points are used (Mueller and Drewelow, 2013). Therefore, further studies are needed to clarify if limited sampling strategies for CYP3A phenotyping can eventually be combined with our novel BF dosage form.

In addition to liver and small intestine (Thummel et al., 1996; Paine et al., 1996), CYP3A is also present in other tissues, such as in the salivary glands (Kragelund et al., 2008) and in the gingival tissue (Zhou et al., 1996). The question arises, which fraction of the administered midazolam is metabolized by each of these tissues. Metabolism in the oral epithelium seems to be unlikely based on previous reports (Vondracek et al., 2001). Since plasma concentrations using our buccal dosing strategy were comparable to intravenously administered midazolam, buccal absorption of midazolam within 2 min and avoidance of first-pass metabolism seems to be likely. Our BF formulation can therefore be used to determine hepatic (EMA, 2012) but not intestinal metabolic activity (Galetin and Houston, 2006). As a word of caution, part of the administered dose of midazolam could have been prematurely swallowed by the volunteers. In addition, drinking of 200 mL of water 2 min after drug administration might have washed away residual midazolam in the oral cavity. Thus, a contribution of intestinal CYP3A to the observed effects cannot be excluded. However, data from

the present study suggests that bioavailability of buccally administered midazolam might be close to 100%. Additional studies with bigger sample size are needed to optimize administration protocols in specific patient populations.

In terms of patient compliance (in particular if children are involved), BFs can be placed both into the buccal pouch and onto the palate. It seems to be unlikely that this might influence the outcome of phenotyping, especially if metabolic ratios are determined. However, future studies will be needed to confirm this assumption.

While phenotyping with microdoses of midazolam solutions has already been reported (Halama et al., 2013), in the present study a novel BF formulation was used. BFs are already clinically used as nausea-prevention (Zuplenz®), analgesic treatment (Onsolis®/Breakyl®, Belbuca®) (FDA; Meda Pharma GmbH), or anti-allergic treatment with olopatadine (Maruho Ltd). BFs might be especially useful for phenotyping of very vulnerable patient populations, for example geriatric patients or pediatric patients including neonates. BFs stick to the oral mucosa, cannot be spit out, and dissolve within minutes. It should be noted that solid dosage forms such as the herein presented BF have a longer shelf life, do not need refrigeration, and are easier to be administered as compared to liquids. By simply cutting the film, doses can be rapidly and easily adjusted for small pediatric patients, further minimizing the risk of potential pharmacological effects of the probe substance midazolam.

5. Conclusion

The midazolam BF and reference solution showed overlapping concentration-time profiles, but they were not bioequivalent. Microdoses of midazolam were buccally absorbed, avoiding first-pass metabolism, and allowing for a determination of hepatic CYP3A activity. One single blood sampling at least 1 h after application of midazolam BF seems to be sufficient to phenotype patients and to

determine the metabolic activity of CYP3A isozymes. Besides CYP3A phenotyping, additional uses of the BF formulation could be envisaged. For example, drug-drug interaction studies can be carried out by coadministration of an isotope labelled BF, a microdosed tablet formulation, and a potential drug-drug-interaction perpetrator. This could possibly yield the same information as the combination of an intravenous and oral dosing but in a much more convenient way. In conclusion, our microdosed midazolam BF can therefore be considered to be a convenient, safe, and reliable diagnostic tool.

Acknowledgements

Compliance with ethical standards

All procedures performed in this study were in accordance with the ethical standards of the 1964 Helsinki declaration and its subsequent amendments. Informed consent was obtained from all individual participants prior to inclusion into the trial. The study was approved by the Swiss EKNZ ethics committee on research involving humans (permission BASEC 2017-00545).

Appendix A. Supplementary data

Supplementary data to this article can be found online at https://doi.org/10.1016/j.ejps.2019.05.010.

References

Backman, J.T., Kivistö, K.T., Olkkola, K.T., Neuvonen, P.J., 1998. The area under the plasma concentration-time curve for oral midazolam is 400-fold larger during treatment with itraconazole than with rifampicin. Eur. J. Clin. Pharmacol. 54, 53–58.

Borges, A.F., Silva, C., Coelho, J.F.J., Simões, S., 2015. Oral films: current status and future perspectives: I — galenical development and quality attributes. J. Control. Release 206, 1–19.

Burhenne, J., Halama, B., Maurer, M., Riedel, K-D., Hohmann, N., Mikus, G., et al., 2012. Quantification of femtomolar concentrations of the CYP3A substrate midazolam and its main metabolite 1'-hydroxymidazolam in human plasma using ultra performance liquid chromatography coupled to tandem mass spectrometry. Anal. Bioanal. Chem. 402, 2439–2450.

Burk, O., Wojnowski, L., 2004. Cytochrome P450 3A and their regulation. Naunyn Schmiedeberg's Arch. Pharmacol. 369, 105–124.

Donzelli, M., Derungs, A., Serratore, M.-G., Noppen, C., Nezic, L., Krähenbühl, S., et al., 2014. The basel cocktail for simultaneous phenotyping of human cytochrome P450 isoforms in plasma, saliva and dried blood spots. Clin. Pharmacokinet. 53, 271–282.

EMA, 2010. Guideline on the investigation of bioequivalence; CPMP/EWP/QWP/1401/98 rev. 1/Corr (2010) [internet]. Available from European Medicines Agency, Committee for Medicinal Products for Human Use (CHMP)http://www.ema.europa.eu/docs/en_GB/document_library/Scientific_guideline/2010/01/WC500070039.pdf.

EMA, 2012. Guideline on the Investigation of Drug Interactions; CPMP/EWP/560/95/Rev. 1 Corr. 2. pp. 59.

Faul, F., Erdfelder, E., Lang, A.-G., Buchner, A., 2007. G*Power 3: a flexible statistical power analysis program for the social, behavioral, and biomedical sciences. Behav. Res. Methods 39, 175–191.

Faul, F., Erdfelder, E., Buchner, A., Lang, A.-G., 2009. Statistical power analyses using G*Power 3.1: tests for correlation and regression analyses. Behav. Res. Methods 41,

1149–1160.

FDA, 2001. Guidance for industry: statistical approaches to establishing bioequivalence. vol. 2001 U.S. Department of Health and Human Services Food and Drug Administration Center for Drug Evaluation and Research (CDER) Internet. Available from. https://www.fda.gov/downloads/drugs/guidances/ucm070244.pdf.

FDA, 2003. Guidance for industry: bioavailability and bioequivalence studies for orally administered drug products - general considerations (2003) [internet]. Available from U.S. Department of Health and Human Services Food and Drug Administration Center for Drug Evaluation and Research (CDER)https://www.fda.gov/ohrms/dockets/ac/03/briefing/3995B1_07_GFI-BioAvail-BioEquiv.pdf.

FDA Drugs@FDA: FDA approved drug products. [Internet]. [cited 2018 Jan 23]. Available from. https://www.accessdata.fda.gov/scripts/cder/daf/index.cfm.

Galetin, A., Houston, J.B., 2006. Intestinal and hepatic metabolic activity of five cytochrome P450 enzymes: impact on prediction of first-pass metabolism. J. Pharmacol. Exp. Ther. 318, 1220–1229.

Halama, B., Hohmann, N., Burhenne, J., Weiss, J., Mikus, G., Haefeli, W.E., 2013. A nanogram dose of the CYP3A probe substrate midazolam to evaluate drug interactions. Clin. Pharmacol. Ther. 93, 564–571.

Hohmann, N., Kocheise, F., Carls, A., Burhenne, J., Haefeli, W.E., Mikus, G., 2015. Midazolam microdose to determine systemic and pre-systemic metabolic CYP3A activity in humans. Br. J. Clin. Pharmacol. 79, 278–285.

Katzenmaier, S., Markert, C., Riedel, K-D., Burhenne, J., Haefeli, W.E., Mikus, G., 2011. Determining the time course of CYP3A inhibition by potent reversible and irreversible CYP3A inhibitors using a limited sampling strategy. Clin. Pharmacol. Ther. 90, 666–673.

Kim, J.S., Nafziger, A.N., Tsunoda, S.M., Choo, E.F., Streetman, D.S., Kashuba, A.D.M., et al., 2002. Limited sampling strategy to predict AUC of the CYP3A phenotyping probe midazolam in adults: application to various assay techniques. J. Clin. Pharmacol. 42, 376–382.

Kragelund, C., Hansen, C., Torpet, L.A., Nauntofte, B., Brøsen, K., Pedersen, A.M.L., et al., 2008. Expression of two drug-metabolizing cytochrome P450-enzymes in human salivary glands. Oral Dis. 14, 533–540.

Lee, L.S., Bertino, J.S., Nafziger, A.N., 2006. Limited sampling models for oral midazolam: midazolam plasma concentrations, not the ratio of 1-hydroxymidazolam to midazolam plasma concentrations, accurately predicts AUC as a biomarker of CYP3A activity. J. Clin. Pharmacol. 46, 229–234.

Maruho Co., Ltd Products of Maruho Co., Ltd. [internet]. Maruho Co.Ltd - Contrib. Better health people world. [cited 2018 Jan 23]. Available from. https://www.maruho.co.jp/sp/english/aboutmaruho/corporate/profile/products.html.

Masters, J.C., Harano, D.M., Greenberg, H.E., Tsunoda, S.M., Jang, I.-J., Ma, J.D., 2015. Limited sampling strategy of partial area-under-the-concentration-time-curves to estimate midazolam systemic clearance for cytochrome P450 3A phenotyping. Ther. Drug Monit. 37, 84–89.

Meda Pharma GmbH & Co. KG Breakyl ® Buccalfilm Prescribing Information [Internet]. [cited 2018 Jan 23]. Available from. https://www.fachinfo.de/suche/fi/014069.

Mueller, S.C., Drewelow, B., 2013. Evaluation of limited sampling models for prediction of oral midazolam AUC for CYP3A phenotyping and drug interaction studies. Eur. J. Clin. Pharmacol. 69, 1127–1134.

Orlu, M., Ranmal, S.R., Sheng, Y., Tuleu, C., Seddon, P., 2017. Acceptability of orodispersible films for delivery of medicines to infants and preschool children. Drug Deliv 24, 1243–1248.

Paine, M.F., Shen, D.D., Kunze, K.L., Perkins, J.D., Marsh, C.L., McVicar, J.P., et al., 1996. First-pass metabolism of midazolam by the human intestine. Clin. Pharmacol. Ther. 60, 14–24.

Roche Pharma (Schweiz) AG, 2015. Dormicum ® injectionsolution prescribing information [internet]. [cited 2018 Jan 19]. Available from. http://compendium.ch/mpro/mnr/2535/html/de.

Stoll, F., Burhenne, J., Lausecker, B., Weiss, J., Thomsen, T., Haefeli, W.E., et al., 2013. Reduced exposure variability of the CYP3A substrate simvastatin by dose individualization to CYP3A activity. J. Clin. Pharmacol. 53, 1199–1204.

Thummel, K.E., O'Shea, D., Paine, M.F., Shen, D.D., Kunze, K.L., Perkins, J.D., et al., 1996. Oral first-pass elimination of midazolam involves both gastrointestinal and hepatic CYP3A-mediated metabolism. Clin. Pharmacol. Ther. 59, 491–502.

University of Düsseldorf - Group Allgemeine Psychologie und Arbeitspsychologie. G*Power [Internet]. [cited 2018 Aug 20]. Available from. http://www.gpower.hhu.de/.

Vondracek, M., Xi, Z., Larsson, P., Baker, V., Mace, K., Pfeifer, A., et al., 2001. Cytochrome P450 expression and related metabolism in human buccal mucosa. Carcinogenesis 22, 481–488.

Zhang, H., Zhang, J., Streisand, J.B., 2002. Oral mucosal drug delivery. Clin. Pharmacokinet. 41, 661–680.

Zhang, Y., Huo, M., Zhou, J., Xie, S., 2010. PKSolver: an add-in program for pharmacokinetic and pharmacodynamic data analysis in Microsoft Excel. Comput. Methods Prog. Biomed. 99, 306–314.

Zhou, S.-F., 2008. Drugs behave as substrates, inhibitors and inducers of human cytochrome P450 3A4. Curr. Drug Metab. 9, 310–322.

Zhou, L.X., Pihlstrom, B., Hardwick, J.P., Park, S.S., Wrighton, S.A., Holtzman, J.L., 1996. Metabolism of phenytoin by the gingiva of normal humans: the possible role of reactive metabolites of phenytoin in the initiation of gingival hyperplasia. Clin. Pharmacol. Ther. 60, 191–198.

Supporting information

Microdosed midazolam for the determination of cytochrome P450 3A activity: development and clinical evaluation of a buccal film

Recruitment of healthy volunteers

Healthy volunteers were recruited considering inclusion and exclusion criteria (Table S1) after pre-study clinical, medical, and laboratory examinations (Table S2).

Table S1. Inclusion and exclusion criteria for volunteers participating in the pharmacokinetic study.

Inclusion Criteria
Healthy male or female subjects, 18-50 years, BMI 18.0-29.9 kg/m^2. Ability to understand and willingness to comply with study interventions and restrictions.
Signed informed consent after full explanation of the study to the participant.
Physical and mental health; medical assessment determined by medical history, physical examination, especially ECG, and laboratory evaluation shows no clinically relevant abnormalities.
Normal renal function and normal liver blood tests (minor deviations of laboratory values from normal range are acceptable, if judged by the investigator to be of no clinical relevance).
Females of child bearing potential are only included if using reliable contraception with a Pearl Index <1% (i.e. two independent effective contraceptive methods) during the study and 1 week after the last administration of study medication.

Exclusion Criteria
Any regular drug treatment within the last two weeks, except for oral contraceptives.
Exclusion of the trial due to irregular drug treatment or regular substitution of endogenous substances, minerals, and trace elements will be decided on an individual basis (considering the potential impact on CYP3A activity and drug absorption).
Any intake of a substance known to induce or inhibit drug metabolising enzymes or transport system enzymes within a period of less than 10 times the respective elimination half-life or 3 weeks (whatever is longer).
Any participation in a clinical trial within the last four weeks before inclusion.
Blood donation within 4 weeks before the trial or hemoglobin ≤11 g/dL.
Vaccination (active or passive) within one month before inclusion into the trial.
Any physical disorder that could interfere with the participant's safety during the clinical trial or with the study objectives.
Any acute or chronic illness, or clinically relevant findings in the pre-study examination.
History or clinical evidence of any disease or medical condition, which may interfere with the pharmacokinetics of midazolam or which may increase the risk for toxicity or adverse events.
Allergies (except for mild forms of hay fever) or history of hypersensitivity reactions.
Active liver disease.
Regular smoking (≥5 cigarettes/week).
Excessive alcohol drinking (>20 g alcohol/day).
Inability to communicate well with the investigator due to language problems or poor mental development.
Inability or unwillingness to give written informed consent.
For female participants: pregnancy or lactation.

68

Results – Microdosed midazolam for the determination of CYP 3A activity: development and clinical evaluation of a BF – SI

Table S2. Medical Examination of the volunteers prior to participation.

Medical Examination
Medical history.
Physical examination including measurement of height and weight, blood pressure, pulse rate and temperature, a review of organ systems including lungs, heart, abdomen, liver, kidneys, and peripheral pulses, eyes, nose, throat, skin, and short neurological status.
12-lead electrocardiogram.
Safety laboratory screening (red blood cell count, haematocrit, haemoglobin, white blood cell count with differential (neutrophils, eosinophils, basophils, monocytes, and lymphocytes), AST, ALT, AP, CK, total bilirubin, creatinine, total protein, albumin, INR, electrolytes (sodium, potassium, calcium, chloride).
Urine analysis: chemical testing by a strip.
Urine screening for illicit drugs.
Qualitative urine pregnancy test in female participants.

Stability of the buccal film

Stability tests were performed under stress conditions at 60°C. Results from the stress tests are summarised in Table S3.

Table S3. Stability testing of the midazolam-containing buccal film at 60°C for up to 3 weeks.

Storage condition	Outer appearance	Midazolam content (%)	Water content (%)	Color difference (ΔE * ab)
Initial	white film preparation	99.4	3.88	-
60°C – 1 week	white film preparation	96.7	3.21	0.38
60°C – 2 weeks	white film preparation	96.5	3.35	0.68
60°C – 3 weeks	white film preparation	96.1	3.32	0.94

69

Results – Microdosed midazolam for the determination of CYP 3A activity: development and clinical evaluation of a BF – SI

2.4 ORAL DISINTEGRATING TABLETS BASED ON FUNCTIONALISED CALCIUM CARBONATE: A PALATABILITY STUDY IN CHILDREN FROM 2 TO 10 YEARS
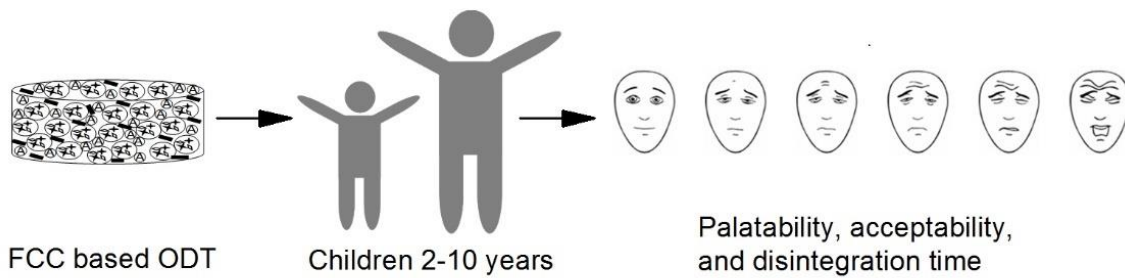
Key Points

Question: Are orally dispersible tablets acceptable for oral administration of medications to preschool and school-age children?

Findings: In this cross-sectional study that included 40 children aged 2 to 10 years, a single dose of an orally dispersible placebo carrier tablet was deemed to be highly acceptable by 93% of parents and staff, and had even higher acceptability (97%) based on observation of the participating children.

Meaning: Greater use of this or similar child-appropriate solid oral formulations could improve access to high-quality medicines and adherence for children globally.

Abstract

Importance: Despite offering advantages for stability and handling, very few solid oral formulations appropriate for young children are available.

Objective: To evaluate the acceptability of a novel oral dispersible tablet formulation for administration to preschool and school-age children.

Design: Cross-sectional acceptability study of a novel child-appropriate monolithic calcium carbonate based orally dispersible placebo carrier tablet.

Setting: Outpatient surgical and fracture clinic of a Swiss university children's hospital.

Participants: Children aged 2 to 10 years without underlying diseases and not wearing fixed dental braces were eligible. Children indicating their verbal assent to take part and for whom parents provided their written informed consent to participation were recruited.

Exposure: One orally dispersible placebo carrier tablet (5 mm diameter) was administered by a member of the research staff to each participating child by placement on the tongue or into the buccal pouch.

Main outcomes and Measures: Acceptability was rated by parents on a 5-point Likert scale ("very acceptable" to "completely inacceptable"), and by research staff on a 4-point acceptability scale ("child wants to try tablet" to "refusal"). Child behaviour and responses were observed to identify poor acceptability.

Results: In total, 40 children (2-5 years of age, n=20; 6-10 years of age, n=20) were included in the study. The orally dispersible placebo carrier tablet had a very high acceptability. The majority of parents reported the formulation to be acceptable or very acceptable (37/40, 93%). For the same children, staff reported administering the orally dispersible tablet without problems. Parents whose

children had previously received oral medications, 13/35 (37%), reported difficulties in administering conventional marketed child-appropriate formulations. The orally dispersible tablet was reported to be easier to administer by 27/35 (77%) parents. None of the children showed distress on receipt of the tablet and only 1/40 children spat out the tablet.

Conclusion and Relevance: A novel oral dispersible placebo carrier tablet was reported to be highly acceptable for administration to preschoolers and school-age children by parents and healthcare staff. Due to advantageous physiochemical properties, this and similar formulations may simultaneously improve access to high-quality medicines and adherence for children globally.

Introduction

Among paediatric patients, medication palatability is essential for patient acceptance, therapeutic compliance and successful outcome of a therapy [1, 2]. Oral dosage forms are preferred to treat children [3]. A medication's taste and the ability of children to swallow their medicine may greatly influence the selection of a drug, therefore therapy and prescribing practice. Despite offering advantages for stability and handling, very few solid oral dosage formulations appropriate for young children are available. Most of the drugs on the market are authorised only for adult use [4]. Therefore, paediatricians need to prepare and administer unlicensed formulations by manipulating adult dosage forms ("off-label use"). This includes splitting or crushing tablets, opening capsules, dispersing tablets or capsules in liquids and taking proportions of them, cutting suppositories, or applying injectable solutions by other routes. However, such manipulations might extremely influence bioavailability and safety of a medicinal product [5]. Additionally to deeper and more exact information on the consequences of such manipulations, the manufacturers are asked to perform paediatric investigations with the products intended for paediatric use [5]. Formulating medicines for children is challenging due to different aspects. Paediatric formulations have to allow for accurate dosing and show good palatability to support patient's compliance with the therapy [6]. So far, there is not much known about the acceptability of different dosage forms, administration volumes, dosage form size, taste, and acceptability and safety of excipients with regard to age and developments status of the child [5]. Different age classes and interregional differences make it necessary to produce different types of galenical formulations in several drug concentrations, flavours, and colours [6, 7].

When planning a clinical trial with children it is necessary to adapt the methods to the child's developmental stage, and to focus on practical and ethical considerations and limitations [8]. According to the EMA, palatability studies for children should be short, entertaining, easily understandable and with as little variables as possible. The younger the children, the more important

it is to respect these principles. Moreover, it has to be kept in mind that younger children have difficulties in communicating their feeling and preferences. Generally, the EMA considers children older than 4 years as capable of participating in taste trials [5].

Speaking of solid oral dosage forms for children, orally dispersible tablets (ODTs) are very interesting formulations [9]. The palatability of a novel oral dispersible tablet formulation based on Functionalised Calcium Carbonate (FCC) was already assessed in adults, showing good acceptability, pleasant taste and no bad sensations during administration [10]. It remains to be tested whether the palatability in children is as positive as in adults, because it is not possible to transfer the findings from adults directly to children due to different taste and mouthfeel sensations [5, 11]. So far, there has not been much systematic methodological research on how to evaluate taste and mouthfeel of age-appropriate formulations in paediatric patient populations. This work aims to evaluate the acceptability of a novel placebo ODT for administration to preschool and school-age children.

Subjects and Methods

This single-centre cross-sectional observational study included 40 children attending the outpatient surgical and fracture clinic of the University Children's Hospital Basel (UKBB). The children were between 2 years and 10 years old, as this is the target group that is most likely to benefit from an ODT formulation being available as an alternative to oral suspensions. The younger group (20 children) was aged between 2 and 5 years, the older volunteers (20 children) were 6 to 10 years old. Keeping in mind the difficulties of younger children to communicate preferences between several formulations, the focus was on acceptance of the ODT's palatability [12]. Administration and children's acceptance of the tablet was rated by research staff on a 4-point acceptability scale (from "child wants to take the ODT" to "refusal") and by parents on a 5-point Likert scale (from "very acceptable" to "completely inacceptable"). For the older subpopulation, additional closed questions were combined with a facial hedonic scale (FHS, Figure 1).

Population	Centre	Test tablet	Palatability assessment
2 to 5 years, 20 children	UKBB outpatient surgical and fracture clinic	single dose of a placebo, orange flavoured, FCC-based ODT	1. assessment by staff 2. parenteral evaluation
6 to 10 years, 20 children	UKBB outpatient surgical and fracture clinic	single dose of a placebo, orange flavoured, FCC-based ODT	1. assessment by staff 2. parenteral evaluation 3. child-appropriate questions 4. FHS

Figure 1. Study design

Female and male volunteers were eligible for enrolment if they were 2 to 10 years of age, indicating their verbal assent to take part and for whom the parents provided their written informed consent. Volunteers were excluded for any of the following reasons: wearing fixed dental braces; suffering from injuries or inflammations affecting the oral cavity or throat; suffering from dysphagia, olfactory impairment, kidney impairment, or hypercalcaemia; known allergy against medications; ongoing antibiotic treatment at the time of the study; known moderate to severe developmental delay as reported by the parents; participation in any other study within the 30 days preceding and during the study; if parents were unlikely to reliably complete the structured questionnaire or understand informed consent due to significant language barriers.

Study protocol and consent forms were approved by an Institutional Ethics Committee. Each study consisted of an approximately 30-min visit without follow-up visits.

Placebo ODTs with a diameter of 5 mm, containing FCC, orange aroma, citric acid, hydrogen carbonate, and a cyclamate/saccharine mix, were provided by University of Basel [10].

The participants were screened on days of routine appointments in the fracture and surgical outpatient clinic of the UKBB and approached during waiting times. If a child was identified to meet the inclusion criteria, designated and trained research staff obtained informed consent from the legal guardian and verbal assent from the child. After administration of one ODT onto the tongue or into the buccal pouch the parents were asked to complete a questionnaire together with the study personnel. A questionnaire developed for adult participants [10] and adapted to suit parental reporting of acceptability and palatability was used. The spontaneous reactions of the children (e.g. positive comments, spitting out of ODT, or crying,) were observed and recorded by the staff to identify poor acceptability. In addition, the older children were asked whether they would like to have a second tablet, how fast the ODT disintegrated and where residues were felt within the mouth. The latter answers were checked visually by the study personnel. Moreover, the older subjects were questioned how they had liked the ODT by pointing to the appropriate face on an FHS (Figure 2) [13, 14]. After finishing the assessment, children and parents were free to leave.
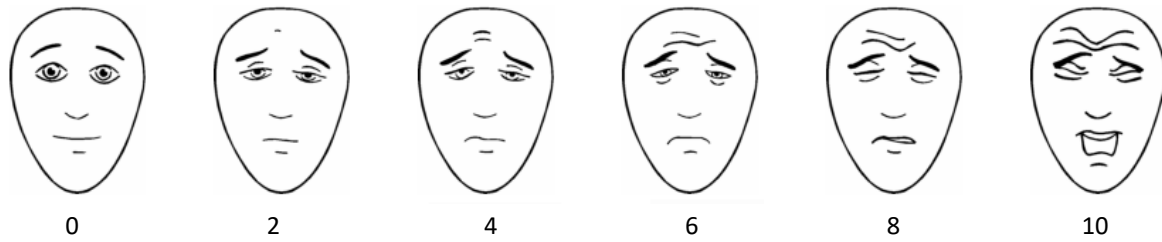
Figure 2. Facial hedonic scale (FHS) used to evaluate the taste sensation of children between 6 to 10 years. The children reported the face that described their experience with the ODT best, ranging from 0 ("very good") to 10 ("very bad").

Statistical Analysis

The objective of the statistical analysis was to assess taste acceptance which was the primary study variable. Subjects were included in the palatability analyses if they satisfied the entry criteria and finished taste evaluation.

Results

In total, 40 children (2-5 years of age, n=20; 6-10 years of age, n=20) were included in the study. 78 children were screened for this palatability study and 38 were excluded for several reasons: they did not appear at the hospital, or enough children in their age group were already included (17/78, 22%); their parents had not enough time to participate (3/78, 4%); their parents refused to participate (8/78, 10%); children did not give verbal assent (1/78, 1%); no reliable communication between staff and parents was possible due to language barriers (4/78, 5%); children met medical exclusion criteria (5/78, 6%).

The orally dispersible placebo carrier tablet had a very high acceptability. The staff reported administering the ODT without any problems for almost all children (39/40, 98%). The majority of parents reported the formulation to be acceptable or very acceptable (37/40, 93%). Parents whose children had previously received oral medications, 13/35 (37%), reported difficulties in administering conventional marketed child-appropriate formulations. The ODT was reported to be easier to administer by 27/35 (77%) of parents. None of the children showed distress on receipt of the tablet and only 1/40 children spat out the tablet.

Using the FHS, all children of the older subpopulation (20/20, 100%) rated the palatability of the ODT between 0 and 2. Moreover, 80% (16/20) of them wanted to take a second ODT when asked for it. Evaluating the older volunteers, the mean disintegration time within the children's mouth was 26 s ± 21 s, reflecting very well the disintegration time assessed by the research personnel. ODT

residues were distributed mainly on the tongue and within the cheek pouch, but neither were they detected in the corners of the mouth of any child, nor did any child try to get rid of ODT residues, e.g. by spitting them out or communicating an urge to drink. Moreover, no unpleasant mouthfeel was described. No adverse events were reported.

Conclusive Discussion

The children were divided into two subgroups. It was already recommended previously to assess taste acceptance in children younger than 5 years by using the child's own spontaneous verbal judgements. Moreover, it was suggested to involve parents by asking about any discomfort or other observations in relation to the acceptance of the study medication by their child. This would ensure reliable outcome of a palatability study with young children [12, 15]. In contrast, children older than 6 years were considered to be able to express acceptability using an FHS as well as verbal judgement [16, 17].

The mean disintegration time measured in children between 6 and 10 years was slightly longer than in adults (26 s vs. 22 s). This shows that the formulation of such ODT is well suited for children even if it is assumed that the mouth and tongue movement during administration have a big influence on the ODT's disintegration time.

Analysis of the palatability study revealed very good acceptance of an FCC-based ODT by preschool as well as school-aged children. Greater use of this or similar child-appropriate solid oral formulations could improve world-wide access to high-quality medicines and adherence for children. A palatable inert carrier ODT could be formulated to contain a wide range of active pharmaceutical ingredients for oral delivery that are currently available only as bad tasting liquid formulations or are unavailable as child-friendly formulations [4]. These include frequently used drugs, such as antibiotics and steroids.

References

1. Toscani M, Drehobl M, Freed J, Stool S (2000) A multicenter, randomized, comparative assessment in healthy pediatric volunteers of the palatability of oral antibiotics effective in the therapy of otitis media. Current Therapeutic Research 61:278–285 . doi: 10.1016/S0011-393X(00)80018-1

2. Powers JL, Gooch WM, Oddo LP (2000) Comparison of the palatability of the oral suspension of cefdinir vs. amoxicillin/clavulanate potassium, cefprozil and azithromycin in pediatric patients. Pediatr Infect Dis J 19:S174-180

3. Breitkreutz J, Boos J (2007) Paediatric and geriatric drug delivery. Expert Opinion on Drug Delivery 4:37–45 . doi: 10.1517/17425247.4.1.37

4. Tan E, Cranswick NE, Rayner CR, Chapman CB (2003) Dosing information for paediatric patients: are they really "therapeutic orphans"? Med J Aust 179:195–198

5. EMA (2006) Reflection paper: formulations of choice for the paediatric population - EMEA/CHMP/194810/2005

6. EMA (2001) ICH Topic E 11 - clinical investigation of medicinal products in the paediatric population - CPMP/ICH/2711/99

7. Nunn T, Williams J (2005) Formulation of medicines for children. Br J Clin Pharmacol 59:674–676 . doi: 10.1111/j.1365-2125.2005.02410.x

8. Davies EH, Tuleu C (2008) Medicines for Children: A Matter of Taste. The Journal of Pediatrics 153:599-604.e2 . doi: 10.1016/j.jpeds.2008.06.030

9. Panchal DM, Tiwari A, Srivastava P (2013) A review on orodispersible tablets - a novel formuation for oral drug delivery system and its future perspective. Indo American Journal of Pharmaceutical Research 3:4149–4168

10. Wagner-Hattler L, Wyss K, Schoelkopf J, et al (2017) In vitro characterization and mouthfeel study of functionalized calcium carbonate in orally disintegrating tablets. International Journal of Pharmaceutics 534:50–59 . doi: 10.1016/j.ijpharm.2017.10.009

11. Segovia C, Hutchinson I, Laing DG, Jinks AL (2002) A quantitative study of fungiform papillae and taste pore density in adults and children. Brain Res Dev Brain Res 138:135–146

12. Sjövall J, Fogh A, Huitfeldt B, et al (1984) Methods for evaluating the taste of paediatric formulations in children: A comparison between the facial hedonic method and the patients' own spontaneous verbal judgement. Eur J Pediatr 141:243–247 . doi: 10.1007/BF00572770

13. Young JR, Sih C, Hogg MM, et al (2018) Qualitative Assessment of Face Validity and Cross-Cultural Acceptability of the Faces Pain Scale: "Revised" in Cameroon. Qual Health Res 28:832–843 . doi: 10.1177/1049732318757488

14. Freeman K, Smyth C, Dallam L, Jackson B (2001) Pain Measurement Scales: A Comparison of the Visual Analogue and Faces Rating Scales in Measuring Pressure Ulcer Pain. Journal of Wound, Ostomy and Continence Nursing 28:290–296

15. Bagger-Sjöbäck D, Bondesson G (1989) Taste evaluation and compliance of two paediatric formulations of phenoxymethylpenicillin in children. Scand J Prim Health Care 7:87–92

16. Matsui D, Lim R, Tschen T, Rieder MJ (1997) Assessment of the palatability of β-lactamase-resistant antibiotics in children. Arch Pediatr Adolesc Med 151:599–602 .
 doi: 10.1001/archpedi.1997.02170430065013

17. Angelilli ML, Toscani M, Matsui DM, Rieder MJ (2000) Palatability of oral antibiotics among children in an urban primary care center. Arch Pediatr Adolesc Med 154:267–270 . doi: 10.1001/archpedi.154.3.267

Supporting information

Oral disintegrating tablets based on Functionalised Calcium Carbonate: a palatability study in children from 2 to 10 years

Data collection about safety of the ODT's excipients

Pharmaceutical excipients are defined as chemically and pharmacologically inactive substances serving the formulation's needs. Typical classes of excipients used in solid dosage forms are fillers, binders, lubricants, disintegrants, coating and matrix polymers or waxes, and glidants. Excipients are often comprising a major part of a medicinal form. Therefore, they have to be checked for their safety and drug compatibility. Paediatric formulations need to be assessed especially regarding their risk for toxicity. Herein, application ranges of the excipients used in the taste-masked ODT formulations for children 2 to 10 years old are summarised. The handbook of excipients and the Food Legislation Europa served as reliable sources.

(I) Calcium carbonate is generally regarded as a nontoxic material. It may cause constipation and flatulence and between 4 and 60 g it can result in hypercalcemia or renal impairment. Calcium carbonate may interfere with the absorption of other drugs from gastrointestinal tract if administered concomitantly [1]. It is commercially available as Calcium Sandoz® 500. For children between 1 and 6 years it is recommended to give 500 mg calcium, that yield in the tablet to 875 mg calcium carbonate [2]. Calcium carbonate E 170 is authorised to be used in the category "dietary foods for infants for special medical purposes and special formulae for infants" with the term *quantum satis* according to the Food Legislation Europa [3].

(II) Calcium phosphate tribasic is widely used in oral pharmaceutical formulations and food products. It is generally regarded as non-toxic and non-irritant at the concentrations that are used for drug formulations. In excessive amounts crystals may deposit in tissues. Oral ingestion may cause abdominal discomfort such as nausea and vomiting [1]. The Food Legislation Europa limited calcium phosphate (E 341) in dietary foods for infants for special medical purposes and special formulae for infants to 1000 mg/kg [3].

(III) Croscarmellose sodium is regarded as non-toxic and non-irritant excipient, mainly used as disintegrant in oral pharmaceutical formulations. In the UK, croscarmellose sodium is accepted for use in dietary supplements [1]. Following commercially available products for children contain croscarmellose sodium as disintegrant: Clarithromycin Basics® 250 mg/5 mL Granulat, Euthyrox®

25 microgram [4, 5]. Crosslinked carmellose sodium E 468 is authorised to be used in tablets up to 5% by weight (50'000 mg/1 kg) by the Food Legislation Europa [3].

(IV) Citric acid is found naturally in the human body, mainly in the bone. It is commonly consumed as part of a normal diet. Citric acid is regarded as non-toxic excipient. Frequent and excessive consumption has been associated with erosion of teeth. Moreover, citric acid can enhance intestinal aluminium absorption in patients with impaired renal function resulting in increased, harmful serum aluminium levels. Therefore, patients with renal failure taking aluminium should not take citric acid containing products [1]. Citric acid is used in ACC® akut Junior Hustenlöser, licensed for children [6]. Citric acid E 330 is authorised to be used in Infant formulae with the term *quantum satis* according to the Food Legislation Europa [3].

(V) Sodium hydrogen carbonate is used in many pharmaceutical formulations, also including injections, ontological, or ophthalmic preparations. Administration of excessive amounts may disturb the body's electrolyte balance resulting in metabolic alkalosis or possible sodium overload due to metabolism of sodium bicarbonate. The amount in antacids or effervescent tablets has been sufficient to exacerbate chronic heart failure, especially in elderly patients [1]. Sodium bicarbonate is also called baking soda. It is used in effervescent tablets and ACC akut® Junior Hustenlöser [6]. Sodium hydrogen carbonate (E 500 (ii)) is authorised by the Food Legislation Europa to be used in dehydrated milk with the term *quantum satis* [3].

(VI) Sodium cyclamate has been discussed controversially. The FDA banned it in 1970, but extensive long-term animal feeding studies and epidemiological studies in humans failed to show any evidence for carcinogenic or mutagenic potential of sodium cyclamate. The WHO set an estimated acceptable daily intake for sodium cyclamate to 11 mg/kg body weight. Sodium cyclamate is used in the product Algifor® Dolo Junior being widely used in all paediatric age groups. The suspension contains 2 mg/mL sodium cyclamate. If a 6-8 month old infant with 5 kg body weight is dosed 3 times daily with 2.5 mL this results in an exposure of 3 mg/kg [7]. According to the Food Legislation Europa sodium cyclamate is authorised under E 952 to be used in solid food supplements (e.g. capsules or tablets) in a maximum dosage of 500 mg/kg [3].

(VII) Sodium saccharine is considered a safe intense sweetener. According to the WHO limit of intake is 2.5 mg/kg body weight, whereas the Committee on Toxicity of Chemicals in Food, Consumer Goods, and the Environment defines it as up to 5 mg/kg body weight [1]. In Switzerland, sodium saccharine is an excipient of Convulex®, for long-term treatment of epilepsy of paediatric patients [8]. The Food Legislation Europa authorised sodium saccharine (E 954) as an additive in dietary foods for special medical purposes with the restriction of 200 mg/kg [3].

(VIII) Orange aroma Givaudan permaseal was used in a novel paediatric formulation, so far not tested in children, but not considered as problematic either [9]. The supplier company Givaudan stated in the ingredients' declaration that this aroma is suitable for all human food related to end use applications where flavouring is permitted. In the technical data sheet, the provider shows values of 0.08-2.5% formulation content for Pharma purposes [10].

(IX) Magnesium stearate is widely used as pharmaceutical excipient and generally regarded as non-toxic upon oral administration. Consuming large quantities may result in laxative effects or mucosal irritation. In a toxicity study with rats magnesium stearate was shown to be non-toxic when administered orally or inhaled. It was also not carcinogenic when implanted in the bladder of mice [1]. Magnesium stearate is a standard lubricant, used in Euthyrox®, which is also licensed for children [5].

In conclusion, all the excipients used in the placebo ODT formulation are in concentration ranges recommended in literature. The used excipients are found in abundance in different formulations world-wide including paediatric medicines.

References

1. Rowe RC, Sheskey PJ, Quinn, Marian E. (2009) Handbook of pharmaceutical excipients, 6th ed. Pharmaceutical Press and American Pharmacists Association

2. Sandoz Pharmaceuticals AG (2012) Calcium Sandoz® 500/1000 prescribing information

3. Food Legislation Europa. Food additives. https://webgate.ec.europa.eu/foods_system/main/index.cfm. Accessed 26 July 2018

4. Basics GmbH (2018) Clarithromycin Basics® 250 mg/5 ml Granulat zur Herstellung einer Suspension zum Einnehmen prescribing information

5. Merck Serono GmbH (2017) Euthyrox® 25 Mikrogramm Tabletten prescribing information

6. Hexal AG (2015) ACC® akut junior Hustenlöser, 100 mg Brausetbl. prescribing information

7. Vifor Consumer Health SA (2017) Algifor® Dolo Junior prescribing information

8. Axapharm AG (2017) Convulex® Kapseln und Sirup prescribing information

9. Orlu-Gul M, Fisco G, Parmar D, et al (2013) A new reconstitutable oral paediatric hydrocortisone solution containing hydroxypropyl-β-cyclodextrin. Drug Development and Industrial Pharmacy 39:1028–1036 . doi: 10.3109/03639045.2012.696654

10. Givaudan Technical Data Sheet. Givaudan Schweiz AG. 3 February 2016

3   DISCUSSION

In the chapters above, several different drug delivery devices – mainly based on polymers – were described. In chapters 1.1 and 2.1 it was shown how synthetic polymers such as PDMS-*b*-MOXA can be used to formulate polymeric nanoparticles. Moreover, it was explained how these polymeric vesicles can be targeted towards hepatocytes and which important points should be considered when formulating such targeted nanomedicines. Thereafter, in chapters 1.2 and 2.2, the focus was again on polymers, but this time on natural polymers, namely chitosan. It was described how these polymers can be used to formulate hydrogels and how hydrogels can serve as devices for chronic wound healing.

Regarding clinical application, PDMS-*b*-PMOXA polymersomes, modified with asialofetuin to achieve hepatocyte targeting, are still far away from entering the clinics. The project described herein was mainly based on *in vitro* analyses and early *in vivo* results obtained in zebrafish embryos. The same is valid for the chitosan hydrogel. The method we used to formulate this hydrogel seems very promising for further use as it does not require potentially toxic chemicals. However, a clinical application is not going to happen soon in this case as well. To still get a link to clinical practice, the following sections (3.1 and 3.2) focus on nanoparticles and hydrogels for clinical applications in general. What is known so far? Which hurdles might need to be overcome? Which achievements were already made?

Chapters 1.3, 2.3, 1.4, and 2.4 are about clinical studies with two different formulations. In chapters 1.3 and 2.3 a BF for CYP3A phenotyping is described. It is explained why phenotyping is necessary and why this new formulation offers advantages against established phenotyping strategies. Chapters 1.4, and 2.4 are dedicated to a palatability study in children, using ODTs. Herein, focus is on the need for such formulations for children and which important points need to be considered when performing paediatric clinical studies. In the following sections (3.3 and 3.4) the potential of BFs and ODTs for further use in daily clinical practice is discussed, with special emphasis on paediatric patients.

3.1 NANOPARTICLES FOR TARGETED DRUG DELIVERY

3.1.1 TARGETED NANOPARTICLES IN CLINICAL STUDIES

Nanomedicines are one of the hot topics of today's research in the field of drug delivery. One common definition of the term nanomedicine is "the use of nanoscale or nanostructured materials in medicine that according to their structure have unique medical effects" [226]. Research in this field already resulted in successful development of therapeutics, *in vitro* diagnostics, agents for diagnostic imaging, or medical devices [227]. To achieve clinical translation, it is important to invest adequate resources into preclinical research. To make preclinical research as impactful as possible, it needs to be tailored to the clinical approach that is finally intended from the very beginning. Thereafter, the design of clinical studies needs to optimally suit their purpose and it is obviously of paramount importance to successfully complete these studies [227]. The first nanoparticulate drug carriers were liposomes and in 1995, the first FDA-approved liposomal formulation entered the market: Doxil®, doxorubicin encapsulated into PEGylated nanoliposomes. Doxil® is a passively targeted nanomedicine, reaching its target cells via the EPR effect [228]. Already in the 1980s, liposomes were modified with targeting ligands and proposed to increase the transport of these nanocarriers to diseased tissue compared to unspecific drug delivery [229, 230]. However, there is still a huge gap between numerous preclinically evaluated targeted nanocarriers and only few entering clinical trials. Searching the website clinicaltrials.gov, several trials investigate for example the non-targeted paclitaxel albumin-stabilised nanoparticle formulation nab-paclitaxel (Abraxane®) combined with various chemotherapeutics and for different indications. But only few clinical trials investigate targeted nanoparticles in clinical trials: doxorubicin-loaded anti-EGFR immunoliposomes were successfully tested in a phase I dose-escalation study (NCT01702129) [231] and a phase II study is going on at the moment (NCT02833766). HER2-targeted PEGylated liposomal doxorubicin (NCT01304797) and liposomal formulations of a docetaxel prodrug targeting the EphA2 receptor were assessed with and without other anti-cancer drugs (NCT03076372) [232, 233]. It was also tested in a phase I study whether the novel, tumour-targeted, systemic gene therapy agent SGT-94 could be delivered when entrapped into liposomes targeted to the transferrin receptor (NCT01517464) [234]. So far, no targeted liposomal carrier has been approved for therapy. In terms of polymeric nanocarriers, the situation is even worse with less clinical trials registered using polymeric nanoparticles for targeted drug delivery: one is a polymeric nanoparticle formulation of docetaxel, named BIND-014, targeted against the prostate-specific membrane antigen. It is already tested in a phase II clinical trial against different cancers (NCT01812746, NCT01792479, NCT02283320, NCT02479178).

Recently, several reviews tried to analyse why preclinical studies and clinically usable nanomedicines remain disconnected [235, 236]. For Rosenblum and co-workers, the main hurdles for successful implementation of actively targeted nanomedicines into clinical practice are physiological barriers such as endothelial barriers, the uptake by target cells and lysosomal escape, as well as shielding of the nanocarriers from the MPS. Moreover, therapeutic benefit from actively targeted nanomedicines is limited because of tumour heterogeneity, relative hypoxia, and hampered endosomal escape. In addition to physiological reasons, regulatory hurdles and complex manufacturing processes negatively influence the success of actively targeted nanocarriers [236].

3.1.2 SUCCESSFUL HEPATOCYTE TARGETING ACHIEVED?

In chapter 2.1 the *in vitro* results of targeted PDMS-*b*-PMOXA polymersomes are described. The polymersomes were designed according to the four principles mentioned in section 1.1.3 to successfully deliver a potential cargo to hepatocytes.

(I) Their **pharmacokinetic properties** were optimised to be well suited for liver targeting. With a diameter around 150 nm the PDMS-*b*-PMOXA polymersomes would be able to pass the fenestration of liver sinusoids and to arrive at the hepatocytes [68]. The polymersomes' surface charge was slightly negative, again ideal to reach hepatocytes [72]. Moreover, the polymersomes were stable even upon incubation in 3% bovine serum albumin or 50% foetal calf serum at 37°C. PMOXA was reported to add stealth properties to nanocarriers resulting in prolonged blood circulation times *in vivo*. De Vocht and co-workers reported that particles prepared of a triblock PMOXA-*b*-PDMS-*b*-PMOXA were neither cytotoxic nor did they provoke an inflammatory response by the MPS [31]. But it needs to be kept in mind that – according to Kierstead and colleagues – PMOXA triggered an IgM response upon injection into rodents even though it could prolong circulation time of the respective nanoparticles. The inflammatory response towards the tested polymer was comparable to results seen with PEGylated nanoparticles [237]. Such IgM response could result in enhanced blood clearance upon second injection, called accelerated blood clearance phenomenon [237–239]. In terms of the polymeric nanoparticles described in chapter 2.1, further investigations regarding the *in vivo* behaviour of PDMS-*b*-PMOXA polymersomes would be needed. Even though these polymersomes were non-toxic during an early screening in an *in vivo* model of zebrafish embryos, efficacy in an *in vivo* system has not been proven. Unpublished and preliminary results displayed that PMOXA was not capable of adding enough stealth properties to the polymersomes to avoid recognition by the MPS upon injection into zebrafish embryos.

(II) The **target receptor** for the herein described PDMS-*b*-PMOXA polymersomes was the ASGPR. As already outlined elsewhere, this receptor is well suited to target hepatocytes [66, 89]. With the PDMS-*b*-PMOXA study an efficient internalisation of targeted polymersomes into HepG2 cells via the ASGPR could be confirmed *in vitro*.

(III) The chosen **targeting ligand** was asialofetuin, a ligand that is known to be selective for the ASGPR [78, 89]. Upon asialofetuin binding, the ASGPR is internalised via clathrin-coated pits, followed by endosomal fusion, and transfer to lysosomes [59]. In chapter 2.1 it was mechanistically shown that the internalisation mechanism of the ASGPR was not altered upon binding of asialofetuin-modified PDMS-*b*-PMOXA polymersomes. These were internalised into the early endosomes and accumulated in the lysosomes. As mentioned above, lysosomal escape is one prerequisite for successful clinical translation, because many therapeutics (e.g. nucleic acids, proteins, or peptides) will be degraded and inactivated under lysosomal conditions [236]. In contrast, for lysosomal storage diseases it would be beneficial to have drug delivery systems that transport their cargo via the bloodstream to the target cells and release their cargo not before entering the lysosomes. Examples for hepatic lysosomal storage diseases are lysosomal enzyme deficiencies (e.g. Gaucher's disease and multiple sulfatase deficiency), defects in soluble non-enzymatic lysosomal proteins (e.g. Niemann-Pick disease), and defects in lysosomal membrane proteins (e.g. free sialic acid storage disorder) [240]. Increasing the activity of the defective enzyme or protein is already clinically used to treat patients with lysosomal storage diseases. This is called enzyme replacement therapy. Other therapy approaches aim to restore the equilibrium between synthesis of substrates and their degradation within lysosomes by either reducing the synthesis or by increasing the substrate clearance [241]. The asialofetuin-modified PDMS-*b*-PMOXA polymersomes could protect respective therapeutic enzymes from degradation and clearance in the bloodstream. Upon asialofetuin-targeted uptake into hepatocytes the enzyme could be delivered to the lysosomes where it would be needed.

(IV) The polymersomes were tested with **suitable *in* vitro and *in* vivo models**. Successful targeting of PDMS-*b*-PMOXA polymersomes towards hepatocytes was shown *in vitro* using HepG2 cells. Moreover, cytotoxicity of these nanocarriers was assessed *in vitro* as well as *in vivo*. For *in vivo* studies zebrafish embryos were chosen. Zebrafish embryos are increasingly used as early screening tools and to close the gap between cell-assays and experiments in rodents [242]. Zebrafish embryos possess several advantages such as small size, high reproducibility, rapid development, *ex utero* embryonic growth, and almost complete transparency until 120 hours post fertilisation. Regarding the signalling pathways zebrafish and human beings share a high level of genomic homology. In addition, their cardiovascular, digestive, and nervous systems resemble mammalian systems. This makes zebrafish embryos highly valuable for toxicity assessments *in vivo* [93, 243, 244].

3.1.3 Necessary steps before entering clinical trials

The considerations made above reflect only the first steps in the development of a new drug formulation. The Nanotechnology Characterization Lab (NCL) summarised the key preclinical steps required by FDA before a new drug is allowed to transit from the discovery phase into clinical trials [245].

(I) The preclinical characterisation contains **tests for sterility and endotoxins** (e.g. coagulation assays with Limulus Amoebocyte Lysate) to exclude misinterpretation of any data – especially immunological assays – due to microbial or endotoxin contaminations.

(II) In a second step, **physicochemical characterisations** of the new formulation are performed. Therefore, size and size distribution, ligand distribution, surface charge, surface chemistry, composition, purity, and stability of the nanomaterials are assessed because these might influence the *in vivo* behaviour and tolerability. Moreover, batch-to-batch variability needs to be addressed and reduced to a minimum. The PDMS-*b*-PMOXA polymersomes described in this thesis were analysed regarding their size, size distribution, ligand distribution, surface charge, surface chemistry, and stability. However, scale-up of their production cycle would be very difficult. The thin-film-rehydration method by using a rotary evaporator is well suited for millilitre scales but not for volumes in litre-ranges. Moreover, extrusion of larger scales might be very complex and slow. Another issue, which might be faced, is reproducibility of ligand binding in case several small batches would be produced instead of less and larger ones. Therefore, it would be worth investigating alternative production methods such as microfluidics, which might be more efficient to scale-up the manufacturing of nanoparticles [246].

(III) The physicochemical classification is followed by extensive ***in vitro* assays**. These biochemical analyses and cell-based assays are designed to mimic the *in vivo* conditions as close as possible. Binding and internalisation capacities of the nanomedicines, coagulation, plasma protein binding, haemolysis, and platelet aggregation upon blood contact are evaluated. Some of these assays were performed with the herein described PDMS-*b*-PMOXA polymersomes but not enough to draw final conclusions. Further studies would be needed.

(IV) The ***in vivo* characterisation** suggested by the NCL is divided into three topics: pharmacology and toxicology, efficacy, and immunotoxicity. Pharmacokinetics (i.e. absorption, distribution, metabolism, and excretion (ADME)) and acute and repeated dose toxicity are determined in at least two different species (one rodent and one non-rodent). The results obtained from these trials are important to select potential starting doses for phase I clinical trials in humans. As mentioned above, toxicity screening of PDMS-*b*-PMOXA polymersomes was successfully performed in zebrafish embryos, but not in higher

vertebrates. Also ADME characterisations are lacking. If the efficacy of nanomedicines should be evaluated it is of paramount importance to use appropriate and a variety of tumour models such as transgenic, orthotopic, xenograft, or metastatic models in rodents. Tests for immunotoxicity consist of *in vivo* tests in rodents, assessing adjuvanticity, T-cell dependent antibody response, lymph node proliferation tests, and pyrogenicity assessment [245]. All these characterisations are a prerequisite before entering any clinical trial with human beings. Since with the PDMS-*b*-PMOXA polymersomes none of these was performed, it is obvious that this formulation is still far away from clinics.

Even if a nanoparticulate formulation has been tested according to all the aforementioned points and developed to proceed into clinics, it is important to design the trials carefully. This includes distinct pre-selection of the patient population to choose the patients who will – most probably – benefit most from the new approach. To achieve best possible therapeutic outcomes, the patient pre-selections should focus on presence of the target receptor, the ability of the actively targeted formulation to bind this receptor, tumour heterogenicity, and the extent of EPR effect. It might be beneficial to use companion diagnostics for this purpose [66, 236].

Discussion – Nanoparticles for targeted drug delivery

3.2 CHITOSAN HYDROGEL TO TREAT CHRONIC WOUNDS

3.2.1 CHITOSAN FORMULATIONS USED FOR CLINICAL APPLICATIONS

At the moment, several clinical studies are investigating chitosan scaffolds as potential material for wound healing: In a phase III study, the efficacy of a chitosan gel combined with isosorbide dinitrate in diabetic foot ulcers was investigated (NCT02789033). In another phase III study, a sponge composed of glycosaminoglycans and collagen ionically crosslinked with chitosan (Dermagen®) was tested regarding its ability heal diabetic foot ulcers (NCT00521937). Carboxymethyl chitosan (Surgi shield®) was successfully tested in a phase I study to achieve haemostasis immediately after endoscopic sinus surgery and to prevent adhesion formation (NCT01895933) [247]. Also chitosan/dextran gels were confirmed to be sufficient for the same purpose [248]. In a phase I study slow release Tb4 collagen and chitosan porous sponge scaffolds skin substitutes were evaluated regarding their efficacy and safety in wounds that were rated as difficult to heal (NCT02668055). Other clinical trials rated bioactive chitosan dressings superior to conservative treatment for ulcer treatment [249, 250]. Chitosan was also shown to be effective as haemostatic dental dressing (HemCon® Dental Dressing) after oral surgical procedures [251, 252]. Another field for chitosan is plastic surgery, where it was shown that chitosan dressings on skin graft donor sites fastened wound re-epithelialisation, promoted nerve regeneration, and led to faster return to normal skin colour than areas that were not treated with chitosan [253]. Moreover, a chitosan gel mixed with autologous whole blood (BST-CarGel) showed superior repair of cartilage lesions in the knee compared to microfracture – an articular cartilage repair surgical technique – alone [254].

There are already wound healing materials containing chitosan on the market. For example Tricol Biomedical Inc. sells wound dressings coated with chitosan to increase antibacterial activity (ChitoGauze® PRO, ChitoFlex® PRO) [255]. Medline vends a wound dressing containing chitosan and antimicrobial ionic silver (Opticell® Ag+), which has been shown to be effective against gram positive and gram negative bacteria [256]. Chitosan as haemostatic component in CELOX® has been tested in several clinical studies, being helpful even against life-threatening bleedings. A selection can be found in references [257–259].

3.2.2 DELIVERY OF GROWTH FACTORS FROM CHITOSAN SCAFFOLDS

From these many examples above, it becomes obvious that chitosan has already made its way into clinics, mainly in the field of wound treatments. Often, chitosan is combined with other drugs to support its antimicrobial and wound healing characteristics. The drug categories that are mainly

delivered via chitosan scaffolds are growth factors, anti-inflammatory drugs, antimicrobial drugs, and other supplementary drugs advantageous for wound healing (e.g. nitric oxide) [260]. The chitosan hydrogel described above (chapter 2.2) was designed to deliver therapeutic proteins, for example growth factors. Therefore, the next section will focus on delivery of growth factors from chitosan systems to improve wound healing. In section 1.2.4 it was already mentioned that growth factors are important players for wound healing as they regulate cell growth, proliferation, migration, and differentiation. Moreover, chronic wounds are characterised by decreased levels of growth factors. This brought up the idea to provide the wound with necessary growth factors delivered via external wound healing materials [261, 262]. However, it needs to be kept in mind that growth factors could be enzymatically degraded or inactivated by the extracellular matrix after being brought into contact with a wound environment. Therefore, it is necessary to deliver growth factors in a wound dressing that protects and ensures controlled and prolonged release of its payload.

Combining a recombinant human vascular endothelial growth factor (rhVEGF) with the antibiotic gentamicin in a delivery system of collagen and chitosan resulted in facilitated cell adhesion and proliferation. The researchers called their two-compartment structure a dermal scaffold. The two active compounds were encapsulated in PLGA microspheres and lyophilised. Afterwards, these were added to mixed solutions of collagen and chitosan and the resulting mixtures were lyophilised, too. The scaffold was built of two layers, containing different concentrations of loaded PLGA microspheres. It took more than 28 and 49 days, respectively, to release gentamicin and rhVEGF from this two-compartment structured scaffold *in vitro*. These two different release times were the key characteristic of this delivery system. The time frame of antibiotic gentamicin release of almost one month was stated to be ideal during the inflammatory phase of wound healing. The two-month long release of rhVEGF could be helpful during remodelling by supporting vascular regeneration and skin repair. The dermal scaffold was successfully tested for cell proliferation capability *in vitro* using mouse fibroblasts. Moreover, antibacterial activity was evaluated by inhibiting proliferation of *Staphylococcus aureus* and *Serratia marcescens* [263].

Another research group developed a sponge of chitosan and hyaluronic acid. This sponge was loaded with vascular endothelial growth factor (VEGF)-containing nanofibrin to deliver it to diabetic wounds. Chitosan and hyaluronic acid were blended and homogenously mixed with the VEGF-containing fibrin nanoparticles. The resulting mixture was lyophilised. VEGF was released within one week, which was stated as appropriate for wound dressing. The sponges were shown to be cytocompatible *in vitro* in HDF cells and HUVECs. Moreover, the angiogenic characteristics of VEGF containing scaffolds were determined with endothelial cells. They proliferated and formed capillary-like tubes after being seeded onto the chitosan sponge [264].

Ribeiro and co-workers presented a dextran hydrogel loaded with growth factor containing chitosan microparticles. Chitosan microparticles were prepared by ionotropic gelation between the anionic chelating agent sodium triphosphate (TPP) and cationic chitosan. Epidermal growth factor (EGF) and VEGF were dissolved in chitosan solutions and the microparticles were obtained by electrospinning. Afterwards, these were added to dextran solutions prior to crosslinking and gelation with adipic acid dihydrazide. Biocompatibility was shown *in vitro* using human fibroblasts. *In vivo* experiments in rats showed that the hydrogel containing VEGF and EGF supported the formation of moist wounds resulting in faster wound healing and closure than controls. Moreover, reactive or granulomatous inflammatory reactions in skin lesions were absent according to histological analyses [265].

Another option to entrap chitosan nanoparticles was described by Zhou and colleagues. They prepared chitosan nanoparticles loaded with recombinant human EGF (rhEGF) via ionotropic gelation with TPP. Afterwards, these were entrapped within a fibrin gel matrix during polymerisation, consisting of fibrinogen and thrombin. It was possible to deliver rhEGF via sustained and controlled release over more than 96 h without loss of bioactivity (as shown *in vitro* in BALB/c 3T3 cells) [266].

3.2.3 How advanced is our chitosan hydrogel?

The publications mentioned above clearly indicate the capabilities offered by chitosan based hydrogels in the field of wound healing and tissue engineering. Chitosan scaffolds combined with growth factors were shown to be biocompatible, bioabsorbable, and cell-stimulating, allowing sustained and controlled release of bioactive growth factors. In comparison to the hydrogel described in chapter 2.2, the herein presented formulations are further developed. They all contained growth factors instead of model proteins and all of them were at least tested *in vitro*, showing biocompatibility of the whole delivery systems. Moreover, some of them were already tested successfully *in vivo,* presenting improved wound healing characteristics, and some were even authorised for tissue regeneration purposes (section 3.2.1).

However, the main focus of the work described in chapter 2.2 was the development of a hydrogel that is chemically crosslinked under mild and aqueous reaction conditions via Michael addition. No potentially toxic crosslinking agents [101] were needed and therefore, no removal of such by-products or excess of crosslinkers had to be performed after gelation whilst still providing the advantage of a strongly crosslinked hydrogel. Nevertheless, it was shown that the hydrogel was still biodegradable. Many chitosan delivery systems designed for wound healing make use of ionic crosslinking, as for example the ones described above [264–266]. Such formulations do not need crosslinking chemicals

but they tend to lack long-term stability and should be used only for short-term clinical applications [267].

Generally spoken, many chitosan hydrogels are used after lyophilisation to be applied onto wounds. As already outlined in chapter 2.2, lyophilisation bears the advantage of increasing long-term stability and handling properties of the lyophilised product compared to a liquid or semisolid formulation. Moreover, a lyophilised formulation could be fixed on a wound – either using an occlusive dressing or a semipermeable one – with the ability to imbibe large amounts of wound exudate but not drying out the wound. This would result in a moist wound environment and painless dressing changes. Especially chronic diabetic wounds need careful observations and daily dressing changes [268, 269]. The diffusion mediated release of protein from the chitosan hydrogel described in chapter 2.2 was achieved within one day. Therefore, this would be a good candidate for wounds that need daily checking and dressings changes. In contrast, most hydrogels containing growth factors release their cargos over 10-40 days [260]. By introducing ionic or covalent interactions between cargo and scaffold, release times would increase significantly. This would be very useful to reduce the number of dressing changes to a minimum and to avoid disturbance of the wound healing process by removal of wound dressings. To tailor the release profile of therapeutic proteins from their scaffold, different types of hydrogels should be chosen depending on the intended use.

3.3 BUCCAL FILMS FOR PHENOTYPING: A PHARMACOKINETIC STUDY

3.3.1 PHENOTYPING IN DAILY CLINICAL ROUTINE?

To identify variations in the enzymatic activity of CYPs, genotyping as well as phenotyping are used in clinical practice and are covered by EMA guidelines [270]. With these approaches, physicians try to individualise dose recommendations for their patients with the aim to anticipate the ones being at risk for therapeutic inefficacies or toxic reactions [271]. Using genotyping, the individual DNA sequence of each patient can be precisely determined, and functional genetic mutations coding for specific enzymes can be analysed. The major drawback of this approach is its inability to detect the influence of environmental factors on the enzymatic activity such as drug-drug interactions. For this purpose, phenotyping is used. It reflects a combination of genetic, endogenous, and environmental factors, finally providing information on the actual activity of CYPs (Figure 5) [272].

So far, phenotyping has not been established on a clinical routine basis. Especially, for patients at risk such as cancer patients, this would however offer very interesting options [273]. In contrast to therapeutic drug monitoring, phenotyping identifies patients at risk for over- or under-treatment before starting a therapy, and not only during therapy. Actually, phenotyping in general would be beneficial for all patients. The majority of individuals might not be categorised as normal metaboliser for all five main CYPs (CYP3A4, CYP3A5, CYP2D6, CYP2C9, and CYP2C19), according to a retrospective study in more than 22'000 male and female patients, with different ethnical background, aged between 1 and 108 years [274].

Phenotyping can be performed either for one specific CYP (individual), or for multiple enzyme subfamilies, using a cocktail approach [275, 276]. In general, the major drawback of phenotyping results from possible side effects due to pharmacologically active doses of probe drugs. Therefore, the probability for such undesired effects needs to be reduced to a minimum by using doses as low as possible. The keyword here is microdosing [171, 174]. According to the EMA, a "microdose is defined as less than 1/100th of the dose calculated to yield a pharmacological effect of the test substance [...] and at a maximum dose of ≤ 100 µg" [277]. As already outlined in chapter 1.3, preparation of microdosed formulations can be laborious and error-prone. Consequently, a new method for microdosing, i.e. a BF containing 30 µg of midazolam, was evaluated. The midazolam BF (chapter 2.3) was used for an individual phenotyping approach and might be highly relevant to phenotype patients who will be treated exclusively with one or even several drugs that are metabolised by CYP3A. To disturb the patients as little as possible, a limited sampling strategy had already been evaluated, reducing required blood sampling times to a minimum [190, 278]. However, there are conflicting reports regarding the reliability of limited sampling strategies. Masters and co-workers found that

partial AUCs ($AUC_{0\text{-}1\,h}$, $AUC_{0\text{-}2\,h}$, and $AUC_{0\text{-}4\,h}$) were not suitable to assess hepatic CYP3A activity after intravenous midazolam administration, neither as baseline measurement nor under inhibited CYP3A conditions. Only induced CYP3A activity could be predicted using such limited sampling approach [279]. Moreover, Mueller and colleagues retrospectively analysed data of 123 healthy volunteers who had received oral midazolam. They came to the conclusion that a four-sampling point limited sampling strategy could accurately predict oral midazolam AUC for CYP3A phenotyping, but not one-, two-, or three-sampling point models [280]. Therefore, further studies will be needed to clarify necessary prerequisites for limited sampling strategies for CYP3A phenotyping and their usability in clinical settings. If already for one single substance limited sampling strategies are difficult to achieve, it is even more problematic for phenotyping cocktails containing several probe drugs. This further increases patients' discomfort during phenotyping [281]. To reduce at least the quantity of collected fluids like blood or urine, new sampling procedures have been investigated [282]. These include dried blood spots [172, 283], hair [284, 285], saliva [172], exhaled breath [286], or sweat [287]. Another important point to be considered when applying phenotyping cocktails are mutual interactions between the single components, which need to be excluded in advance [283].

Before any phenotyping approach can be established for clinical routine, it is essential to validate it not only in patients with normal CYP activity, but also with inhibited and induced CYP-function [276]. Regarding a microdosing method such as a microdosed BF, this becomes even more important because CYP induction or inhibition might result in very low concentrations of parent or metabolite being difficult to analyse. For the method described in chapter 2.3, it is known that lower limits of detection are 0.093 pg/mL and 0.255 pg/mL for midazolam and 1'-OH-midazolam, respectively. It remains to be further evaluated whether these limits would be reached with altered CYP activities. Such studies would also set the range for low or high CYP activity, which could then serve as a reference for future applications of the substance as phenotyping probe. Another important point is to test the phenotyping approach in male and female volunteers [288], in older and younger patient populations, and in people of different weight to be able to generalise the results obtained from former studies [276].

It can be concluded that the ideal phenotyping cocktail should allow **fast and simple analysis** of **several CYPs** in **one experiment** while requiring **minimal sample amounts** for analysis as well as administering **minimal doses** of **optimal probe drugs** [289]. Keller and co-workers reviewed several different phenotyping cocktails and concluded that most of them show satisfactory data validation and clinical evidence to be used as near-future applications. Adverse reactions during therapy could be anticipated, improving the balance between efficacy and safety [290].

3.3.2 BFs in clinical practice

In general, thin films represent a valuable alternative to conventional drug dosage forms. Their advantages include being easy to swallow, self-administrable, fast-dissolving, easy to handle and transport, and cost-effective to develop. Systemic as well as local actions could be achieved via oral, buccal, sublingual, ocular, or transdermal applications [291].

Some drug delivery platforms based on polymeric films are already on the market: e.g. Zuplenz® oral soluble film (ondansetron) against opioid dependence [292], Suboxone® sublingual film (buprenorphine and naloxone) against nausea and vomiting [292], Breakyl® Buccalfilm (fentanyl) for opioid therapy [293], or Zolmitriptan RapidFilm® (zolmitriptan) against migraine [294]. It is assumed that the market for BFs is going to substantially grow in the near future [295, 296].

3.3.3 Potential applications for a midazolam BF beyond phenotyping

As already outlined, BFs are easy to swallow and hard to be spat out. This makes them especially interesting for patients with dysphagia, such as paediatric, geriatric, or bedridden patients, as well as non-cooperative ones. The difficulties encountered when tablets or capsules must be swallowed could be circumvented. Patient safety would be increased by avoiding the risk of choking. Another advantage is that BF administration does not require additional water. This makes BFs convenient to be consumed anytime anywhere. Moreover, patients with repeated emesis, mental disorders, or motion sickness seem to prefer dosage forms that can be administered without drinking large amounts of water and without swallowing [183].

In Switzerland, midazolam can be obtained as intravenous or intramuscular injection solution, rectal solution, or filmtablets with a size of at least 11.6 mm x 61 mm [176, 297]. Even if Dormicum® film tablets can be crushed and suspended to be applied as liquid or semisolid formulation [298] this is an inconvenient alternative. In Germany, there are midazolam solutions for buccal application in cases of seizures [299]. It is also possible to dilute injection solutions for oral application or to prepare midazolam nasal sprays. However, this is always work-intensive and error-prone. A ready-to-use formulation, in several midazolam concentrations, easy and safe to apply would be highly desirable.

Therefore, a midazolam BF could be imagined to be beneficial for all the patient populations mentioned above. Its use is not limited to phenotyping with microdoses, but it could be formulated as well to contain higher concentrations of midazolam. This would result in a pharmacologically active product with the same indication options as other midazolam-containing dosage forms. The buccal absorption of midazolam from such BF and rapid onset of action would favour its use in the fields of

epileptic seizures, sedation, induction of anaesthesia, or sleep disorders [176]. It remains to be tested what would be the maximal concentration of midazolam that could be loaded into a BF. Moreover, it needs to be investigated whether loading with higher amounts would influence the route of absorption due to limited buccal absorption capacity. Absorption could be a combination of buccal and intestinal, resulting in altered pharmacokinetic profiles compared to a microdosed midazolam BF.

3.4 ORAL DISINTEGRATING TABLETS BASED ON FUNCTIONALISED CALCIUM CARBONATE: A PALATABILITY STUDY IN CHILDREN

It is well known that palatability is an important factor to be considered when developing oral formulations for children [300, 301]. In addition, swallowability is essential, especially for younger children [199]. Therefore, ODTs offer a very interesting alternative to conventional tablets or capsules. According to the FDA, ODTs are defined as "a solid dosage form containing medical substances, which disintegrates rapidly, usually within a matter of seconds, when placed upon the tongue. […] A large majority of these products have *in vitro* disintegrations times of approximately 30 seconds or less" [302].

3.4.1 IMPORTANT POINTS TO CONSIDER WHEN PERFORMING CLINICAL STUDIES WITH CHILDREN

Among paediatric patients, the medication's palatability is essential for patient acceptance, therapeutic compliance and successful outcome of a therapy [303, 304]. As outlined in chapter 1.4.2, medicine's taste and the ability of children to swallow their medication may greatly influence the selection of a drug, therefore therapy, and prescribing practice. So far, there has not been much systematic methodological research on taste and mouthfeel evaluation of age-appropriate formulations in children. The study described above (chapter 2.4) was designed according to the special characteristics of paediatric patients [222].

(I) The study procedure was kept as **short** as possible, lasting at maximum 30 minutes per volunteer in total. This included the informed consent procedure as well as explanation of the study, administration of the ODT, and palatability assessment and evaluation with children and parents.

(II) It is important that the research personnel is well experienced in handling children to **motivate** them and to obtain honest answers and reactions from them. This requires close interactions with parents and caregivers to ensure study support from their side. Without their help it might be difficult to build the basis for fruitful interactions with the paediatric patients. Moreover, such support might be beneficial when it comes to interpreting facial expressions of the children and getting verbal answers from them.

(III) To obtain verbal assent of a child and to make sure that it understood the procedure a **child-appropriate language** is of paramount importance. This could be accompanied by leveraging cartoons to explain the procedure and showing the study product before administering it. For the ODT study it was important to explain to parents and children where to place the ODT and how to give feedback on its disintegration behaviour.

(IV) Since children are easily confused and become taste-fatigue by too many variables, it was decided to **focus on taste acceptance** and not to evaluate children's preferences between several formulations. According to the recommendations by Sjövall and colleagues [223], exclusively verbal feedback regarding ODT acceptability was obtained from the younger sub-population. To increase objectivity of the results obtained from older children, an FHS and closed questions were additionally used. Moreover, they were asked for feedback on the disintegration time and behaviour of the FCC based ODTs. For both groups further information regarding acceptability of the tested ODT was obtained by seeking parental feedback.

3.4.2 FUNCTIONALISED CALCIUM CARBONATE IS A SAFE EXCIPIENT FOR ODTS

Functionalised Calcium Carbonate (FCC) consists of calcium carbonate and calcium phosphate, which are both considered to be non-toxic excipients and safe for paediatric use (chapter 2.4, [305]). Its unique and highly porous surface structure makes FCC well suited to prepare ODTs [225, 306]. Moreover, it was already used to formulate gastro-retentive drug delivery systems [307] as well as mucoadhesive particles for colonic drug delivery [308]. In accordance with their porous structure, FCC particles were successfully loaded with high amounts of different small molecule drugs (hydrophilic as well as lipophilic ones) and even proteins [308, 309]. In addition, the porous structure of FCC allows for rapid water uptake and fast disintegration upon contact with liquid, accelerating drug release of poorly water-soluble drugs [225, 308]. Therefore, FCC based ODTs offer very interesting options as safe, inert, and functional oral drug delivery systems.

3.4.3 CAN OUR FCC BASED ODT BE CONSIDERED CHILD-APPROPRIATE?

According to the criteria for paediatric medicines [208], the FCC based ODT was successfully tested in children in a clinical study. It can be considered a child-appropriate drug delivery device.

(I) The FCC based ODTs presented in chapter 2.4 were designed as carrier tablets for drugs to be administered *per os*. As outlined above, FCC is a **safe excipient** and well suited for paediatric purposes [305].

(II) Due to rapid disintegration of the ODT upon contact with saliva it does not need to be swallowed [225]. This makes FCC based ODTs highly acceptable for patients who have difficulties with swallowing solid dosage forms. In adults as well as in children **palatability and acceptability** of the tested ODT were rated as very positive and highly acceptable, respectively (chapter 2.4, [225]). Taste

masking was achieved by using artificial sweetener in combination with citric acid reacting with sodium bicarbonate. This results in a pleasant, sweet, and tickly feeling in the mouth.

(III) For the different subgroups of the paediatric population **dose adjustments** can be easily achieved, since FCC is a very versatile multifunctional excipient. For this purpose, ODTs could be either formulated containing different amounts of active drug, or they could be compacted to large tablets or mini-tablets. The latter approach would permit dosing per kilogram of body weight without additional formulation work.

(IV) Since ODTs can be put into the buccal pouch or directly onto the tongue, their **administration** even to very young children is easy and safe. Moreover, application of an ODT is highly accepted in almost every cultural background (in contrast to suppositories, for example). Such high acceptability of an easy-to-administer formulation increases patient compliance and lowers the risk for wrongly administered medications.

3.4.4 ODTs APPROVED FOR PAEDIATRIC USE

In Switzerland, there are several fused or dispersible tablets available on the market [310]. These include over the counter products as well as prescription drugs. Exclusively licensed for use in **adolescents** are: Abilify® (aripiprazole), a neuroleptic drug; Domperidon®/Neogast-X® LINGUAL (domperidone) against nausea and emesis; Felden® (piroxicam) to treat rheumatoid arthritis; and Temesta® Expidet (lorazepam) for sedation. Some of the products on the market are also approved for **children**: Co-Amoxi® (amoxicillin and clavulanic acid), an antibiotic drug; Dafalgan® ODIS (paracetamol), an analgesic and antipyretic substance; Fluimucil® lingual (acetylcysteine) to treat cough; Imodium® lingual (loperamide) against diarrhoea; Ondansetron® ODT (ondansetron) to treat chemotherapy-induced nausea and emesis; and Risperidon® oro (risperidone) for children with autism. In Switzerland, no orally disintegrating formulation for **infants** younger than 2 years is approved.

Since FCC – the excipient investigated in the study described in chapter 2.4 – consists of two already well-known excipients [305], a safety assessment becomes much easier than for a completely novel substance, which should be introduced to the market. FCC based ready-to-use granules are already available (Omyapharm® ODG, [311]) and could serve as standard platform fulfilling the requirements in a PIP. The processes, which were implemented to produce the FCC based ODTs, were shown to be efficient and effective. Moreover, the resulting tablets were of high physical stability and easy to handle. Therefore, ODTs containing FCC as novel and safe excipient present a promising option to formulate child-appropriate medications in the future.

3.4.5 ODTs AND BFs

BFs (chapters 1.3 and 2.3) as well as ODTs (chapters 1.4 and 2.4) are promising options to treat special and vulnerable patient populations. Both formulations can be easily administered to paediatric, elderly, or mentally disabled patients. As both formulations disintegrate rapidly upon contact with saliva there is no risk for suffocation upon swallowing, resulting in an improved safety profile. Moreover, direct contact of both formulations with the oral mucosa requires good taste-masking strategies, especially for bad-tasting drugs. ODTs and BFs can be formulated to offer well-accepted medications with good palatability. The latter is particularly important to be assessed carefully when designing an ODT, since particles from ODT disintegration could leave an unpleasant mouthfeel.

Due to fast dissolution and absorption of loaded drugs a rapid onset of action can be expected. In addition, drug absorption within mouth, pharynx, or oesophagus through saliva increases bioavailability by avoiding first pass metabolism. Advantages of ODTs and BFs over liquid oral formulations include enhanced dosing accuracy as well as increased stability during storage and transport. Moreover, ODTs and BFs do not require special packaging, except for being protected from humidity. In terms of drug loading, ODTs might be beneficial compared to BFs, especially if ODTs are based on highly porous FCC [182, 183, 312, 313]. In conclusion, BFs as well as ODTs are worth to be further investigated to improve the medical options for vulnerable patient populations. Still their respective advantages and disadvantages might steer the decision more towards one or the other.
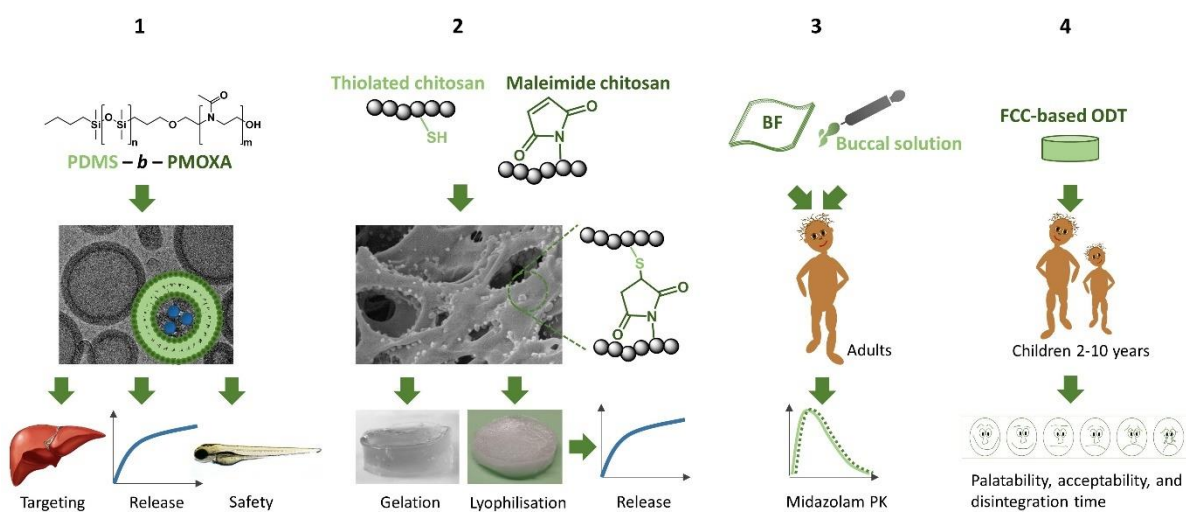
4   CONCLUSION

Figure 9. The variety of drug delivery devices presented in this thesis. From development of polymeric vesicles for targeted drug delivery to hepatocytes (1), over a self-assembling chitosan hydrogel for wound healing (2) towards buccal films (BFs) for phenotyping (3) and oral disintegrating tablets (ODTs) as child-appropriate carrier formulations (4).

In this work, a broad spectrum of different drug delivery systems was explained and evaluated (Figure 9). Nanoparticles, i.e. **polymersomes**, synthesised from the synthetic diblock copolymer PDMS-*b*-PMOXA were successfully characterised and modified. The targeting strategy towards hepatocytes included coupling of asialofetuin onto the polymersomes' surface and proof of receptor-mediated uptake via the ASGPR. Loading of a model drug into the polymersomes and its sustained release were achieved. In addition, all polymersomes variations were biocompatible *in vitro* as well as *in vivo*. However, preliminary results displayed that PMOXA was not capable of adding enough stealth properties to the polymersomes to avoid recognition by the MPS upon injection into zebrafish embryos. These results remain to be fully understood.

The second polymeric drug delivery system being evaluated was a self-assembling chitosan **hydrogel**. Upon successful thiolation and modification with maleimide moieties, respectively, gelation started immediately after mixing aqueous solutions of these two polymers. The hydrogel revealed a porous structure, was able to imbibe excess of water and was biodegradable. Moreover, protein loading and release were achieved. Release properties were the same from freshly prepared as well as from lyophilised hydrogels. Spreadability of the self-assembling chitosan hydrogel was comparable to formulations that are already on the market.

These two formulations were mainly analysed *in vitro*. Within the last years, continuous progress was made regarding clinical application of targeted nanoparticles, e.g. in cancer therapy, and growth factor containing hydrogels to improve healing of chronic wounds. However, there is still a big gap from preclinical research to clinical studies and applications.

Two more drug delivery systems were successfully tested in clinical settings. The **buccal film (BF)** containing microdoses of midazolam was successfully evaluated for phenotyping of CYP3A activity in healthy adults. Pharmacokinetic parameters such as AUC, C_{max}, or metabolic ratios of midazolam and its main metabolite 1'-OH-midazolam were assessed and compared between application via BF and via a buccal reference solution (i.e. a diluted Dormicum® solution). It was shown that a microdosed BF could be an interesting novel diagnostic tool for phenotyping, especially of vulnerable populations such as children or geriatric patients.

These patient groups might also benefit from the last drug delivery system presented in this thesis. **Oral disintegrating tablets (ODTs)** based on Functionalised Calcium Carbonate were tested for their palatability and disintegration behaviour in children from 2 to 10 years. These ODTs disintegrated within less 30 seconds, and children as well as their parents rated them as very convenient. Due to their good taste and mouth feeling they were highly accepted. Therefore, such ODTs could well serve as inert carrier for a broad variety of drugs, which – until now – do not exist in age-appropriate or good-tasting formulations.

REFERENCES

1. Wicki A, Witzigmann D, Balasubramanian V, Huwyler J (2015) Nanomedicine in cancer therapy: challenges, opportunities, and clinical applications. J Control Release 200:138–157 . doi: 10.1016/j.jconrel.2014.12.030

2. Tinkle S, McNeil SE, Mühlebach S, et al (2014) Nanomedicines: addressing the scientific and regulatory gap. Ann N Y Acad Sci 1313:35–56 . doi: 10.1111/nyas.12403

3. The European Commission (2013) Commission Delegated Regulation (EU) No 1363/2013 of 12 December 2013 amending Regulation (EU) No 1169/2011 of the European Parliament and of the Council on the provision of food information to consumers as regards the definition of "engineered nanomaterials" (Text with EEA relevance). Official Journal of the European Union 343/26-343/28

4. Liang R, Wei M, Evans DG, Duan X (2014) Inorganic nanomaterials for bioimaging, targeted drug delivery and therapeutics. Chem Commun (Camb) 50:14071–14081 . doi: 10.1039/c4cc03118k

5. Gautier J, Allard-Vannier E, Hervé-Aubert K, et al (2013) Design strategies of hybrid metallic nanoparticles for theragnostic applications. Nanotechnology 24:432002 . doi: 10.1088/0957-4484/24/43/432002

6. Robbins PD, Ghivizzani SC (1998) Viral vectors for gene therapy. Pharmacol Ther 80:35–47

7. Zhang X, Godbey WT (2006) Viral vectors for gene delivery in tissue engineering. Adv Drug Deliv Rev 58:515–534 . doi: 10.1016/j.addr.2006.03.006

8. Gregoriadis G (2008) Liposome research in drug delivery: the early days. J Drug Target 16:520–524 . doi: 10.1080/10611860802228350

9. Talluri SV, Kuppusamy G, Karri VVSR, et al (2016) Lipid-based nanocarriers for breast cancer treatment - comprehensive review. Drug Deliv 23:1291–1305 . doi: 10.3109/10717544.2015.1092183

10. Yingchoncharoen P, Kalinowski DS, Richardson DR (2016) Lipid-based drug delivery systems in cancer therapy: what is available and what is yet to come. Pharmacol Rev 68:701–787 . doi: 10.1124/pr.115.012070

11. van Hoogevest P, Wendel A (2014) The use of natural and synthetic phospholipids as pharmaceutical excipients. Eur J Lipid Sci Technol 116:1088–1107 . doi: 10.1002/ejlt.201400219

12. van Meer G, Voelker DR, Feigenson GW (2008) Membrane lipids: where they are and how they behave. Nat Rev Mol Cell Biol 9:112–124 . doi: 10.1038/nrm2330

13. Elzoghby AO (2013) Gelatin-based nanoparticles as drug and gene delivery systems: reviewing three decades of research. J Control Release 172:1075–1091 . doi: 10.1016/j.jconrel.2013.09.019

14. Kodama Y, Nakamura T, Kurosaki T, et al (2014) Biodegradable nanoparticles composed of dendrigraft poly-L-lysine for gene delivery. Eur J Pharm Biopharm 87:472–479 . doi: 10.1016/j.ejpb.2014.04.013

15. Loyer P, Cammas-Marion S (2014) Natural and synthetic poly(malic acid)-based derivates: a family of versatile biopolymers for the design of drug nanocarriers. J Drug Target 22:556–575 . doi: 10.3109/1061186X.2014.936871

16. dos Santos MA, Grenha A (2015) Polysaccharide nanoparticles for protein and Peptide delivery: exploring less-known materials. Adv Protein Chem Struct Biol 98:223–261 . doi: 10.1016/bs.apcsb.2014.11.003

17. Prabhu RH, Patravale VB, Joshi MD (2015) Polymeric nanoparticles for targeted treatment in oncology: current insights. Int J Nanomedicine 10:1001–1018 . doi: 10.2147/IJN.S56932

18. Grossen P, Witzigmann D, Sieber S, Huwyler J (2017) PEG-PCL-based nanomedicines: a biodegradable drug delivery system and its application. J Control Release 260:46–60 . doi: 10.1016/j.jconrel.2017.05.028

19. Liu G-Y, Chen C-J, Ji J (2012) Biocompatible and biodegradable polymersomes as delivery vehicles in biomedical applications. Soft Matter 8:8811–8821 . doi: 10.1039/C2SM25721A

20. Torchilin VP (2001) Structure and design of polymeric surfactant-based drug delivery systems. J Control Release 73:137–172

21. Discher DE, Eisenberg A (2002) Polymer vesicles. Science 297:967–973 . doi: 10.1126/science.1074972

22. Messager L, Gaitzsch J, Chierico L, Battaglia G (2014) Novel aspects of encapsulation and delivery using polymersomes. Curr Opin Pharmacol 18:104–111 . doi: 10.1016/j.coph.2014.09.017

23. Thambi T, Park JH, Lee DS (2016) Stimuli-responsive polymersomes for cancer therapy. Biomater Sci 4:55–69 . doi: 10.1039/c5bm00268k

24. De Oliveira H, Thevenot J, Lecommandoux S (2012) Smart polymersomes for therapy and diagnosis: fast progress toward multifunctional biomimetic nanomedicines. Wiley Interdiscip Rev Nanomed Nanobiotechnol 4:525–546 . doi: 10.1002/wnan.1183

25. Broz P, Benito SM, Saw C, et al (2005) Cell targeting by a generic receptor-targeted polymer nanocontainer platform. J Control Release 102:475–488 . doi: 10.1016/j.jconrel.2004.10.014

26. Egli S, Nussbaumer MG, Balasubramanian V, et al (2011) Biocompatible functionalization of polymersome surfaces: a new approach to surface immobilization and cell targeting using polymersomes. J Am Chem Soc 133:4476–4483 . doi: 10.1021/ja110275f

27. Camblin M, Detampel P, Kettiger H, et al (2014) Polymersomes containing quantum dots for cellular imaging. Int J Nanomedicine 9:2287–2298 . doi: 10.2147/IJN.S59189

28. Figueiredo P, Balasubramanian V, Shahbazi M-A, et al (2016) Angiopep2-functionalized polymersomes for targeted doxorubicin delivery to glioblastoma cells. Int J Pharm 511:794–803 . doi: 10.1016/j.ijpharm.2016.07.066

29. Zalipsky S, Hansen CB, Oaks JM, Allen TM (1996) Evaluation of blood clearance rates and biodistribution of poly(2-oxazoline)-grafted liposomes. J Pharm Sci 85:133–137 . doi: 10.1021/js9504043

30. Konradi R, Pidhatika B, Mühlebach A, Textor M (2008) Poly-2-methyl-2-oxazoline: a peptide-like polymer for protein-repellent surfaces. Langmuir 24:613–616 . doi: 10.1021/la702917z

31. De Vocht C, Ranquin A, Willaert R, et al (2009) Assessment of stability, toxicity and immunogenicity of new polymeric nanoreactors for use in enzyme replacement therapy of MNGIE. J Control Release 137:246–254 . doi: 10.1016/j.jconrel.2009.03.020

32. Hare JI, Lammers T, Ashford MB, et al (2017) Challenges and strategies in anti-cancer nanomedicine development: an industry perspective. Advanced Drug Delivery Reviews 108:25–38 . doi: 10.1016/j.addr.2016.04.025

33. Godin B, Sakamoto JH, Serda RE, et al (2010) Emerging applications of nanomedicine for therapy and diagnosis of cardiovascular diseases. Trends Pharmacol Sci 31:199–205 . doi: 10.1016/j.tips.2010.01.003

34. Katsuki S, Matoba T, Koga J-I, et al (2017) Anti-inflammatory nanomedicine for cardiovascular disease. Front Cardiovasc Med 4:87 . doi: 10.3389/fcvm.2017.00087

35. Dolati S, Babaloo Z, Jadidi-Niaragh F, et al (2017) Multiple sclerosis: therapeutic applications of advancing drug delivery systems. Biomed Pharmacother 86:343–353 . doi: 10.1016/j.biopha.2016.12.010

36. Prosperi D, Colombo M, Zanoni I, Granucci F (2017) Drug nanocarriers to treat autoimmunity and chronic inflammatory diseases. Semin Immunol 34:61–67 . doi: 10.1016/j.smim.2017.08.010

37. Dos Santos Ramos MA, Da Silva PB, Spósito L, et al (2018) Nanotechnology-based drug delivery systems for control of microbial biofilms: a review. Int J Nanomedicine 13:1179–1213 . doi: 10.2147/IJN.S146195

38. Infoholic Research (2017) Global nanomedicine market – drivers, opportunities, trends, and forecasts: 2017–2023. https://www.researchandmarkets.com/reports/4092019/global-nanomedicine-market-drivers. Accessed 9 May 2018

39. Williams R (2006) Global challenges in liver disease. Hepatology 44:521–526 . doi: 10.1002/hep.21347

40. Guengerich FP (1999) Cytochrome P-450 3A4: regulation and role in drug metabolism. Annu Rev Pharmacol Toxicol 39:1–17 . doi: 10.1146/annurev.pharmtox.39.1.1

41. Brown MS, Kovanen PT, Goldstein JL (1981) Regulation of plasma cholesterol by lipoprotein receptors. Science 212:628–635

42. Harrison PM, Arosio P (1996) The ferritins: molecular properties, iron storage function and cellular regulation. Biochim Biophys Acta 1275:161–203

43. Bartneck M, Warzecha KT, Tacke F (2014) Therapeutic targeting of liver inflammation and fibrosis by nanomedicine. Hepatobiliary Surg Nutr 3:364–376 . doi: 10.3978/j.issn.2304-3881.2014.11.02

44. Halma C, Daha MR, Van Es LA (1992) In vivo clearance by the mononuclear phagocyte system in humans: an overview of methods and their interpretation. Clinical and Experimental Immunology 89:1–7

45. Sanyal AJ (2011) Zakim and Boyer's hepatology - 6th Edition. Saunders

46. Mishra N, Yadav NP, Rai VK, et al (2013) Efficient hepatic delivery of drugs: novel strategies and their significance. Biomed Res Int 2013:382184 . doi: 10.1155/2013/382184

47. Sørensen KK, Simon-Santamaria J, McCuskey RS, Smedsrød B (2015) Liver sinusoidal endothelial cells. In: Comprehensive Physiology. American Cancer Society, pp 1751–1774

48. Bacon B, O'Grady J, DiBisceglie A, Lake J (2005) Comprehensive clinical hepatology - 2nd edition. Mosby

49. Flisiak R (1997) Role of Ito cells in the liver function. Pol J Pathol 48:139–145

50. Maurel P (2010) Hepatocytes: methods and Protocols. Humana Press

51. Paxton S, Peckham M, Adele K (2003) The Leeds histology guide. https://www.histology.leeds.ac.uk/digestive/liver_hepatocyte.php. Accessed 16 May 2018

52. El-Serag HB (2011) Hepatocellular carcinoma. New England Journal of Medicine 365:1118–1127 . doi: 10.1056/NEJMra1001683

53. Bouchard MJ, Navas-Martin S (2011) Hepatitis B and C virus hepatocarcinogenesis: lessons learned and future challenges. Cancer Lett 305:123–143 . doi: 10.1016/j.canlet.2010.11.014

54. Stoller JK, Aboussouan LS (2012) A review of α1-antitrypsin deficiency. Am J Respir Crit Care Med 185:246–259 . doi: 10.1164/rccm.201108-1428CI

55. Byrne BJ, Falk DJ, Pacak CA, et al (2011) Pompe disease gene therapy. Hum Mol Genet 20:R61-68 . doi: 10.1093/hmg/ddr174

56. Fagiuoli S, Daina E, D'Antiga L, et al (2013) Monogenic diseases that can be cured by liver transplantation. J Hepatol 59:595–612 . doi: 10.1016/j.jhep.2013.04.004

57. Hoppe B (2012) An update on primary hyperoxaluria. Nat Rev Nephrol 8:467–475 . doi: 10.1038/nrneph.2012.113

58. Kay MA (2011) State-of-the-art gene-based therapies: the road ahead. Nature Reviews Genetics 12:316–328 . doi: 10.1038/nrg2971

59. Poelstra K, Prakash J, Beljaars L (2012) Drug targeting to the diseased liver. J Control Release 161:188–197 . doi: 10.1016/j.jconrel.2012.02.011

60. Reddy LH, Couvreur P (2011) Nanotechnology for therapy and imaging of liver diseases. J Hepatol 55:1461–1466 . doi: 10.1016/j.jhep.2011.05.039

61. Maurice R (2017) Travel into the liver. In: Rob Maurice | Medical / Scientific Animator | Travel into the liver. http://www.robmaurice.com/portfolio_page/liver-lobules/. Accessed 17 Jul 2018

62. Lau AH, Szabo G, Thomson AW (2009) Antigen-presenting cells under the influence of alcohol. Trends in Immunology 30:13–22 . doi: 10.1016/j.it.2008.09.005

63. Bartneck M, Keul HA, Wambach M, et al (2012) Effects of nanoparticle surface-coupled peptides, functional endgroups, and charge on intracellular distribution and functionality of human primary reticuloendothelial cells. Nanomedicine 8:1282–1292 . doi: 10.1016/j.nano.2012.02.012

64. Huang X, Peng X, Wang Y, et al (2010) A reexamination of active and passive tumor targeting by using rod-shaped gold nanocrystals and covalently conjugated peptide ligands. ACS Nano 4:5887–5896 . doi: 10.1021/nn102055s

65. Webster DM, Sundaram P, Byrne ME (2013) Injectable nanomaterials for drug delivery: carriers, targeting moieties, and therapeutics. Eur J Pharm Biopharm 84:1–20 . doi: 10.1016/j.ejpb.2012.12.009

66. Witzigmann D, Quagliata L, Schenk SH, et al (2016) Variable asialoglycoprotein receptor 1 expression in liver disease: implications for therapeutic intervention. Hepatol Res 46:686–696 . doi: 10.1111/hepr.12599

67. He C, Hu Y, Yin L, et al (2010) Effects of particle size and surface charge on cellular uptake and biodistribution of polymeric nanoparticles. Biomaterials 31:3657–3666 . doi: 10.1016/j.biomaterials.2010.01.065

68. Gaumet M, Vargas A, Gurny R, Delie F (2008) Nanoparticles for drug delivery: the need for precision in reporting particle size parameters. Eur J Pharm Biopharm 69:1–9 . doi: 10.1016/j.ejpb.2007.08.001

69. Walkey CD, Olsen JB, Guo H, et al (2012) Nanoparticle size and surface chemistry determine serum protein adsorption and macrophage uptake. J Am Chem Soc 134:2139–2147 . doi: 10.1021/ja2084338

70. Ishiwata H, Suzuki N, Ando S, et al (2000) Characteristics and biodistribution of cationic liposomes and their DNA complexes. J Control Release 69:139–148

71. Rothkopf C, Fahr A, Fricker G, et al (2005) Uptake of phosphatidylserine-containing liposomes by liver sinusoidal endothelial cells in the serum-free perfused rat liver. Biochim Biophys Acta 1668:10–16 . doi: 10.1016/j.bbamem.2004.10.013

72. Xiao K, Li Y, Luo J, et al (2011) The effect of surface charge on in vivo biodistribution of PEG-oligocholic acid based micellar nanoparticles. Biomaterials 32:3435–3446 . doi: 10.1016/j.biomaterials.2011.01.021

73. Bazile D, Prud'homme C, Bassoullet M, et al (1995) Stealth me. PEG-PLA nanoparticles avoid uptake by the mononuclear phagocytes system. Journal of Pharmaceutical Sciences 84:493–498 . doi: 10.1002/jps.2600840420

74. Lammers T, Kiessling F, Hennink WE, Storm G (2012) Drug targeting to tumors: principles, pitfalls and (pre-) clinical progress. J Control Release 161:175–187 . doi: 10.1016/j.jconrel.2011.09.063

75. Kamaly N, Xiao Z, Valencia PM, et al (2012) Targeted polymeric therapeutic nanoparticles: design, development and clinical translation. Chem Soc Rev 41:2971–3010 . doi: 10.1039/c2cs15344k

76. Bareford LM, Swaan PW (2007) Endocytic mechanisms for targeted drug delivery. Advanced Drug Delivery Reviews 59:748–758 . doi: 10.1016/j.addr.2007.06.008

77. Kang J-H, Toita R, Murata M (2016) Liver cell-targeted delivery of therapeutic molecules. Critical Reviews in Biotechnology 36:132–143 . doi: 10.3109/07388551.2014.930017

78. Tolleshaug H, Berg T, Blomhoff R (1984) Uptake of mannose-terminated glycoproteins in isolated rat liver cells. Evidence for receptor-mediated endocytosis in hepatocytes. Biochemical Journal 223:151–160 . doi: 10.1042/bj2230151

79. Dini Luciana, Autuori Francesco, Lentini Alessandro, et al (1992) The clearance of apoptotic cells in the liver is mediated by the asialoglycoprotein receptor. FEBS Letters 296:174–178 . doi: 10.1016/0014-5793(92)80373-O

80. Harris EN, Weigel JA, Weigel PH (2008) The human hyaluronan receptor for endocytosis (HARE/Stabilin-2) is a systemic clearance receptor for heparin. J Biol Chem 283:17341–17350 . doi: 10.1074/jbc.M710360200

81. D'Souza AA, Devarajan PV (2015) Asialoglycoprotein receptor mediated hepatocyte targeting - strategies and applications. J Control Release 203:126–139 . doi: 10.1016/j.jconrel.2015.02.022

82. Alexis F, Pridgen E, Molnar LK, Farokhzad OC (2008) Factors affecting the clearance and biodistribution of polymeric nanoparticles. Mol Pharm 5:505–515 . doi: 10.1021/mp800051m

83. Stockert RJ (1995) The asialoglycoprotein receptor: relationships between structure, function, and expression. Physiol Rev 75:591–609 . doi: 10.1152/physrev.1995.75.3.591

84. Hashida M, Nishikawa M, Yamashita F, Takakura Y (2001) Cell-specific delivery of genes with glycosylated carriers. Advanced Drug Delivery Reviews 52:187–196 . doi: 10.1016/S0169-409X(01)00209-5

85. Drickamer K (1988) Two distinct classes of carbohydrate-recognition domains in animal lectins. J Biol Chem 263:9557–9560

86. Geffen I, Spiess M (1992) Asialoglycoprotein receptor. Int Rev Cytol 137B:181–219

87. Baenziger JU, Maynard Y (1980) Human hepatic lectin. Physiochemical properties and specificity. J Biol Chem 255:4607–4613

88. Díez S, Miguéliz I, Tros de Ilarduya C (2009) Targeted cationic poly(D,L-lactic-co-glycolic acid) nanoparticles for gene delivery to cultured cells. Cell Mol Biol Lett 14:347–362 . doi: 10.2478/s11658-009-0003-7

89. Detampel P, Witzigmann D, Krähenbühl S, Huwyler J (2013) Hepatocyte targeting using pegylated asialofetuin-conjugated liposomes. J Drug Target. doi: 10.3109/1061186X.2013.860982

90. Discher DE, Ahmed F (2006) Polymersomes. Annu Rev Biomed Eng 8:323–341 . doi: 10.1146/annurev.bioeng.8.061505.095838

91.   Dieu L-H, Wu D, Palivan CG, et al (2014) Polymersomes conjugated to 83-14 monoclonal antibodies: in vitro targeting of brain capillary endothelial cells. Eur J Pharm Biopharm 88:316–324 . doi: 10.1016/j.ejpb.2014.05.021

92.   Zon LI, Peterson RT (2005) In vivo drug discovery in the zebrafish. Nat Rev Drug Discov 4:35–44 . doi: 10.1038/nrd1606

93.   Chakraborty C, Sharma AR, Sharma G, Lee S-S (2016) Zebrafish: A complete animal model to enumerate the nanoparticle toxicity. Journal of Nanobiotechnology 14:65 . doi: 10.1186/s12951-016-0217-6

94.   Rani M, Agarwal A, Negi YS (2010) Review: chitosan based hydrogel polymeric beads - as drug delivery system. BioResources 5:2765–2807 . doi: 10.15376/biores.5.4.2765-2807

95.   Wichterle O, Lím D (1960) Hydrophilic gels for biological use. Nature 185:117–118 . doi: 10.1038/185117a0

96.   Mathew AP, Uthaman S, Cho K-H, et al (2018) Injectable hydrogels for delivering biotherapeutic molecules. Int J Biol Macromol 110:17–29 . doi: 10.1016/j.ijbiomac.2017.11.113

97.   Giri TK, Thakur A, Alexander A, et al (2012) Modified chitosan hydrogels as drug delivery and tissue engineering systems: present status and applications. Acta Pharmaceutica Sinica B 2:439–449 . doi: 10.1016/j.apsb.2012.07.004

98.   Hoffman AS (2002) Hydrogels for biomedical applications. Adv Drug Deliv Rev 54:3–12 . doi: 10.1016/S0169-409X(01)00239-3

99.   Peppas NA, Hilt JZ, Khademhosseini A, Langer R (2006) Hydrogels in biology and medicine: from molecular principles to bionanotechnology. Advanced Materials 18:1345–1360 . doi: 10.1002/adma.200501612

100. Vashist A, Vashist A, Gupta YK, Ahmad S (2013) Recent advances in hydrogel based drug delivery systems for the human body. J Mater Chem B 2:147–166 . doi: 10.1039/C3TB21016B

101. Bhattarai N, Gunn J, Zhang M (2010) Chitosan-based hydrogels for controlled, localized drug delivery. Advanced Drug Delivery Reviews 62:83–99 . doi: 10.1016/j.addr.2009.07.019

102. Berger J, Reist M, Mayer JM, et al (2004) Structure and interactions in covalently and ionically crosslinked chitosan hydrogels for biomedical applications. European Journal of Pharmaceutics and Biopharmaceutics 57:19–34 . doi: 10.1016/S0939-6411(03)00161-9

103. Wu ZM, Zhang XG, Zheng C, et al (2009) Disulfide-crosslinked chitosan hydrogel for cell viability and controlled protein release. European Journal of Pharmaceutical Sciences 37:198–206 . doi: 10.1016/j.ejps.2009.01.010

104. Tan H, Chu CR, Payne KA, Marra KG (2009) Injectable in situ forming biodegradable chitosan–hyaluronic acid based hydrogels for cartilage tissue engineering. Biomaterials 30:2499–2506 . doi: 10.1016/j.biomaterials.2008.12.080

105. Pritchard CD, O'Shea TM, Siegwart DJ, et al (2011) An injectable thiol-acrylate poly(ethylene glycol) hydrogel for sustained release of methylprednisolone sodium succinate. Biomaterials 32:587–597 . doi: 10.1016/j.biomaterials.2010.08.106

106. Nie W, Yuan X, Zhao J, et al (2013) Rapidly in situ forming chitosan/ε-polylysine hydrogels for adhesive sealants and hemostatic materials. Carbohydrate Polymers 96:342–348 . doi: 10.1016/j.carbpol.2013.04.008

107. Yang K, Han Q, Chen B, et al (2018) Antimicrobial hydrogels: promising materials for medical application. Int J Nanomedicine 13:2217–2263 . doi: 10.2147/IJN.S154748

108. Alami-Milani M, Zakeri-Milani P, Valizadeh H, et al (2017) Novel pentablock copolymers as thermosensitive self-assembling micelles for ocular drug delivery. Adv Pharm Bull 7:11–20 . doi: 10.15171/apb.2017.003

109. Salatin S, Barar J, Barzegar-Jalali M, et al (2016) Hydrogel nanoparticles and nanocomposites for nasal drug/vaccine delivery. Arch Pharm Res 39:1181–1192 . doi: 10.1007/s12272-016-0782-0

110. Thambi T, Phan VHG, Lee DS (2016) Stimuli-sensitive injectable hydrogels based on polysaccharides and their biomedical applications. Macromol Rapid Commun 37:1881–1896 . doi: 10.1002/marc.201600371

111. Dalwadi C, Patel G (2015) Application of nanohydrogels in drug delivery systems: recent patents review. Recent Pat Nanotechnol 9:17–25

112. Fakhari A, Anand Subramony J (2015) Engineered in-situ depot-forming hydrogels for intratumoral drug delivery. J Control Release 220:465–475 . doi: 10.1016/j.jconrel.2015.11.014

113. Vedadghavami A, Minooei F, Mohammadi MH, et al (2017) Manufacturing of hydrogel biomaterials with controlled mechanical properties for tissue engineering applications. Acta Biomater 62:42–63 . doi: 10.1016/j.actbio.2017.07.028

114. Tsou Y-H, Khoneisser J, Huang P-C, Xu X (2016) Hydrogel as a bioactive material to regulate stem cell fate. Bioact Mater 1:39–55 . doi: 10.1016/j.bioactmat.2016.05.001

115. Shukla SK, Mishra AK, Arotiba OA, Mamba BB (2013) Chitosan-based nanomaterials: A state-of-the-art review. International Journal of Biological Macromolecules 59:46–58 . doi: 10.1016/j.ijbiomac.2013.04.043

116. Ravi Kumar MNV (2000) A review of chitin and chitosan applications. Reactive and Functional Polymers 46:1–27 . doi: 10.1016/S1381-5148(00)00038-9

117. Mima S, Miya M, Iwamoto R, Yoshikawa S (1983) Highly deacetylated chitosan and its properties. Journal of Applied Polymer Science 28:1909–1917 . doi: 10.1002/app.1983.070280607

118. Pan Y, Li Y, Zhao H, et al (2002) Bioadhesive polysaccharide in protein delivery system: chitosan nanoparticles improve the intestinal absorption of insulin in vivo. International Journal of Pharmaceutics 249:139–147 . doi: 10.1016/S0378-5173(02)00486-6

119. Jayakumar R, Menon D, Manzoor K, et al (2010) Biomedical applications of chitin and chitosan based nanomaterials—a short review. Carbohydrate Polymers 82:227–232 . doi: 10.1016/j.carbpol.2010.04.074

120. Chatterjee S, Chatterjee BP, Guha AK (2014) A study on antifungal activity of water-soluble chitosan against Macrophomina phaseolina. Int J Biol Macromol 67:452–457 . doi: 10.1016/j.ijbiomac.2014.04.008

121. Sundaram N, Mony U, Jayakumar R (2016) Chitin and chitosan as hemostatic agents. In: Encyclopedia of Polymer Science and Technology. American Cancer Society, pp 1–12

122. Sugano M, Fujikawa T, Hiratsuji Y, et al (1980) A novel use of chitosan as a hypocholesterolemic agent in rats. Am J Clin Nutr 33:787–793 . doi: 10.1093/ajcn/33.4.787

123. Nishimura K, Nishimura S, Nishi N, et al (1984) Immunological activity of chitin and its derivatives. Vaccine 2:93–99

124. Pattani A, Patravale VB, Panicker L, Potdar PD (2009) Immunological effects and membrane interactions of chitosan nanoparticles. Mol Pharm 6:345–352 . doi: 10.1021/mp900004b

125. Sorlier P, Denuzière A, Viton C, Domard A (2001) Relation between the degree of acetylation and the electrostatic properties of chitin and chitosan. Biomacromolecules 2:765–772 . doi: 10.1021/bm015531+

126. Chhabra P, Tyagi P, Bhatnagar A, et al (2016) Optimization, characterization, and efficacy evaluation of 2% chitosan scaffold for tissue engineering and wound healing. Journal of Pharmacy And Bioallied Sciences 8:300 . doi: 10.4103/0975-7406.199346

127. Croisier F, Jérôme C (2013) Chitosan-based biomaterials for tissue engineering. European Polymer Journal 49:780–792 . doi: 10.1016/j.eurpolymj.2012.12.009

128. Devlieghere F, Vermeulen A, Debevere J (2004) Chitosan: antimicrobial activity, interactions with food components and applicability as a coating on fruit and vegetables. Food Microbiology 21:703–714 . doi: 10.1016/j.fm.2004.02.008

129. Ham-Pichavant F, Sèbe G, Pardon P, Coma V (2005) Fat resistance properties of chitosan-based paper packaging for food applications. Carbohydrate Polymers 61:259–265 . doi: 10.1016/j.carbpol.2005.01.020

130. Suntornsuk W, Pochanavanich P, Suntornsuk L (2002) Fungal chitosan production on food processing by-products. Process Biochemistry 37:727–729 . doi: 10.1016/S0032-9592(01)00265-5

131. Sun L, Du Y, Yang J, et al (2006) Conversion of crystal structure of the chitin to facilitate preparation of a 6-carboxychitin with moisture absorption–retention abilities. Carbohydrate Polymers 66:168–175 . doi: 10.1016/j.carbpol.2006.02.036

132. Rinaudo M (2006) Chitin and chitosan: properties and applications. Progress in Polymer Science 31:603–632 . doi: 10.1016/j.progpolymsci.2006.06.001

133. Northcott KA, Snape I, Scales PJ, Stevens GW (2005) Dewatering behaviour of water treatment sludges associated with contaminated site remediation in Antarctica. Chemical Engineering Science 60:6835–6843 . doi: 10.1016/j.ces.2005.05.049

134. Crini G (2005) Recent developments in polysaccharide-based materials used as adsorbents in wastewater treatment. Progress in Polymer Science 30:38–70 . doi: 10.1016/j.progpolymsci.2004.11.002

135. Zhang J, Xia W, Liu P, et al (2010) Chitosan modification and pharmaceutical/biomedical applications. Marine Drugs 8:1962–1987 . doi: 10.3390/md8071962

136. Strobl GR (2007) The physics of polymers: concepts for understanding their structures and behavior, 3rd ed. Springer-Verlag, Berlin Heidelberg

137. Abolhasani MM, Arefazar A, Mozdianfard M (2009) Effect of dispersed phase composition on morphological and mechanical properties of PET/EVA/PP ternary blends. Journal of Polymer Science Part B: Polymer Physics 48:251–259 . doi: 10.1002/polb.21857

138. Khoo CGL, Frantzich S, Rosinski A, et al (2003) Oral gingival delivery systems from chitosan blends with hydrophilic polymers. European Journal of Pharmaceutics and Biopharmaceutics 55:47–56 . doi: 10.1016/S0939-6411(02)00155-8

139. Gibson HW, Bailey FC (1980) Chemical modification of polymers. 13. sulfonation of polystyrene surfaces. Macromolecules 13:34–41 . doi: 10.1021/ma60073a007

140. Kurita K (2001) Controlled functionalization of the polysaccharide chitin. Progress in Polymer Science 26:1921–1971 . doi: 10.1016/S0079-6700(01)00007-7

141. Avadi MR, Sadeghi AMM, Tahzibi A, et al (2004) Diethylmethyl chitosan as an antimicrobial agent: synthesis, characterization and antibacterial effects. European Polymer Journal 40:1355–1361 . doi: 10.1016/j.eurpolymj.2004.02.015

142. Aoi K, Takasu A, Okada M, Imae T (2003) Nano-scale molecular shapes of water-soluble chitin derivatives having monodisperse poly(2-alkyl-2-oxazoline) side chains. Macromolecular Chemistry and Physics 203:2650–2657 . doi: 10.1002/macp.200290040

143. Qu X, Wirsén A, Albertsson A-C (1999) Synthesis and characterization of pH-sensitive hydrogels based on chitosan and D,L-lactic acid. Journal of Applied Polymer Science 74:3193–3202 . doi: 10.1002/(SICI)1097-4628(19991220)74:13<3193::AID-APP23>3.0.CO;2-V

144. Moura LIF, Dias AMA, Carvalho E, de Sousa HC (2013) Recent advances on the development of wound dressings for diabetic foot ulcer treatment—a review. Acta Biomaterialia 9:7093–7114 . doi: 10.1016/j.actbio.2013.03.033

145. Han G, Ceilley R (2017) Chronic wound healing: a review of current management and treatments. Adv Ther 34:599–610 . doi: 10.1007/s12325-017-0478-y

146. Lloyd LL, Kennedy JF, Methacanon P, et al (1998) Carbohydrate polymers as wound management aids. Carbohydrate Polymers 37:315–322 . doi: 10.1016/S0144-8617(98)00077-0

147. Harding KG, Jones V, Price P (2000) Topical treatment: which dressing to choose. Diabetes Metab Res Rev 16 Suppl 1:S47-50

148. Stadelmann WK, Digenis AG, Tobin GR (1998) Physiology and healing dynamics of chronic cutaneous wounds. The American Journal of Surgery 176:26S-38S . doi: 10.1016/S0002-9610(98)00183-4

149. Robson MC (1997) Wound infection: a failure of wound healing caused by an imbalance of bacteria. Surgical Clinics of North America 77:637–650 . doi: 10.1016/S0039-6109(05)70572-7

150. Steed DL (1997) The role of growth factors in wound healing. Surg Clin North Am 77:575–586

151. Wahl SM, Wahl LM, McCarthy JB (1978) Lymphocyte-mediated activation of fibroblast proliferation and collagen production. J Immunol 121:942–946

152. Diegelmann RF, Cohen IK, Kaplan AM (1981) The role of macrophages in wound repair: a review. Plast Reconstr Surg 68:107–113

153. Thiruvoth FM, Mohapatra DP, Sivakumar DK, et al (2015) Current concepts in the physiology of adult wound healing. Plastic and Aesthetic Research 2:250–256 . doi: 10.4103/2347-9264.158851

154. Pitts DG, Willoughby J, Morgan RK (2016) Clinical reasoning and problem solving to prevent pitfalls in hand injuries. In: Musculoskeletal Key - Fastest Muscoloskeletal Insight Engine. https://musculoskeletalkey.com/clinical-reasoning-and-problem-solving-to-prevent-pitfalls-in-hand-injuries/. Accessed 20 Jul 2018

155. Jones V, Grey JE, Harding KG (2006) Wound dressings. BMJ 332:777–780 . doi: 10.1136/bmj.332.7544.777

156. Park JW, Hwang SR, Yoon I-S (2017) Advanced growth factor delivery systems in wound management and skin regeneration. Molecules 22:1259 . doi: 10.3390/molecules22081259

157. Mittal B, Tulsyan S, Kumar S, et al (2015) Chapter four - cytochrome P450 in cancer susceptibility and treatment. In: Makowski GS (ed) Advances in Clinical Chemistry. Elsevier, pp 77–139

158. Nebert DW, Russell DW (2002) Clinical importance of the cytochromes P450. The Lancet 360:1155–1162 . doi: 10.1016/S0140-6736(02)11203-7

159. Preissner SC, Hoffmann MF, Preissner R, et al (2013) Polymorphic cytochrome P450 enzymes (CYPs) and their role in personalized therapy. PLOS ONE 8:e82562 . doi: 10.1371/journal.pone.0082562

160. Gundert-Remy U, Bernauer U, Blömeke B, et al (2014) Extrahepatic metabolism at the body's internal–external interfaces. Drug Metabolism Reviews 46:291–324 . doi: 10.3109/03602532.2014.900565

161. Wilkinson GR (2005) Drug metabolism and variability among patients in drug response. New England Journal of Medicine 352:2211–2221 . doi: 10.1056/NEJMra032424

162. Anzenbacher P, Anzenbacherová E (2001) Cytochromes P450 and metabolism of xenobiotics. Cell Mol Life Sci 58:737–747

163. Backman JT, Kivistö KT, Olkkola KT, Neuvonen PJ (1998) The area under the plasma concentration-time curve for oral midazolam is 400-fold larger during treatment with itraconazole than with rifampicin. Eur J Clin Pharmacol 54:53–58

164. Ray WA, Murray KT, Meredith S, et al (2004) Oral erythromycin and the risk of sudden death from cardiac causes. N Engl J Med 351:1089–1096 . doi: 10.1056/NEJMoa040582

165. (2011) Statin interactions: reports of serious myopathy. In: Medsafe -New zealand medicines andmedical devices safety authority. http://www.medsafe.govt.nz/profs/PUArticles/StatinInteractionsJune2011.htm. Accessed 13 Jun 2018

166. Bailey DG, Dresser G, Arnold JMO (2013) Grapefruit–medication interactions: forbidden fruit or avoidable consequences? CMAJ 185:309–316 . doi: 10.1503/cmaj.120951

167. Ruschitzka F, Meier PJ, Turina M, et al (2000) Acute heart transplant rejection due to Saint John's wort. The Lancet 355:548–549 . doi: 10.1016/S0140-6736(99)05467-7

168. Piscitelli SC, Burstein AH, Chaitt D, et al (2000) Indinavir concentrations and St John's wort. The Lancet 355:547–548 . doi: 10.1016/S0140-6736(99)05712-8

169. Ionescu C, Caira MR (2006) Drug metabolism: current concepts. Springer Science & Business Media

170. Nicholson JK, Holmes E, Kinross JM, et al (2012) Metabolic phenotyping in clinical and surgical environments. Nature 491:384–392 . doi: 10.1038/nature11708

171. Burhenne J, Halama B, Maurer M, et al (2012) Quantification of femtomolar concentrations of the CYP3A substrate midazolam and its main metabolite 1'-hydroxymidazolam in human plasma using ultra performance liquid chromatography coupled to tandem mass spectrometry. Anal Bioanal Chem 402:2439–2450 . doi: 10.1007/s00216-011-5675-y

172. Donzelli M, Derungs A, Serratore M-G, et al (2014) The Basel Cocktail for simultaneous phenotyping of human cytochrome P450 isoforms in plasma, saliva and dried blood spots. Clin Pharmacokinet 53:271–282 . doi: 10.1007/s40262-013-0115-0

173. Eap CB, Buclin T, Cucchia G, et al (2004) Oral administration of a low dose of midazolam (75 μg) as an in vivo probe for CYP3A activity. Eur J Clin Pharmacol 60:237–246 . doi: 10.1007/s00228-004-0762-z

174. Halama B, Hohmann N, Burhenne J, et al (2013) A nanogram dose of the CYP3A probe substrate midazolam to evaluate drug interactions. Clin Pharmacol Ther 93:564–571 . doi: 10.1038/clpt.2013.27

175. Hohmann N, Kocheise F, Carls A, et al (2015) Midazolam microdose to determine systemic and pre-systemic metabolic CYP3A activity in humans. Br J Clin Pharmacol 79:278–285 . doi: 10.1111/bcp.12502

176. Roche Pharma (Schweiz) AG (2015) Dormicum® injectionsolution prescribing information

177. Wandel C, Böcker R, Böhrer H, et al (1994) Midazolam is metabolized by at least three different cytochrome P450 enzymes. British Journal of Anaesthesia 73:658–661 . doi: 10.1093/bja/73.5.658

178. Heizmann P, Eckert M, Ziegler WH (1983) Pharmacokinetics and bioavailability of midazolam in man. Br J Clin Pharmacol 16:43S-49S

179. Nordt SP, Clark RF (1997) Midazolam: a review of therapeutic uses and toxicity. J Emerg Med 15:357–365

180. Zhu B, Bush D, Doss GA, et al (2008) Characterization of 1'-hydroxymidazolam glucuronidation in human liver microsomes. Drug Metab Dispos 36:331–338 . doi: 10.1124/dmd.107.017962

181. Hyland R, Osborne T, Payne A, et al (2009) In vitro and in vivo glucuronidation of midazolam in humans. Br J Clin Pharmacol 67:445–454 . doi: 10.1111/j.1365-2125.2009.03386.x

182. Borges AF, Silva C, Coelho JFJ, Simões S (2015) Oral films: current status and future perspectives: I — galenical development and quality attributes. Journal of Controlled Release 206:1–19 . doi: 10.1016/j.jconrel.2015.03.006

183. Dixit RP, Puthli SP (2009) Oral strip technology: overview and future potential. J Control Release 139:94–107 . doi: 10.1016/j.jconrel.2009.06.014

184. Sucker H, Fuchs P, Speiser P (1991) Pharmazeutische Technologie, 2nd ed. Georg Thieme Verlag Stuttgart, Stuttgart, Germany

185. ElMeshad AN, Hagrasy ASE (2011) Characterization and optimization of orodispersible mosapride film formulations. AAPS PharmSciTech 12:1384–1392 . doi: 10.1208/s12249-011-9713-z

186. Liew KB, Tan YTF, Peh K-K (2014) Effect of polymer, plasticizer and filler on orally disintegrating film. Drug Development and Industrial Pharmacy 40:110–119 . doi: 10.3109/03639045.2012.749889

187. Alanazi FK, Abdel Rahman AA, Mahrous GM, Alsarra IA (2007) Formulation and physicochemical characterisation of buccoadhesive films containing ketorolac. Journal of Drug Delivery Science and Technology 17:183–192 . doi: 10.1016/S1773-2247(07)50034-1

188. Xie F, Halley PJ, Avérous L (2012) Rheology to understand and optimize processibility, structures and properties of starch polymeric materials. Progress in Polymer Science 37:595–623 . doi: 10.1016/j.progpolymsci.2011.07.002

189. Cilurzo F, Cupone IE, Minghetti P, et al (2010) Nicotine fast dissolving films made of maltodextrins: a feasibility study. AAPS PharmSciTech 11:1511–1517 . doi: 10.1208/s12249-010-9525-6

190. Katzenmaier S, Markert C, Riedel K-D, et al (2011) Determining the time course of CYP3A inhibition by potent reversible and irreversible CYP3A inhibitors using a limited sampling strategy. Clinical Pharmacology & Therapeutics 90:666–673 . doi: 10.1038/clpt.2011.164

191. Orlu M, Ranmal SR, Sheng Y, et al (2017) Acceptability of orodispersible films for delivery of medicines to infants and preschool children. Drug Deliv 24:1243–1248 . doi: 10.1080/10717544.2017.1370512

192. Rushil S, Priti M (2014) Paediatric formulation development: challenges and opportunities. Int J Pharm Sci Rev Res 24:137–143

193. Slavkova M, Breitkreutz J (2015) Orodispersible drug formulations for children and elderly. European Journal of Pharmaceutical Sciences 75:2–9 . doi: 10.1016/j.ejps.2015.02.015

194. ICH Expert Working Group (2000) Clinical investigation of medicinal products in the pediatric population E11, ICH harmonised tripartite guideline

195. EMA (2007) Guideline on the investigation of medicinal products in the term and preterm neonate, Doc. Ref. EMEA/267484/2007. 1–19

196. World Health Organization (2015) What is a preterm baby? In: WHO. http://www.who.int/features/qa/preterm_babies/en/. Accessed 27 Jun 2018

197. Piñeiro-Carrero VM, Piñeiro EO (2004) Liver. Pediatrics 113:1097–1106

198. Lee PA (1980) Normal ages of pubertal events among American males and females. J Adolesc Health Care 1:26–29

199. EMA (2006) Reflection paper: formulations of choice for the paediatric population - EMEA/CHMP/194810/2005

200. Schirm E, Tobi H, Vries T de, et al (2007) Lack of appropriate formulations of medicines for children in the community. Acta Paediatrica 92:1486–1489 . doi: 10.1111/j.1651-2227.2003.tb00837.x

201. Bruns CM, Kemnitz JW (2004) Sex hormones, insulin sensitivity, and diabetes mellitus. ILAR J 45:160–169 . doi: 10.1093/ilar.45.2.160

202. Schachter SC (1988) Hormonal considerations in women with seizures. Arch Neurol 45:1267–1270 . doi: 10.1001/archneur.1988.00520350105025

203. Weathermon R, Crabb DW (1999) Alcohol and medication interactions. 23:15

204. Kroon LA (2007) Drug interactions with smoking. Am J Health Syst Pharm 64:1917–1921 . doi: 10.2146/ajhp060414

205. Macfarlane A (1975) Olfaction in the development of social preferences in the human neonate. Ciba Found Symp 103–117

206. Segovia C, Hutchinson I, Laing DG, Jinks AL (2002) A quantitative study of fungiform papillae and taste pore density in adults and children. Brain Res Dev Brain Res 138:135–146

207. EMA (2001) ICH Topic E 11 - clinical investigation of medicinal products in the paediatric population - CPMP/ICH/2711/99

208. Breitkreutz J, Boos J (2007) Paediatric and geriatric drug delivery. Expert Opinion on Drug Delivery 4:37–45 . doi: 10.1517/17425247.4.1.37

209. Salunke S, Giacoia G, Tuleu C (2012) The STEP (safety and toxicity of excipients for paediatrics) database. Part 1—a need assessment study. International Journal of Pharmaceutics 435:101–111 . doi: 10.1016/j.ijpharm.2012.05.004

210. Salunke S, Brandys B, Giacoia G, Tuleu C (2013) The STEP (safety and toxicity of excipients for paediatrics) database: Part 2 – the pilot version. International Journal of Pharmaceutics 457:310–322 . doi: 10.1016/j.ijpharm.2013.09.013

211. Salunke S, Tuleu C (2015) The STEP database through the end-users eyes—usability study. International Journal of Pharmaceutics 492:316–331 . doi: 10.1016/j.ijpharm.2015.06.016

212. Steffensen GK, Pachaï A, Pedersen SE (1998) Peroral drug administration to children - are there any problems? Ugeskr Laeg 160:2249–2252

213. Baguley D, Lim E, Bevan A, et al (2012) Prescribing for children – taste and palatability affect adherence to antibiotics: a review. Archives of Disease in Childhood 97:293–297 . doi: 10.1136/archdischild-2011-300909

214. Kaplan BJ, Steiger RA, Pope J, et al (2010) Successful treatment of pill-swallowing difficulties with head posture practice. Paediatr Child Health 15:e1–e5

215. Brown D, Ford JL, Nunn AJ, Rowe PH (2004) An assessment of dose-uniformity of samples delivered from paediatric oral droppers. J Clin Pharm Ther 29:521–529 . doi: 10.1111/j.1365-2710.2004.00595.x

216. Johnson A, Meyers R (2016) Evaluation of measuring devices packaged with prescription oral liquid medications. J Pediatr Pharmacol Ther 21:75–80 . doi: 10.5863/1551-6776-21.1.75

217. van Santen E, Barends DM, Frijlink HW (2002) Breaking of scored tablets: a review. Eur J Pharm Biopharm 53:139–145

218. Sirisha K. VR, Vijaya Sri K, Suresh K, et al (2013) A review of pellets and pelletization process – a multiparticulate drug delivery system. Int J Pharm Sci Res 4:2145–2158 . doi: http://dx.doi.org/10.13040/IJPSR.0975-8232.4(6).2145-58

219. Aleksovski A, Dreu R, Gašperlin M, Planinšek O (2015) Mini-tablets: a contemporary system for oral drug delivery in targeted patient groups. Expert Opinion on Drug Delivery 12:65–84 . doi: 10.1517/17425247.2014.951633

220. Neuspiel DR, Taylor MM (2013) Reducing the risk of harm from medication errors in children. Health Serv Insights 6:47–59 . doi: 10.4137/HSI.S10454

221. EMA (2008) Ethical considerations for clinical trials on medicinal products with the paediatric population - Recommendations of the ad hoc group for the development of implementing guidelines for Directive 2001/20/EC relating to good clinical practice in the conduct of clinical trials on medicinal products for human use

222. Davies EH, Tuleu C (2008) Medicines for Children: A Matter of Taste. The Journal of Pediatrics 153:599-604.e2 . doi: 10.1016/j.jpeds.2008.06.030

223. Sjövall J, Fogh A, Huitfeldt B, et al (1984) Methods for evaluating the taste of paediatric formulations in children: A comparison between the facial hedonic method and the patients' own spontaneous verbal judgement. Eur J Pediatr 141:243–247 . doi: 10.1007/BF00572770

224. Ghaderi F, Banakar S, Rostami S (2013) Effect of pre-cooling injection site on pain perception in pediatric dentistry: "A randomized clinical trial." Dent Res J (Isfahan) 10:790–794

225. Wagner-Hattler L, Wyss K, Schoelkopf J, et al (2017) In vitro characterization and mouthfeel study of functionalized calcium carbonate in orally disintegrating tablets. International Journal of Pharmaceutics 534:50–59 . doi: 10.1016/j.ijpharm.2017.10.009

226. Wagner V, Dullaart A, Bock A-K, Zweck A (2006) The emerging nanomedicine landscape. In: Nature Biotechnology. https://www.nature.com/articles/nbt1006-1211. Accessed 3 Jul 2018

227. Min Y, Caster JM, Eblan MJ, Wang AZ (2015) Clinical translation of nanomedicine. Chem Rev 115:11147–11190 . doi: 10.1021/acs.chemrev.5b00116

228. Barenholz Y (Chezy) (2012) Doxil® — the first FDA-approved nano-drug: lessons learned. Journal of Controlled Release 160:117–134 . doi: 10.1016/j.jconrel.2012.03.020

229. Leserman LD, Barbet J, Kourilsky F, Weinstein JN (1980) Targeting to cells of fluorescent liposomes covalently coupled with monoclonal antibody or protein A. Nature 288:602–604

230. Fraley R, Papahadjopoulos D (1981) New generation liposomes: the engineering of an efficient vehicle for intracellular delivery of nucleic acids. Trends in Biochemical Sciences 6:77–80 . doi: 10.1016/0968-0004(81)90028-1

231. Mamot C, Ritschard R, Wicki A, et al (2012) Tolerability, safety, pharmacokinetics, and efficacy of doxorubicin-loaded anti-EGFR immunoliposomes in advanced solid tumours: a phase 1 dose-escalation study. The Lancet Oncology 13:1234–1241 . doi: 10.1016/S1470-2045(12)70476-X

232. Lee H, Shields AF, Siegel BA, et al (2017) 64Cu-MM-302 positron emission tomography quantifies variability of enhanced permeability and retention of nanoparticles in relation to treatment response in patients with metastatic breast cancer. Clin Cancer Res 23:4190–4202 . doi: 10.1158/1078-0432.CCR-16-3193

233. Merrimack MM-310. In: Merrimack Pipeline. http://www.merrimack.com/strategies/mm-310/. Accessed 3 Jul 2018

234. Siefker-Radtke A, Zhang X, Guo CC, et al (2016) A phase l study of a tumor-targeted systemic nanodelivery system, SGT-94, in genitourinary cancers. Molecular Therapy 24:1484–1491 . doi: 10.1038/mt.2016.118

235. Belfiore L, Saunders DN, Ranson M, et al (2018) Towards clinical translation of ligand-functionalized liposomes in targeted cancer therapy: Challenges and opportunities. Journal of Controlled Release 277:1–13 . doi: 10.1016/j.jconrel.2018.02.040

236. Rosenblum D, Joshi N, Tao W, et al (2018) Progress and challenges towards targeted delivery of cancer therapeutics. Nat Commun 9: . doi: 10.1038/s41467-018-03705-y

237. Kierstead PH, Okochi H, Venditto VJ, et al (2015) The effect of polymer backbone chemistry on the induction of the accelerated blood clearance in polymer modified liposomes. J Control Release 213:1–9 . doi: 10.1016/j.jconrel.2015.06.023

238. Laverman P, Carstens MG, Boerman OC, et al (2001) Factors affecting the accelerated blood clearance of polyethylene glycol-liposomes upon repeated injection. J Pharmacol Exp Ther 298:607–612

239. Oussoren C, Storm G (1999) Effect of repeated intravenous administration on the circulation kinetics of poly(ethyleneglycol)-liposomes in rats. Journal of Liposome Research 9:349–355 . doi: 10.3109/08982109909018655

240. Platt FM, Boland B, van der Spoel AC (2012) Lysosomal storage disorders: the cellular impact of lysosomal dysfunction. J Cell Biol 199:723–734 . doi: 10.1083/jcb.201208152

241. Parenti G, Andria G, Ballabio A (2015) Lysosomal storage diseases: from pathophysiology to therapy. Annual Review of Medicine 66:471–486 . doi: 10.1146/annurev-med-122313-085916

242. Sieber S, Grossen P, Detampel P, et al (2017) Zebrafish as an early stage screening tool to study the systemic circulation of nanoparticulate drug delivery systems in vivo. J Control Release 264:180–191 . doi: 10.1016/j.jconrel.2017.08.023

243. Rizzo LY, Golombek SK, Mertens ME, et al (2013) In vivo nanotoxicity testing using the zebrafish embryo assay. J Mater Chem B 1: . doi: 10.1039/C3TB20528B

244. Bodewein L, Schmelter F, Di Fiore S, et al (2016) Differences in toxicity of anionic and cationic PAMAM and PPI dendrimers in zebrafish embryos and cancer cell lines. Toxicology and Applied Pharmacology 305:83–92 . doi: 10.1016/j.taap.2016.06.008

245. Nanotechnology Characterization Lab (NCL) Assay cascade protocols. https://ncl.cancer.gov/resources/assay-cascade-protocols. Accessed 4 Jul 2018

246. Jahn A, Vreeland WN, Gaitan M, Locascio LE (2004) Controlled vesicle self-assembly in microfluidic channels with hydrodynamic focusing. J Am Chem Soc 126:2674–2675 . doi: 10.1021/ja0318030

247. Chung Y-J, An S-Y, Yeon J-Y, et al (2016) Effect of a chitosan gel on hemostasis and prevention of adhesion after endoscopic sinus surgery. Clin Exp Otorhinolaryngol 9:143–149 . doi: 10.21053/ceo.2015.00591

248. Valentine R, Athanasiadis T, Moratti S, et al (2010) The efficacy of a novel chitosan gel on hemostasis and wound healing after endoscopic sinus surgery. American Journal of Rhinology & Allergy 24:70–75 . doi: 10.2500/ajra.2010.24.3422

249. Kordestani S, Shahrezaee M, Tahmasebi M n., et al (2008) A randomised controlled trial on the effectiveness of an advanced wound dressing used in Iran. J Wound Care 17:323–327 . doi: 10.12968/jowc.2008.17.7.30525

250. Mo X, Cen J, Gibson E, et al (2015) An open multicenter comparative randomized clinical study on chitosan. Wound Rep and Reg 23:518–524 . doi: 10.1111/wrr.12298

251. Malmquist JP, Clemens SC, Oien HJ, Wilson SL (2008) Hemostasis of oral surgery wounds with the HemCon Dental Dressing. J Oral Maxillofac Surg 66:1177–1183 . doi: 10.1016/j.joms.2007.12.023

252. Pippi R, Santoro M, Cafolla A (2017) The use of a chitosan-derived hemostatic agent for postextraction bleeding control in patients on antiplatelet treatment. J Oral Maxillofac Surg 75:1118–1123 . doi: 10.1016/j.joms.2017.01.005

253. Stone CA, Wright H, Devaraj VS, et al (2000) Healing at skin graft donor sites dressed with chitosan. British Journal of Plastic Surgery 53:601–606 . doi: 10.1054/bjps.2000.3412

254. Stanish WD, McCormack R, Forriol F, et al (2013) Novel scaffold-based BST-CarGel treatment results in superior cartilage repair compared with microfracture in a randomized controlled trial. J Bone Joint Surg Am 95:1640–1650 . doi: 10.2106/JBJS.L.01345

255. Tricol Biomedical Inc. Products archive. In: Tricol Biomedical. https://www.hemcon.com/welcome/shop/. Accessed 5 Jul 2018

256. Medline (2013) Product brochure Opticell®wound dressings - powerful yet gentle moisture management

257. Pozza M, Millner RWJ (2011) Celox (chitosan) for haemostasis in massive traumatic bleeding: experience in Afghanistan. Eur J Emerg Med 18:31–33 . doi: 10.1097/MEJ.0b013e32833a5ee4

258. Kozen BG, Kircher SJ, Henao J, et al (2008) An alternative hemostatic dressing: comparison of CELOX, HemCon, and QuikClot. Academic Emergency Medicine 15:74–81 . doi: 10.1111/j.1553-2712.2007.00009.x

259. Schmid BC, Reznicek GA, Rolf N, Maul H (2012) Postpartum hemorrhage: use of hemostatic combat gauze. Am J Obstet Gynecol 206:e12-13 . doi: 10.1016/j.ajog.2011.09.018

260. Elviri L, Bianchera A, Bergonzi C, Bettini R (2017) Controlled local drug delivery strategies from chitosan hydrogels for wound healing. Expert Opinion on Drug Delivery 14:897–908 . doi: 10.1080/17425247.2017.1247803

261. Cross KJ, Mustoe TA (2003) Growth factors in wound healing. Surg Clin North Am 83:531–545, vi . doi: 10.1016/S0039-6109(02)00202-5

262. Meier K, Nanney LB (2006) Emerging new drugs for wound repair. Expert Opinion on Emerging Drugs 11:23–37 . doi: 10.1517/14728214.11.1.23

263. Wang F, Wang M, She Z, et al (2015) Collagen/chitosan based two-compartment and bi-functional dermal scaffolds for skin regeneration. Materials Science and Engineering: C 52:155–162 . doi: 10.1016/j.msec.2015.03.013

264. Mohandas A, Anisha BS, Chennazhi KP, Jayakumar R (2015) Chitosan–hyaluronic acid/VEGF loaded fibrin nanoparticles composite sponges for enhancing angiogenesis in wounds. Colloids and Surfaces B: Biointerfaces 127:105–113 . doi: 10.1016/j.colsurfb.2015.01.024

265. Ribeiro MP, Espiga A, Silva D, et al (2009) Development of a new chitosan hydrogel for wound dressing. Wound Repair and Regeneration 17:817–824 . doi: 10.1111/j.1524-475X.2009.00538.x

266. Zhou W, Zhao M, Zhao Y, Mou Y (2011) A fibrin gel loaded with chitosan nanoparticles for local delivery of rhEGF: preparation and in vitro release studies. J Mater Sci: Mater Med 22:1221–1230 . doi: 10.1007/s10856-011-4304-9

267. Aduba DC, Yang H (2017) Polysaccharide fabrication platforms and biocompatibility assessment as candidate wound dressing materials. Bioengineering 4:1 . doi: 10.3390/bioengineering4010001

268. Lindholm C, Searle R (2016) Wound management for the 21st century: combining effectiveness and efficiency. International Wound Journal 13:5–15 . doi: 10.1111/iwj.12623

269. Hilton JR, Williams DT, Beuker B, et al (2004) Wound dressings in diabetic foot disease. Clin Infect Dis 39:S100–S103 . doi: 10.1086/383270

270. EMA (2011) Guideline on the use of pharmacogenetic methodologies in the pharmacokinetic evaluation of medicinal products; EMA/CHMP/37646/2009

271. Samer CF, Lorenzini KI, Rollason V, et al (2013) Applications of CYP450 testing in the clinical setting. Mol Diagn Ther 17:165–184 . doi: 10.1007/s40291-013-0028-5

272. Kivistö KT, Kroemer HK (1997) Use of probe drugs as predictors of drug metabolism in humans. J Clin Pharmacol 37:40S-48S

273. Wit D de, Gelderblom H, Sparreboom A, et al (2014) Midazolam as a phenotyping probe to predict sunitinib exposure in patients with cancer. Cancer Chemother Pharmacol 73:87–96 . doi: 10.1007/s00280-013-2322-7

274. Hocum BT, White JR, Heck JW, et al (2016) Cytochrome P-450 gene and drug interaction analysis in patients referred for pharmacogenetic testing. American Journal of Health-System Pharmacy 73:61–67 . doi: 10.2146/ajhp150273

275. Jerdi MC, Daali Y, Oestreicher MK, et al (2004) A simplified analytical method for a phenotyping cocktail of major CYP450 biotransformation routes. J Pharm Biomed Anal 35:1203–1212 . doi: 10.1016/j.jpba.2004.03.021

276. Derungs A, Donzelli M, Berger B, et al (2016) Effects of cytochrome P450 inhibition and induction on the phenotyping metrics of the Basel Cocktail: a randomized crossover study. Clin Pharmacokinet 55:79–91 . doi: 10.1007/s40262-015-0294-y

277. EMA (2003) Position paper on non-clinical safety studies to support clinical trials with a single microdose; CPMP/SWP/2599/02 (2003)

278. Kim JS, Nafziger AN, Tsunoda SM, et al (2002) Limited sampling strategy to predict AUC of the CYP3A phenotyping probe midazolam in adults: application to various assay techniques. The Journal of Clinical Pharmacology 42:376–382 . doi: 10.1177/00912700222011418

279. Masters JC, Harano DM, Greenberg HE, et al (2015) Limited sampling strategy of partial area-under-the-concentration-time-curves to estimate midazolam systemic clearance for cytochrome P450 3A phenotyping. Ther Drug Monit 37:84–89 . doi: 10.1097/FTD.0000000000000116

280. Mueller SC, Drewelow B (2013) Evaluation of limited sampling models for prediction of oral midazolam AUC for CYP3A phenotyping and drug interaction studies. Eur J Clin Pharmacol 69:1127–1134 . doi: 10.1007/s00228-012-1437-9

281. Fuhr U, Jetter A, Kirchheiner J (2007) Appropriate phenotyping procedures for drug metabolizing enzymes and transporters in humans and their simultaneous use in the "cocktail" approach. Clinical Pharmacology & Therapeutics 81:270–283 . doi: 10.1038/sj.clpt.6100050

282. Kesel PMMD, Lambert WE, Stove CP (2016) Alternative sampling strategies for cytochrome P450 phenotyping. Clin Pharmacokinet 55:169–184 . doi: 10.1007/s40262-015-0306-y

283. Bosilkovska M, Samer C, Déglon J, et al (2016) Evaluation of mutual drug–drug interaction within Geneva Cocktail for cytochrome P450 phenotyping using innovative dried blood sampling method. Basic & Clinical Pharmacology & Toxicology 119:284–290 . doi: 10.1111/bcpt.12586

284. Mizuno A, Uematsu T, Gotoh S, et al (1996) The measurement of caffeine concentration in scalp hair as an indicator of liver function. J Pharm Pharmacol 48:660–664

285. De Kesel PMM, Lambert WE, Stove CP (2015) Paraxanthine/caffeine concentration ratios in hair: an alternative for plasma-based phenotyping of cytochrome P450 1A2? Clin Pharmacokinet 54:771–781 . doi: 10.1007/s40262-015-0237-7

286. Park GJ-H, Katelaris PH, Jones DB, et al (2003) Validity of the 13C-caffeine breath test as a noninvasive, quantitative test of liver function. Hepatology 38:1227–1236 . doi: 10.1053/jhep.2003.50475

287. Delahunty T, Schoendorfer D (1998) Caffeine demethylation monitoring using a transdermal sweat patch. J Anal Toxicol 22:596–600

288. Anderson GD (2005) Sex and racial differences in pharmacological response: where is the evidence? Pharmacogenetics, pharmacokinetics, and pharmacodynamics. J Womens Health (Larchmt) 14:19–29 . doi: 10.1089/jwh.2005.14.19

289. de Andrés F, LLerena A (2016) Simultaneous determination of cytochrome P450 oxidation capacity in humans: a review on the phenotyping cocktail approach. Curr Pharm Biotechnol 17:1159–1180 . doi: 10.2174/1389201017666160926150117

290. Keller GA, Gago MLF, Diez RA, Di Girolamo G (2017) In vivo phenotyping methods: cytochrome P450 probes with emphasis on the cocktail approach. Curr Pharm Des 23:2035–2049 . doi: 10.2174/1381612823666170207100724

291. Karki S, Kim H, Na S-J, et al (2016) Thin films as an emerging platform for drug delivery. Asian Journal of Pharmaceutical Sciences 11:559–574 . doi: 10.1016/j.ajps.2016.05.004

292. Aquestive Therapeutics List of marketed PharFilm products. In: Aquestive. https://aquestive.com/products/. Accessed 13 Jul 2018

293. Meda Pharma GmbH & Co. KG (2015) Breakyl ® Buccalfilm prescribing information

294. tesa Labtec GmbH (2012) APR and Labtec announce approval in Europe of Zolmitriptan Rapidfilm®. In: tesa SE. http://www.tesa-labtec.com/eng/company/press/apr-and-labtec-announce-approval-in-europe-of-zolmitriptan-rapidfilm,3097354,1.html. Accessed 13 Jul 2018

295. Irfan M, Rabel S, Bukhtar Q, et al (2016) Orally disintegrating films: a modern expansion in drug delivery system. Saudi Pharmaceutical Journal 24:537–546 . doi: 10.1016/j.jsps.2015.02.024

296. RootsAnalysis Business Research & Consulting (2015) Oral Thin Films Market, 2015 - 2025. In: Oral Thin Films Market, 2015 - 2025. https://www.rootsanalysis.com/reports/view_document/oral-thin-films-market-2015-2025/81.html. Accessed 13 Jul 2018

297. Gelbe Liste Dormicum® 7.5 mg Filmtabletten prescribing information

298. Bornand D (2017) Crushing of tablets (Liste: Zermörserbarkeit und Verabreichungshinweise von Tabletten) - LL0019-V07-B01

299. Gelbe Liste (2016) Buccolam® oral solution for buccal application prescribing information

300. Cram A, Breitkreutz J, Desset-Brèthes S, et al (2009) Challenges of developing palatable oral paediatric formulations. International Journal of Pharmaceutics 365:1–3 . doi: 10.1016/j.ijpharm.2008.09.015

301. Florence AT (2008) Neglected diseases, neglected technologies, neglected patients? International Journal of Pharmaceutics 350:1–2 . doi: 10.1016/j.ijpharm.2007.11.028

302. FDA (2008) Guidance for industry: orally disintegrating tablets (2008)

303. Powers JL, Gooch WM, Oddo LP (2000) Comparison of the palatability of the oral suspension of cefdinir vs. amoxicillin/clavulanate potassium, cefprozil and azithromycin in pediatric patients. Pediatr Infect Dis J 19:S174-180

304. Toscani M, Drehobl M, Freed J, Stool S (2000) A multicenter, randomized, comparative assessment in healthy pediatric volunteers of the palatability of oral antibiotics effective in the therapy of otitis media. Current Therapeutic Research 61:278–285 . doi: 10.1016/S0011-393X(00)80018-1

305. Rowe RC, Sheskey PJ, Quinn, Marian E. (2009) Handbook of pharmaceutical excipients, 6th ed. Pharmaceutical Press and American Pharmacists Association

306. Stirnimann T, Di Maiuta N, Gerard DE, et al (2013) Functionalized calcium carbonate as a novel pharmaceutical excipient for the preparation of orally dispersible tablets. Pharm Res 30:1915–1925 . doi: 10.1007/s11095-013-1034-3

307. Eberle VA, Schoelkopf J, Gane PAC, et al (2014) Floating gastroretentive drug delivery systems: comparison of experimental and simulated dissolution profiles and floatation behavior. Eur J Pharm Sci 58:34–43 . doi: 10.1016/j.ejps.2014.03.001

308. Preisig D, Haid D, Varum FJO, et al (2014) Drug loading into porous calcium carbonate microparticles by solvent evaporation. European Journal of Pharmaceutics and Biopharmaceutics 87:548–558 . doi: 10.1016/j.ejpb.2014.02.009

309. Roth R, Schoelkopf J, Huwyler J, Puchkov M (2018) Functionalized calcium carbonate microparticles for the delivery of proteins. European Journal of Pharmaceutics and Biopharmaceutics 122:96–103 . doi: 10.1016/j.ejpb.2017.10.012

310. compendium.ch. In: Disperisble, disintegrating, and liquid oral formulations. https://compendium.ch/search/tablette/de. Accessed 16 Jul 2018

311. Oma International AG Omya product offer - Pharma & Nutra

312. Rameesa CK, Drisya MK (2015) Orodispersible tablet: a patient friendly dosage form (a review). Bali Medical Journal 4:17–20

313. Panchal DM, Tiwari A, Srivastava P (2013) A review on orodispersible tablets - a novel formuation for oral drug delivery system and its future perspective. Indo American Journal of Pharmaceutical Research 3:4149–4168

APPENDIX

CRS newsletter: biocompatible PDMS-*b*-PMOXA polymersomes for cell type specific targeting.

K. Kiene, S.H. Schenk, D. Witzigmann, J. Huwyler; **CRS Newsletter** 2017, Volume 34 Number 5, 15

Biocompatible PDMS-*b*-PMOXA Polymersomes for Cell Type Specific Drug Targeting

Klara Kiene,[a] Susanne H. Schenk, Dominik Witzigmann, and Jörg Huwyler
University of Basel, Switzerland

Introduction

Many promising therapeutic compounds suffer from disadvantages such as low bioavailability, rapid clearance, and high systemic toxicity. To overcome these challenges, nanoparticles such as polymersomes can be used as promising drug delivery systems. Polymersomes are vesicles formed by self-assembly of amphiphilic block co-polymers such as poly(dimethylsiloxane)-*b*-poly(2-methyloxazoline) (PDMS-*b*-PMOXA). PDMS-*b*-PMOXA is a promising block co-polymer because the individual polymer blocks have been reported to be biocompatible.

Herein, we present the formulation of polymersomes based on PDMS-*b*-PMOXA, and we demonstrate slow drug release of incorporated model drug (i.e., carboxyfluorescein, CF) *in vitro*. In addition, we focus on the surface modification of PDMS-*b*-PMOXA polymersomes (PP) for targeted drug delivery to hepatocytes. Potential toxicity of the resulting polymersomes is assessed *in vitro* and *in vivo*.[1]

Experimental Approach and Results

PP were prepared by thin-film rehydration and subsequently modified to obtain targeted vesicles (Fig. 1). All PP variants were routinely analyzed by dynamic light scattering (DLS) for average size and size distribution (Table 1). The different modifications resulted in monodisperse suspensions of particles with hydrodynamic diameters of around 150 nm. Cryo-transmission electron microscopy (cryo-TEM) confirmed size and vesicle morphology (Fig. 2A). The polymersomes could be stored in Dulbecco's phosphate-buffered saline (DPBS) at 4°C for at least 4 months without significant change in particle size and polydispersity index (PDI) and without loss of functionality as confirmed by cellular uptake experiments. In addition, the integrity of the particles was tested under forced stress conditions. Unmodified PP were incubated
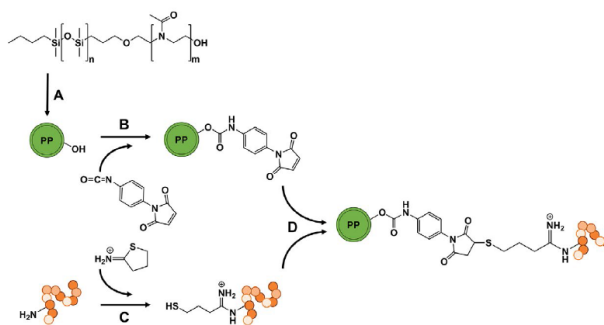
Figure 1. *Preparation of AF targeted PP. (A) Formulation of PP using the thin film rehydration method. (B) Modification of the polymersomes' surface using p-maleimidophenyl-isocyanate to obtain maleimide-functionalized PP and (C) in parallel thiolation of AF using 2-iminothiolane (Traut's activation). (D) Finally, maleimide-functionalized PP and activated AF were covalently linked via Michael addition to achieve PP-AF.*

Table 1. Size and Size Distribution of PDMS-*b*-PMOXA Based Polymersomes[a]

Abbreviation	Full Name of Polymersomes	Diameter (nm)	PDI
PP	PDMS-*b*-PMOXA polymersomes	156.9 ± 8.8	0.082 ± 0.041
PP-F	PP modified with fetuin	155.4 ± 15.0	0.097 ± 0.015
PP-AF	PP modified with asialofetuin	149.8 ± 7.9	0.103 ± 0.019
PP-488	PP modified with HiLyte Fluor 488	161.3 ± 10.2	0.175 ± 0.057
PP-F-488	PP modified with HiLyte Fluor 488 labeled F	148.4 ± 6.3	0.098 ± 0.039
PP-AF-488	PP modified with HiLyte Fluor 488 labeled AF	149.3 ± 1.5	0.098 ± 0.027
PP-CF	PP loaded with CF	155.9 ± 17.5	0.133 ± 0.034

[a] Hydrodynamic diameters (DLS-intensity peaks) and polydispersity index (PDI) of different polymersome formulations were measured by DLS. Data represent mean values ± SD (*n* = 5). Abbreviations used for the different formulations are indicated.

15

in DPBS, 3% bovine serum albumin (BSA), or 50% fetal calf serum (FCS) for 7 days at 37°C. As outlined in Figure 2B, no statistically significant changes in particle diameters occurred over time. To demonstrate that PDMS-*b*-PMOXA forms tight vesicles, we encapsulated CF as a model drug into PP and subsequently measured CF release into DPBS at different temperatures over 96 h using a microdialysis device (Fig. 2C). CF release was temperature dependent and occurred in a slow and sustained manner over a long period of time. No initial burst release was observed at any of the tested temperatures, and no plateau was reached within the duration of the experiment. Moreover, a similar release profile was observed in buffers containing naturally occurring serum proteins (3% BSA and 50% FCS, observation period 48 h). Using the standard thin-film rehydration method, the achieved loading capacity was 1.5 ± 0.2 nmol of CF per mg of PP. This seems low. However; to achieve therapeutic effects, alteration of pharmacokinetics is the most important factor. Nanoparticles can shift the balance in off- and on-target accumulation. Therefore, already a low percentage of nanoparticles delivered to the diseased tissue may offer a benefit to the patients by reducing severe side effects of encapsulated drugs.[2]

For hepatocyte-specific targeting, we selected the asialoglycoprotein receptor (ASGPR),[3] and its naturally occurring ligand asialofetuin (AF) was covalently linked to PP (PP-AF). Using confocal microscopy and flow cytometry (FACS), we showed receptor-mediated and energy-dependent uptake of PP-AF by the hepatocarcinoma cell line HepG2 (Fig. 3).
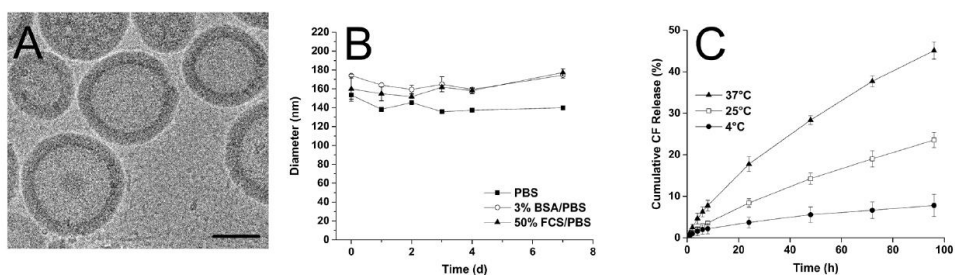
Figure 2. *Characterization of PP. (A) Cryo–TEM analysis of PP showed the formation of hollow spheres. Scale bar = 100 nm. (B) Stability of PP in different buffers at 37°C. Changes in hydrodynamic diameters were measured by DLS. Values are means ± SD (n = 3). (C) Cumulative release profile of CF from PP-CF in DPBS measured at different temperatures. SD is shown with error bars (n = 3).*
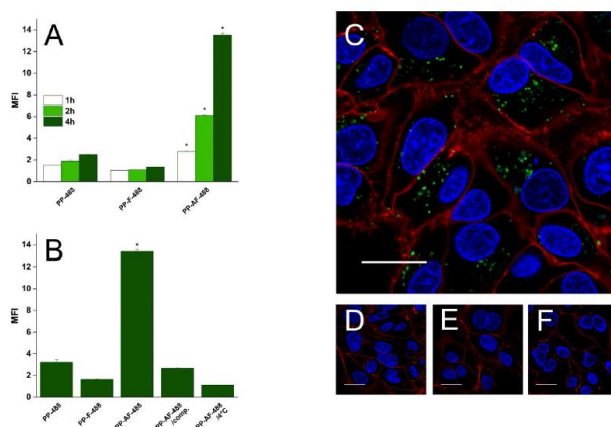

Figure 3. *Time-dependent and receptor-specific cellular uptake of targeted PP. (A) HepG2 cells were incubated with PP-488, PP-F-488, and PP-AF-488 and analyzed by FACS to quantify uptake of the differently modified PP. Mean fluorescence intensity (MFI) was normalized to untreated control cells. SD is shown with error bars (n = 3); asterisk (*) indicates P < 0.01. (B) ASGPR specific uptake of PP-AF-488 by HepG2 cells. PP-488 (negative control) and PP-AF-488: cells were incubated with the indicated polymersomes for 4 h at 37°C. PP-AF-488/comp: for competitive inhibition, cells were pre-incubated for 1 h with an excess of free AF before adding PP-AF-488. PP-AF-488/4°C: HepG2 cells were incubated at 4°C in the presence of PP-AF-488. Uptake determined by FACS is shown as MFI normalized to untreated control cells. SD is shown with error bars (n = 3); asterisk (*) indicates P < 0.01. (C–F) Confocal microscopy after 4 h uptake of respective polymersomes. Nuclei are blue, cell membranes red, and PP-488 and PP-AF-488 green. Scale bar = 20 μm. (C) PP-AF-488. (D) PP-488. (E) PP-AF-488/comp. (F) PP-AF-488/4°C.*

16

To confirm the biocompatibility of various PP formulations *in vitro*, we performed MTT assays. For all concentrations and formulations, cell viability was at least 80% (Fig. 4A). To investigate whether our polymersomes exhibit adverse effects *in vivo*, we used zebrafish embryos (ZFE). This vertebrate model is becoming increasingly recognized as an "intermediate" model for toxicity screening of small molecules but also nanoparticles before turning to experiments in rodents.[4] ZFE with chorion as well as dechorionized ZFE were exposed up to 96 h postfertilization (hpf) to the highest concentration of different PP formulations that were non-toxic *in vitro* (500 μg/mL). As a result, no signs of developmental toxicity were observed during the whole experiment (equal hatching rate, no malformations such as pericardial edema or tail malformations), suggesting good biocompatibility of all PP variants (Fig. 4B–D). In addition, preliminary experiments indicate that even direct injection of our polymersomes into the blood circulation of 72 hpf ZFE (using a microinjection device) did not result in acute toxicity. We conclude from these experiments that our polymersomes are well tolerated within a typical dose range suggested for use of nanomedicines.[5]
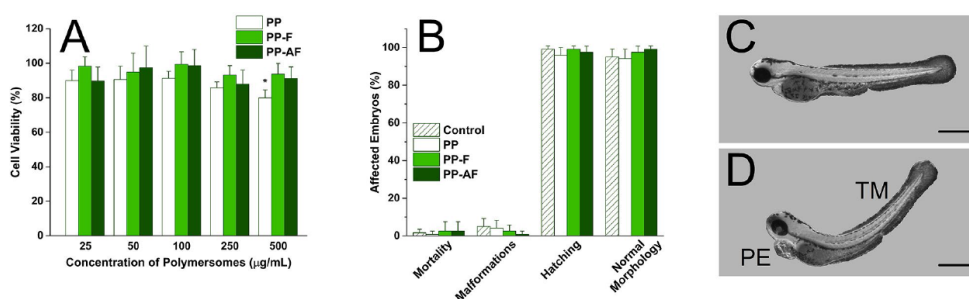
Figure 4. *In vitro and in vivo toxicity. (A) MTT-assay. Cell viability of HepG2 cells after incubation for 24 h with increasing concentrations of differently modified PP. Cell viability of untreated control cells is 100%. SD is shown with error bars (n = 8); asterisk (*) indicates P < 0.01. (B) Toxicity of differently modified polymersomes in zebrafish (96 hpf). Percentages of mortality in the early zebrafish larvae, larvae affected by morphological malformations, hatching rate, and larvae with normal morphology are shown. The polymersome formulations were tested and compared to control (no polymersomes). Values are means ± SD (n = 30). (C, D) Representative images of ZFE 96 hpf. (C) ZFE with normal morphology. (D) Exemplified ZFE with malformations (PE pericardial edema, TM tail malformation). Scale bar = 0.5 mm.*

Conclusion

In conclusion, we achieved a targeted drug delivery system that is biocompatible *in vitro* and presumably also *in vivo*. It could be loaded with a hydrophilic model compound, and sustained release over a long time was achieved in DPBS as well as in serum protein containing media. Successful AF conjugation and therefore effective ASGPR targeting make our polymersomes a promising tool for clinical application in the field of liver disorders.

References

1 Kiene, K, Schenk, SH, Porta, F, Ernst, A, Witzigmann, D, Grossen, P, Huwyler, J. PDMS-*b*-PMOXA polymersomes for hepatocellular targeting and assessment of toxicity. Eur. J. Pharm. Biopharm. 119: 322-332 (2017). doi:10.1016/j.ejpb.2017.07.002.
2 Lammers, T, Kiessling, F, Ashford, M, Hennink, W, Storm, G. Cancer nanomedicine: Is targeting our target ? Nat. Rev. Mater. 1: 1-4 (2016). doi:10.1038/natrevmats.2016.76.
3 Witzigmann, D, Quagliata, L, Schenk, SH, Quintavalle, C, Terracciano, LM, Huwyler, J. Variable asialoglycoprotein receptor 1 expression in liver disease: Implications for therapeutic intervention. Hepatol. Res. 46: 686-696 (2016). doi:10.1111/hepr.12599.
4 Rizzo, LY, Golombek, SK, Mertens, ME, Pan, Y, Laaf, D, Broda, J, Jayapaul, J, Möckel, D, Subr, V, Hennink, WE, Storm, G, Simon, U, Jahnen-Dechent, W, Kiessling, F, Lammers, T. *In vivo* nanotoxicity testing using the zebrafish embryo assay. J. Mater. Chem. B Mater. Biol. Med. 1: 3918-3925 (2013). doi:10.1039/C3TB20528B.
5 Kettiger, H, Sen, D, Schiesser, L, Rosenholm, JM, Huwyler, J. Comparative safety evaluation of silica-based particles. Toxicol. Vitr. 30: 355-363 (2015). doi:10.1016/j.tiv.2015.09.030. ■

PDMS-PMOXA Polymer Vesicles for Targeted Delivery to Lectin Receptors

Fabiola Porta[1], **Klara Kiene**[1], Marine Camblin[1], Martina Konantz[2], Philip Grossen[1], Dominik Witzigmann[1], Susanne Schenk[1] and Jörg Huwyler[1]

1 Department of Pharmaceutical Technology, University of Basel, Klingelbergstrasse 50, 4056 Basel, Switzerland
2 Department of Biomedicine, University Hospital Basel, Hebelstrasse 20, 4031 Basel, Switzerland

Introduction

Poly(dimethylsiloxane)-poly(2-methyloxazoline) (PDMS-PMOXA) are diblock-copolymers which self-assemble in water in stable vesicular polymer based nanostructures, named polymersomes. These vesicles present several potential applications ranging from nanoreactors to targeted drug delivery systems. In this study we formulated polymer vesicles based on PDMS-PMOXA covalently modified with asialofetuin (AF), an essential ligand for asialoglycoprotein receptors (ASGPR) abundantly expressed on the surface of hepatocytes. Intracellular uptake was demonstrated using AF modified PDMS-PMOXA polymer vesicles in HepG2 cells lines. Intracellular internalization was competitively inhibited using free AF. The behaviour of PDMS-PMOXA polymersomes and protein modified polymersomes was further investigated using zebrafish, showing biocompatible and circulating nanoparticles.

Methods
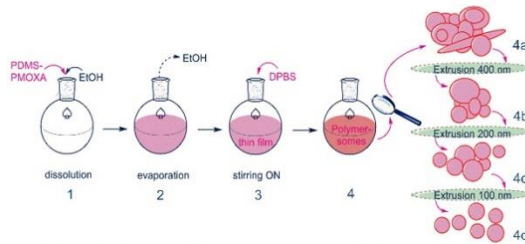
Fig. 1 General scheme of polymersome synthesis. (1) A homogeneous solution of PDMS-PMOXA is performed in Ethanol (EtOH). (2) The polymeric thin film is achieved in high vacuum. (3) Rehydration of the PDMS-PMOXA thin film with physiological phosphate buffer (DPBS) is performed. (4) Poylmersomes are formed during overnight stirring at room temperature. (4a,b,c,d) To achieve the final formulation an extrusion with 400nm, 200nm and 100nm is necessary.
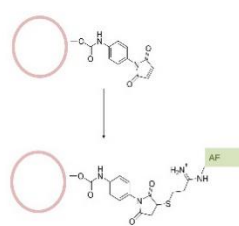
Fig. 2 Synthesis of AF/PDMS-PMOXA polymersomes. Polymeric vesicles were modified with *p*-maleimidophenyl isocyanate (PMPI), obtaining a maleimide functionalized surface. Next, the thiolated AF was coupled via Michael addition.
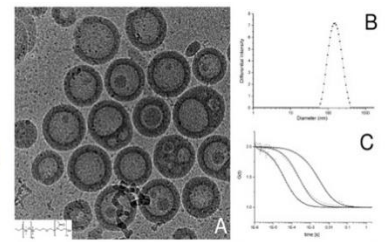
Fig. 3 (A) Cryo-TEM of PDMS-PMOXA polymeric vesicles. (B) Dynamic light scattering (DLS) shows a average diameter of 137nm (STD ±0.074). (C) Successful modification was measured with fluorescence correlation spectroscopy (FCS) and resulted in 26 molecules of AF per polymersome (C).
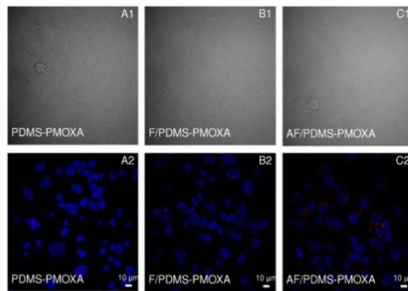
Results

Uptake in HepG2

Fig. 4 Uptake of differently modified PDMS-PMOXA polymersomes in HepG2 cells after 4hours; 1: bright field, 2: Hoechst 33342, Ex=405nm and DiI, Ex=550nm. (A1,2) Intracellular uptake of PDMS-PMOXA polymersomes. (B1,2) Cellular uptake of F/PDMS-PMOXA polymeric vesicles. (C1,2) AF/PDMS-PMOXA intracellular uptake. Significant intracellular accumulation of AF/PDMS-PMOXA is shown. Therefore, receptor mediated active uptake is demonstrated.
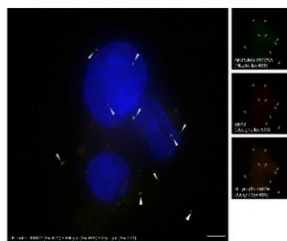
Endosomal staining in HepG2

Fig. 5 Uptake of AF-modified polymersomes (green) into early endosomes (EEA1, red) of HepG2 after 1 hour (Pearson's corr. coeff. 0.896). Scale bar 5µm.
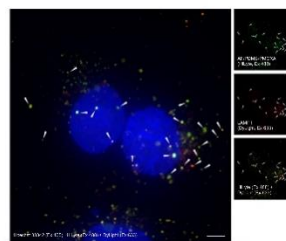
Fig. 6 Uptake of AF/PDMS-PMOXA (green) into late endosomes (LAMP1, red) of HepG2 after 4 hours (Pearson's corr. coeff. 0.857). Scale bar 5µm.

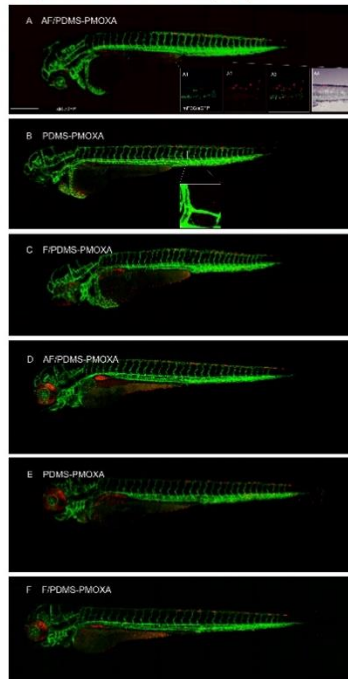### Injection into Zebrafish (2dpf)

Fig. 7 Laser confocal microscopy of fluorescently labelled zebrafish. (A) 1hpi of AF/PDMS-PMOXA polymeric vesicles in zebrafish trans-genic line kdrl:eGFP and mPEG:eGFP. Magnification of macrophage uptake of fluorescent nanoparticles is shown in A1,2,3,4. (B) Biodistribution of unmodified polymersomes in zebrafish embryo (1hpi), with included magnification of extravasating vesicles. (C) 1hpi confocal microscopy of F/PDMS-PMOXA polymer vesicles. (D,E,F) 1dpi of polymeric nanovesicles formulation visualized using confocal microscopy in kdrl:eGFP line. Polymeric nanovesicles were observed in the embryo circulation as free flotating nanoparticles. Any abnormal accumulation or aggretion was not obserserved. Therefore, the nanovesicles did not undergo opsonization. In contrast, AF/PDMS-PMOXA polymersomes were visualized in macrophages already after 1 hpi. Thus, active uptake via lectin receptors was achieved. This behaviour was not observed for the other two formulations (data not shown). Scale bar 300µm.

Conclusions

Targeted PDMS-PMOXA polymersomes were successfully synthesized. Asialofetuin was used as targeting moiety for HepG2 cell line due to significant expression of ASGPR receptors on the cellular membrane. Receptor mediated uptake of such formulation was confirmed by confocal laser microscopy after 4 hours. Intracellular trafficking of AF/PDMS-PMOXA polymeric nanovesicles was investigated studying the permanence of the vesicles in early and late endosomes. After 4 hours of incubation polymersomes were observed in the late endosomes as correlated with the Pearson's coefficient. Moreover, real time blood circulation of the polymersomes formulations was investigated using zebrafish embryos. These nanoparticles resulted being long circulating and did not induce any opsonization. Furthermore, AF/PDMS-PMOXA polymersomes were actively taken up by macrophages after 1 hpi as demonstrated by the mPEG line. Finally, we achieved the synthesis of a biocompatible targeted delivery system with potential clinical applications.

University of Basel

DEPARTMENT OF PHARMACEUTICAL SCIENCES

Formation of a Self - Assembling Chitosan Hydrogel

Klara Kiene, Dr. Fabiola Porta, Prof. Dr. Jörg Huwyler
Division of Pharmaceutical Technology, University of Basel, Switzerland
Email: klara.kiene@unibas.ch

Abstract

We used the biocompatible polymer chitosan to prepare a self-assembling hydrogel. By Michael addition between a sulfhydryl modified and a maleimide functionalized chitosan polymer, we achieved a covalently crosslinked hydrogel. The microscopic aspect of the hydrogel matrix was investigated with scanning electron microscopy (SEM). A defined porous structure was observed with a pore diameter around 100 μm. Release kinetics were investigated using a model biomolecule, bovine serum albumin (BSA) with a molecular weight of 66 kDa. The gel showed sustained release properties. A post-loading of BSA was also performed; however, in this case an evident burst release was observed. Lyophilization of the hydrogel after loading and self-assembly showed that the release properties of the hydrogel maintained unchanged. Therefore, we can conclude that we synthesized a self-assembling biocompatible hydrogel with sustained release properties. As a next step, studies will be performed to optimize release kinetics in a model of human skin and to apply the technology to the treatment of wounds.

A. We prepared a gel which was loaded with BSA before gelation by dissolving thiolated chitosan in a solution of BSA. This gel showed sustained release of BSA over 10 hours (**A.1**). The release kinetics were not changed if we lyophilized the gel before release (**A.2**).
B. It is also possible to load the gel superficially with BSA after gelation, leading to burst release of BSA (**B.1**). For all the three gels we did not observe significant differences ($p = 0.01$) between the release at physiological pH (7.4, bright blue) and pH 8.0 (dark blue).
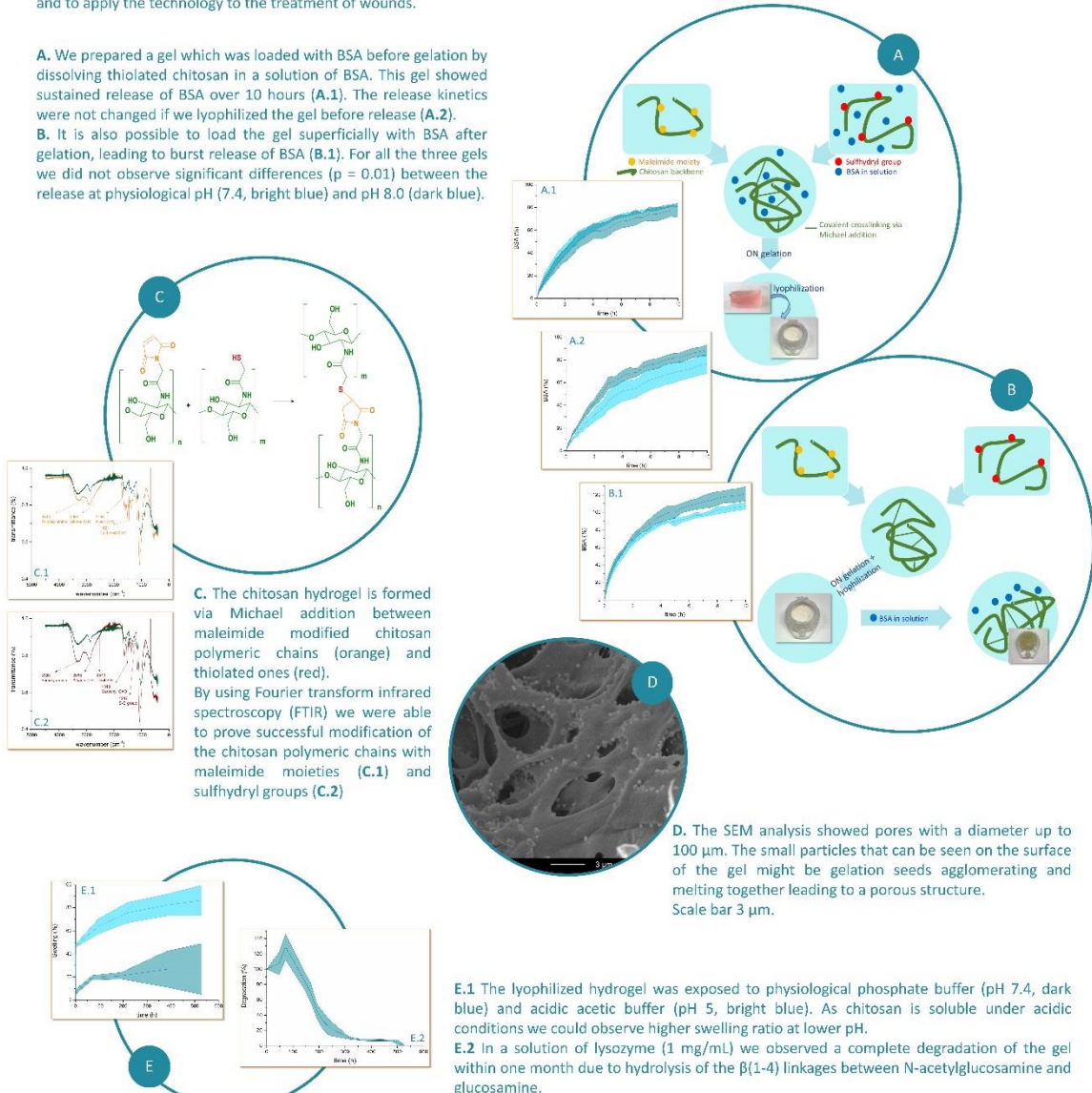
C. The chitosan hydrogel is formed via Michael addition between maleimide modified chitosan polymeric chains (orange) and thiolated ones (red).
By using Fourier transform infrared spectroscopy (FTIR) we were able to prove successful modification of the chitosan polymeric chains with maleimide moieties (**C.1**) and sulfhydryl groups (**C.2**)

D. The SEM analysis showed pores with a diameter up to 100 μm. The small particles that can be seen on the surface of the gel might be gelation seeds agglomerating and melting together leading to a porous structure.
Scale bar 3 μm.

E.1 The lyophilized hydrogel was exposed to physiological phosphate buffer (pH 7.4, dark blue) and acidic acetic buffer (pH 5, bright blue). As chitosan is soluble under acidic conditions we could observe higher swelling ratio at lower pH.
E.2 In a solution of lysozyme (1 mg/mL) we observed a complete degradation of the gel within one month due to hydrolysis of the β(1-4) linkages between N-acetylglucosamine and glucosamine.

Outlook

We synthesized a self-assembling chitosan hydrogel which is able to act as a drug carrier for proteins leading to sustained release. The gel can be stored for prolonged periods of time, as it is possible to lyophilize the complete gel without changing its properties. We imagine this gel to serve as a wound dressing delivering proteins (e.g. growth factors) to the wound in order to improve wound healing. Chitosan itself is known to be biocompatible, antiinfectious, immune-stimulating and promoting tissue-regeneration, which makes it a great polymer for wound dressings. The gel could be applied in its lyophilized form and swell due to the wet wound ground. By closing the whole system, the gel would help keeping a moisture wound environment on the one hand; on the other hand it shows sustained release kinetics in a pH range of superficial chronic wounds and in which many proteolytic enzymes exhibit maximum activity. Therefore, our self-assembling chitosan hydrogel could be a great technology to design future wound dressings.

References: Mather Prog. Polym. Sci. 31, 487–531 (2006); Chatterjee. Int. J. Biol. Macromol. 67, 452–7 (2014); Pattani Mol. Pharm. 6, 345–52 (2009); Rani BioResources 5, 2765–2807 (2010); Dissemond Der Hautarzt; Zeitschrift für Dermatologie, Venerol. und verwandte Gebiete 54, 930–65 (2003)

PDMS-*b*-PMOXA Polymersomes:
Hepatocyte Targeting & Assessment of Toxicity*

Klara Kiene, Susanne H. Schenk, Dominik Witzigmann, Jörg Huwyler
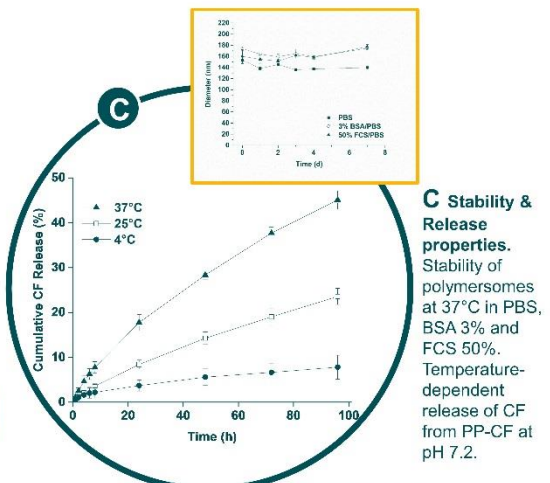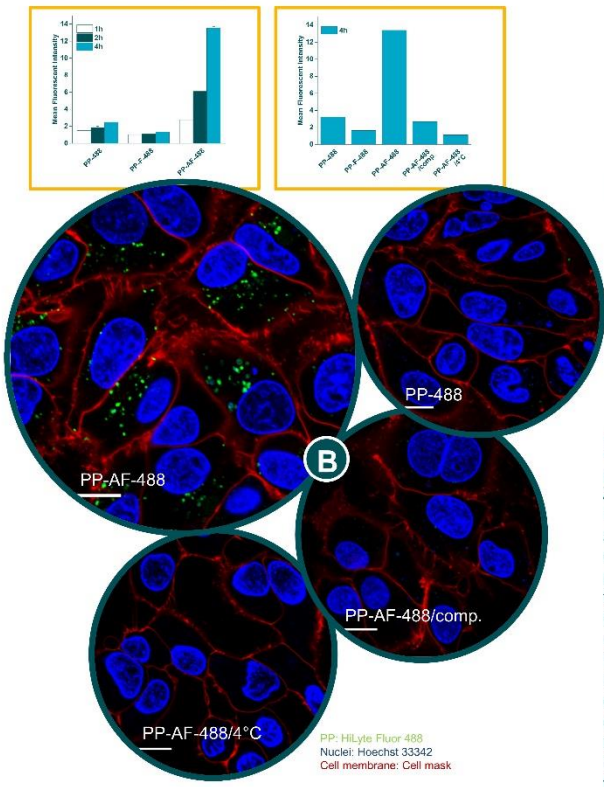*Division of Pharmaceutical Technology, University of Basel, Switzerland*

Nanoparticles, such as polymersomes, can be directed to the hepatic asialoglycoprotein receptor to achieve targeted drug delivery. In this study, we prepared asialofetuin conjugated polymersomes based on the biocompatible amphiphilic di-block copolymer poly(dimethylsiloxane)-*b*-poly(2-methyl-oxazoline) (PDMS-*b*-PMOXA). We assessed their targeting ability, as well as their potential toxicity *in vitro* and *in vivo* using zebrafish embryos.

A Chemical Structure, Cryo-Tem & DLS. Chemical Structre of PDMS-*b*-PMOXA. Cryo-TEM image of polymersomes (Scale bar 50 nm). DLS analysis of various polymersome formulations.
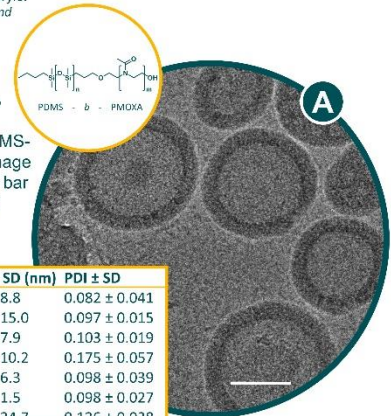
Abbreviation	Type of Polymersomes	Diam. ± SD (nm)	PDI ± SD
PP	PDMS-PMOXA Polymersomes	156.9 ± 8.8	0.082 ± 0.041
PP-F	PP modified with Fetuin	155.4 ± 15.0	0.097 ± 0.015
PP-AF	PP modified with Asialofetuin	149.8 ± 7.9	0.103 ± 0.019
PP-488	PP modified with HiLyte Fluor 488	161.3 ± 10.2	0.175 ± 0.057
PP-F-488	PP modified with 488-labelled F	148.4 ± 6.3	0.098 ± 0.039
PP-AF-488	PP modified with 488-labelled AF	149.3 ± 1.5	0.098 ± 0.027
PP-CF	PP loaded with (5,6)-Carboxyfluorescein	156.7 ± 34.7	0.136 ± 0.038

B Cellular uptake of polymersomes by HepG2 cells. AF-modified polymersomes show receptor mediated uptake within 4 hours. Qualitative analysis by confocal fluorescence microscopy (Scale bar 10 μm), quantitative analysis by FACS.

PP-AF-488

PP-488

PP-AF-488/comp.

PP-AF-488/4°C

PP: HiLyte Fluor 488
Nuclei: Hoechst 33342
Cell membrane: Cell mask

C Stability & Release properties. Stability of polymersomes at 37°C in PBS, BSA 3% and FCS 50%. Temperature-dependent release of CF from PP-CF at pH 7.2.

D Toxicity of polymersomes in ZF embryos. Incubation of zebrafish embryos with different polymersome formulations (500 μg/mL) until 96 hpf. Malformations include yolk sac edema, pericardial edema (PE), tail malformations (TM) and head deformations. Scale bar 0.5 mm.
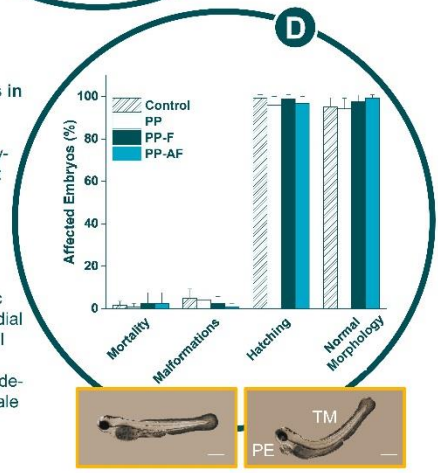
Klara Kiene
PhD Student - Pharmaceutical Technology
email: klara.kiene@unibas.ch
phone: +41 (0)61 207 1509
web: pharma.unibas.ch

In conclusion, a hepatocyte specific drug delivery system was designed, which is safe and biocompatible.

* Kiene et al. "PDMS-b-PMOXA Polymersomes for Hepatocyte Targeting and Assessment of Toxicity", submitted and revised

Pharmaceutical Technology – Drug Targeting Group

University of Basel

DIVISION OF PHARMACEUTICAL TECHNOLOGY

Introduction and Aim

There is a growing interest in therapeutic applications based on nanomedicines. To this end, nanoparticles (NPs) are used, which consist of inorganic materials, lipids, natural and synthetic polymers, or viruses. NPs can have inherent therapeutic effects (e.g. induction of oxidative stress or DNA damage), can be used as drug carriers, and can further be used as imaging agents or theranostics. Although the principles of nanomedicine are applicable to a broad range of diseases, treatment of cancer remains the most challenging therapeutic field. In our group, we use a broad range of nanomaterials for passive and active drug targeting and for imaging and test these systems in various *in vitro* and *in vivo* settings.

Particle Design

Lipid nanoparticles (i.e. liposomes). Representative TEM picture. Diameter 60 nm.

Inorganic Nanoparticles i.e. gold NPs (AuNPs) and supramagnetic iron oxide NPs (SPIONs). Representative TEM pictures. Diameter 10-20 nm.

Polymer nanoparticles i.e. polymersomes and solid sphere NPs. Representative TEM images. Diameter 150 nm and 80 nm respectively.

Hydrophobic molecule
Hydrophilic molecule

Surface Modifications

Targeted Drug Delivery
To achieve active targeted delivery, NPs must be modified on their surface with an agent that confers specificity for its cognate receptor. A wide range of ligands have been used for such purposes including small molecules for example folic acid and carbohydrates, or macromolecules such as peptides, proteins, antibodies, aptamers, and oligonucleotides.

~12 nm
Antibodies
Fab scFv
Peptides
Aptamers
Small molecules
<1 nm

NPs: HiLyte Fluor 488
Nuclei: Hoechst 33342
Cell membrane: Cell mask
Scale bar 10 µm

Animal Models

From Zebrafish to Rats
The transfer of experimental drug delivery systems to *in vivo* applications remains a challenge since it is difficult to assess their circulation behavior (pharmacokinetics) in the body at an early stage of drug discovery.
Thus, innovative and improved concepts are urgently needed to overcome this issue and to close the gap between empiric NP design, *in vitro* assessment, and first *in vivo* experiments using rodent animal models. Therefore, we are validating the zebrafish as an early and easy accessible *in vivo* tool for the optimization of nanoparticulate drug delivery systems.

Safety

Physico-Chemical Properties
Biological Systems
Chemical Composition

Nanotoxicology
We focus our research on NP-mediated acute toxic effects *in vitro* and *in vivo*. We aim to establish characterization strategies and assay toolboxes that provide robust information on how NPs interact with organisms. These insights should ultimately help authorities to establish nanosafety guidelines.

3D reconstructions of synchrotron phase contrast projections of zebrafish embryos (grey, otoliths in blue) showing the bio-distribution of AuNPs (yellow) and SPIONs (red). Scale bars 100 µm and 50 µm respectively.

Gene Delivery and Pharmacological Effects

Schematic overview of the therapeutic approach to clone H-1 parvovirus NS1 into a pDNA vector and deliver it via lipoplex NPs to healthy cells and hepato-cellular carcinoma derived cell lines. NS1 expression decreases cell viability in liver cancer derived cell lines (e.g. Hep3B) whereas healthy liver cells (primary human hepatocytes, PHH) are not influenced.

parental plasmid   bacterial backbone is removed   mcDNA

Minicircle DNA (mcDNA) obtained by removal of the bacterial backbone sequences of a parental plasmid is associated with higher transfection efficiency as well as higher transgene expression.
Moreover, a long persisting trans-gene expression can be achieved using mcDNA despite the fact that mcDNA is not integrated in the host genome.
Therefore, the use of mcDNA represents a safe alternative for gene therapy due to non-integration and avoidance of potentially cytotoxic transfection reagents.

Conclusion

Gene therapy is one of the most rapidly growing areas in nanomedicine research. The delivery of foreign nucleic acids, e.g. siRNA, mRNA or DNA, into human cells offers fascinating opportunities for biomedical applications. Gene delivery systems can be used to exert a therapeutic effect, to modulate cellular functions, or for monitoring purposes. Our translational research is focused on the development of new nanomaterials for an optimized loading and retention of nucleic acids and for a systemic administration *in vivo* with high cytocompatibility.